

**Adaptive Algorithms Design for Active
Noise Control Systems with
Disturbance at Reference and Error
Microphones**

by

Muhammad Saeed Aslam

Thesis submitted for the degree of

Doctor of Philosophy

in

School of Electrical & Electronic Engineering
Faculty of Engineering, Computer & Mathematical Sciences
The University of Adelaide, Australia

November 2020

© 2020
Muhammad Saeed Aslam
All Rights Reserved



Contents

Contents	iii
Abstract	v
Statement of Originality	vii
Acknowledgements	ix
Publications	xi
List of Figures	xiii
List of Tables	xv
List of Acronyms	xvii
List of Symbols	xix
Chapter 1. Introduction	1
1.1 Introduction	3
1.2 Literature Review	4
1.2.1 Feedforward Active Noise Control Systems	4
1.2.2 Secondary Path Estimation	6
1.2.3 Acoustic Feedback Neutralization	7
1.2.4 Hybrid Active Noise Control Systems for Disturbances	9
1.3 Motivation	10
1.4 Methodology	11
1.5 Contributions	11
1.6 Thesis outline	13
Chapter 2. Variable Threshold-Based Selective Updating Algorithms in Feed- Forward Active Noise Control Systems	15

Chapter 3. Novel Fast Recursive Least Squares Filter Design for Active Noise Control	31
Chapter 4. Robust Active Noise Control Design by Optimal Weighted Least Squares Approach	43
Chapter 5. Self-adapting variable step size strategies for active noise control systems with acoustic feedback	59
Chapter 6. New control structure for estimation-less acoustic feedback neutralization in active noise control systems	71
Chapter 7. Thesis Conclusion	93
7.1 Summary	94
7.2 Future work	95
References	97

Abstract

Active noise control (ANC) is a popular choice for mitigating the acoustic noise in the surrounding environment resulting from industrial and medical equipment, appliances, and consumer electronics. ANC cancels the low frequency acoustic noise by generating a cancelling sound from speakers. The speakers are triggered by noise control filters and produce sound waves with the same amplitude and inverted phase to the original sound. Noise control filters are updated by adaptive algorithms. Successful applications of this technology are available in headsets, earplugs, propeller aircraft, cars and mobile phones. Since multiple applications are running simultaneously, efficiency of the adaptive control algorithms in terms of implementation, computations and performance is critical to the performance of the ANC systems. The focus of the present project is on the development of efficient adaptive algorithms that perform optimally in different configurations of ANC systems suitable for real world applications.

Statement of Originality

I certify that this work contains no material which has been accepted for the award of any other degree or diploma in my name, in any university or other tertiary institution and, to the best of my knowledge and belief, contains no material previously published or written by another person, except where due reference has been made in the text. In addition, I certify that no part of this work will, in the future, be used in a submission in my name, for any other degree or diploma in any university or other tertiary institution without the prior approval of the University of Adelaide and where applicable, any partner institution responsible for the joint-award of this degree.

I acknowledge that copyright of published works contained within this thesis resides with the copyright holder(s) of those works.

I also give permission for the digital version of my thesis to be made available on the web, via the University's digital research repository, the Library Search and also through web search engines, unless permission has been granted by the University to restrict access for a period of time.

I acknowledge the support I have received for my research through the provision of an Australian Government Research Training Program Scholarship.

November 8, 2020

Signed

Date

Acknowledgements

I wish to express my sincere gratitude to my supervisors, Prof. Peng Shi and Prof. Cheng-Chew Lim, for their support, guidance and encouragement. I would like to thank them for providing me all the facilities, for allowing me to carry out the research in my own way and sharing insightful suggestions.

I would like to acknowledge School of Electrical and Electronic Engineering at The University of Adelaide for the financial support to cover all my expenses. At last, but not the least I owe my deepest gratitude to Di Shen and Syed Imranul Islam for their help, treasuring memories, and support during the entire period.

Muhammad Saeed Aslam

Nov 2020

Adelaide, SA, Australia

Publications

Journal publications

- MUHAMMAD SAEED ASLAM, PENG SHI, CHENG-CHEW LIM (2019).** Variable Threshold-Based Selective Updating Algorithms in Feed-Forward Active Noise Control Systems, *IEEE Transactions on Circuits and Systems I: Regular Papers*, **66(2)**, pp. 782–795.
- MUHAMMAD SAEED ASLAM, PENG SHI, CHENG-CHEW LIM (2019).** Robust Active Noise Control Design by Optimal Weighted Least Squares Approach, *IEEE Transactions on Circuits and Systems I: Regular Papers*, **66(10)**, pp. 3955–3967.
- MUHAMMAD SAEED ASLAM, PENG SHI, CHENG-CHEW LIM (2020).** Self-Adapting Variable Step Size Strategies for Active Noise Control Systems with Acoustic Feedback, *Automatica*, <https://doi.org/10.1016/j.automatica.2020.109354>.
- MUHAMMAD SAEED ASLAM, PENG SHI, CHENG-CHEW LIM (2020).** Novel Fast Recursive Least Squares Filter Design for Active Noise Control, *IEEE Transactions on Signal Processing*, under review.
- MUHAMMAD SAEED ASLAM, PENG SHI, CHENG-CHEW LIM (2020).** New Control Structure for Estimation-less Acoustic Feedback Neutralization in Active Noise Control Systems, *Automatica*, under review.

List of Figures

1.1	Feed-forward configuration of single channel ANC system	5
1.2	Block diagram of the conventional feedforward ANC systems.	6
1.3	Feed-forward configuration of single channel ANC system with acoustic feedback.	8



List of Tables

List of Acronyms

ANC	Active noise control
FIR	Finite impulse response
SNR	Signal-to-Noise ratio
FxLMS	Filtered-x least mean square
LMS	Least mean square
SU	Selective updating
VT	Variable threshold
FxLMS-Newton		Filtered-x least mean square-Newton
VT-SULMS	...	variable threshold based selective updating least mean square
SMF	Set membership filtering
MSE	Mean square error
PM	Proposed method
SAVSS	Self-adapting variable step size
NLMS	Normalized least mean square
NF	Notch filtering
FxOWRLS	Filtered-x optimally weighted recursive least squares
FTRLs	Fast transversal recursive least squares
RLS	Recursive least squares
FxFTRLs	Filtered-x fast transversal recursive least squares
VTFxEFRLS	..	Variable threshold filtered-x efficient fast recursive least squares
ADC	Analog-to-digital converter
DAC	Digital-to-analog converter

List of Symbols

$d(n)$	desired response/output of primary path
$E\{\cdot\}$	Expectation operator
$e(n)$	Residual error/error signal
f	Signal frequency
$F(z)$	Acoustic feedback path transfer function
$P(z)$	Primary path transfer function
$S(z)$	Secondary path transfer function
$W(z)$	Noise control filter
$\hat{F}(z)$	Estimated acoustic feedback path transfer function
$\hat{S}(z)$	Estimated secondary path transfer function
$f(n)$	Impulse response of acoustic feedback path
$p(n)$	Impulse response of primary path
$s(n)$	Impulse response of secondary path
$w(n)$	Impulse response of noise control filter
$\hat{f}(n)$	Impulse response of estimated acoustic feedback path
$\hat{s}(n)$	Impulse response of estimated secondary path
$\mathbf{f}(n)$	Impulse response vector for acoustic feedback path
$\mathbf{p}(n)$	Impulse response vector for primary path
$\mathbf{s}(n)$	Impulse response vector for secondary path
$\mathbf{w}(n)$	Impulse response vector for noise control filter
$\hat{\mathbf{f}}(n)$	Impulse response vector for estimated acoustic feedback path

List of Symbols

$\hat{\mathbf{s}}(n)$	Impulse response vector for estimated secondary path
$G(n)$	Time-varying gain for auxiliary noise
$x(n)$	Reference signal
$y(n)$	Control signal
$*$	Linear convolution
$v(n)$	Auxiliary noise
L_s	Length of $\hat{\mathbf{s}}(n)$
L_f	Length of $\hat{\mathbf{f}}(n)$
L_w	Length of $\mathbf{w}(n)$
n	Time index
$v_g(n)$	Gain modulated auxiliary noise
$x_f(n)$	Output of $F(z)$
$\hat{x}_f(n)$	Output of $\hat{F}(z)$
$\hat{d}(n)$	Cancelling noise
λ	Forgetting factor
μ	Step size parameter
μ_s	Step size parameter for $\hat{\mathbf{s}}(n)$
μ_w	Step size parameter for $\mathbf{w}(n)$
μ_f	Step size parameter for $\hat{\mathbf{f}}(n)$
$B(z)$	Predictor filter
$\mathbf{b}(n)$	Impulse response vector for predictor filter
μ_b	Step size parameter for $\mathbf{b}(n)$
Δ	Delay
L_d	Delay length

$\|\cdot\|^2$ Square of the Euclidean norm

$\hat{x}_s(n)$ $x(n)$ filtered through $\hat{s}(n)$

Chapter 1

Introduction

ACTIVE noise control is a popular choice for cancelling the low frequency noises using the secondary sources or speakers. This chapter introduces the configurations of active noise control systems along with the recent developments. The research motivations and contributions are highlighted for each configuration followed by the outline of the remaining chapters.

1.1 Introduction

Increase in the use of mechanical and electronic devices in daily life, yield the noise which has adverse effects on stress levels, health and productivity (Kajikawa *et al.* 2012). Currently available methods to mitigate this noise issue are categorised as active and passive. Passive methods perform well at higher frequencies and are known to become impractical for low frequencies as the dimension of passive materials is selected in relation with the wavelength. Active noise control (ANC) is preferred for performance against low frequency noises by generating a cancelling noise with identical amplitude and opposite phase using a secondary source in a controlled manner (Lueg 1936, Aslam *et al.* 2021, Aslam *et al.* 2019a). Recently, the ANC has gained popularity in commercial products like automobiles, headphones and mobile phones alongside numerous successful reported results including aircraft cabin noise, magnetic resonance imaging scanner, incubators and air conditioning ducts (Lee *et al.* 2021, Aslam *et al.* 2019b, Aslam 2016).

The cancellation of the primary noise is primarily dependent on the closeness of the amplitude and phase of the cancelling noise. In practice, noise sources and environment are time varying which means variations exist in the amplitude, frequency content and phase of the primary noise and adaptive filters are usually used to design control strategies to track the time varying problems (Kuo and Morgan 1996). Adaptive filters can be updated using Least mean square (LMS) and least squares (LS) algorithms. The adaptive algorithms are designed to meet requirements including steady state error, convergence speed, computational complexity, robustness and tunable parameters. Of these adaptive algorithms, LMS algorithm is extensively used for simplicity and computational efficiency (Lopes *et al.* 2017, Aslam 2016, Lopes and Gerald 2015, Aslam and Raja 2015, Ahmed *et al.* 2013b, Liao and Lin 2007, Lin and Liao 2008, Eriksson and Allie 1989, Kuo and Vijayan 1997, Zhang *et al.* 2001, Zhang *et al.* 2003, Akhtar *et al.* 2006, Akhtar *et al.* 2007, Carini and Malatini 2008, Davari and Hassanpour 2009, Basin *et al.* 2011). However, its performance is strongly dependent on the value of the step size parameter and correlation of the input data (Diniz 2008). By contrast, LS algorithm can be used to overcome the convergence speed and steady state issues, but at the cost of increase in computations. Hence, there is a need for designing adaptive algorithms that can combine best of LMS and LS algorithms and function efficiently.

1.2 Literature Review

The aim of the present research is to design the adaptive control algorithms for ANC systems that robustly achieve small steady state error at a relatively high convergence speed with low computational demand and manageable tuning parameters. The approach to designing algorithms with such characteristics can involve efficient implementations of the LS algorithms with a selective updating mechanism to achieve fast convergence with reduced computations (Diniz 2008). Alternative approach is to design multi-innovation or data-reusing algorithms (Diniz 2008) with self-adjusting step sizes and selective updating strategy. These possibilities will be explored during this research project.

1.2 Literature Review

The control mechanism of the ANC systems is classified as either feedforward or feedback. In a single channel feedforward ANC systems, a reference microphone is used to detect reference noise, a secondary source or loudspeaker is used to generate a canceling noise and an error microphone to sense the residual noise. In contrast, the single channel feedback ANC system only uses an error microphone and a loudspeaker. Feedforward ANC systems can be used in a variety of general applications but feedback ANC is used in situations where sensing or internal generation of coherent reference signal is not possible. These situations include spatially incoherent turbulence noise, multi-source noise, noise from multiple propagation paths and induced resonance (Kuo and Vijayan 1997). In addition, controllable bandwidth of feedback systems is very limited compared to feedforward systems (Kajikawa *et al.* 2012, Kuo and Vijayan 1997). Therefore, feedforward ANC systems are the primary focus of attention in this research work.

1.2.1 Feedforward Active Noise Control Systems

This section considers the feedforward ANC systems and schematic of a basic feedforward ANC system is shown in Fig. 1.1, where reference signal $x(n)$ is detected by a reference microphone and one error microphone is used for residual signal $e(n)$. Primary noise, $d(n)$, results from $x(n)$ passing through primary path $P(z)$ (from digital outcome of reference sensor to digital outcome of error sensor). Cancelling noise, $\hat{d}(n)$, is formed by $x(n)$ passing through adaptive noise controller $W(z)$ and secondary path

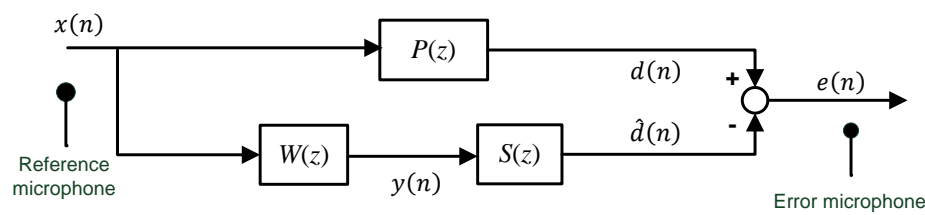


Figure 1.1. Feed-forward configuration of single channel ANC system

$S(z)$ (digital trigger of the speaker to the digital outcome of error sensor). In this configuration, noise controller is responsible for triggering the speaker by using the reference and error signals and design of noise controller is critical to the working of ANC systems.

Owing to the time varying nature of the environment and noise sources, noise controllers are updated online using adaptive algorithms to compensate for changes. Numerous adaptive algorithms have been designed so far for noise control filters in ANC systems, but least mean square (LMS) algorithm (Lopes *et al.* 2017, Aslam 2016, Lopes and Gerald 2015, Aslam and Raja 2015, Ahmed *et al.* 2013b, Liao and Lin 2007, Lin and Liao 2008, Eriksson and Allie 1989, Kuo and Vijayan 1997, Zhang *et al.* 2001, Zhang *et al.* 2003, Akhtar *et al.* 2006, Akhtar *et al.* 2007, Carini and Malatini 2008, Davari and Hassanpour 2009, Basin *et al.* 2011) and least squares (LS) algorithm (Bouchard 2002, Hong *et al.* 2007, Huffel *et al.* 2007, Söderström 2007, Reddy *et al.* 2011, Hong and Söderström 2009, Bouchard and Quednau 2000, Montazeri and Poshtan 2011, Söderström 2013) are the most celebrated ones to date. Conventional LS and LMS algorithms need to be modified to avoid convergence issues caused by $S(z)$ at the output of $W(z)$ (Kuo and Morgan 1996). Consequently, filtered-x variants were developed in which $x(n)$ is filtered through an estimated secondary path $\hat{S}(z)$ before being used as input for conventional adaptive algorithm (see Fig. 1.2). Filtered-x least mean square (FxLMS) algorithm is the most preferred variant due to its computational simplicity, unbiased convergence and robustness (Eriksson and Allie 1989, Kuo and Vijayan 1997, Zhang *et al.* 2001, Zhang *et al.* 2003, Diniz 2008).

The convergence speed and tracking capability of the LMS algorithm is degraded by the increase in eigen-spread of the input signal (Diniz 2008, Glentis *et al.* 1999). One possible solution is to use LS algorithm or LMS-Newton algorithm that have convergence and steady-state error properties significantly better than the LMS algorithm (Kuo and Morgan 1996). This solution, however, requires a relatively large number

purpose involves injection of auxiliary noise with LMS adaptive algorithm as shown in Fig. 1.2. Algorithms in (Eriksson and Allie 1989, Kuo and Vijayan 1997, Zhang *et al.* 2001, Akhtar *et al.* 2006, Aslam and Raja 2015) involve a continuous injection of fixed power auxiliary noise which results in a high level noise at the error microphone, while (Davari and Hassanpour 2009, Aslam 2016) also use similar approach but deactivate auxiliary noise in steady state. In (Zhang *et al.* 2003, Akhtar *et al.* 2007, Carini and Malatini 2008, Ahmed *et al.* 2013b, Lopes and Gerald 2015, Shi *et al.* 2013), different power variation strategies are designed for auxiliary noise to achieve superior convergence rate, online estimation and noise reduction. In (Carini and Malatini 2008, Ahmed *et al.* 2013b, Aslam and Raja 2015) variable step size strategies are also designed for fast convergence. Recently, a method is reported in (Lopes *et al.* 2017) that uses the reference signal and the controller output to model the secondary and primary paths, but is extremely unstable due to dependence on the frequency content of the reference signal. The LMS algorithm is used in all previous algorithms for its simplicity, small computations and ease of implementation. However, performance of the LMS algorithm degrades for signals with high correlation or speech signals (Glentis *et al.* 1999). Variable step size strategies are used by some methods to overcome these issues but this increases the number of tunable parameters and decreases robustness. Improvement in these properties is the highlight of this research project.

1.2.3 Acoustic Feedback Neutralization

In feedforward ANC systems, reflections of the sound generated by the speakers can propagate upstream and can be detected by the reference microphone. This undesired detection is the acoustic feedback from the secondary source to the reference microphone. This undesired acoustic feedback makes system unstable. The signal detected at the reference microphone includes the original reference signal $x(n)$ and the feedback signal $x_f(n)$ (see Fig. 1.3). The feedback signal $x_f(n)$ forms a closed loop which causes system instability if left unattended (Ahmed and Akhtar 2017, Ahmed *et al.* 2015, Ahmed *et al.* 2013a). The instability caused by acoustic feedback can be solved by use of directional speakers and reference microphones, or by electronic neutralization using a feedback compensation filter that also models the feedback path (from the loudspeaker to the reference sensor) (Kajikawa *et al.* 2012, Kuo and Morgan 1996). The latter approach has been explored by many researchers over the past few decades (Ahmed and Akhtar 2017, Ahmed *et al.* 2015, Ahmed *et al.* 2013a, Kuo 2002, Kuo and

1.2 Literature Review

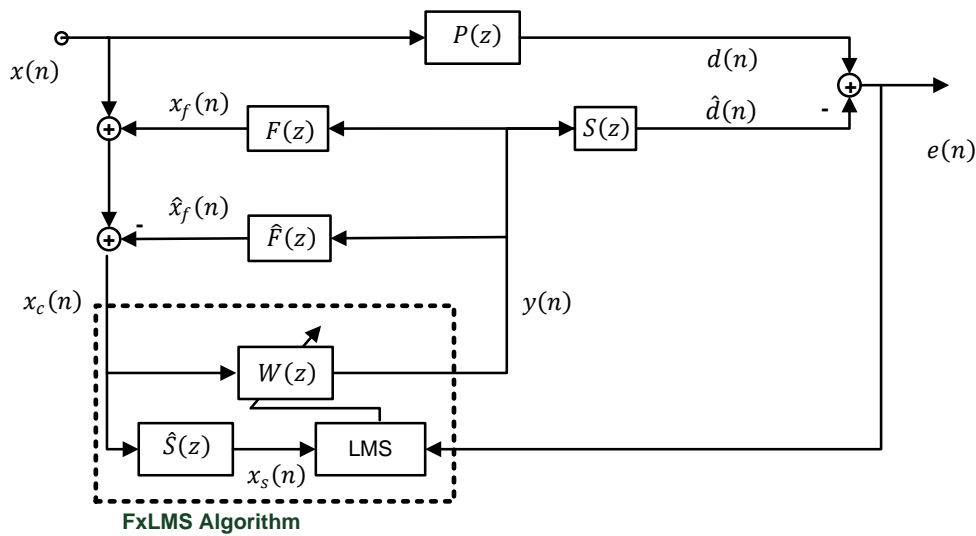


Figure 1.3. Feed-forward configuration of single channel ANC system with acoustic feedback.

Luan 1994, Egtesadi and Leventhall 1981, Eriksson 1987, Swinbanks 1973) and will be addressed in this project. In this approach, $x(n)$ is extracted from the signal detected at the reference microphone by compensation of feedback path $F(z)$ (digital trigger of the speaker to the digital outcome of reference sensor) by using the estimated feedback path $\hat{F}(z)$. A fixed feedback neutralization filter is introduced in (Warnaka *et al.* 1984) to remove the feedback interference. However, time-varying properties of the acoustic feedback limit the scope of this solution and necessitate the techniques involving online estimation and compensation of the feedback path (Ahmed and Akhtar 2017).

For online estimation, an auxiliary noise is introduced at the output of the control filter (Ahmed and Akhtar 2017, Ahmed *et al.* 2015, Ahmed *et al.* 2013a, Akhtar and Mitsuhashi 2011b, Kuo 2002). The method proposed in (Kuo 2002) use a constant power auxiliary noise and fixed step size parameters for feedback path compensation and noise control. However, the continuous injection of the auxiliary noise limits the robustness, convergence speed and the steady state performance. A variable step size is presented in (Akhtar and Mitsuhashi 2011b) for feedback path modeling filter which improves the convergence speed with some compromise in the steady state performance as the step size increases from small to large value with improvement in estimation accuracy. Additionally, lower and upper bounds for the step size of each feedback path estimation filter increase the tunable parameters. The methods in (Akhtar and Mitsuhashi 2011b, Kuo 2002) use a fixed power auxiliary noise that means its contribution in the residual error and reference signal stays through out the operation time. The power variation of auxiliary noise is highlighted in (Ahmed and

Akhtar 2017, Ahmed *et al.* 2015, Ahmed *et al.* 2013a) and gain scheduling is designed for varying the power of auxiliary noise in relation with estimation accuracy. In terms of step size parameter, the method in (Ahmed *et al.* 2013a) uses fixed step sizes for adaptive filters, while a variable step size scheme is introduced for the single channel ANC systems in (Ahmed *et al.* 2015) which is extended to the multi-channel systems in (Ahmed and Akhtar 2017). The gain variation scheme in (Ahmed and Akhtar 2017, Ahmed *et al.* 2015) is tuningless compared to (Ahmed *et al.* 2013a). Similar to (Akhtar and Mitsuhashi 2011b), the step size strategy of (Ahmed and Akhtar 2017, Ahmed *et al.* 2015) also increases from a small value at the start up to a large value in the steady state, which may lead to a large steady state error. The power variation schemes of (Ahmed and Akhtar 2017, Ahmed *et al.* 2015, Ahmed *et al.* 2013a) have a noteworthy contribution in the residual error from the auxiliary noise in the steady state, which is a disturbance for the noise control filter and result in performance deterioration. Methods presented in (Ahmed and Akhtar 2017, Ahmed *et al.* 2015, Ahmed *et al.* 2013a, Akhtar and Mitsuhashi 2011b, Kuo 2002) use a fixed step size in FxLMS algorithms for the noise control filter, which limits the robustness and convergence properties of the noise control filter. Hence, there is a gap to fill for adaptive control algorithm that can achieve fast convergence with minimum number of tunable parameters and computations. There is a scope for modeling a scheme that stops auxiliary noise after the convergence of modeling adaptive filter.

1.2.4 Hybrid Active Noise Control Systems for Disturbances

Hybrid ANC systems are used when reference signal is not available for all the primary noises detected at error microphone. These situation occurs when sensing or internal generation of completely coherent reference signal is not possible which include spatially incoherent turbulence noise, multi-source noise, noise from multiple propagation paths and induced resonance (Kuo and Vijayan 1997). In these situations, Hybrid ANC (Sun and Kuo 2007, Akhtar and Mitsuhashi 2011a, Mokhtarpour and Hassanpour 2012, Wu *et al.* 2015, Padhi *et al.* 2017) is most commonly used to compensate for the periodic disturbances. Algorithms in (Sun and Kuo 2007, Akhtar and Mitsuhashi 2011a, Wu *et al.* 2015) use fixed step size parameters which limits the convergence speed of these methods. Empirical formulas are presented for step size variation in (Mokhtarpour and Hassanpour 2012), which also include additional tunable

1.3 Motivation

parameters. The variable step size scheme of (Padhi *et al.* 2017) is based on the minimization of mis-alignment vector of the adaptive filters which requires an estimate of the disturbance signal variance. The variance of disturbance signal is not available directly and offline estimation is not useful for time varying disturbances.

In summary, various methods discussed in this section for different control configurations have margins of improvement in different performance measures which include convergence speed, steady state error, computational complexity, tracking ability and tunable parameters. This project is aimed at developing control algorithms with optimality in these performance measures.

1.3 Motivation

Extensive research is witnessed in the different configurations of ANC systems with commercial products launched in the last decade. The control algorithms developed so far excel in some performance measures but lag in others (performance measures include convergence speed, steady state error, computational complexity, tracking ability and tunable parameters). The use of efficient algorithms can help in reducing the processing needs in ANC applications which means reduction in the use of power and processing resources. Numerous algorithms have been reported for single channel and multi-channel feedforward ANC systems which use LMS algorithms for low computational cost, but these are poor performers for speech signals. So, such adaptive algorithms are in demand that converge at a fast rate to a small steady state error without any additional computational cost and tunability issues. These types of algorithms are the contribution of this research. Stable operation under disturbances of any kind is another contribution. Algorithms that perform under disturbances and mitigate these disturbances if they are correlated, are significant to the field of active noise cancellation. In various control configurations mentioned in the literature review, adaptive algorithms are updated even after reaching the convergence, which is not useful. Development of pro-active algorithms that perform frequent updates in the transition phase and fewer updates in the steady state, is the natural step in forward direction. The algorithms will be designed to improve the performance without any additional computations and this makes them suitable for higher order systems. The thesis is focused on designing control strategies that converge to small steady state error in reduced time with minimum computational effort and able to track the changes in

the properties of the environment or noise source. The reduction in number and simplicity of the associated tunable parameters is added advantage to simplify the use of designed adaptive algorithms in various scenarios.

1.4 Methodology

Most commonly used algorithms for parameter estimation are: Least square (LS) algorithm and least mean square (LMS) algorithm. LS algorithms are expensive in terms of computations and are not suitable for high order systems. LMS algorithms are simple, but perform poorly for highly correlated input signals. A number of methods can be adopted to achieve the objectives mentioned in previous section. One approach is to use data selective adaptive filtering based methods (Diniz 2008), like partial-update algorithms and set-membership algorithms, can be used to reduce the computational complexity of adaptive algorithms without any degrading effects on performance. Self-adapting step size strategies can be developed on the basis of the statistics of the observable data to make ANC system robust and easy to use in different scenarios. Use of pro-active step size variation can alleviate the convergence issues of LMS algorithms for speech signals and reduce the number of tunable parameters. Similarly, a self adapting variable forgetting factor can be derived from the statistics of measured data for LS algorithms. This can result in a fast convergence rate and small steady state error, which are not possible with a fixed forgetting factor. Also, LS algorithms with data selective filtering can result in reduced operations with high end noise reduction at a fast convergence rate. Further reduction in operations can be achieved by use of efficient implementations of the LS algorithms like array LS algorithms or fast recursive LS algorithms (Diniz 2008). The improved performance with reduced computational requirements shall make the proposed algorithms an equally preferred choice for lower and higher order ANC systems.

1.5 Contributions

Adaptive algorithms have been designed fore various configurations of ANC systems that gives optimal performance in terms of steady state noise reduction level, convergence speed, computational complexity, tracking and tunability. The contributions achieved are

- Selective updating least mean square algorithm and filtered-x LMS-Newton algorithm are designed for secondary path estimation and noise control filter in feed-forward active noise control systems. Variable thresholding mechanism is used to reduce computations while maintaining estimation accuracy and convergence speed.
- Power scheduling schemes designed for online secondary path estimation and acoustic feedback path estimation discontinue auxiliary noise injection after the convergence of the estimation filters. Therefore, contribution of auxiliary noise is negligible in the normal operation of ANC systems.
- The proposed variable threshold selective updating methods work in a pro-active manner to make designed methods suitable for devices where multiple applications are running simultaneously. At the system startup and in the transition phase, frequent coefficient updates are allowed while fewer coefficient updates are performed in the steady state.
- For narrowband disturbances at the error microphone, an optimal weighting factor is derived for robust performance of feedforward and feedback noise controllers. The designed method computes the weighting factor recursively and updates the noise controllers when there is new information in the current data to improve the noise reduction. Covariance matrices for noise control filters are guaranteed to be non-increasing and positive-definite to ensure a non-increasing and bounded error.
- For systems with acoustic feedback, self-adapting variable step sizes based adaptive algorithms are derived. Moreover, a tuningless power schedule is designed for auxiliary noise to vary the gain in relation to the predictor filter output. In the steady state, noise reduction performance is improved and computations are reduced by discontinuing the feedback compensation and predictor filters.
- A numerically stable filtered-x fast recursive least squares algorithm is derived using forward prediction only. Convergence analysis shows that the developed method can deliver improved convergence speed and tracking.
- A new control structure is designed to neutralize the acoustic feedback for narrowband noises. A frequency estimation algorithm is designed to predict the narrowband frequencies and generate the corresponding reference signals for

noise control filters. The designed control structure does not require acoustic feedback path estimation and therefore, offers improvement in noise reduction performance.

1.6 Thesis outline

Organisation of the thesis is as follows.

Chapter 2 presents the variable threshold based selective updating least mean square and filtered-x LMS-Newton algorithms designed for fast convergence and improved noise reduction irrespective. A robust schedule has been designed for auxiliary signal power to facilitate fast online estimation of secondary path with negligible contribution to residual noise in the steady state.

Chapter 3 derives the numerically stable filtered-x fast recursive least squares algorithm for noise control filter using forward prediction only. Convergence analysis has also been performed along with the computational comparisons.

Chapter 4 derives the optimal weighting factor for feed-forward and feedback noise controllers for ANC systems with narrowband disturbances at the error microphone. Detailed analysis has been provided for the various properties of the designed method.

Chapter 5 presents the derivation and analysis of the self-adapting variable step size normalized least mean square algorithms for acoustic feedback neutralization filter, predictor filter and noise control filter.

Chapter 6 provides the design of new control structure for ANC systems with acoustic feedback that does not require feedback path estimation. A frequency estimation algorithm has been implemented to internally generate the reference signals for noise control filters. Steady state properties of frequency estimation algorithm have also derived.

Chapter 7 provides the areas for further improvements along with possible methods for achieving the optimal performance.

Chapter 2

Variable Threshold-Based Selective Updating Algorithms in Feed-Forward Active Noise Control Systems

SELECTIVE updating based adaptive algorithms are introduced for secondary path estimation and noise control. A variable threshold mechanism is used for selective updating to reduce the computations of filtered-x LMS-Newton algorithm for noise control filter to allow quick convergence to small steady state error. A variable threshold based selective updating least mean square algorithm is proposed for secondary path estimation along with pro-active auxiliary noise variation scheme. The proposed variable threshold allows frequent updates in the transition phase and fewer updates in the steady state. Therefore reducing computations without deteriorating the performance as shown by comparison with established state-of-the-art methods in terms of estimation accuracy, steady-state residual error, convergence speed, number of tunable parameters and tracking capability.

Statement of Authorship

Title of Paper	Variable Threshold-Based Selective Updating Algorithms in Feed-Forward Active Noise Control Systems
Publication Status	Published
Publication Details	Muhammad Saeed Aslam, Peng Shi, Cheng-Chew Lim (2019). Variable Threshold-Based Selective Updating Algorithms in Feed-Forward Active Noise Control Systems, <i>IEEE Transactions on Circuits and Systems I: Regular Papers</i> , 66(2), pp. 782–795.

Principal Author

Name of Principal Author (Candidate)	Muhammad Saeed Aslam	
Contribution to the Paper	Designed the core idea and performed analysis on the concept, interpreted data, wrote manuscript and acted as corresponding author	
Overall percentage (%)	80%	
Certification:	This paper reports on original research I conducted during the period of my Higher Degree by Research candidature and is not subject to any obligations or contractual agreements with a third party that would constrain its inclusion in this thesis. I am the primary author of this paper.	
Signature	Date	8/11/2020

Co-Author Contributions

By signing the Statement of Authorship, each author certifies that:

- the candidate's stated contribution to the publication is accurate (as detailed above);
- permission is granted for the candidate to include the publication in the thesis; and
- the sum of all co-author contributions is equal to 100% less the candidate's stated contribution.

Name of Co-Author	Peng Shi	
Contribution to the Paper	Supervised development of work, helped in refining core concept and manuscript evaluation.	
Signature	Date	8 Nov 2020

Name of Co-Author	Cheng-Chew Lim	
Contribution to the Paper	Supervised development of work, helped in data interpretation and manuscript evaluation.	
Signature	Date	8/11/2020

Please cut and paste additional co-author panels here as required.

Variable Threshold-Based Selective Updating Algorithms in Feed-Forward Active Noise Control Systems

Muhammad Saeed Aslam^{ID}, Peng Shi^{ID}, *Fellow, IEEE*, and Cheng-Chew Lim^{ID}, *Senior Member, IEEE*

Abstract—Selective updating (SU)-based adaptive algorithms are proposed for secondary path estimation and noise control in active noise control systems. Use of the proposed variable threshold (VT) for noise control filter aids in reducing the computational complexity of filtered-x LMS-Newton algorithm to achieve fast convergence and improved noise reduction irrespective of the eigen-spread of input signal correlation matrix. A VT-SU least mean square algorithm is presented for the online estimation of the secondary path that reduces computational cost while maintaining estimation accuracy and convergence speed. A power scheduling scheme is presented that requires only one tunable parameter and discontinues auxiliary noise for power level below a predefined limit to reduce the residual error signal. The proposed VT-SU algorithms allow frequent updates in the transition phase and fewer updates in the steady state. Simulations are performed under benchmark conditions to validate the improved performance of the proposed method in comparison with established state-of-the-art methods in terms of estimation accuracy, steady-state residual error, convergence speed, number of tunable parameters, tracking capability, and computational complexity.

Index Terms—FxLMS-Newton, gain scheduling, active noise control, selective filtering, online secondary path estimation, parameter estimation.

I. INTRODUCTION

ACOUSTIC noise has become a critical issue with increase in use of mechanical and electronic devices for its adverse effects on stress levels, health and productivity. The methods adopted to mitigate acoustic noise are categorized as active and passive. Active noise control (ANC) is preferred for performance against low frequency noises by generating a cancelling noise with identical amplitude and opposite phase using a secondary source in a controlled manner [1]. Recently, it has gained popularity in commercial products like automobiles, headphones and mobile phones while numerous successful industrial applications are reported including aircraft cabin noise, magnetic resonance imaging scanner, incubators and

air conditioning ducts. A schematic of a basic ANC system is shown in Fig. 1, where a reference microphone is used to detect the reference signal $x(n)$ which passes through the primary path $P(z)$ to form the primary noise, $d(n)$. The noise controller $W(z)$ uses $x(n)$ to produce the trigger signal for speaker. The speaker is the secondary source used to produce the cancelling noise, $\hat{d}(n)$. The objective of ANC system is to adaptively update $W(z)$ such that $d(n)$ and $\hat{d}(n)$ have equal magnitude but opposite phase. The resultant signal is detected by an error microphone and is called residual error signal $e(n)$. Numerous variants of least mean square (LMS) algorithm [2]–[4] and least squares (LS) algorithm [5]–[7] algorithms are designed for noise control filters in ANC systems, but filtered-x LMS (FxLMS) algorithm is usually preferred for its computational simplicity, unbiased convergence and robustness [8]–[10]. The convergence speed and tracking capability of the LMS algorithm is primarily affected by eigen-spread of the input signal [11], [12]. LS algorithm or LMS-Newton algorithm offer superior convergence and steady-state error properties with increased computations [13]. Consequently, a proactive approach is presented in this paper for updating filter coefficients using LMS-Newton algorithm that alleviates the computational load without degrading the performance.

It can be seen in Fig. 1 that there is an estimate of secondary path, $\hat{S}(z)$, in the update path of $W(z)$ and adverse influence of an erroneous secondary path estimate on system performance is presented in [14]–[17]. Estimate of $S(z)$ is usually obtained by the auxiliary noise injection with LMS adaptive algorithm as shown in Fig. 1. Algorithms in [3], [8], [9], [18], and [19] use fixed power auxiliary noise which results in high level noise at the error microphone, while [2] and [20] also use a similar approach but deactivate auxiliary noise in the steady state. In [4], [10], and [21]–[24], different power variation strategies are designed for auxiliary noise to achieve superior convergence rate, online estimation and noise reduction. In [3], [4], and [23], variable step size strategies are also designed for fast convergence. Recently, the reference signal and the controller output are used to model the secondary and primary paths in [25]. This method has strong dependence on the frequency content of the reference signal [9]. In this paper, a data dependent updating mechanism and simplistic power variation strategy is devised for the efficient $S(z)$ estimation. The distinct contributions made in this paper are as follows

- 1) A variable threshold based selective updating LMS (VT-SULMS) algorithm is derived for obtaining $\hat{S}(z)$ online with following distinct properties

Manuscript received June 7, 2018; revised August 7, 2018; accepted August 23, 2018. Date of publication September 26, 2018; date of current version January 18, 2019. This work was supported in part by the National Nature Science Foundation of China under Grant 61773131 and Grant U1509217 and in part by the Australian Research Council under Grant DP170102644. This paper was recommended by Associate Editor H. R. Karimi. (Corresponding author: Muhammad Saeed Aslam.)

The authors are with the School of Electrical and Electronic Engineering, The University of Adelaide, Adelaide, SA 5005, Australia (e-mail: muhammad.aslam@adelaide.edu.au; peng.shi@adelaide.edu.au; cheng.lim@adelaide.edu.au).

Color versions of one or more of the figures in this paper are available online at <http://ieeexplore.ieee.org>.

Digital Object Identifier 10.1109/TCSI.2018.2868662

1549-8328 © 2018 IEEE. Personal use is permitted, but republication/redistribution requires IEEE permission.

See http://www.ieee.org/publications_standards/publications/rights/index.html for more information.

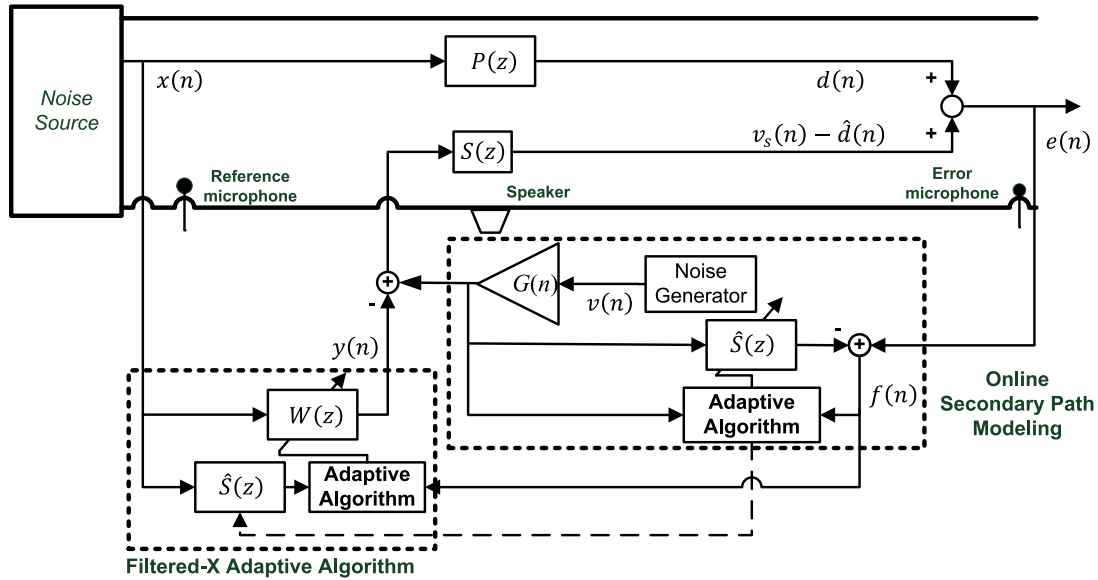


Fig. 1. Block diagram of the conventional feed-forward ANC systems.

- The computational requirements of the proposed algorithm are less demanding than the algorithms available in relevant literature while maintaining estimation accuracy that does not compromise the performance of noise controller.
 - It performs equally well in transient and steady state. Therefore, it requires the auxiliary noise injection for a small number of iterations.
 - It requires tuning of one parameter.
- 2) A scheme is formulated for the gain variation of auxiliary noise that takes into account the level of secondary path estimation. The important features of this scheme are
 - In this scheduling scheme, the noise injection is stopped when power falls below a minimum pre-defined limit. As a weak auxiliary noise signal is not contributing in secondary path estimation, then there is no significant advantage in injecting it and updating the estimation filter.
 - It has one tunable parameter which is a forgetting factor.
 - It improves the convergence speed for secondary path estimation and thus auxiliary noise is injected for small number of iterations.
 - It requires less computations compared to previous schemes and its impact accumulates as gain of auxiliary noise is continuously calculated.
 - It helps the system in maintaining stability in case of perturbations in acoustic paths.
 - 3) Variable threshold based filtered-x selective updating LMS-Newton (VT-FxSULMS-Newton) algorithm is derived for $W(z)$ to improve the noise reduction performance with significantly reduced computational requirements while maintaining fast convergence and small steady state error.

The comparative study of the proposed methods with their counterparts validate the supremacy for different ANC scenarios in terms of residual noise, estimation accuracy,

convergence speed, response to perturbations, computational complexity and number of tuning parameters.

The organization of upcoming sections is as follows: Section II describes the system model. VT-SULMS algorithm and variation of $G(n)$ for online estimation of $S(z)$ are derived in section III along with convergence analysis. Section IV derives a VT-FxSULMS-Newton algorithm for $W(z)$. Section V presents the computational requirements. Computer simulation results are analyzed in section VI followed by concluding remarks in section VII.

II. ANC SYSTEM MODEL

A schematic of the proposed methodology is given in Fig. 2. The objective is to reduce $e(n)$ by using the noise control filter $W(z)$ which has to model primary path $P(z)$ and inversely model secondary path $S(z)$ for optimal noise control filter [9]. The reference signal $x(n)$ and residual error signal $e(n)$ are detected by reference microphone and error microphone respectively. Primary signal, $d(n)$, can be written as

$$d(n) = p(n) * x(n), \quad (1)$$

where $*$ denotes linear convolution and $p(n)$ is the impulse response of primary path $P(z)$ at time n . The control signal, $y(n)$, is

$$y(n) = \mathbf{w}^T(n) \mathbf{x}_w(n), \quad (2)$$

where $\mathbf{w}(n)$ is the coefficient vector for $W(z)$

$$\mathbf{w}(n) = [w_0(n), w_1(n), \dots, w_{(L_w-1)}(n)]^T, \quad (3)$$

$$\mathbf{x}_w(n) = [x(n), x(n-1), \dots, x(n-(L_w-1))]^T, \quad (4)$$

and L_w is the length of $\mathbf{w}(n)$. A gain modulated auxiliary signal, $v_g(n)$, is added to the output of $W(z)$ for $S(z)$ estimation and is obtained by

$$v_g(n) = G(n)v(n), \quad (5)$$

where $G(n)$ is a variable gain function (discussed in section III) and $v(n)$ is a white noise sequence with zero mean

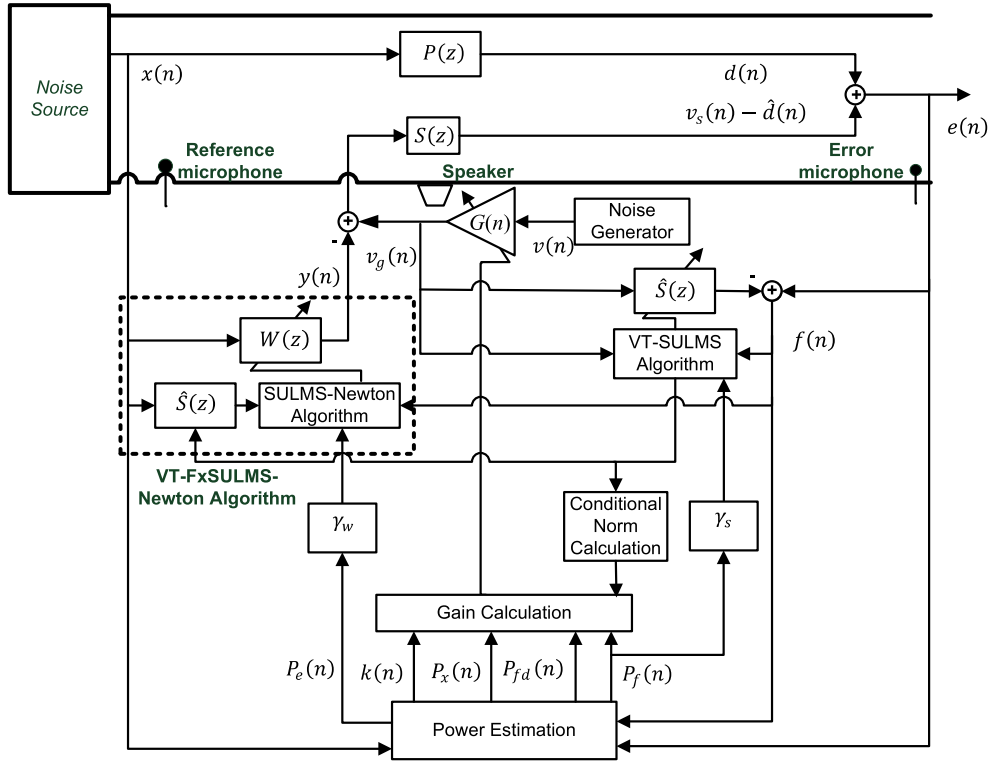


Fig. 2. Block diagram of the proposed method for feed-forward ANC systems.

and unit variance (uncorrelated with $x(n)$). The secondary cancellation signal comprises of $\hat{d}(n)$ and $v_s(n)$. The primary noise canceling signal $\hat{d}(n)$ is obtained by

$$\hat{d}(n) = s(n) * y(n), \quad (6)$$

and $v_s(n)$ can be given as

$$v_s(n) = s(n) * v_g(n), \quad (7)$$

where $s(n)$ is the impulse response of $S(z)$ at time n . The residual error signal, $e(n)$, can be given as

$$e(n) = d(n) - \hat{d}(n) + v_s(n). \quad (8)$$

The objective of the ANC system is to minimize the $e(n)$ signal through use of noise control filter $W(z)$. The adaptive algorithm used for updating the $W(z)$ requires the estimate of secondary path. Therefore, on-line estimation of secondary path using VT-SULMS algorithm will be addressed in the upcoming section, which is followed by the design of adaptive algorithm for $W(z)$.

III. VT-SULMS ALGORITHM FOR ONLINE SECONDARY PATH MODELING

The proposed VT-SULMS algorithm is based on the concepts of the set-membership filtering (SMF) [11], [26]–[29] which is based on a set consisting of coefficients that lead to absolute estimation errors falling below a prescribed threshold. SMF is focused on estimation of this set or its member [11]. The SU mechanism results in significant savings in computations and power since the coefficient updates are performed only for estimation error greater than the pre-defined threshold. This results in frequent updates during the early iterations

when errors are large, and fewer updates in the steady state. The power of the auxiliary signal, $v(n)$ is crucial for the convergence speed of secondary path modeling filter and noise control filter. Therefore, the power of $v(n)$, $G(n)$, should vary in relation with status of secondary path modeling and should become negligible in the steady state. VT-SULMS algorithm is presented in the following subsections along with a scheme to vary $G(n)$ and convergence analysis.

A. Threshold Based Selective Updating LMS Algorithm

This section derives the computationally efficient T-SULMS algorithm that updates the coefficient vector, $\hat{\mathbf{s}}(n)$, of $\hat{S}(z)$. Its output is given by

$$\hat{v}_s(n) = \hat{\mathbf{s}}^T(n) \mathbf{v}_g(n), \quad (9)$$

where

$$\hat{\mathbf{s}}(n) = [\hat{s}_0(n), \hat{s}_1(n), \dots, \hat{s}_{(L_s-1)}(n)]^T, \quad (10)$$

$$\mathbf{v}_g(n) = [v_g(n), v_g(n-1), \dots, v_g(n-(L_s-1))]^T. \quad (11)$$

The vectors $\mathbf{v}_g(n)$ and $\hat{\mathbf{s}}(n) \in \mathbb{R}^{L_s}$, where \mathbb{R} represents the set of real numbers. The estimation error, $f(n)$, can be written as

$$\begin{aligned} f(n) &= e(n) - \hat{v}_s(n) \\ &= e(n) - \hat{\mathbf{s}}^T(n) \mathbf{v}_g(n), \end{aligned} \quad (12)$$

where $\mathbf{v}_g(n)$ is the auxiliary input vector. The objective of the SU is to design $\hat{\mathbf{s}}(n)$ that upper bounds $|f(n)|$ by a prescribed threshold γ_s . There are several valid solutions of $\hat{\mathbf{s}}(n)$ for a properly chosen value of γ_s . For a set, \bar{S} , of all possible data pairs $\{\mathbf{v}_g(n), e(n)\}$, let feasibility set, $H(n)$, contains all vector $\hat{\mathbf{s}}(n)$ that have $|f(n)|$ upper bounded by γ_s

$$H(n) = \left\{ \hat{\mathbf{s}}(n) \in \mathbb{R}^{L_s} : |f(n)| \leq \gamma_s, \{\mathbf{v}_g(n), e(n)\} \in \bar{S} \right\}. \quad (13)$$

The goal of SMF is to adaptively find a member of $H(n)$. The simplest approach is to compute a filter using the information provided by the constraint set H_k . Assume $\hat{\mathbf{s}}(n)$ is trained with k data pairs $\{\mathbf{v}_g(i), e(i)\}$ for $i = 1, \dots, k$, then H_k denotes the set of all vectors $\hat{\mathbf{s}}(n)$ for which $|f(n)|$ is bounded by γ_s

$$H_k = \left\{ \hat{\mathbf{s}}(n) \in \mathbb{R}^{L_s} : \left| e(n) - \hat{\mathbf{s}}^T(n) \mathbf{v}_g(n) \right| \leq \gamma_s \right\}. \quad (14)$$

The key idea of the T-SULMS algorithm is to check the previous estimate $\hat{\mathbf{s}}(n)$ for existence outside the constraint set H_k . If $\left| e(n) - \hat{\mathbf{s}}^T(n) \mathbf{v}_g(n) \right| > \gamma_s$, the new estimate $\hat{\mathbf{s}}(n+1)$ will be obtained to bring error to the closest boundary of H_k . Orthogonal projection of $\hat{\mathbf{s}}(n)$ is used to obtain the update. NLMS algorithm for obtaining $\hat{\mathbf{s}}(n+1)$ is

$$\hat{\mathbf{s}}(n+1) = \hat{\mathbf{s}}(n) + \frac{\mu_s(n)}{\mathbf{v}_g^T(n) \mathbf{v}_g(n)} f(n) \mathbf{v}_g(n), \quad (15)$$

where $\mu_s(n)$ is the variable step size parameter. The update is obtained either if

$$f(n) = e(n) - \hat{\mathbf{s}}^T(n) \mathbf{v}_g(n) > \gamma_s, \quad (16)$$

or

$$f(n) = e(n) - \hat{\mathbf{s}}^T(n) \mathbf{v}_g(n) < -\gamma_s, \quad (17)$$

and the *a-posteriori* error can be given by

$$\begin{aligned} \epsilon(n) &= e(n) - \hat{\mathbf{s}}^T(n+1) \mathbf{v}_g(n) = \pm \gamma_s \\ &= e(n) - \hat{\mathbf{s}}^T(n) \mathbf{v}_g(n) - \frac{\mu_s(n)}{\mathbf{v}_g^T(n) \mathbf{v}_g(n)} f(n) \mathbf{v}_g^T(n) \mathbf{v}_g(n) \\ &= f(n) - \frac{\mu_s(n)}{\mathbf{v}_g^T(n) \mathbf{v}_g(n)} f(n) \mathbf{v}_g^T(n) \mathbf{v}_g(n), \end{aligned} \quad (18)$$

where $\epsilon(n)$ equals $\pm \gamma_s$ for updated coefficients. The equality obtained from (18) is

$$\epsilon(n) = e(n) [1 - \mu_s(n)] = \pm \gamma_s, \quad (19)$$

The above equation leads to

$$1 - \mu_s(n) = \pm \frac{\gamma_s}{f(n)}, \quad (20)$$

where (+) sign is applicable for $f(n) > 0$ and (−) sign applies for the case where $f(n) < 0$. Therefore, $\mu_s(n)$ can be written as

$$\begin{aligned} \mu_s(n) &= 1 - \frac{\gamma_s}{|f(n)|}, \text{ if } |f(n)| > \gamma_s \\ &= 0, \text{ otherwise} \end{aligned} \quad (21)$$

Now $G(n)$ in (5) is variable and can have a value close to 0 (explained in section III-C). This means that the normalizing term, $\mathbf{v}_g^T(n) \mathbf{v}_g(n)$, in (15) can become very small that can result in a very large update in $\hat{\mathbf{s}}(n+1)$. This large update may make $\hat{\mathbf{s}}(n+1)$ to become unstable. To avoid this, we use

$$\hat{\mathbf{s}}(n+1) = \hat{\mathbf{s}}(n) + \frac{\mu_s(n)}{\max(\mathbf{v}^T(n) \mathbf{v}(n), \mathbf{v}_g^T(n) \mathbf{v}_g(n))} f(n) \mathbf{v}_g(n), \quad (22)$$

where $\max(\cdot)$ means maximum of the values separated by commas and

$$\mathbf{v}(n) = [v(n), v(n-1), \dots, v(n-(L_s-1))]^T. \quad (23)$$

Use of $\max(\mathbf{v}^T(n) \mathbf{v}(n), \mathbf{v}_g^T(n) \mathbf{v}_g(n))$ in (22) does not require much computations as

$$\begin{aligned} \mathbf{v}^T(n+1) \mathbf{v}(n+1) &= \mathbf{v}^T(n) \mathbf{v}(n) - v^2(n - (L_s - 1)) + v^2(n+1). \end{aligned} \quad (24)$$

Similar implementation is also possible for $\mathbf{v}_g^T(n) \mathbf{v}_g(n)$. This completes the derivation of threshold based SULMS algorithm for secondary path modeling. A VT parameter, γ_s , is used in (21), and the scheme for its variation is presented in detail in the next section.

B. Variable Threshold Parameter $\gamma_s(n)$

It is crucial to choose a flexible $\gamma_s(n)$ to avoid over-bounding and under-bounding. This subsection proposes a variable $\gamma_s(n)$ that meets the conflicting demands of the transition phase and the steady state. Using (8) and (9), the error signal of expression (12) can be given by

$$f(n) = v_s(n) - \hat{v}_s(n) + f_w(n), \quad (25)$$

where $f_w(n)$ is disturbance for secondary path modeling and can be defined as

$$f_w(n) = d(n) - \hat{d}(n), \quad (26)$$

where $d(n)$ and $\hat{d}(n)$ are already defined using expressions (1) and (6). As a result, expression (8) becomes

$$e(n) = f_w(n) + v_s(n). \quad (27)$$

For the secondary path identification, the effect of under modeling and an estimate of the additional noise, $f_w(n)$, can be obtained from the estimation error signal $f(n)$ [11]. As auxiliary signal, $v_g(n)$, is a white noise, then the mean square error (MSE), $\xi_s = E[f^2(n)]$, can be calculated as

$$\xi_s = E \left\{ \left[\mathbf{s}^T(n) \mathbf{v}_g(n) - \hat{\mathbf{s}}^T(n) \mathbf{v}_g(n) \right]^2 + f_w^2(n) \right\}, \quad (28)$$

where $E[\cdot]$ denotes statistical expectation. Assume $v_g(n)$ is uncorrelated with the additional noise $f_w(n)$ which means that the expected value of the modeling filter and the unknown secondary path impulse response will coincide. Thus

$$\xi_s = E \left\{ \left[\mathbf{s}^T(n) \mathbf{v}_g(n) - \hat{\mathbf{s}}^T(n) \mathbf{v}_g(n) \right]^2 \right\} + \sigma_{f_w}^2, \quad (29)$$

where $\sigma_{f_w}^2(n)$ represents

$$\sigma_{f_w}^2(n) = E[f_w^2(n)]. \quad (30)$$

The VT parameter, $\gamma_s(n)$ can be written as

$$\gamma_s(n+1) = \alpha \gamma_s(n) + (1-\alpha) \sqrt{\beta_s \sigma_{f_w}^2(n)}, \quad (31)$$

where α and β_s are selected for an acceptable compromise between mis-adjustment and convergence rate. Now, $\sigma_{f_w}^2(n)$ is unknown as $f_w(n)$ is not a directly available signal. The estimate of $\sigma_{f_w}^2(n)$ can be obtained by

$$\hat{\sigma}_{f_w}^2(n+1) = \alpha \hat{\sigma}_{f_w}^2(n) + (1-\alpha) f^2(n), \quad (32)$$

and expression (31) becomes

$$\gamma_s(n+1) = \alpha \gamma_s(n) + (1-\alpha) \sqrt{\beta_s \hat{\sigma}_{f_w}^2(n)}. \quad (33)$$

TABLE I

VT-SULMS ALGORITHM FOR ONLINE SECONDARY PATH MODELING

VT-SULMS algorithm
Initialize: $\hat{\mathbf{s}}(0) = \mathbf{v}_g(0) = \mathbf{v}(0) = [0, 0, \dots, 0]^T$ $\hat{\sigma}_{f_w}^2(0) = \gamma_s(0) = 0, \alpha = 0.99$
Do for $n > 0$
{
Obtain $e(n)$ and $v(n)$
Update $\mathbf{v}_g(n)$ and $\mathbf{v}(n)$ (expressions (11) and (23))
$f(n) = e(n) - \hat{\mathbf{s}}^T(n)\mathbf{v}_g(n)$ (expression (12))
$\hat{\sigma}_{f_w}^2(n+1) = \alpha\hat{\sigma}_{f_w}^2(n) + (1-\alpha)f^2(n)$ (expression (32))
$\gamma_s(n+1) = \alpha\gamma_s(n) + (1-\alpha)\sqrt{\beta_s\hat{\sigma}_{f_w}^2(n)}$ (expression (33))
if ($ f(n) > \gamma_s$ and $G(n) > \varepsilon$) (expressions (21) and (22))
{
$\mu_s(n) = 1 - \frac{\gamma_s}{ f(n) }$
$\hat{\mathbf{s}}(n+1) = \hat{\mathbf{s}}(n) + \frac{\mu_s(n)}{\max(\mathbf{v}^T(n)\mathbf{v}(n), \mathbf{v}_g^T(n)\mathbf{v}_g(n))} f(n)\mathbf{v}_g(n)$
}
}

The proposed VT-SULMS algorithm is summarized in Table I. In (5) and (11), a variable gain $G(n)$ is used and the scheme for its variation is discussed in the next subsection.

C. Time-Varying Gain $G(n)$

A suitable time varying gain should have a large value when the estimation of the secondary path is poor and should decrease with improvement in estimation accuracy. In addition, the gain should be zero in steady state which means sufficient estimation accuracy is obtained to ensure the stable noise control performance. The signal $e(n)$ contains information required for estimation as well as noise cancellation. The sub-signal necessary for noise control is $f_w(n)$ given in (26) while $v_s(n)$ is necessary for secondary path estimation. Two important points worth mentioning here are

- Presence of $f_w(n)$ in $e(n)$ is a disturbance for $\hat{\mathbf{s}}(n)$ and $v_s(n)$ is a disturbance for $\mathbf{w}(n)$. So, continuous injection of $v(n)$ is not favourable towards noise cancellation.
- Under-modeling of secondary path may affect the performance of noise control filter due to its presence in update path. So, $v(n)$ of sufficient power should be introduced to achieve fast convergence of $\hat{\mathbf{s}}(n)$ which is desired for effective operation of $\mathbf{w}(n)$.

A time-varying gain of $v(n)$ is an effective approach to achieve these goals. Gain scheduling scheme in [23] aims at keeping $R(n)$ constant for all n

$$R(n) = \frac{\mathbb{E}[f_w^2(n)]}{\mathbb{E}[v_s^2(n)]}, \quad (34)$$

where $G(n)$ is

$$G(n) = \sqrt{\frac{P_e(n)}{(R+1)P_s(n)}}, \quad (35)$$

where

$$P_e(n) = \alpha P_e(n-1) + (1-\alpha)e^2(n), \quad (36)$$

$$P_s(n) = \alpha P_s(n-1) + (1-\alpha)\hat{\mathbf{s}}^T(n)\hat{\mathbf{s}}(n), \quad (37)$$

and $0.9 < \alpha < 1.0$. In [23], $R \equiv 1$, which means

$$\mathbb{E}[f_w^2(n)] = \mathbb{E}[v_s^2(n)], \quad (38)$$

is always satisfied, and $G(n)$ is proportional to $\sqrt{\mathbb{E}[f_w^2(n)]}$ at steady state for method in [23]. This makes an unnecessary contribution to $e(n)$. The proposed scheme utilizes an approach to terminate the auxiliary noise at steady state, reduce the number of tunable parameters and avoid redundant computations. When the accuracy of $\hat{\mathbf{s}}(n)$ is insufficient, like after initialization or after encountering a perturbation in the acoustic paths, then $P_f(n) > P_x(n)$ and

$$G(n) = \sqrt{\frac{P_f(n-1)}{\hat{\mathbf{s}}^T(n)\hat{\mathbf{s}}(n)}}, \quad (39)$$

where $P_f(n)$ and $P_x(n)$ are obtained using the following approximators

$$P_f(n) = \alpha P_f(n-1) + (1-\alpha)f^2(n), \quad (40)$$

$$P_x(n) = \alpha P_x(n-1) + (1-\alpha)x^2(n). \quad (41)$$

Rewriting equation (25) as

$$\begin{aligned} f(n) &= v_s(n) - \hat{v}_s(n) + f_w(n) \\ &= f_s(n) + f_w(n). \end{aligned} \quad (42)$$

Now, $P_f(n)$ can be given as

$$P_f(n) = P_{f_s}(n) + P_{f_w}(n), \quad (43)$$

where $P_{f_s}(n)$ is the power of $f_s(n)$ and $P_{f_w}(n)$ is the power of $f_w(n)$. When $\hat{\mathbf{s}}(n)$ is not close to $\hat{\mathbf{s}}(n)$, $G(n)$ will increase due to $P_{f_s}(n)$ in (43) to ensure fast convergence. Increase in accuracy of $\hat{\mathbf{s}}(n)$ reduces $P_{f_s}(n)$ in (43) and as a result $G(n)$ reduces. However, (39) can only reduce the gain to a level of $R(n) = 0$ dB. Consequently, a different scheme is used for conditions near the steady state, $P_f(n) \leq P_x(n)$

$$G(n) = \begin{cases} \sqrt{P_x(n)}, & \text{if } k(n) > P_x(n) \\ k(n), & \text{otherwise} \end{cases} \quad (44)$$

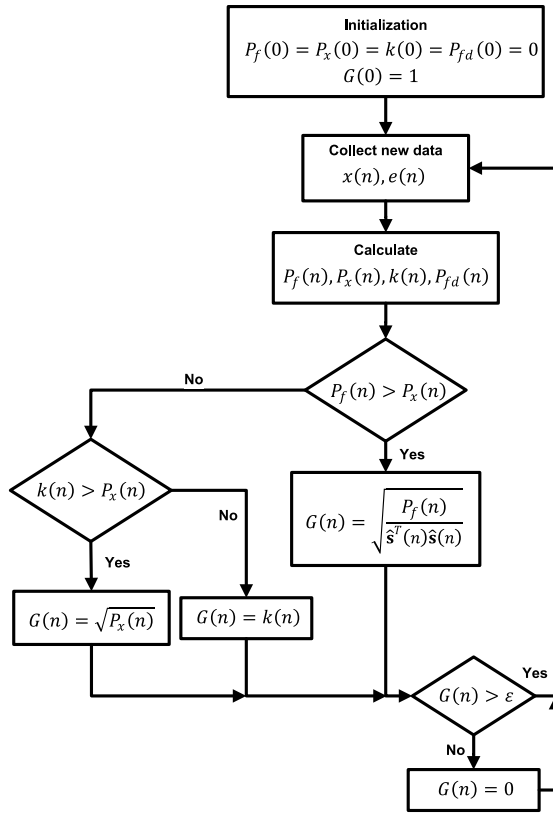
where

$$k(n) = \alpha k(n-1) + P_{f_d}^2(n), \quad (45)$$

and $P_{f_d}(n)$ is the estimate of $\mathbb{E}[f(n)f(n-1)]$, which results in a small gain in steady state

$$P_{f_d}(n) = \alpha P_{f_d}(n-1) + (1-\alpha)f(n)f(n-1). \quad (46)$$

Conditions in (44) keep $G(n)$ in check to avoid divergence of $\mathbf{w}(n)$ and maintain stable operation in the events like acoustic perturbation or uncorrelated interference at error sensor [4]. Lastly, a check is placed on $G(n)$ that if it falls below certain lower limit, ε , then substitute $G(n) = 0$. The reason is to avoid injection of auxiliary noise when it is not powerful enough to contribute in secondary path estimation. A reasonable choice for ε is an estimate of measurement noise at the reference or error microphone. Flow diagram for the selection of $G(n)$ is provided in Fig. 3. The proposed method for online secondary path modeling along with gain variation scheme is complete here, and the convergence analysis is presented in next subsection to highlight the stability of the proposed methodology.


 Fig. 3. Flow diagram for time varying gain $G(n)$.

D. Convergence of the Misalignment

This section presents the convergence analysis of $\hat{\mathbf{s}}(n)$. Define the misalignment vector at time n as

$$\mathbf{m}(n) = \mathbf{s}(n) - \hat{\mathbf{s}}(n). \quad (47)$$

Rewriting (22) in terms of the misalignment gives

$$\mathbf{m}(n+1) = \mathbf{m}(n) - \frac{\mu_s(n)}{L_s \sigma_{v_g}^2} f(n) \mathbf{v}_g(n), \quad (48)$$

where $\sigma_{v_g}^2$ is the auxiliary signal power and the approximation used is $\mathbf{v}_g^T(n) \mathbf{v}_g(n) = L_s \sigma_{v_g}^2 = L_s E\{v_g^2(n)\}$ for $L_s \gg 1$. Taking the l_2 norm and the mathematical expectation of (48) yields

$$\begin{aligned} E[\|\mathbf{m}(n+1)\|_2^2] &= E[\|\mathbf{m}(n)\|_2^2] \\ &\quad - \frac{2\mu_s(n)}{L_s \sigma_{v_g}^2} E[\mathbf{v}_g^T(n) \mathbf{m}(n) f(n)] \\ &\quad + \frac{\mu_s^2(n)}{L_s^2 \sigma_{v_g}^4} E[f^2(n) \mathbf{v}_g^T(n) \mathbf{v}_g(n)]. \end{aligned} \quad (49)$$

Using (7), (9) and (47) the modeling error signal from (25) can be written as

$$f(n) = \mathbf{v}_g^T(n) \mathbf{m}(n) + f_w(n). \quad (50)$$

For the second term on the right hand side of (49), take (50) into account and remove the uncorrelated product to obtain

$$\begin{aligned} E[\mathbf{v}_g^T(n) \mathbf{m}(n) f(n)] &= E[\mathbf{v}_g^T(n) \mathbf{m}(n) \mathbf{v}_g^T(n) \mathbf{m}(n)] \\ &= E[(\mathbf{v}_g^T(n) \mathbf{m}(n))^2]. \end{aligned} \quad (51)$$

Using independence and weakly-dependent assumptions [30], (51) can be written as

$$\begin{aligned} E[(\mathbf{v}_g^T(n) \mathbf{m}(n))^2] &= \text{tr}[E[\mathbf{m}^T(n) \mathbf{R}_{v_g v_g} \mathbf{m}(n)]] \\ &= E[\text{tr}[\mathbf{m}(n) \mathbf{m}^T(n) \mathbf{R}_{v_g v_g}]] \\ &= \text{tr}[E[\mathbf{m}(n) \mathbf{m}^T(n)] \mathbf{R}_{v_g v_g}], \end{aligned} \quad (52)$$

where $\mathbf{R}_{v_g v_g} = E[\mathbf{v}_g(n) \mathbf{v}_g^T(n)]$ and $\text{tr}[\cdot]$ denotes the trace of a matrix. Expectation and trace are linear operators and are exchanged in (52). The identity used in penultimate line of (52) is, $\text{tr}[\mathbf{A}\mathbf{B}] = \text{tr}[\mathbf{B}\mathbf{A}]$, where \mathbf{A} and \mathbf{B} are matrices of order $N \times M$ and $M \times N$ respectively. Two assumptions are considered at this point. The *a posteriori* misalignment, $\mathbf{m}(n)$, at n is uncorrelated with $v_g(n)$ at $n+1$ and the correlation matrix $E[\mathbf{m}(n) \mathbf{m}^T(n)]$ is close to a diagonal matrix. This is valid in the steady-state, since error of the individual coefficients become uncorrelated. Under these assumptions, (52) becomes

$$E[\mathbf{v}_g^T(n) \mathbf{m}(n) f(n)] = \sigma_{v_g}^2 E[\|\mathbf{m}(n)\|_2^2]. \quad (53)$$

For the last expectation term from (49), substitute (50) and remove uncorrelated terms to

$$\begin{aligned} E[f^2(n) \mathbf{v}_g^T(n) \mathbf{v}_g(n)] &= \text{tr}[E[f_w^2(n) \mathbf{v}_g^T(n) \mathbf{v}_g(n)]] \\ &\quad + E[\mathbf{v}_g(n) \mathbf{v}_g^T(n) \mathbf{m}(n) \mathbf{m}^T(n) \mathbf{v}_g(n) \mathbf{v}_g^T(n)]. \end{aligned} \quad (54)$$

Using the independence property of $\mathbf{v}_g(n)$ and $\mathbf{m}(n)$, the second expectation term on right side of (54) can be written as

$$\begin{aligned} E[\mathbf{v}_g(n) \mathbf{v}_g^T(n) \mathbf{m}(n) \mathbf{m}^T(n) \mathbf{v}_g(n) \mathbf{v}_g^T(n)] &= E[\mathbf{v}_g(n) \mathbf{v}_g^T(n) \mathbf{K}(n) \mathbf{v}_g(n) \mathbf{v}_g^T(n)], \end{aligned} \quad (55)$$

where $\mathbf{K}(n) = E[\mathbf{m}(n) \mathbf{m}^T(n)]$. Using the procedure of [30], expression (55) can be written as

$$\begin{aligned} E[\mathbf{v}_g(n) \mathbf{v}_g^T(n) \mathbf{K}(n) \mathbf{v}_g(n) \mathbf{v}_g^T(n)] &= \sigma_{v_g}^4 E[\|\mathbf{m}(n)\|_2^2] \mathbf{I}_{L_s} \\ &\quad + 2\sigma_{v_g}^4 E[\mathbf{m}(n) \mathbf{m}^T(n)], \end{aligned} \quad (56)$$

where \mathbf{I}_{L_s} is an identity matrix of order L_s . Substitute (56) in (54) results in

$$\begin{aligned} E[f^2(n) \mathbf{v}_g^T(n) \mathbf{v}_g(n)] &= \text{tr}[\sigma_{v_g}^4 E[\|\mathbf{m}(n)\|_2^2] \mathbf{I}_{L_s}] \\ &\quad + 2\sigma_{v_g}^4 E[\mathbf{m}(n) \mathbf{m}^T(n)] + L_s \sigma_{v_g}^2 \sigma_{f_w}^2 \\ &= (L_s + 2)\sigma_{v_g}^4 E[\|\mathbf{m}(n)\|_2^2] + L_s \sigma_{v_g}^2 \sigma_{f_w}^2, \end{aligned} \quad (57)$$

where $E[f_w^2(n)] = \sigma_{f_w}^2$, for all n . Substitute (53) and (57) in (49). Rearrange the resulting expression

$$\begin{aligned} E[\|\mathbf{m}(n+1)\|_2^2] &= g(\mu_s(n), L_s) E[\|\mathbf{m}(n)\|_2^2] \\ &\quad + h(\mu_s(n), L_s, \sigma_{v_g}^2, \sigma_{f_w}^2), \end{aligned} \quad (58)$$

where

$$g(\mu_s(n), L_s) = 1 - 2\frac{\mu_s(n)}{L_s} + \frac{(L_s + 2)\mu_s^2(n)}{L_s^2}, \quad (59)$$

$$h(\mu_s(n), L_s, \sigma_{v_g}^2, \sigma_{f_w}^2) = \frac{\mu_s^2(n)}{L_s \sigma_{v_g}^2} \sigma_{f_w}^2. \quad (60)$$

Expression (58) illustrates the relationship of misalignment with two distinct components: convergence rate and mis-adjustment. The term $g(\mu_s(n), L_s)$ influences the convergence rate of the algorithm. It depends on the normalized step size value $\mu_s(n)$ and the filter length L_s . The fastest convergence is obtained when $g(\mu_s(n), L_s)$ reaches its minimum. Taking $\mu_s(n)$ as the reference parameter, result obtained is

$$\mu_s(n) |_{FC} = \frac{L_s}{L_s + 2}, \quad (61)$$

where subscript FC is used to denote fast convergence. For long filters $L_s \gg 2$, the fastest convergence is possible for $\mu_s(n) \approx 1$, which is an established result [30], [31]. Let us evaluate the proposed $\mu_s(n)$ from (21) and $G(n)$ from (39). It is clear from (50) that $f(n)$ is greater than $f_w(n)$ for large estimation errors, $\mathbf{s}(n) - \hat{\mathbf{s}}(n)$. This occurs at the system start up or in case of perturbation in $\mathbf{s}(n)$. At this stage, $G(n)$ is large resulting in $f(n) \gg f_w(n)$. This makes $\mu_s(n) \approx 1$ from (21) which is required for fast convergence. Thus, the proposed method matches the desired functionality at the system start up and perturbation phases.

The stability condition can be expressed by the non-increasing nature of $E[\|\mathbf{m}(n+1)\|_2^2]$ in (58). The decreasing $E[\|\mathbf{m}(n+1)\|_2^2]$ can be obtained by getting $g(\mu_s(n), L_s)$ in (58) to be less than 1, which from (59) leads to

$$g(\mu_s(n), L_s) |_{\text{stable}} = \frac{2L_s}{L_s + 2}. \quad (62)$$

For $L_s \gg 2$, condition in (62) reduces to $\mu_s(n) |_{\text{stable}} < 2$. Applying this condition to $\mu_s(n)$ in (21) results in

$$\left[1 - \frac{\gamma_s(n)}{|f(n)|} \right] < 2. \quad (63)$$

This condition is always true since filter update is only performed when $|f(n)|$ is greater than $\gamma_s(n)$. The minimum value of $|f(n)|$ happens when $\mathbf{s}(n) \approx \hat{\mathbf{s}}(n)$ and this leads to $|f(n)| \approx \gamma_s(n)$, which means $\mu_s(n) \approx 0$. Moreover, the gain $G(n)$ switches to small value from expression (44). Similarly, when estimation error is large, $f(n) \gg \gamma_s(n)$, then $\mu_s(n) \approx 1$. It follows that the proposed $\mu_s(n)$ is always within the stability limit.

The term $h(\mu_s(n), L_s, \sigma_{v_g}^2, \sigma_{f_w}^2)$ in (58) influences the mis-adjustment of the proposed algorithm. As expected, the mis-adjustment decreases with decrease in $\sigma_{f_w}^2$ and increase in $\sigma_{v_g}^2$. The mis-adjustment is minimum when the function in (60) reaches its minimum. Take $\mu_s(n)$ as the reference parameter, the lowest mis-adjustment is obtained for $\mu_s(n) \approx 0$ [31]. The minimum mis-adjustment is a desirable property in the steady state and it is clear from (21) that $\mu_s(n) \approx 0$ and $\sigma_{v_g}^2$ also becomes small as $G(n)$ is set to a small value $k(n)$ as given in (44) in the steady state. Similarly, when modeling accuracy is poor then $\mu_s(n) \approx 1$ and $\sigma_{v_g}^2$ is large as $G(n)$ is set to a large value as given in (39). This limits the mis-adjustment and proves that the proposed algorithm provides the desired properties of fast convergence and small steady state error. This completes the discussion on the proposed secondary path modeling, and the next section is focused on the adaptive algorithm design for $W(z)$.

IV. VARIABLE THRESHOLD BASED FxSULMS-NEWTON ALGORITHM FOR NOISE CONTROL FILTER

This section introduces a variable threshold based filtered-x selective updating LMS-Newton (VTFxSULMS-Newton) algorithm which incorporates estimates of the second-order statistics with significant reduction in computations. The objective is to avoid the slow convergence of the LMS algorithm for highly correlated input signal [11], [12]. Estimated inverse of the input signal auto-correlation matrix is used for this improvement which results in a significant elevation in the computational requirements. Therefore, SU mechanism is proposed to reduce the computations by using a VT to allow frequent updates in transition state and fewer updates in steady state. Expressions for LMS-Newton algorithm can be written as [11]

$$\mathbf{w}(n+1) = \mathbf{w}(n) + 2\mu e(n)\hat{\mathbf{Q}}^{-1}(n)\hat{\mathbf{x}}_s(n), \quad (64)$$

where

$$\hat{\mathbf{Q}}^{-1}(n) = \frac{1}{1-\alpha} \left[\hat{\mathbf{Q}}^{-1}(n-1) - \frac{\psi(n)\psi^T(n)}{\frac{1-\alpha}{\alpha} + \hat{\mathbf{x}}_s^T(n)\psi(n)} \right], \quad (65)$$

$$\psi(n) = \hat{\mathbf{Q}}^{-1}(n-1)\hat{\mathbf{x}}_s(n), \quad (66)$$

and $0 < \alpha < 1$ is weighting factor, μ is a factor introduced to protect the algorithm from divergence resulting from the use of noisy estimates $\hat{\mathbf{Q}}(n)$ and $\hat{\mathbf{g}}_w(n)$ and

$$\hat{\mathbf{x}}_s(n) = [\hat{x}_s(n), \hat{x}_s(n-1), \dots, \hat{x}_s(n-(L_w-1))]^T, \quad (67)$$

$$\hat{x}_s(n) = \hat{s}(n) * x(n). \quad (68)$$

Computations required for (65) are significantly large and can be reduced by using a SU mechanism. A threshold based scheme is proposed for this purpose which means that coefficient vector for noise control is updated only when $|e(n)| > \gamma_w(n)$. It is crucial to choose a flexible $\gamma_w(n)$ as selecting a very large value will not allow sufficient filter updates, and updates without any improvement will occur for a small value. The proposed variable $\gamma_w(n)$ meets the conflicting demands of the transition phase and the steady state. For the noise control filter, the effect of under estimation and an estimate of the additional noise can be obtained from the $e(n)$ [11]. The MSE, $\xi_w = E[e^2(n)]$, can be calculated as

$$\xi_w = E \left\{ \left[d(n) - \mathbf{w}^T(n)\hat{\mathbf{x}}_s(n) \right]^2 + v_s^2(n) \right\}. \quad (69)$$

Assume $x(n)$ is uncorrelated with $v_s(n)$ which means that the expected value of the noise control filter will coincide with actual solution. Thus

$$\xi_w = E \left\{ d(n) - \mathbf{w}^T(n)\hat{\mathbf{x}}_s(n) \right\} + \sigma_{f_s}^2, \quad (70)$$

where $\sigma_{f_w}^2(n)$ represents

$$\sigma_{f_s}^2(n) = E[v_s^2(n)]. \quad (71)$$

The VT parameter, $\gamma_w(n)$ can be written as

$$\gamma_w(n+1) = \alpha\gamma_w(n) + (1-\alpha)\sqrt{\beta_w\sigma_{f_s}^2(n)}, \quad (72)$$

where α and β_w are selected for an acceptable compromise between mis-adjustment and convergence rate.

TABLE II
VARIABLE THRESHOLD BASED FILTERED-X SELECTIVE UPDATE
LMS-NEWTON ALGORITHM FOR NOISE CONTROL FILTER

VT-FxSULMS-Newton algorithm
Initialize:
$\mathbf{w}(0) = \hat{\mathbf{x}}_s(0) = [0, 0, \dots, 0]^T$
$\mathbf{x}(0) = [0, 0, \dots, 0]^T$
$\hat{\mathbf{Q}}^{-1}(0) = 10^{-6}\mathbf{I}$ (\mathbf{I} is identity matrix of dimensions $L_w \times L_w$)
$\sigma_e^2(0) = \gamma_w(0) = 0, \alpha = 0.99, 2\mu = 1 - \alpha$
Do for $n > 0$
{
Obtain $e(n)$ and $x(n)$
Update $\mathbf{x}(n)$
$\hat{x}_s(n) = \hat{\mathbf{s}}^T(n)\mathbf{x}(n)$ (expression (68))
Update $\hat{\mathbf{x}}_s(n) = [\hat{x}_s(n), \hat{x}_s(n-1), \dots, \hat{x}_s(n-(L_w-1))]^T$
$f(n) = e(n) - \hat{\mathbf{s}}^T(n)\mathbf{v}_g(n)$ (as calculated in secondary path modeling)
$\sigma_e^2(n+1) = \alpha\sigma_e^2(n) + (1-\alpha)e^2(n)$ (expression (73))
$\gamma_w(n+1) = \alpha\gamma_w(n) + (1-\alpha)\sqrt{\beta_w\sigma_e^2(n)}$ (expression (74))
if ($ e(n) > \gamma_w(n)$)
{
$\psi(n) = \hat{\mathbf{Q}}^{-1}(n-1)\hat{\mathbf{x}}_s(n)$ (expressions (66) and (65))
$\hat{\mathbf{Q}}^{-1}(n) = \frac{1}{1-\alpha} \left[\hat{\mathbf{Q}}^{-1}(n-1) - \frac{\psi(n)\psi^T(n)}{\frac{1-\alpha}{\alpha} + \hat{\mathbf{x}}_s^T(n)\psi(n)} \right]$
$\mathbf{w}(n+1) = \mathbf{w}(n) + 2\mu e(n)\psi(n)$ (expression (64))
}
}

Now, $\sigma_{f_s}^2(n)$ is unknown as $v_s(n)$ is not a directly available signal. The estimate of $\sigma_{f_s}^2(n)$ is

$$\hat{\sigma}_{f_s}^2(n+1) = \alpha\hat{\sigma}_{f_s}^2(n) + (1-\alpha)e^2(n), \quad (73)$$

and expression (72) becomes

$$\gamma_w(n+1) = \alpha\gamma_w(n) + (1-\alpha)\sqrt{\beta_w\hat{\sigma}_{f_s}^2(n)}. \quad (74)$$

Substitute $2\mu = 1 - \alpha$ in (65) and (64) to reduce the number of tunable parameters. Steps for implementation of VTFxSULMS-Newton algorithm are summarized in Table II.

V. COMPUTATIONAL COMPLEXITY

Comparison of the proposed and established methods in terms of computational complexity is presented in this section. Number of multiplications and additions is the figure of merit considered for comparison. Divisions are not considered here as the considered algorithms do not involve significant number of divisions. Table III lists the computational complexity for algorithms, where there are two entries in the case of [4] since it chooses between two functions to calculate the gain of auxiliary noise. Algorithms proposed in [4] and [20]–[23] use variants of LMS for secondary path modeling and noise controller to keep computations on a low level. In [2], noise controller is updated through LMS algorithm, but least squares algorithm is used for modeling purpose which is responsible for increase in computations. The proposed VT-SULMS and VT-FxSULMS-Newton algorithm use a proactive approach for updating filter coefficients that alleviates the computational load without any negative impact on the performance. Computations of VT-FxSULMS-Newton algorithm are calculated

TABLE III
COMPUTATIONAL REQUIREMENTS FOR ANC SYSTEMS
DICUSSED IN THIS PAPER

	Additions	Multiplications
Akhtar's method [22]	$3L_w + 4L_s + 4$	$3L_w + 4L_s + 13$
Carini's method [23]	$6L_w + 6L_s + 4D - 1$	$7L_w + 6L_s + 4D + 19$
Pooya's method [20]	$3L_w + 3L_s + 7$	$3L_w + 3L_s + 21$
Shakeel's method [4]		
$P_f(n) > P_x(n)$	$4L_w + 6L_s + 7$	$4L_w + 6L_s + 29$
$P_f(n) \leq P_x(n)$	$4L_w + 5L_s + 6$	$4L_w + 5L_s + 29$
Lopes's method [21]	$4L_w + 7L_s + 3$	$4L_w + 7L_s + 20$
Saeed's method [2]	$2L_t^2 + 3L_t + L_p + L_s + 2L_w$	$2L_t^2 + 5L_t + L_p + L_s + 2L_w + 3$
Proposed method		
state 1 ^a		
$P_f(n) > P_x(n)$	$L_w^2 + 3L_w + 4L_s + 9$	$L_w^2 + 5L_w + 4L_s + 21$
$P_f(n) \leq P_x(n)$	$L_w^2 + 3L_w + 3L_s + 10$	$L_w^2 + 5L_w + 3L_s + 21$
state 2 ^b	$L_w^2 + 3L_w + 2L_s + 5$	$L_w^2 + 5L_w + 2L_s + 18$
state 3 ^c		
$P_f(n) > P_x(n)$	$L_w + 4L_s + 9$	$L_w + 4L_s + 20$
$P_f(n) \leq P_x(n)$	$L_w + 3L_s + 10$	$L_w + 3L_s + 20$
state 4 ^d	$L_w + 2L_s + 5$	$L_w + 2L_s + 17$

^a state 1: Both $\hat{\mathbf{s}}(n)$ and $\mathbf{w}(n)$ are updated.

^b state 2: Only $\mathbf{w}(n)$ is updated.

^c state 3: Only $\hat{\mathbf{s}}(n)$ is updated.

^d state 4: No filter update.

for implementation scheme provided in [31]. There are four possible states for the proposed algorithm in terms of computations

- In state 1, both $\hat{\mathbf{s}}(n)$ and $\mathbf{w}(n)$ are being updated. There are two entries for this state as calculation of $\hat{\mathbf{s}}^T(n)\hat{\mathbf{s}}(n)$ is required in (39) only when $P_f(n) > P_x(n)$.
- Only $\mathbf{w}(n)$ is updated in state 2 which means $|f(n)| > \gamma_s$ is not satisfied. This reduces computations by stopping the evaluation of expressions (21) and (22). Furthermore, there is only one entry for this state as secondary path estimation filter is not getting updated, so there is no need to calculate $\hat{\mathbf{s}}^T(n)\hat{\mathbf{s}}(n)$ in (39) when $P_f(n) > P_x(n)$.
- Condition $|f(n)| > \gamma_s$ is valid and $|e(n)| > \gamma_w(n)$ is invalid. Therefore, VT-SULMS algorithm is updating $\hat{\mathbf{s}}(n)$ in state 3. Once again there are two entries in this state due to the occurrence of $\hat{\mathbf{s}}^T(n)\hat{\mathbf{s}}(n)$ in (39) when $P_f(n) > P_x(n)$. The entries in this state are less than the methods in [4] and [20]–[23] due to VT-FxSULMS-Newton algorithm being inactive. This means computationally expensive expressions (65) and (64) are not executed.
- Adaptive algorithms for both $\hat{\mathbf{s}}(n)$ and $\mathbf{w}(n)$ are inactive in state 4. This state also has a single entry and requires least number of multiplications and additions.

The computations in the proposed algorithm switch between these four states. At start up and during perturbations, computations switch to high end while the proposed method

TABLE IV
PARAMETERS VALUES USED IN SIMULATIONS

	Parameters
Akhtar's method [22]	$\mu_w = 5 \times 10^{-4}, \mu_{smax} = 1 \times 10^{-2}, \mu_{smin} = 1 \times 10^{-3}, \lambda = 0.99, \sigma_{max}^2 = 1, \sigma_{min}^2 = 1 \times 10^{-3}$
Carini's method [23]	$D = 8, \mu_{smin} = 4 \times 10^{-3}, \lambda = 0.99, \hat{\lambda} = 0.6, R(n) = 1$
Pooya's method [20]	$\mu_w = 12 \times 10^{-4}, \mu_{smax} = 5 \times 10^{-2}, \mu_{smin} = 9 \times 10^{-3}, \lambda = 0.99, \alpha = 3.28 \times 10^{-5}, \gamma = 0.999$
Shakeel's method [4]	$\mu_1 = 3 \times 10^{-1}, \mu_2 = 8 \times 10^{-2}, \lambda = 0.99, \alpha = 0.997, \gamma_{max} = 0.9, \gamma_{min} = 0.3$
Lopes's method [21]	$\mu = 0.5, \mu_s = 0.5, \lambda = 0.9, k_r = 0.1, \beta = 40, A = 2$
Saeed's method [2]	$\mu_w = 1 \times 10^{-4}, \lambda = 0.99$
Proposed method	$\alpha = 0.99, \beta_w = 4.5, \beta_s = 1.4$

requires least computations in the steady state by proactive use of VT-SU scheme. Alternate forms of the LMS-Newton algorithm like fast traversal filters [11] can also be explored with selective updating mechanism for superior convergence and steady state error performance with significantly reduced computational requirements.

VI. CASE STUDIES

In this section, the performance of the proposed algorithm is demonstrated by conducting simulations under standard conditions. The performance is compared with Akhtar *et al.* (AM) [22], Carini (CM) and Malatini [23], Davari (DM) and Hassanpour [20], Ahmed *et al.* [4], Lopes (LM) and Gerald [21] and Saeed's method (SaM) [2] in terms of secondary path identification error

$$\Delta S(n) = 10 \log_{10} \left(\frac{\|s(n) - \hat{s}(n)\|^2}{\|s(n)\|^2} \right), \quad (75)$$

MSE at the error microphone $E[e^2(n)]$, convergence speed, number of tunable parameters and computational complexity. Recently, an overall modeling based technique is also presented in [25]. Its results are not included for strong dependence on the frequency content of the reference signal. The values used for various parameters are provided in Table IV while sampling frequency is kept at 2 kHz and $v(n)$ is a zero mean white noise of unit variance. The parameter α in the proposed method is the forgetting factor and value used for it is same as used in the previous methods. Primary and secondary paths are obtained from experimental data provided in [13]. For all cases, $W(z)$ remains in inactive state for the first 5000 iterations to ensure stable operation [2], [4]. Also, simulation results are obtained by averaging over 20 runs.

A. Case 1

In this case, reference signal is formed by the mixture of two types of signals: multi-tonal and broadband signals. Multi-tonal noise is produced by machines like fans, generators and compressors [2], [20] while broadband noise occur in ducts [13]. Multi-tonal part is formed by combining sinusoids of frequencies: 100, 200, 300, and 400 Hz and adjusting the

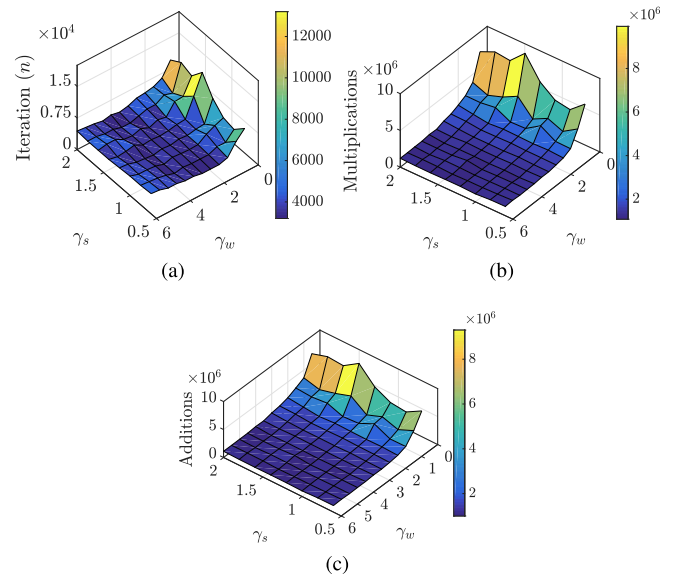


Fig. 4. Surfaces against tuning parameters for: (a) Iteration (n). (b) Multiplications. (c) Additions.

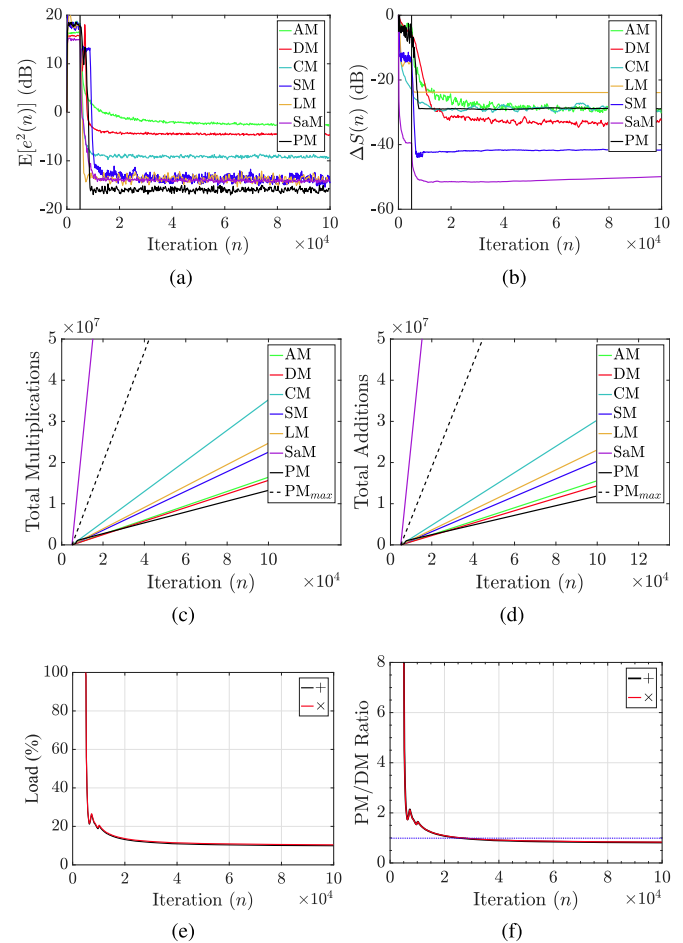


Fig. 5. Performance results for Case 1: (a) The mean-squared error (dB). (b) The relative modeling error (dB). (c) Total multiplications at n . (d) Total additions at n . (e) Load percentage (f) PM/DM ratio.

variance to 2.0. For broadband part, a bandpass filter with 250-500 Hz passband is used to filter a zero mean white Gaussian noise with variance 2.0. Finally, Gaussian noise is mixed to achieve a SNR of 30 dB. The range tested for tunable

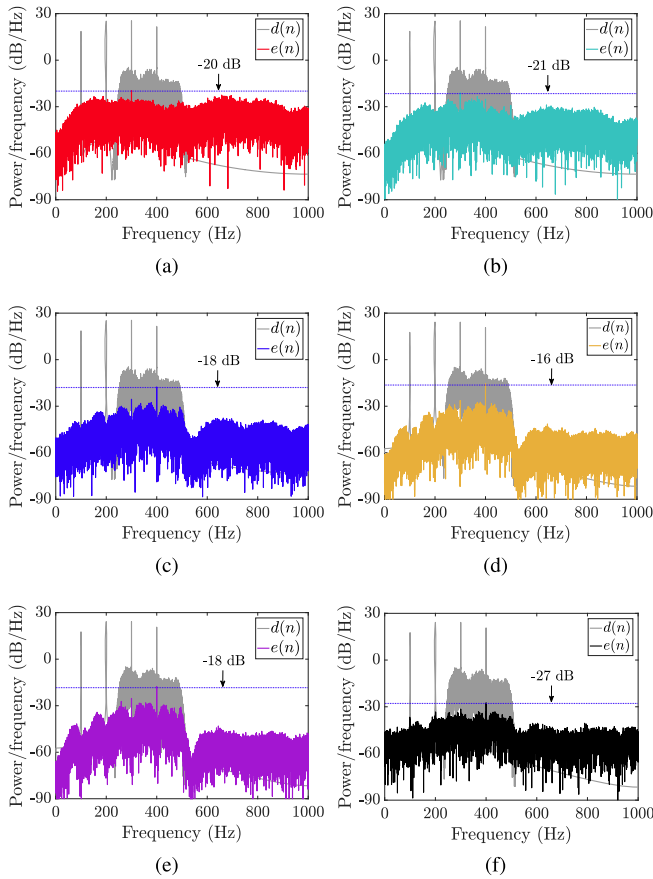


Fig. 6. Power spectra of the primary noise, $d(n)$, and residual noise, $e(n)$, in Case 1. (a) DM. (b) CM. (c) SM. (d) LM. (e) SaM. (f) PM.

parameters is $0.5 \leq \beta_w \leq 6.0$ and $0.6 \leq \beta_s \leq 2.0$. This range ensures convergence with performance similar to when adaptive filters are allowed to update at each iteration. The plots of iterations, total multiplications and total additions at convergence are shown in Fig. 4 for the same level of modeling accuracy and noise reduction. Some observations regarding this figure are

- For $\beta_s > 1.4$ and any value of β_w , iterations required for convergence start to increase (see Fig. 4(a)). This means that updates are happening less frequently than desired and result in rise in iterations to reach steady state despite small numbers of computations (Fig. 4(b) and (c)). Similar behavior is visible for $\beta_w > 4.5$ and any value of β_s .
- Fast convergence with minimum computations is a desirable and difficult task. Suitable range for parameters is: $2.0 \leq \beta_w \leq 4.5$ and $0.6 \leq \beta_s \leq 1.4$.

Simulation results with parameter values provided in Table IV are presented in Fig. 5. The proposed algorithm converges in 3800 iterations and there is an improvement of about 2.5 dB in steady state value of $E[e^2(n)]$ with a modeling error of -30 dB. Fig. 5 (c) and (d) demonstrate total computations performed up to n iterations. In terms of computations, the proposed method is least expensive requiring at least 16% less computations than the previous methods at $n = 95000$. PM_{max} in Fig. 5 (c) and (d) represents the computations required if the proposed algorithm is allowed to update at each iteration.

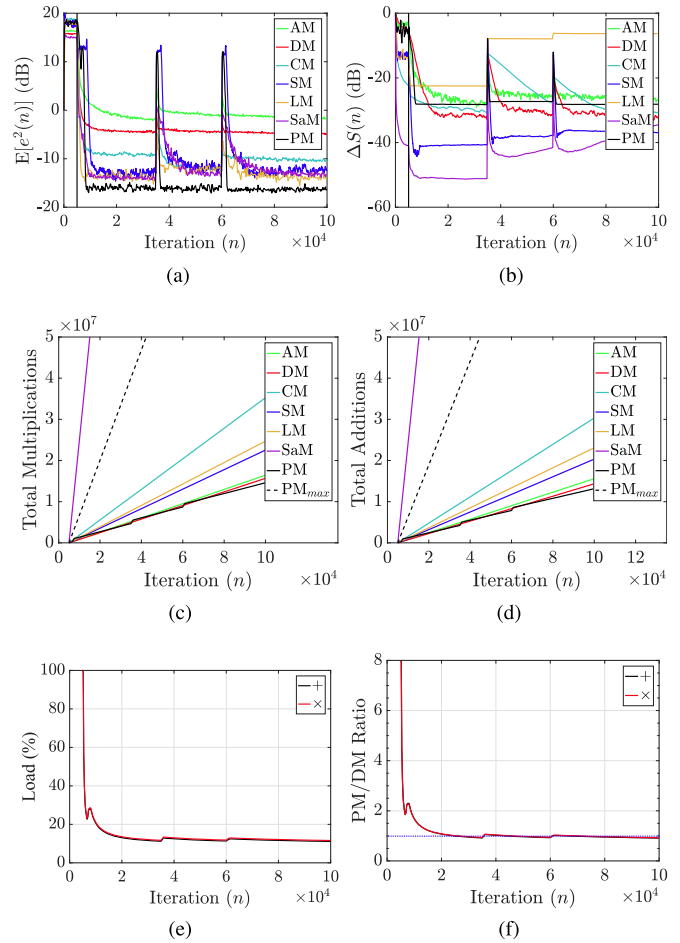


Fig. 7. Performance results for Case 2: (a) The mean-squared error (dB). (b) The relative modeling error (dB). (c) Total multiplications at n . (d) Total additions at n . (e) Load percentage. (f) PM/DM ratio.

Comparing PM_{max} with PM shows that proposed VT scheme has reduced computational cost to less than 50% in first 350 iterations and less than 11% in 45000 iterations (see Fig. 5(e)). Since there are two VT parameters, the individual savings can be achieved for SULMS and Fx-SULMS-Newton algorithm. The second least expensive method in terms of computations is DM. Therefore, ratios of computations between PM and DM are presented in Fig. 5(f) and computations of both become equal in 21500 iterations and the blue line corresponds to ratio equal to 1. For $n > 21500$, PM requires less computations than previous methods and by $n = 95000$ it saves at least 17% computational cost as compared to previous methods. The desired functionality of ANC system is to reduce $e(n)$ in reduced iterations with minimum computations. The proposed method has shown improvement in all desirable areas. Moreover, power spectra of the primary noise, $d(n)$, and residual noise, $e(n)$, are shown in Fig. 6 to compare the behavior of the proposed method with established methods.

B. Case 2

This case addresses the situation of perturbation in both primary and secondary paths during operation with reference signal of case 1. This perturbation in acoustic paths is modeled

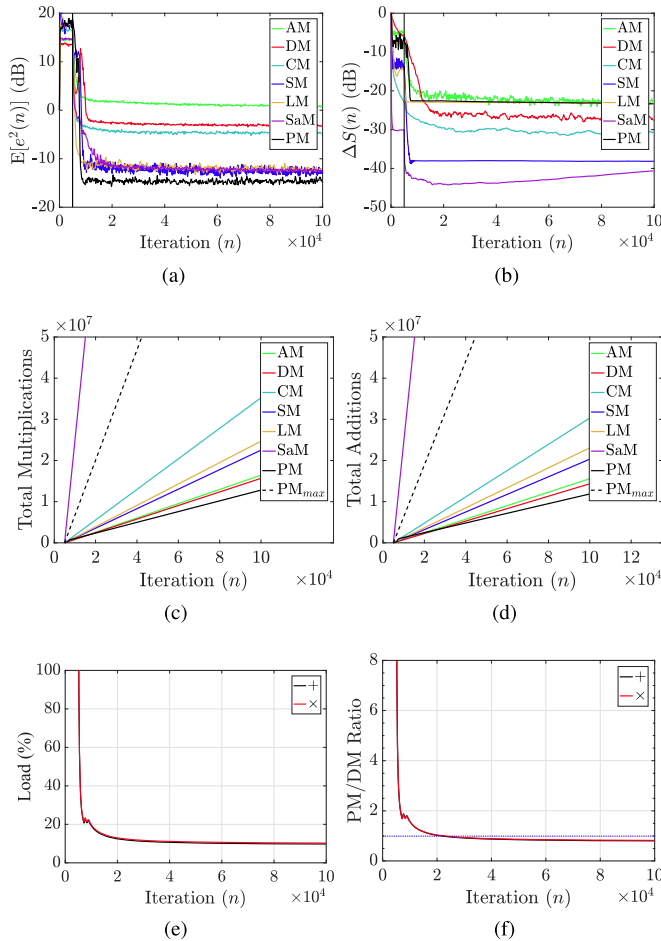


Fig. 8. Performance results for Case 3: (a) The mean-squared error (dB). (b) The relative modeling error (dB). (c) Total multiplications at n . (d) Total additions at n . (e) Load percentage. (f) PM/DM ratio.

by

$$\begin{aligned} \mathbf{s}(n+1) &= 0.9\mathbf{s}(n) + 0.1R_1(n), \\ \mathbf{p}(n+1) &= 0.9\mathbf{p}(n) + 0.1R_2(n), \end{aligned}$$

where $R_1(n)$ and $R_2(n)$ are random vectors. The perturbations are introduced at $n = 35000$ and $n = 60000$. Simulation results are provided in Fig. 7. The proposed algorithm shows improvement in convergence speed and steady state value of $E[e^2(n)]$ (at least 2.5 dB) while maintaining a steady state modeling error of -30 dB. The proposed method achieves noise reduction level of -16 dB while previous methods reach the steady state value of -13.5 dB. In case of acoustic changes, the noise reduction performance of the proposed method is consistent in terms of convergence speed as well as the steady state error (see Fig. 7(a)). As expected, there are small jumps at perturbation instants in the plots for multiplications and additions, still the proposed method achieves low computational cost owing to a flexible VT scheme (see Fig. 7(c) and (d)). Comparing PM_{max} with PM shows that computational cost reduces to half in first 350 iterations and decimates in next 50000 iterations (see Fig. 7(e)). There is an increase of less than 2% due to perturbations in acoustic paths. Ratios of computations between PM and second least expensive method, DM, are presented in Fig. 7(f). The first

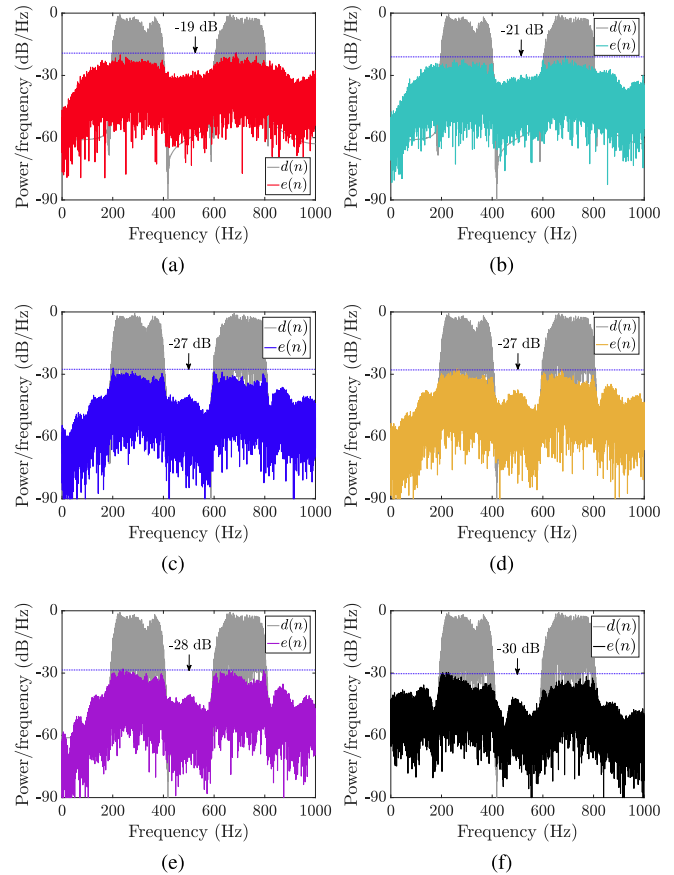


Fig. 9. Power spectra of the primary noise, $d(n)$, and residual noise, $e(n)$, in Case 3. (a) DM. (b) CM. (c) SM. (d) LM. (e) SaM. (f) PM.

perturbation causes a rise from 0.95 to 1.07 and second one produces fluctuation from 0.95 to 1.03. The proposed method still achieves a ratio of 0.92 at $n = 95000$. This means at least 8% less computations even in the presence of acoustic perturbations. The proposed VT scheme works efficiently by allowing frequent updates during perturbations and fewer updates in the steady state without compromising the noise reduction performance highlights the superior performance and robustness of the proposed method.

C. Case 3

Broad-band signal used in this case is formed by addition of signals obtained by filtering a zero mean Gaussian noise with variance 5.0 through two bandpass filters with passbands: 200-400 Hz and 600-800 Hz. Finally, Gaussian noise is mixed to achieve a SNR of 30 dB. Performance results are presented in Fig. 8. The proposed method converges in 4000 iterations to a steady state value of -15 dB which is an improvement of at least 3 dB from previous methods. The computational requirements of various methods are presented in Fig. 8 (c) and (d). The proposed method requires reduced operations with improved noise reduction performance which is a significant improvement. Proactive use of VT in the proposed method is evident from comparison with PM_{max} in Fig. 8(e). The VT parameters allowed frequent updates in the transition phase and fewer updates in the steady state. Ratios of computations between PM and DM in Fig. 8(f) demonstrate a pattern similar to first two cases.

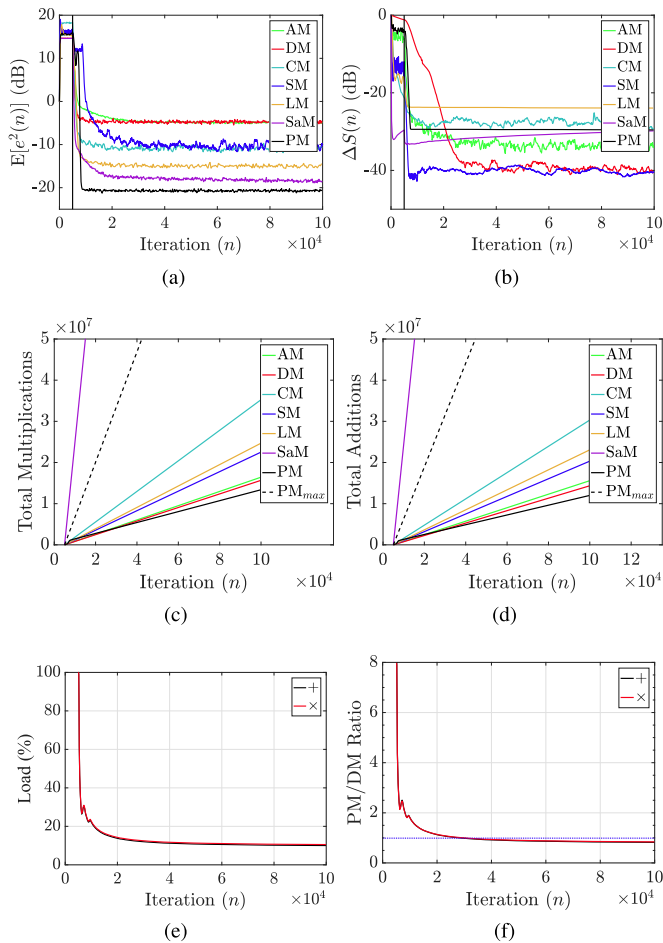


Fig. 10. Performance results for Case 4: (a) The mean-squared error (dB). (b) The relative modeling error (dB). (c) Total multiplications at n . (d) Total additions at n . (e) Load percentage. (f) PM/DM ratio.

Thereby, saving a minimum of 18% computations after 100000 iterations. The computational savings become more prominent with the increase in the iterations which is a preferable characteristic for long term operation. Power spectra for various methods is provided in Fig. 9 for further analysis.

D. Case 4

Tonal signals with frequencies from 100 to 200 Hz with a 20 Hz step are combined and the variance of resulting signal is adjusted to 2.0 to form the reference signal. Also, SNR of 30 dB is achieved by adding Gaussian noise. The simulation results are shown in Fig. 10. The proposed VT-FxSULMS-Newton algorithm converges in 3600 iterations to a steady state value of -21 dB and there is an improvement of about 2.5 dB in steady state value of $E[e^2(n)]$ with a modeling error of -30 dB. The convergence speed of the proposed method is prominent in comparison with previous methods. Fig. 10 (c) and (d) demonstrate total computations performed up to n iterations. In terms of computations, the proposed method is least expensive requiring at least 16% less computations compared to the previous methods at $n = 95000$ (see Fig. 10(f)). Influence of the proposed VT parameters is evident from the noise reduction performance and computational efficiency. The proposed VT scheme allowed frequent updates

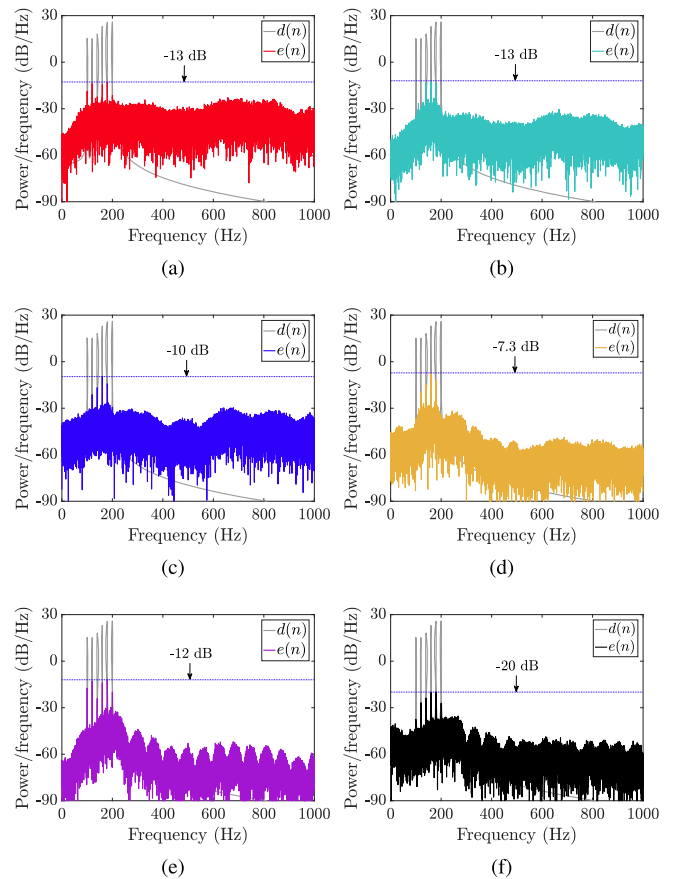


Fig. 11. Power spectra of the primary noise, $d(n)$, and residual noise, $e(n)$, in Case 4. (a) DM. (b) CM. (c) SM. (d) LM. (e) SaM. (f) PM.

in the transition phase and fewer updates in the steady state. The least operations in the steady state without sacrificing the noise reduction performance mark the improvement achieved by the proposed algorithm. Power spectra for methods under discussion are presented in Fig. 11 and the proposed method shows noteworthy improvement.

VII. CONCLUSIONS

This paper introduces two computationally efficient VT schemes for SU based adaptive algorithms used in secondary path estimation and noise control. The proposed VT-FxSULMS-Newton algorithm for noise control filter provides balance between fast convergence and reduced computations while providing improved steady state performance and tracking that is independent of eigen-spread of input signal correlation matrix, which is the cause of deterioration in the performance of LMS based algorithms. In addition, a gain variation method is presented for auxiliary noise that responds effectively to the acoustic changes with reduced number of tunable parameters. The proposed method improves the mean square error by more than 2.5 dB for multi-tonal, broadband and mixed type noise. Similarly, the computational cost of VT-SULMS adaptive algorithm and VT-FxSULMS-Newton algorithm is less than the previous methods by significant margin due to efficient use of separate VT parameter designed for secondary path estimation filter and noise control filter. Computational savings are more than 10% after 100000 iterations

even with acoustic changes. These savings increase in long term operational conditions. In addition, there are only three tunable parameters for the proposed algorithm. Hence, improvements achieved in convergence rate, steady state mean square error, computational cost, tracking ability and number of tunable parameters highlight the contributions of the proposed method. The use of fuzzy control [32], [33] and finite frequency properties [34] may be good alternative to be exploited in future for better performance.

REFERENCES

- [1] P. Lueg, "Process of silencing sound oscillations," U.S. Patent 2043416 A, Jan. 9, 1936.
- [2] M. S. Aslam, "Maximum likelihood least squares identification method for active noise control systems with autoregressive moving average noise," *Automatica*, vol. 69, pp. 1–11, Jul. 2016.
- [3] M. S. Aslam and M. A. Z. Raja, "A new adaptive strategy to improve online secondary path modeling in active noise control systems using fractional signal processing approach," *Signal Process.*, vol. 107, pp. 433–443, Feb. 2015.
- [4] S. Ahmed, M. T. Akhtar, and X. Zhang, "Robust auxiliary-noise-power scheduling in active noise control systems with online secondary path modeling," *IEEE/ACM Trans. Audio, Speech, Language Process.*, vol. 21, no. 4, pp. 749–761, Apr. 2013.
- [5] M. Bouchard, "Numerically stable fast convergence least-squares algorithms for multichannel active sound cancellation systems and sound deconvolution systems," *Signal Process.*, vol. 82, no. 5, pp. 721–736, 2002.
- [6] M. R. Reddy, I. M. S. Panahi, and R. Briggs, "Hybrid FxRLS-FxNLMS adaptive algorithm for active noise control in fMRI application," *IEEE Trans. Control Syst. Technol.*, vol. 19, no. 2, pp. 474–480, Mar. 2011.
- [7] A. Montazeri and J. Poshtan, "A new adaptive recursive RLS-based fast-array IIR filter for active noise and vibration control systems," *Signal Process.*, vol. 91, no. 1, pp. 98–113, 2011.
- [8] L. J. Eriksson and M. C. Allie, "Use of random noise for on-line transducer modeling in an adaptive active attenuation system," *J. Acoust. Soc. Amer.*, vol. 85, no. 2, pp. 797–802, 1989.
- [9] S. M. Kuo and D. Vijayan, "A secondary path modeling technique for active noise control systems," *IEEE Trans. Speech Audio Process.*, vol. 5, no. 4, pp. 374–377, Jul. 1997.
- [10] M. Zhang, H. Lan, and W. Ser, "A robust online secondary path modeling method with auxiliary noise power scheduling strategy and norm constraint manipulation," *IEEE Trans. Speech Audio Process.*, vol. 11, no. 1, pp. 45–53, Jan. 2003.
- [11] P. S. R. Diniz, *Adaptive Filtering: Algorithms and Practical Implementation*. New York, NY, USA: Springer, 2008.
- [12] G.-O. Glentis, K. Berberidis, and S. Theodoridis, "Efficient least squares adaptive algorithms for FIR transversal filtering," *IEEE Signal Process. Mag.*, vol. 16, no. 4, pp. 13–41, Jul. 1999.
- [13] S. M. Kuo and D. R. Morgan, *Active Noise Control Systems: Algorithms and DSP Implementations*. New York, NY, USA: Wiley, 1996.
- [14] S. D. Snyder and C. H. Hansen, "The effect of transfer function estimation errors on the filtered-x LMS algorithm," *IEEE Trans. Signal Process.*, vol. 42, no. 4, pp. 950–953, Apr. 1994.
- [15] N. Sato and T. Sone, "Influence of modeling error on noise reduction performance of active noise control systems using filtered-x LMS algorithm," *J. Acoust. Soc. Jpn., E*, vol. 17, no. 4, pp. 195–202, 1996.
- [16] O. J. Tobias, J. C. M. Bermudez, and N. J. Bershad, "Mean weight behavior of the filtered-x LMS algorithm," *IEEE Trans. Signal Process.*, vol. 48, no. 4, pp. 1061–1075, Apr. 2000.
- [17] I. T. Ardekani and W. H. Abdulla, "Effects of imperfect secondary path modeling on adaptive active noise control systems," *IEEE Trans. Signal Process.*, vol. 20, no. 5, pp. 1252–1262, Sep. 2012.
- [18] M. Zhang, H. Lan, and W. Ser, "Cross-updated active noise control system with online secondary path modeling," *IEEE Trans. Speech Audio Process.*, vol. 9, no. 5, pp. 598–602, Jul. 2001.
- [19] M. T. Akhtar, M. Abe, and M. Kawamata, "A new variable step size LMS algorithm-based method for improved online secondary path modeling in active noise control systems," *IEEE/ACM Trans. Audio, Speech, Language Process.*, vol. 14, no. 2, pp. 720–726, Mar. 2006.
- [20] P. Davari and H. Hassanpour, "Designing a new robust on-line secondary path modeling technique for feedforward active noise control systems," *Signal Process.*, vol. 89, pp. 1195–1204, Jun. 2009.
- [21] P. A. C. Lopes and J. A. B. Gerald, "Auxiliary noise power scheduling algorithm for active noise control with online secondary path modeling and sudden changes," *IEEE Signal Process. Lett.*, vol. 22, no. 10, pp. 1590–1594, Oct. 2015.
- [22] M. T. Akhtar, M. Abe, and M. Kawamata, "Noise power scheduling in active noise control systems with online secondary path modeling," *IEICE Electron. Express*, vol. 4, no. 2, pp. 66–71, 2007.
- [23] A. Carini and S. Malatini, "Optimal variable step-size NLMS algorithms with auxiliary noise power scheduling for feedforward active noise control," *IEEE/ACM Trans. Audio, Speech, Language Process.*, vol. 16, no. 8, pp. 1383–1395, Nov. 2008.
- [24] P. Shi, Y. Yin, and F. Liu, "Gain-scheduled worst-case control on nonlinear stochastic systems subject to actuator saturation and unknown information," *J. Optim. Theory Appl.*, vol. 156, no. 3, pp. 844–858, 2013.
- [25] P. A. C. Lopes, J. A. B. Gerald, and M. S. Piedade, "The MMFLMS algorithm for active noise control with on-line secondary path modeling," *Digit. Signal Process.*, vol. 60, pp. 75–80, Jan. 2017.
- [26] J. R. Deller, "Set membership identification in digital signal processing," *IEEE Acoust., Speech, Signal Process. Mag.*, vol. 6, no. 4, pp. 4–20, Oct. 1989.
- [27] J. R. Deller, Jr., M. Nayeri, and S. F. Odeh, "Least-square identification with error bounds for real-time signal processing and control," *Proc. IEEE*, vol. 81, no. 6, pp. 815–849, Jun. 1993.
- [28] S. Dasgupta and Y.-F. Huang, "Asymptotically convergent modified recursive least-squares with data-dependent updating and forgetting factor for systems with bounded noise," *IEEE Trans. Inf. Theory*, vol. IT-33, no. 3, pp. 383–392, May 1987.
- [29] S. Gollamudi, S. Nagaraj, S. Kapoor, and Y.-F. Huang, "Set-membership filtering and a set-membership normalized LMS algorithm with an adaptive step size," *IEEE Signal Process. Lett.*, vol. 5, no. 5, pp. 111–114, May 1998.
- [30] B. Farhang-Boroujeny, *Adaptive Filters: Theory and Applications*. Hoboken, NJ, USA: Wiley, 1999.
- [31] A. H. Sayed, *Adaptive Filters*. Hoboken, NJ, USA: Wiley, 2008.
- [32] Y. Wang, H. Shen, H. R. Karimi, and D. Duan, "Dissipativity-based fuzzy integral sliding mode control of continuous-time T-S fuzzy systems," *IEEE Trans. Fuzzy Syst.*, vol. 26, no. 3, pp. 1164–1176, Jun. 2018.
- [33] Y. Wang, H. R. Karimi, H. Shen, Z. Fang, and M. Liu, "Fuzzy-model-based sliding mode control of nonlinear descriptor systems," *IEEE Trans. Cybern.*, to be published, doi: [10.1109/TCYB.2018.2842920](https://doi.org/10.1109/TCYB.2018.2842920).
- [34] H. Gao, X. Li, and J. Qiu, "Finite frequency H_∞ deconvolution with application to approximated bandlimited signal recovery," *IEEE Trans. Autom. Control*, vol. 63, no. 1, pp. 203–210, Jan. 2018.



Muhammad Saeed Aslam received the bachelor's degree in electrical engineering from the University of Engineering and Technology, Lahore, Pakistan, in 2007, and the master's degree in control systems engineering from the Pakistan Institute of Engineering and Applied Sciences, Islamabad, Pakistan, in 2009. He is currently pursuing the Ph.D. degree in electrical engineering with The University of Adelaide. His research interests include digital signal processing, filter design theory, adaptive algorithms, system identification, and active noise control.



Peng Shi (M'95–SM'98–F'15) received the Ph.D. degree in electrical engineering from The University of Newcastle, Australia, in 1994, the second Ph.D. degree in mathematics from the University of South Australia in 1998, the Doctor of Science degree from the University of Glamorgan, Wales, in 2006, and the Doctor of Engineering degree from The University of Adelaide, Australia, in 2015.

He is currently a Professor at The University of Adelaide. His research interests include system and control theory, intelligent systems, and operational research. He is a Member-at-Large of Board of Governors, the IEEE SMC Society, and an IEEE Distinguished Lecturer. He is a fellow of the Institution of Engineering and Technology, and the Institute of Engineers, Australia.

He received the Andrew Sage Best Transactions Paper Award from the IEEE SMC Society in 2016. He has served on the editorial board of a number of journals in the fields of automation, fuzzy systems, cybernetics, signal processing, and information sciences.



Cheng-Chew Lim (M'82–SM'02) received the B.Sc. degree (Hons.) in electronic and electrical engineering and the Ph.D. degree in electronic and electrical engineering from Loughborough University, Leicestershire, U.K. He is currently a Professor with The University of Adelaide, Adelaide, SA, Australia. His research interests include control and systems theory, autonomous systems, machine learning, and optimization techniques and applications. He serves as an Associate Editor for the IEEE TRANSACTIONS OF SYSTEMS, MAN, AND

CYBERNETICS: SYSTEMS and an Editorial Board Member for the *Journal of Industrial and Management Optimization*, and has served as a Guest Editor for a number of journals, including *Discrete and Continuous Dynamical System-Series B*.

Chapter 3

Novel Fast Recursive Least Squares Filter Design for Active Noise Control

NOVEL fast least squares algorithm is derived for noise control filter which is numerically stable to quantization errors. Thus, making it suitable for finite precision implementation. Only forward prediction is used to calculate updation gain which reduces the computational complexity significantly. Convergence analysis of the proposed method is given to demonstrate the stability, robustness and convergence speed. Simulation examples are provided to demonstrate the effectiveness and improved performance achieved by the proposed method.

Statement of Authorship

Title of Paper	Novel Fast Recursive Least Squares Filter Design for Active Noise Control
Publication Status	Submitted for Publication
Publication Details	Muhammad Saeed Aslam, Peng Shi, Cheng-Chew Lim (2020). Novel Fast Recursive Least Squares Filter Design for Active Noise Control, <i>IEEE Transactions on Signal Processing</i> , Third round (Minor Revision) under review.

Principal Author

Name of Principal Author (Candidate)	Muhammad Saeed Aslam	
Contribution to the Paper	Designed the core idea and performed analysis on the concept, interpreted data, wrote manuscript and acted as corresponding author	
Overall percentage (%)	80%	
Certification:	This paper reports on original research I conducted during the period of my Higher Degree by Research candidature and is not subject to any obligations or contractual agreements with a third party that would constrain its inclusion in this thesis. I am the primary author of this paper.	
Signature	Date	8/11/2020

Co-Author Contributions

By signing the Statement of Authorship, each author certifies that:

- i. the candidate's stated contribution to the publication is accurate (as detailed above);
- ii. permission is granted for the candidate to include the publication in the thesis; and
- iii. the sum of all co-author contributions is equal to 100% less the candidate's stated contribution.

Name of Co-Author	Peng Shi	
Contribution to the Paper	Supervised development of work, helped in refining core concept and manuscript evaluation.	
Signature	Date	8 Nov 2020

Name of Co-Author	Cheng-Chew Lim	
Contribution to the Paper	Supervised development of work, helped in data interpretation and manuscript evaluation.	
Signature	Date	8/11/2020

Please cut and paste additional co-author panels here as required.

Novel Fast Recursive Least Squares Filter Design for Active Noise Control

Muhammad Saeed Aslam, Peng Shi, *Fellow, IEEE*, and Cheng-Chew Lim, *Senior Member, IEEE*

Abstract—Fast transversal recursive least squares (FTRLs) algorithms have numerical stability issues arising from parameters in backward prediction. In this paper, a novel filtered-x fast RLS algorithm is derived to address numerical stability for finite-precision implementation. Unlike FTRLs algorithms which use forward and backward predictors simultaneously, the approach presented uses forward prediction only to avoid stability issues arising from the backward prediction. The new method is robust and stable in the presence of quantization errors while delivers performance similar to that by FTRLs and RLS algorithms. Convergence analysis of the developed method is also presented. It is shown that lower bound for forgetting factor is smaller than that for standard FTRLs algorithm, that indicates the designed method can achieve improved convergence rate and tracking performance. Also the computational requirement of the new algorithm is significantly less than existing algorithms. Furthermore, a variable threshold based updating mechanism is deployed to further reduce the computations in the long term operation sense. Simulation examples are provided to demonstrate the effectiveness and better performance of the proposed new algorithm.

Index Terms—active noise control; adaptive filter; fast algorithms; recursive least squares.

I. INTRODUCTION

ACTIVE noise control (ANC) is an attractive approach for cancelling noises from low frequency band by generating a similar amplitude and opposite phase cancelling noise through a secondary source [1]. Apart from popular consumer products such as headphones, mobile phones and automobiles, ANC is applied in numerous applications including incubators, aircraft cabin, transformers [2]–[4]. In most applications, feedforward ANC systems are used to drive the controlled secondary source [5]–[7]. In a single channel feedforward ANC system, two microphones are used: one to detect the reference signal $x(n)$ and other to detect residual error signal $e(n)$ (see Fig. 1(a)). Primary noise, $d(n)$ results from $x(n)$ passing through primary path $P(z)$. Cancelling noise, $\hat{d}(n)$ is produced by the speaker. The speaker is a secondary source which is triggered by the adaptive noise controller $W(z)$. The adaptive algorithm used to update $W(z)$ makes use of $x(n)$ and $e(n)$ to reduce the noise at the error microphone.

Least mean square (LMS) algorithm is widely used for reasons including simple implementation, small computational requirements, convergence to the Wiener solution in the mean sense, and guaranteed convergence under stationary conditions [8]. However, convergence rate for LMS is dependent on the

eigenvalue spread of correlation matrix for input signal [2]–[4], [8]. On the other hand, recursive least squares (RLS) algorithms exhibit fast convergence independent of the eigenvalue spread of correlation matrix for input signal [4], [8]. RLS algorithms recursively minimize the sum of the squares of error between the desired and the filter outputs at each iteration. Also, RLS algorithms have superior performance in time-varying environments [8], [9]. The downside of RLS algorithms includes high computations to calculate correlation matrix, and stability issues [10], [11]. Among algorithms developed for $W(z)$, filtered-x LMS (FxLMS) algorithms in [2], [12] use fixed step size for updating the noise filter coefficients, while [5], [13]–[16] employ various variable step size schemes to improve the performance of FxLMS algorithm. The main disadvantage of FxLMS algorithm is slow convergence for input signals with high correlation [3], [4]. On the contrary, filtered-x recursive least squares (FxRLS) algorithms [3], [4], [6] provide fast convergence response irrespective of spectral properties of input signal. Standard FxRLS algorithm requires significantly higher computations per sample for improved performance [6]. Algorithm designed in [3] makes use of selective updating mechanism to reduce the overall computations required for long term operation of ANC system. In [4], a variable weighting factor is devised to accelerate the convergence rate and to decide the coefficient vector update of $W(z)$.

Amid various algorithms that solve the least squares (LS) problem recursively, fast transversal recursive least-squares (FTRLs) algorithms offer performance similar to RLS algorithms [8], [9]. Derivation of FTRLs algorithms involves simultaneous solution to the forward and backward prediction problems, along with an auxiliary filter and a joint-process estimator. The predictors are used to model the input signal, which allows the vector and scalar expressions contrary to matrix relations for RLS algorithms. In terms of performance and computations, FTRLs algorithms offer a good substitute for LMS and RLS algorithms [8], [10].

FTRLs algorithms are computationally attractive, but have stability issues which arise from backward predictor as proven in [10]. The numerically stabilized FTRLs algorithm introduced in [10] involves calculation of backward predictor error signal from alternate formulas. A weighted sum of these redundant error signals is used to update backward predictor and maintain stability. This algorithm gives suitable performance for stationary signals, but may become unstable for non-stationary signals [8]. Also, after the convergence of FTRLs algorithms with the speech signals, likelihood variable and Kalman gain decay to zero as shown in [17]. These values

Authors are with the School of Electrical and Electronic Engineering, The University of Adelaide, Adelaide, SA, 5005, Australia. E-mail: muhammad.aslam; peng.shi; cheng.lim@adelaide.edu.au. This work is supported by the Australian Research Council (DP170102644).

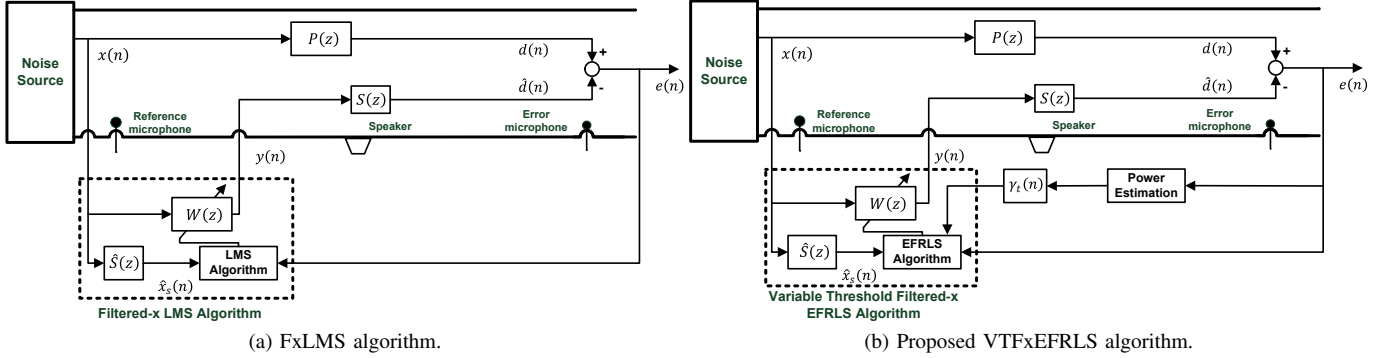


Fig. 1. ANC System with different adaptive control algorithms.

restrict the adaptability of FTRL algorithms. Therefore, the algorithm is rescued by reinitializing the variables whenever likelihood variable and Kalman gain decay to zero as explained in [8], [11]. The objective of this paper is to design a stable and effective FTRL algorithm by removing the backward predictor.

This contribution proposes a filtered-x efficient fast RLS (FxEFRLS) algorithm where variables from only forward predictor are used to obtain the adaptation gain. Numerical instability arises mainly from variables of backward predictor. Therefore, backward prediction is completely avoided. The proposed algorithm uses variables from forward predictor, a leakage factor, and a regularization constant to deliver performance similar to RLS and FTRL algorithms while being robust and numerically stable to quantization errors. The computational demands of the presented method are less than that of standard FTRL algorithm, and these requirements are further reduced by using a variable threshold developed in [3]. The proposed algorithm combines the strengths of LMS and LS algorithms along with numerical stability to deliver a performance that is desirable and an improvement to the previous methods.

The prominent attributes of the presented method are as follows

- 1) The presented algorithm uses variables from forward predictor only to obtain the adaptation gain. The variables from backward predictor are completely avoided for numerical stability which is verified by convergence analysis and extensive simulations.
- 2) The use of forward predictor reduces the computational demands of the proposed method compared with RLS and FTRL algorithms. Moreover, variable threshold is used to further reduce the computations.
- 3) For the proposed method, lower bound on forgetting factor is derived, and is found to be smaller than that of the standard FTRL algorithm. A small valued lower bound for proposed method can result in improved convergence rate and tracking performance.

Performance measures used to compare the various algorithms discussed in this paper are convergence rate, steady state error, computational complexity, stability under numerical errors from finite-precision implementation, and tracking

ability. Moreover, $E\{\cdot\}$ denotes expected value, $*$ represents the linear convolution, and \approx stands for approximation.

This paper is organized as follows: Section II gives a system description. Standard filtered-x fast transversal recursive least squares (FxFTRL) algorithm is presented in Section III. Derivation of variable threshold filtered-x efficient fast recursive least squares (VTFxEFRLS) algorithm and stability analysis are presented in Section IV. Section V discusses the computational and memory demands of various methods discussed in this paper. Simulation results are analyzed in Section VI with conclusions summarized in Section VII.

II. MODEL DESCRIPTION

In the proposed ANC system as given in Fig. 1(b), residual error, $e(n)$, is reduced by recursively updating the noise control filter $W(z)$. Let n denote the number of iterations and z denote the z -transform. The error microphone detects the signal, $e(n)$,

$$e(n) = d(n) + \hat{d}(n), \quad (1)$$

where $d(n)$ is the primary noise and $\hat{d}(n)$ is the noise cancelling signal. Signal $d(n)$ can be written as

$$d(n) = p(n) * x(n), \quad (2)$$

where $x(n)$ is the reference signal detected at the reference microphone. Impulse response of primary path $P(z)$ is represented by $p(n)$. Signal $\hat{d}(n)$ in (1) can be written as

$$\hat{d}(n) = s(n) * y(n), \quad (3)$$

where $s(n)$ represents the impulse response of secondary path $S(z)$. Let $\mathbf{w}(n)$ be the coefficient vector of $W(z)$, then control signal, $y(n)$, can be given as

$$y(n) = \mathbf{w}^T(n)\mathbf{x}(n), \quad (4)$$

where

$$\mathbf{w}(n) = [w_1(n), w_2(n), \dots, w_K(n)]^T, \quad (5)$$

$$\mathbf{x}(n) = [x(n), x(n-1), \dots, x(n-(K-1))]^T, \quad (6)$$

T denotes matrix transpose, and K represents the number of weights in $\mathbf{w}(n)$. This paper addresses the derivation of a novel adaptive algorithm to update $\mathbf{w}(n)$ and therefore, standard and proposed fast recursive least squares algorithms for $W(z)$ are discussed in the upcoming sections.

III. FILTERED-X FAST TRANSVERSAL RECURSIVE LEAST SQUARES ALGORITHM

This section presents a brief overview of the standard filtered-x fast transversal recursive least squares (FxFTRLS) algorithm [9], [10] for $\mathbf{w}(n)$. FxFTRLS algorithm uses the divergence control parameter presented in [10] to address the unstable behavior. The divergence control parameter modifies the error signal for the backward predictor to stabilize the FxFTRLS algorithm. The recursive expression for updating $\mathbf{w}(n)$ is

$$\mathbf{w}(n) = \mathbf{w}(n-1) - \Psi(n, K)\gamma(n)e(n), \quad (7)$$

where $\gamma(n)$ is the likelihood variable [18]

$$\gamma(n) = \frac{1}{1 - \Psi^T(n, K)\hat{\mathbf{x}}_s(n)}, \quad (8)$$

and $\Psi(n, K)$ is a dual Kalman gain vector of length K

$$\Psi(n, K) = -\frac{Q^{-1}(n-1, K)\hat{\mathbf{x}}_s(n)}{\lambda}, \quad (9)$$

$$\hat{\mathbf{x}}_s(n) = [\hat{x}_s(n), \hat{x}_s(n-1), \dots, \hat{x}_s(n-(K-1))]^T, \quad (10)$$

$$\hat{x}_s(n) = \hat{s}(n) * x(n). \quad (11)$$

$0 < \lambda \leq 1$, $Q(n, K)$ represents the covariance matrix of $\hat{x}_s(n)$ with dimension $K \times K$, and $\hat{s}(n)$ represents impulse response of an estimate of secondary path $\hat{S}(z)$. This paper addresses the derivation of a novel adaptive algorithm to update $\mathbf{w}(n)$ and for simplicity, assuming that secondary path has already been estimated (recent developments are available in [2], [5], [16]).

Efficient estimation of $\Psi(n, K)$ and $\gamma(n)$ in (7) is critical for the development of FxFTRLS algorithm. For $\Psi(n, K)$ in (9), expressions for $Q^{-1}(n, K+1)$ with respect to forward predictor $\mathbf{w}_f(n)$ and backward predictor $\mathbf{w}_b(n)$ are

$$\mathbf{Q}^{-1}(n, K+1) = \begin{bmatrix} 0 & 0 \\ 0 & \mathbf{Q}^{-1}(n-1, K) \end{bmatrix} + \begin{bmatrix} 1 \\ -\mathbf{w}_f^T(n) \end{bmatrix} [1 \quad -\mathbf{w}_f^T(n)] \alpha^{-1}(n), \quad (12)$$

$$\mathbf{Q}^{-1}(n, K+1) = \begin{bmatrix} \mathbf{Q}^{-1}(n-1, K) & 0 \\ 0 & 0 \end{bmatrix} + \begin{bmatrix} -\mathbf{w}_b^T(n) \\ 1 \end{bmatrix} [-\mathbf{w}_b^T(n) \quad 1] \beta^{-1}(n), \quad (13)$$

$$\alpha(n) = \lambda\alpha(n-1) + \gamma(n-1)e_f^2(n), \quad (14)$$

$$\beta(n) = \lambda\beta(n-1) + \gamma(n-1)e_b^2(n), \quad (15)$$

where $\alpha(n)$ is the variance of forward predictor error $e_f(n)$, and $\beta(n)$ is the variance of backward prediction error $e_b(n)$. Coefficient vectors for predictors, $\mathbf{w}_f(n)$ and $\mathbf{w}_b(n)$, are of length K . Post-multiply (12) and (13) with $-\lambda^{-1}[\hat{\mathbf{x}}_s^T(n), x_s(n-K)]$, rearrange the resulting expressions and use (9) to obtain $\Psi(n, K)$ recursively

$$\begin{bmatrix} \Psi(n, K) \\ \Psi(n, K+1) \end{bmatrix} = \begin{bmatrix} 0 \\ \Psi(n-1, K) \end{bmatrix} - \frac{e_f(n)}{\lambda\alpha(n-1)} \begin{bmatrix} 1 \\ -\mathbf{w}_f^T(n-1) \end{bmatrix} + \frac{e_b(n)}{\lambda\beta(n-1)} \begin{bmatrix} -\mathbf{w}_b^T(n-1) \\ 1 \end{bmatrix}. \quad (16)$$

where

$$e_f(n) = \hat{x}_s(n) - \mathbf{w}_f^T(n)\hat{\mathbf{x}}_s(n-1), \quad (17)$$

$$e_b(n) = \hat{x}_s(n-K) - \mathbf{w}_b^T(n)\hat{\mathbf{x}}_s(n), \quad (18)$$

and $\Psi(n, K+1)$ is used to calculate the divergence control parameter for stable backward predictor [10]

$$\zeta(n) = e_b(n) + \lambda^{-K+1}\gamma(n-1)\alpha(n-1)\Psi(n, K+1). \quad (19)$$

By using (8) and (16)–(19), $\mathbf{w}_f(n)$ and $\mathbf{w}_b(n)$ can be obtained recursively by

$$\mathbf{w}_f(n) = \mathbf{w}_f(n-1) - \Psi(n-1, K)\gamma(n-1)e_f(n), \quad (20)$$

$$\mathbf{w}_b(n) = \mathbf{w}_b(n-1) - \Psi(n, K)\gamma(n)e_{b1}(n),$$

$$e_{b1}(n) = e_b(n) + \mu\zeta(n),$$

where μ is used to control the propagation of numerical error in the computation of $\mathbf{w}_b(n)$. For a Gaussian input signal with $\mu = 1$, the stability condition for $\mathbf{w}_b(n)$ is [17]:

$$\lambda > \sqrt{\frac{K+1}{K+2}}, \quad (21)$$

which in turn limits the convergence rate and tracking capability.

IV. VARIABLE THRESHOLD FILTERED-X EFFICIENT FAST RECURSIVE LEAST SQUARES ALGORITHM

In the proposed VTFxFTRLS algorithm, forward prediction is used to obtain the adaptation gain for $W(z)$. Using forward predictor only helps in avoiding instability arising from backward predictor. The proposed method is completely different from methods given in [9], [10], which use both forward and backward predictors. In this section, a detailed analysis is carried out to consolidate the stable behavior claim regarding the proposed method. The stability condition is derived for the presented method to depict significant improvement in convergence rate and tracking. The computations of this method are reduced by using forward predictor only and by using a variable threshold developed in [3].

Consider $\Psi(n, K)$ of (16) in the absence of prediction components ($\mathbf{w}_f(n)$ and $\mathbf{w}_b(n)$)

$$\begin{bmatrix} \Psi(n, K) \\ 0 \end{bmatrix} = \begin{bmatrix} -\frac{\hat{x}_s(n)}{\lambda\alpha(n-1)} \\ \Psi(n-1, K) \end{bmatrix}.$$

After K iterations, all the components of $\Psi(n, K)$ are delayed versions of the first element as shown below

$$\Psi(n, K) = - \begin{bmatrix} \frac{\hat{x}_s(n)}{\lambda\alpha(n-1)} \\ \frac{\hat{x}_s(n-1)}{\lambda\alpha(n-2)} \\ \vdots \\ \frac{\hat{x}_s(n-K+1)}{\lambda\alpha(n-K)} \end{bmatrix}. \quad (22)$$

In the steady state, approximation of $\alpha(n)$ for stationary $\hat{x}_s(n)$ can be given as

$$\begin{aligned} \alpha(n) &= \lambda\alpha(n-1) + \gamma(n-1)\hat{x}_s^2(n) \\ &\approx \gamma_{ss} \frac{\sigma_x^2}{1-\lambda}, \end{aligned} \quad (23)$$

where γ_{ss} denotes steady state of slowly varying $\gamma(n)$, and σ_x^2 is the variance of $\hat{x}_s(n)$. Thus, terms $\lambda\alpha(n-i)$ in (22) converge to a value proportional to σ_x^2

$$\gamma(n)\Psi(n, K) \approx -c_0 \frac{\hat{\mathbf{x}}_s(n)}{\sigma_x^2},$$

where constant $c_0 > 0$. Coefficient update expression from (7) and (23) is similar to that of NLMS algorithm. This observation means that FxFTRLs algorithm should perform similar to NLMS in the absence of $\mathbf{w}_f(n)$ and $\mathbf{w}_b(n)$.

In practice, impulse responses of physical systems have significant starting entries. The later entries decrease in significance with increase in index. For backward predictor, the end elements in $\mathbf{w}_b(n)$ are the significant ones. The significant end coefficients of $\mathbf{w}_b(n)$ contribute strongly in the end terms of $\Psi(n, K)$ in (16) [8], [10], [17]. The significant contribution from end elements in $\mathbf{w}_b(n)$ does not propagate to other terms of $\Psi(n, K)$ due to the down-shift property [17], [19], [20]. Therefore, initial significant terms of $\mathbf{w}(n)$ come from $-e_f(n)/\lambda\alpha(n-1)$ and the initial terms of $\mathbf{w}_f(n)$ (from (7) and (16)). Overall, $\mathbf{w}_b(n)$ majorly contributes to the last coefficients of $\mathbf{w}(n)$ which are insignificant. Therefore, $\mathbf{w}_b(n)$ can be discarded from (16) without causing deterioration in performance. The proposed algorithm uses $\mathbf{w}_f(n)$ only to update $\Psi(n, K)$

$$\begin{bmatrix} \Psi(n, K) \\ 0 \end{bmatrix} = \begin{bmatrix} 0 \\ \Psi(n-1, K) \end{bmatrix} - \frac{e_f(n)}{\lambda\alpha(n-1)} \begin{bmatrix} 1 \\ -\mathbf{w}_f(n-1) \end{bmatrix}, \quad (24)$$

where $\gamma(n)$ is defined in (8), $\alpha(n)$ is defined in (14) and $\mathbf{w}_f(n)$ is defined in (20). It would be interesting to analyze the proposed algorithm, when input signal becomes very small or zero. The associated terms can be written as

$$\begin{bmatrix} e_f(n) = 0, \\ \Psi(n, K) = \mathbf{0}, \\ \alpha(n) = \lambda\alpha(n-1), \\ \mathbf{w}_f(n) = \mathbf{w}_f(n-1), \\ \gamma(n) = 1. \end{bmatrix}$$

From (14), we can see that $\alpha(n) = \lambda\alpha(n-1) \rightarrow 0$. This results in instability in all FTRLs algorithms due to division by $\alpha(n)$ for $\Psi(n, K)$ (see (24) for the proposed method). This situation can be avoided by adding a small positive constant c_0

$$\frac{e_f(n)}{\lambda\alpha(n-1)} \text{ replaced with } \frac{e_f(n)}{\lambda\alpha(n-1) + c_0}.$$

The updated expression for $\Psi(n, K)$ becomes

$$\begin{bmatrix} \Psi(n, K) \\ 0 \end{bmatrix} = \begin{bmatrix} 0 \\ \Psi(n-1, K) \end{bmatrix} - \frac{e_f(n)}{\lambda\alpha(n-1) + c_0} \begin{bmatrix} 1 \\ -\mathbf{w}_f(n-1) \end{bmatrix}. \quad (25)$$

In (20), $\mathbf{w}_f(n)$ holds on to its last values when input signal disappears. After some time, input signal reappearance may cause divergence due to poor initialization or non-zero $\mathbf{w}_f(n)$. In the presented method, $\mathbf{w}_f(n)$ is brought back to zero by

$$\mathbf{w}_f(n) \text{ replaced with } \eta\mathbf{w}_f(n),$$

TABLE I
VTFxEFRLS ALGORITHM TO UPDATE $\mathbf{w}(n)$.

VTFxEFRLS algorithm
Initialize:
$\mathbf{w}(0) = \hat{\mathbf{x}}_s(0) = [0, 0, \dots, 0]^T$
$\mathbf{x}(0) = [0, 0, \dots, 0]^T$
$\Psi(0, K) = \mathbf{0}, \sigma_t^2(0) = \gamma_t(0) = 0, \gamma(0) = 1, \alpha(0) = 10^{-6},$ $\beta(0) = 10^{-6}, c_0 = 10^{-3}, \lambda, \alpha_t, \beta_t, \eta$
Do for $n > 0$ {
Obtain $e(n)$ and $x(n)$
$\hat{x}_s(n) = s(n) * x(n)$ (expression (11))
Update $\hat{\mathbf{x}}_s(n) = [\hat{x}_s(n), \hat{x}_s(n-1), \dots, \hat{x}_s(n-(K-1))]^T$ (expression (10))
$\sigma_t^2(n+1) = \alpha_t \sigma_t^2(n) + (1 - \alpha_t) e^2(n)$ (expression (28))
$\gamma_t(n+1) = \alpha_t \gamma_t(n) + (1 - \alpha_t) \sqrt{\beta_t \sigma_t^2(n)}$ (expression (27))
if ($ e(n) > \gamma_t(n)$){
$e_f(n) = \hat{x}_s(n) - \mathbf{w}_f^T(n) \hat{\mathbf{x}}_s(n-1)$ (expression (17))
$\alpha(n) = \lambda\alpha(n-1) + \gamma(n-1) e_f^2(n)$ (expression (14))
$\begin{bmatrix} \Psi(n, K) \\ 0 \end{bmatrix} = \begin{bmatrix} 0 \\ \Psi(n-1, K) \end{bmatrix} - \frac{e_f(n)}{\lambda\alpha(n-1) + c_0} \begin{bmatrix} 1 \\ -\mathbf{w}_f(n-1) \end{bmatrix}$ (expression (25))
$\mathbf{w}_f(n) = \eta[\mathbf{w}_f(n-1) + \gamma(n-1) e_f(n) \Psi(n-1, K)]$ (expression (26))
$\gamma(n) = \frac{1}{1 - \Psi^T(n, K) \hat{\mathbf{x}}_s(n)}$ (expression (8))
$\mathbf{w}(n) = \mathbf{w}(n-1) - \Psi(n, K) \gamma(n) e(n)$ (expression (7))
}
}

where $0 << \eta < 1$ [19], [20]. Therefore, $\mathbf{w}_f(n)$ of (20) can be written as

$$\mathbf{w}_f(n) = \eta[\mathbf{w}_f(n-1) + \gamma(n-1) e_f(n) \Psi(n-1, K)]. \quad (26)$$

Without any impact on performance, computations for Fx-EFRLS algorithm can be significantly minimized by using the variable threshold mechanism presented by authors in [3]. Condition for updating $\mathbf{w}_f(n)$ can be given as $|e(n)| > \gamma_t(n)$, where $\gamma_t(n)$ is the variable threshold parameter. A variable $\gamma_t(n)$ allows suitable updates in the transition phase and steady state to achieve improved performance. The variable threshold parameter can be written as

$$\gamma_t(n+1) = \alpha_t \gamma_t(n) + (1 - \alpha_t) \sqrt{\beta_t \sigma_t^2(n)}, \quad (27)$$

$$\sigma_t^2(n+1) = \alpha_t \sigma_t^2(n) + (1 - \alpha_t) e^2(n), \quad (28)$$

where α_t and β_t are positive constants selected for small misadjustment and fast convergence rate. The proposed VTFx-EFRLS algorithm is summarized in Table I.

A. Stability Analysis

The stability analysis of the proposed method is performed using procedure provided in [10], [17]. Error propagation in the prediction stage of the proposed method is studied. The linear model used to approximate the error propagation can be written as

$$\Delta\Phi(n) = \mathbf{T}(n)\Delta\Phi(n-1) + \mathbf{V}(n), \quad (29)$$

where $\Delta\Phi(n)$ is the error vector, $\mathbf{T}(n)$ is the transition matrix and $\mathbf{V}(n)$ is the round off error vector. Error vector $\Delta\Phi(n)$ can be defined as

$$\Delta\Phi(n) = \begin{bmatrix} \Delta\mathbf{P}(n) \\ \Delta\mathbf{G}(n) \end{bmatrix}, \quad (30)$$

$$\Delta\mathbf{P}(n) = \begin{bmatrix} \Delta\mathbf{w}_f(n) \\ \Delta\alpha(n) \end{bmatrix}, \quad (31)$$

$$\Delta\mathbf{G}(n) = \begin{bmatrix} \Delta\Psi(n, K) \\ 0 \end{bmatrix}. \quad (32)$$

Vector $\Delta\mathbf{w}_f(n)$ denotes error in $\mathbf{w}_f(n)$, $\Delta\alpha(n)$ denotes error in $\alpha(n)$, and $\Delta\Psi(n, K)$ represents error in $\Psi(n, K)$. Errors in $\Psi(n, K)$ are declared in $\Delta\mathbf{G}(n)$.

Steady state stability of (29) in the mean sense can be guaranteed, if magnitudes of all the eigenvalues of $\mathbf{E}\{\mathbf{T}(n)\}$ are less than one [10]. Matrix $\mathbf{T}(n)$ is obtained by using (31), (32) and the corresponding definitions in Table I. Differentiating $\mathbf{w}_f(n)$ and $\alpha(n)$ provided in Table I results in

$$\begin{aligned} \Delta\mathbf{w}_f(n) = & \eta\Delta\mathbf{w}_f(n-1) - \eta\gamma(n-1)\Psi(n-1, K)\Delta e_f(n) \\ & - \eta e_f(n)\gamma(n-1)\Delta\Psi(n-1, K) - \\ & \eta e_f(n)\Delta\gamma(n-1)\Psi(n-1, K), \end{aligned} \quad (33)$$

$$\begin{aligned} \Delta\alpha(n) = & \lambda\Delta\alpha(n-1) + 2e_f(n)\gamma(n-1)\Delta e_f(n) + \\ & e_f^2(n)\Delta\gamma(n-1), \end{aligned} \quad (34)$$

where

$$\Delta e_f(n) = -\hat{\mathbf{x}}_s^T(n-1)\Delta\mathbf{w}_f(n-1), \quad (35)$$

$$\Delta\gamma(n) = \gamma^2(n)\hat{\mathbf{x}}_s^T(n)\Delta\Psi(n, K). \quad (36)$$

Similarly, $\Delta\mathbf{G}(n)$ can also be obtained as

$$\begin{aligned} \begin{bmatrix} \Delta\Psi(n, K) \\ 0 \end{bmatrix} = & \begin{bmatrix} 0 \\ \Delta\Psi(n-1, K) \end{bmatrix} + c_1 e_f(n) \begin{bmatrix} 0 \\ \Delta\mathbf{w}_f(n-1) \end{bmatrix} \\ & - c_1 \Delta e_f(n) \begin{bmatrix} 1 \\ -\mathbf{w}_f(n-1) \end{bmatrix} + \\ & c_1^2 \lambda e_f(n) \begin{bmatrix} 1 \\ -\mathbf{w}_f(n-1) \end{bmatrix} \Delta\alpha(n-1), \end{aligned} \quad (37)$$

where

$$c_1 = \frac{1}{\lambda\alpha(n-1) + c_0}. \quad (38)$$

Rearranging (37) results in

$$\begin{aligned} \Delta\mathbf{G}(n) = & \begin{bmatrix} \mathbf{0} & 0 \\ \mathbf{I}_K & \mathbf{0} \end{bmatrix} \Delta\mathbf{G}(n-1) + \\ & c_1 e_f(n) \begin{bmatrix} \mathbf{0} \\ \mathbf{I}_K \end{bmatrix} \Delta\mathbf{w}_f(n-1) - \\ & c_1 \begin{bmatrix} 1 \\ -\mathbf{w}_f(n-1) \end{bmatrix} \hat{\mathbf{x}}_s^T(n-1) \Delta\mathbf{w}_f(n-1) + \\ & c_1^2 \lambda e_f(n) \begin{bmatrix} 1 \\ -\mathbf{w}_f(n-1) \end{bmatrix} \Delta\alpha(n-1), \end{aligned} \quad (39)$$

where \mathbf{I}_K is an identity matrix of dimensions $K \times K$. Substitute (33)-(36) and (39) in (29), and simplify the resulting expression to obtain $\mathbf{T}(n)$

$$\mathbf{T}(n) = \begin{bmatrix} \mathbf{T}_1 & \mathbf{T}_2 \\ \mathbf{T}_3 & \mathbf{T}_4 \end{bmatrix}, \quad (40)$$

with

$$\mathbf{T}_1(n) = \begin{bmatrix} \eta(\mathbf{I}_K + \mathbf{C}(n-1)) & \mathbf{0} \\ -2\gamma(n-1)e_f(n)\hat{\mathbf{x}}_s^T(n-1) & \lambda \end{bmatrix}, \quad (41)$$

$$\begin{aligned} \mathbf{T}_2(n) = & \gamma(n-1) \times \\ & \begin{bmatrix} -\eta e_f(n)(\mathbf{I}_K + \mathbf{C}(n-1)) & \mathbf{0} \\ \gamma(n-1)e_f^2(n)\hat{\mathbf{x}}_s^T(n-1) & 0 \end{bmatrix}, \end{aligned} \quad (42)$$

$$\begin{aligned} \mathbf{T}_3(n) = & c_1 \times \\ & \begin{bmatrix} \hat{\mathbf{x}}_s^T(n-1) & \lambda c_1 e_f(n) \\ -\mathbf{w}_f(n-1)\hat{\mathbf{x}}_s^T(n-1) + e_f(n)\mathbf{I}_K & -\lambda c_1 e_f(n)\mathbf{w}_f(n-1) \end{bmatrix}, \end{aligned} \quad (43)$$

$$\mathbf{T}_4(n) = \begin{bmatrix} \mathbf{0} & \mathbf{0} \\ \mathbf{I}_K & \mathbf{0} \end{bmatrix}, \quad (44)$$

$$\mathbf{C}(n-1) = \gamma(n-1)\Psi(n-1, K)\hat{\mathbf{x}}_s^T(n-1), \quad (45)$$

where c_1 is given in (38). Average analysis of (29) is determined by obtaining the steady state value of $\mathbf{E}[\mathbf{T}(n)]$ from (39) assuming signals $\hat{\mathbf{x}}_s(n)$ and $e_f(n)$ are zero-mean, stationary, and independent of each other. Steady state values for slowing varying quantities in (41)-(45) are

$$\begin{aligned} \mathbf{C}(n-1) = & -\mathbf{Q}^{-1}(n-1, K)\hat{\mathbf{x}}_s(n-1)\hat{\mathbf{x}}_s^T(n-1), \\ = & -\mathbf{Q}^{-1}(n-1, K)[\mathbf{Q}(n-1, K) - \lambda\mathbf{Q}(n-2, K)], \\ \approx & \lambda\mathbf{I}_K - \mathbf{I}_K, \end{aligned} \quad (46)$$

$$\gamma(n) = \lambda^K \frac{\det(\mathbf{Q}(n-1, K))}{\det(\mathbf{Q}(n, K))} \approx \lambda^K, \quad (47)$$

$$\gamma(n-1)e_f^2(n) = \alpha(n) - \lambda\alpha(n-1) \approx (1-\lambda)\alpha_{ss}, \quad (48)$$

where α_{ss} is the steady state value of $\alpha(n)$. Similarly, approximation of $\mathbf{Q}(n, K)$ in the steady state is $(1-\lambda)^{-1}\mathbf{Q}$ where $\mathbf{Q} = \mathbf{E}\{\hat{\mathbf{x}}_s(n)\hat{\mathbf{x}}_s^T(n)\}$. Using steady state values (46)-(48), $\mathbf{E}[\mathbf{T}(n)]$ obtained from (40) is

$$\mathbf{E}\{\mathbf{T}(n)\} = \begin{bmatrix} \begin{bmatrix} \eta\lambda\mathbf{I}_K & \mathbf{0} \\ \mathbf{0} & \lambda \end{bmatrix} & \mathbf{0} \\ \mathbf{0} & \begin{bmatrix} \mathbf{0} & \mathbf{0} \\ \mathbf{I}_N & \mathbf{0} \end{bmatrix} \end{bmatrix}. \quad (49)$$

It is clear from (49) that all the eigenvalues of $\mathbf{E}\{\mathbf{T}(n)\}$ are less than one for $0 < \lambda < 1$ and $0 < \eta < 1$. The errors in forward prediction subsystem $\Delta\mathbf{P}(n)$ have K eigenvalues equal to $\eta\lambda$ and one equal to λ . All the eigenvalues of $\Delta\mathbf{G}(n)$ are zero due to the down-shift property used for calculating $\Psi(n, K)$ as numerical errors do not integrate in the same element, instead they pass on from one element to the next element of $\Psi(n, K)$. As all the eigenvalues of $\mathbf{E}[\mathbf{T}(n)]$ are less than one, numerical stability of the system is established in the mean sense.

For the condition on λ and η , first order linear approximations for errors in $\mathbf{w}_f(n)$ and $\alpha(n)$ are [17]

$$\Delta\mathbf{w}_f(n) = \eta(\mathbf{I}_K - \mathbf{F}_1(n-1))\Delta\mathbf{w}_f(n-1) + \mathbf{P}_{w_f}(n), \quad (50)$$

$$\Delta\alpha(n) = \lambda\Delta\alpha(n-1) + a_\alpha(n), \quad (51)$$

$$\mathbf{F}_1(n) = \mathbf{Q}^{-1}(n, K)\hat{\mathbf{x}}_s(n)\hat{\mathbf{x}}_s^T(n),$$

where $\mathbf{P}_{w_f}(n)$ in (50) depends on $\Delta\mathbf{G}(n-1)$, $\Delta\alpha(n-1)$ and $\mathbf{V}(n)$. Term $a_\alpha(n)$ in (51) depends on $\Delta\mathbf{G}(n-1)$, $\Delta\mathbf{w}_f(n-1)$ and $\mathbf{V}(n)$.

Independence hypothesis between $\Delta\alpha(n-1)$ and $a_\alpha(n)$ makes it simple to verify the stability of $E[\Delta\alpha(n)\Delta\alpha(n)]$ from (51). Assuming independence between errors $\Delta\mathbf{w}_f(n-1)$ and the additive term $\mathbf{P}_{w_f}(n)$, covariance matrix $\mathbf{R}(n) = E[\Delta\mathbf{w}_f(n)\Delta\mathbf{w}_f^T(n)]$ can be written as

$$\begin{aligned} \mathbf{R}(n) &= \eta^2\mathbf{R}(n-1) - 2\eta^2E\{\mathbf{F}_1(n-1)\}\mathbf{R}(n-1) \\ &\quad + \eta^2\mathbf{F}_2(n-1) + E\{\mathbf{P}_{w_f}(n)\mathbf{P}_{w_f}^T(n)\}. \end{aligned} \quad (52)$$

where $\mathbf{F}_2(n) = E\{\mathbf{F}_1(n)\Delta\mathbf{w}_f(n)\Delta\mathbf{w}_f^T(n)\mathbf{F}_1^T(n)\}$. Replace $\mathbf{Q}(n-1, K)$ in (52) with asymptotic value $(1-\lambda)^{-1}\mathbf{Q}$,

$$\begin{aligned} \mathbf{R}(n) &= \eta^2\mathbf{R}(n-1) - 2\eta^2(1-\lambda)\mathbf{R}(n-1) \\ &\quad + \eta^2(1-\lambda)^2\mathbf{Q}^{-1}\mathbf{F}_3(n-1)\mathbf{Q}^{-1} + E\{\mathbf{P}_a(n)\mathbf{P}_a^T(n)\}. \end{aligned} \quad (53)$$

where $\mathbf{F}_3(n) = E\{\hat{\mathbf{x}}_s(n)\hat{\mathbf{x}}_s^T(n)\Delta\mathbf{w}_f(n)\Delta\mathbf{w}_f^T(n)\hat{\mathbf{x}}_s(n)\hat{\mathbf{x}}_s^T(n)\}$. Elements of $\mathbf{F}_3(n)$ are $f_{i,j} = \sum_{k=1}^K \sum_{l=1}^K E\{\Delta w_{f,k}(n-1)\Delta w_{f,l}(n-1)\hat{x}_s(n-k)\hat{x}_s(n-l)\hat{x}_s(n-j)\hat{x}_s(n-i)\}$, where $\Delta w_{f,j}(n)$ is j th element of $\Delta\mathbf{w}_f(n)$. For Gaussian input signal, elements of $\Delta\mathbf{w}_f(n)$ and $\hat{x}_s(n)$ are independent. Therefore, $f_{i,j}$ can be written as

$$f_{i,j} = \begin{cases} 0 & i \neq j, \\ (K+2)\sigma_X^2 R_{i,j}^2(n-1) & i = j, \end{cases} \quad (54)$$

where $R_{i,j}(n)$ are the elements of $\mathbf{R}(n)$. Substitute (54) in (53) results in

$$\mathbf{R}(n) = h(\lambda, \eta, K)\mathbf{R}(n-1) + E\{\mathbf{P}_{w_f}(n)\mathbf{P}_{w_f}^T(n)\}, \quad (55)$$

where the quantity $h(\lambda, \eta, K)$ is given by

$$h(\lambda, \eta, K) = \eta^2(1 - 2(1-\lambda) + (K+2)(1-\lambda)^2).$$

The system in (55) is stable for

$$0 \leq h(\lambda, \eta, K) < 1. \quad (56)$$

For $0 < \eta \leq 1$, condition in (56) can be satisfied for the following λ

$$\lambda \geq \frac{K+1}{K+2} - \frac{\sqrt{1+(K+2)(\frac{1}{\eta^2}-1)}}{K+2}. \quad (57)$$

From (57), it can be seen that lower limit on λ is smaller than that in (21). The lower bound for proposed method can result in improved convergence rate and tracking performance.

V. COMPUTATIONAL COMPLEXITY

This section discusses the recent developments in the ANC systems in terms of computational complexity. The standard measures for computations are the numbers of multiplications and additions required by respective algorithms at each iteration, and are given in Table II [2]–[4], [8], [13]. Importance of small computational complexity is a desirable feature for battery powered systems and systems with multiple applications sharing same resources. LMS algorithms presented in [2], [13], [14] require small computations while [3], [4] require more computations in the transition state for using RLS algorithm variations. The second rows for [3], [4] denote the computations required when controller update is not performed by using a threshold parameter. The proposed algorithm also has two entries due to use of a variable threshold parameter

TABLE II
COMPUTATIONS REQUIRED FOR ANC SYSTEMS UNDER DISCUSSION.

	Additions	Multiplications
FxFTRLs algorithm	$9K + L + 4$	$9K + L + 17$
Shakeel's method [13]	$4K + 2L - 1$	$4K + 2L + 5$
Lopes's method [14]	$4K + 2L - 1$	$4K + 2L + 5$
Saeed's method [2]	$2K + L - 2$	$2K + L + 1$
Saeed's method [3] $\mathbf{w}(n)$ is updated	$K^2 + 3K + L + 1$	$K^2 + 5K + L + 3$
No filter update	$K + L + 1$	$K + L + 3$
Saeed's method [4] $\mathbf{w}(n)$ is updated	$K^2 + 3K + L - 1$	$K^2 + 5K + L + 1$
No filter update	$K + L - 1$	$K + L$
Proposed method $\mathbf{w}(n)$ is updated	$6K + L + 3$	$7K + L + 14$
No filter update	$K + L$	$K + L + 7$

TABLE III
NUMBER OF VARIABLES TO BE STORED FOR ANC SYSTEMS UNDER DISCUSSION.

	Number of variables
FxFTRLs algorithm	$6K + 2L + 10$
Shakeel's method [13]	$3K + 2L + 9$
Lopes's method [14]	$3K + 2L + 10$
Saeed's method [2]	$3K + 2L + 4$
Saeed's method [3]	$K^2 + 3K + 2L + 7$
Saeed's method [4]	$K^2 + 3K + 2L + 9$
Proposed method	$5K + 2L + 14$

given in (29). In either row, the presented method requires computations very similar to the LMS algorithm, but performance is similar to RLS algorithm as demonstrated in the next section. Computing tasks can be significantly accelerated by using frequency-domain block processing [21], as time-domain convolution can be converted to multiplication in the frequency domain. In addition to operations, memory requirements are also compared in terms of variables stored at each iteration (see Table III). Algorithms designed in [3], [4] demand more memory than the algorithms in [2], [13], [14] and the proposed method. The presented design provides optimal solution in terms of computational complexity and convergence performance. For the proposed system, the memory demand remains constant throughout the operation while computations vary between two values provided in Table III. Therefore, only operations are compared in the Section VI.

VI. CASE STUDIES

The proposed method (PM) is compared with Shakeel (SM) [13], Lopes (LM) [14], Saeed (SaM1) [2], Saeed (SaM2) [3], Saeed (SaM3) [4] under standard performance measures which include mean-squared error, convergence rate, steady state residual error and computational complexity. The methods in [2]–[4], [13], [14] represent the recent research work on the relevant topic. Parameter settings are given in Table IV for all established cases [2]–[4], [13], [14] with sampling

TABLE IV
PARAMETER VALUES FOR SIX METHODS DISCUSSED IN THIS PAPER.

	Parameters
FxFTRLs	$\lambda = 0.9995$
Shakeel's method [13]	$\mu_1 = 3 \times 10^{-1}, \mu_2 = 8 \times 10^{-2}, \lambda = 0.99, \alpha = 0.997, \gamma_{max} = 0.9, \gamma_{min} = 0.3$
Lopes's method [14]	$\mu = 0.5, \mu_s = 0.5, \lambda = 0.9, k_r = 0.1, \beta = 40, A = 2$
Saeed's method [2]	$\mu_w = 1 \times 10^{-4}, \lambda = 0.99$
Saeed's method [3]	$\alpha = 0.99, \beta_w = 1.5$
Saeed's method [4]	$\lambda = 0.99, \gamma_f = \gamma_b = 0.05$
Proposed method	$\lambda = 0.995, \alpha_t = 0.995, \beta_t = 1.0, \eta = 0.995$

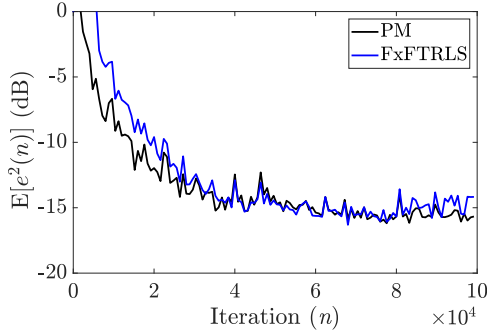


Fig. 2. Mean-squared error for two methods under Case 1 setting.

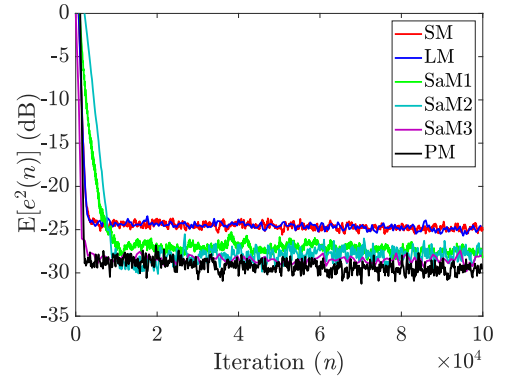
frequency set to 4 kHz and ensemble-average obtained over 20 independent runs. Benchmark acoustic channels, $P(z)$ and $S(z)$, are obtained from [6]. The corresponding lengths for coefficient vectors of $P(z)$, $S(z)$ and $W(z)$ are 256, 64 and 192. Using these coefficient vectors and parameter values from Table IV, the pseudo-code for the proposed method given in Table I can be implemented for various $x(n)$ and conditions addressed in subsequent cases.

A. Case 1

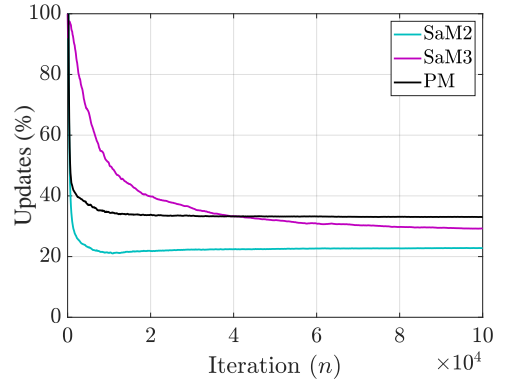
A real-world scenario is considered in this case to compare the proposed method with FxFTRLs algorithm. The data used for $x(n)$ is from a washing machine with frequency band 50-650Hz (available in MATLAB Audio library). Washing machine is a common household appliance and produces considerable noise during operation. Cancelling such noise by ANC can be a strong selling feature. Both methods, PM and FxFTRLs, converge to a similar steady state value as demonstrated in Fig. 2. PM has slightly better convergence rate than FxFTRLs algorithm which is coherent with the stability condition derived for PM in (57). The results from real data verify that removing the backward predictor has insignificant impact on the performance of PM.

B. Case 2

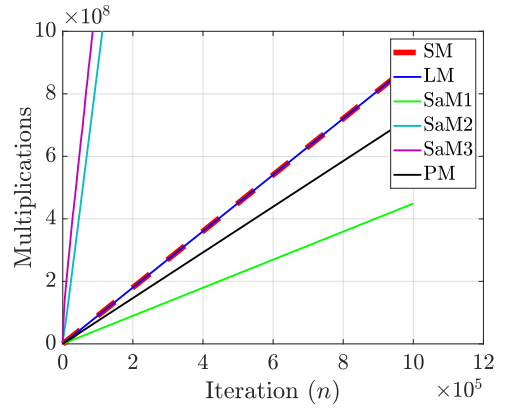
A multi-tonal $x(n)$ is obtained by combining sinusoids of frequencies 165, 235, 290, 315, 410 and 600 Hz, and adjusted the variance to 2.0 [4]. Gaussian noise is added to $x(n)$ for maintaining a signal-to-noise ratio of 30 dB [2]–[4], [13], [14]. The proposed method converges at a similar rate to a



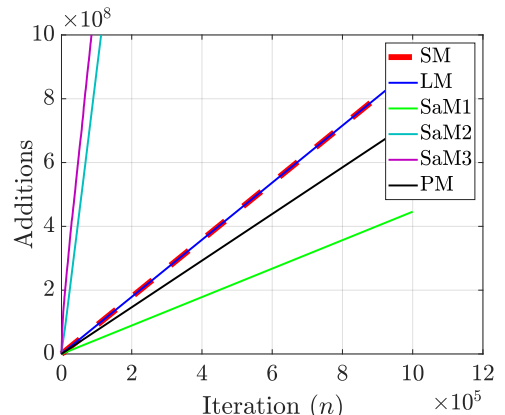
(a) Mean-squared error



(b) Update percentage



(c) Total multiplications



(d) Total additions

Fig. 3. Performance measures for six methods under Case 2 setting.

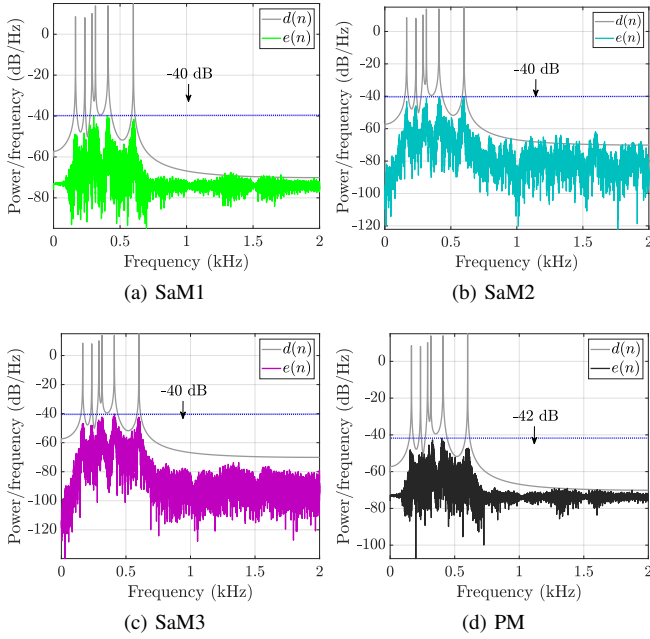


Fig. 4. Steady state power spectra for various methods under Case 2 setting.

same steady state value as [3], [4] as demonstrated in Figs. 3 and 4. Similar performance is achieved as methods in [3], [4] use RLS algorithm, and PM delivers stable and efficient fast implementation of RLS algorithm. The computational requirements of proposed method are very close to [2] which uses a fixed step LMS algorithm for $W(z)$ (see Fig. 3(b)-(d)). Therefore, the proposed method offers fast convergence using fewer computations than achieved by RLS and LMS algorithms, respectively.

C. Case 3

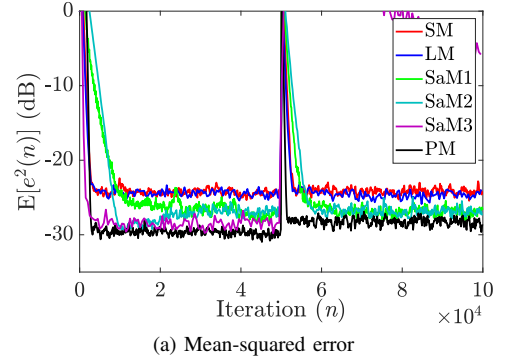
The response of the proposed method to a change in primary path is addressed in this case. The perturbation is introduced at $n = 50000$, and modeled by

$$\mathbf{p}(n+1) = 0.9\mathbf{p}(n) + 0.1\mathbf{r}(n)$$

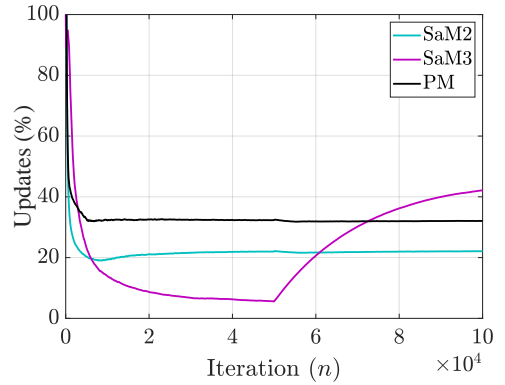
where $\mathbf{r}(n)$ is a random vector. Before the occurrence of perturbation in $P(z)$, performance of all methods is similar to Case 1 as same reference signal is used (see Fig. 5). After change in $P(z)$, the proposed method converges faster than the previous methods as shown in Fig. 5(a). The operations required for PM are similar to the LMS variants [2], [13], [14]. Thus, PM delivers the prominent features of both LMS and RLS.

D. Case 4

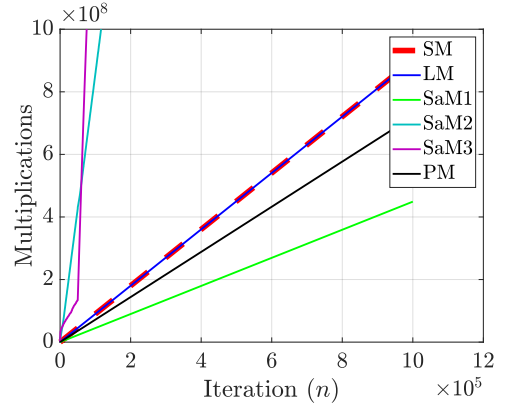
The reference signal is a mixture of multi-tonal and broadband signals. The multi-tonal signal has variance 2.0 and consists of sinusoids with frequencies: 300 and 400 Hz. The broadband signal is a Gaussian noise of zero mean and variance 2.0 passing through a band-pass filter of passband 500-800 Hz. Measurement noise is added to maintain a SNR of 30 dB. The proposed method and RLS methods of [3], [4]



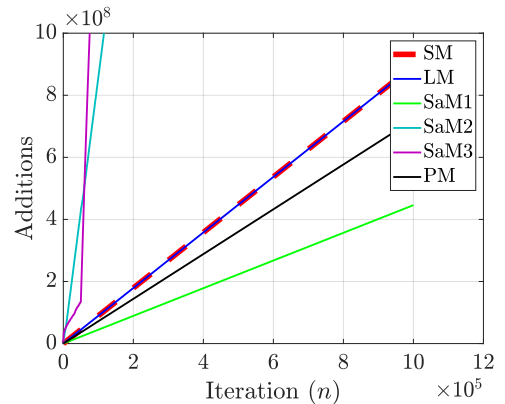
(a) Mean-squared error



(b) Update percentage



(c) Total multiplications



(d) Total additions

Fig. 5. Performance measures for six methods under Case 3 setting.

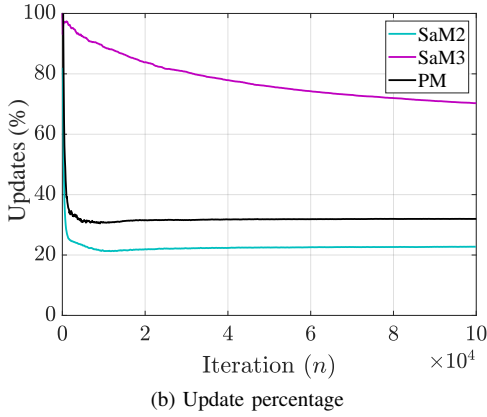
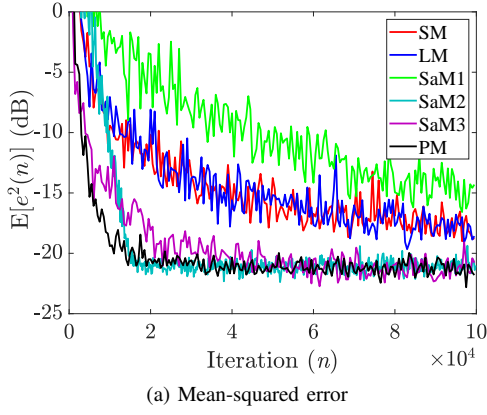


Fig. 6. Performance measures for six methods under Case 4 setting.

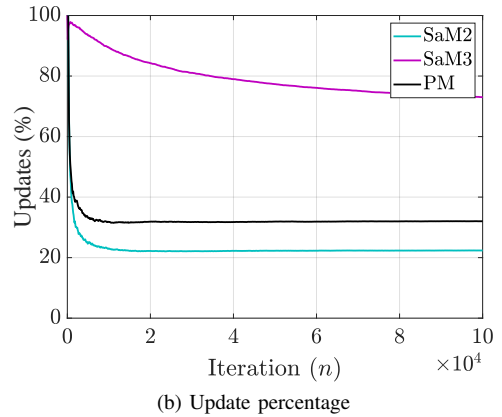
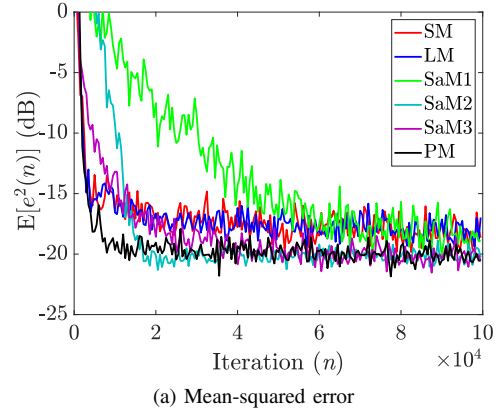


Fig. 8. Performance measures for six methods under Case 5 setting.

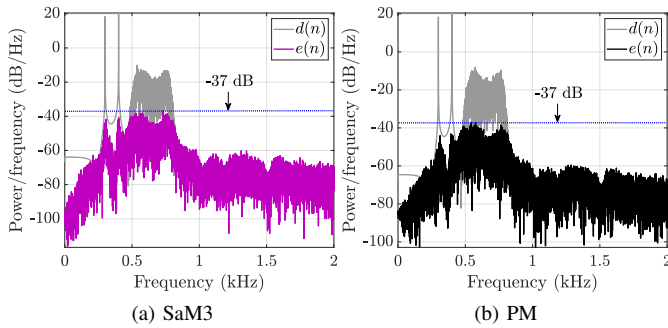


Fig. 7. Steady state power spectra for various methods under Case 4 setting.

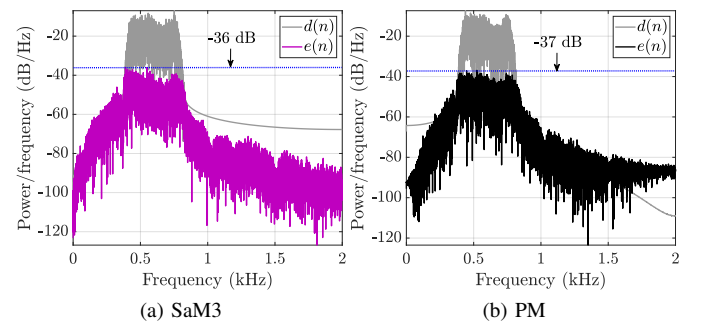


Fig. 9. Steady state power spectra for various methods under Case 5 setting.

converge at similar rate to a same steady state value as shown in Figs. 6(a) and 7. The LMS based methods of [2], [13], [14] converge at significantly slower rate than LS based methods (SaM2, SaM3 and PM).

E. Case 5

A broadband signal, $x(n)$, is obtained by filtering a Gaussian noise with a zero mean and variance 2.0 through a band-pass filter: 400-800 Hz. The proposed algorithm exhibits noise reduction performance similar to [3], [4] and significantly improved compared to [2], [13], [14] (see Figs. 8(a) and 9). The proposed method provides the convergence rate and steady state error of RLS algorithms [3], [4] while requiring computations similar to LMS algorithms [2], [13], [14]. Thus, the designed method provides desirable properties of fast con-

vergence and ease of implementation which are individually available in RLS and LMS algorithms, respectively.

F. Case 6

This case illustrates the stable performance of the proposed method under finite precision implementation. A multi-tonal $x(n)$ is obtained by combining sinusoids of frequencies 100, 200, 300 and 400 Hz, and adjusted the variance to 2.0. The quantized environment used for simulation is adopted from [11]. Noise reduction performance of the proposed algorithm for various word-lengths is given in Fig. 10. Word-length includes the sign bit, and is used for both coefficients and data. The stable behavior exhibited by the proposed method under finite precision conditions verifies its robustness to quantization errors.

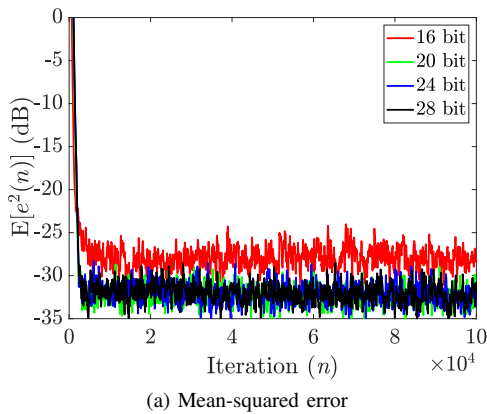


Fig. 10. Mean-squared error curves for PM under Case 6 setting.

VII. CONCLUSIONS

The new recursive least squares algorithm derived in this paper obtains adaptation gain only from parameters in the forward prediction stage. Convergence analysis is performed to establish the stable behavior in the mean sense along with estimating bound on the forgetting factor. For the proposed method, lower bound on forgetting factor is smaller than FTRL algorithms that means the proposed method can offer better convergence rate and tracking performance. The computational demands for the proposed method are significantly less than the RLS based methods, and comparable to the LMS based methods. Simulations show that the proposed method is numerically stable to finite-precision implementation, and provides improved performance in all standard measures.

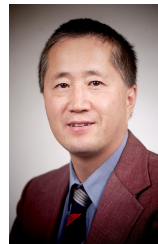
REFERENCES

- [1] P. Lueg. "Process of silencing sound oscillations". Patent US2043416 A, Jun. 1936.
- [2] M. S. Aslam. "Maximum likelihood least squares identification method for active noise control systems with autoregressive moving average noise". *Automatica*, 69:1–11, Jul. 2016.
- [3] M. S. Aslam, P. Shi, and C. C. Lim. "Variable threshold-based selective updating algorithms in feed-forward active noise control systems". *IEEE Trans. Circuits Syst. I, Reg. Papers*, 66(2):782–795, Feb. 2019.
- [4] M. S. Aslam, P. Shi, and C. C. Lim. "Robust active noise control design by optimal weighted least squares approach". *IEEE Trans. Circuits Syst. I, Reg. Papers*, 66(10):3955–3967, Oct. 2019.
- [5] M. S. Aslam and M. A. Z. Raja. "A new adaptive strategy to improve online secondary path modeling in active noise control systems using fractional signal processing approach". *Signal Process.*, 107:433–443, Feb. 2015.
- [6] S. M. Kuo and D. R. Morgan. *Active Noise Control Systems—Algorithms and DSP Implementations*. Wiley, New York, 1996.
- [7] M. A. Z. Raja, M. S. Aslam, N. I. Chaudhary, and W. U. Khan. "Bio-inspired heuristics hybrid with interior-point method for active noise control systems without identification of secondary path". *Front. Inf. Technol. Electron. Eng.*, 19(2):246–259, Apr. 2018.
- [8] P. S. R. Diniz. *Adaptive Filtering: Algorithms and Practical Implementation*. Springer, New York, NY, USA, 2008.
- [9] M. Bouchard. "Numerically stable fast convergence least-squares algorithms for multichannel active sound cancellation systems and sound deconvolution systems". *Signal Process.*, 82(5):721–736, May 2002.
- [10] D. T. M. Slock, and T. Kailath. "Numerically stable fast transversal filters for recursive least squares adaptive filtering". *IEEE Trans. Signal Process.*, 39(1):92–114, Jan. 1991.
- [11] A. H. Sayed. *Adaptive Filters*. John Wiley & Sons, New Jersey, 2008.
- [12] M. Zhang, H. Lan, and W. Ser. "Cross-updated active noise control system with online secondary path modeling". *IEEE Trans. Speech Audio Process.*, 9:598–602, Jul. 2001.

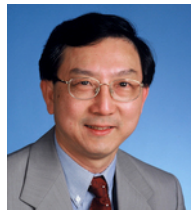
- [13] S. Ahmed, M. T. Akhtar, and X. Zhang. "Robust auxiliary-noise-power scheduling in active noise control systems with online secondary path modeling". *IEEE Trans. Audio, Speech, Language Process.*, 21:749–761, Apr. 2013.
- [14] P. A. C. Lopes and J. A. B. Gerald. "Auxiliary noise power scheduling algorithm for active noise control with online secondary path modeling and sudden changes". *IEEE Signal Process. Lett.*, 22:1590–1594, Oct. 2015.
- [15] P. Davari and H. Hassanpour. "Designing a new robust online secondary path modeling technique for feedforward active noise control systems". *Signal Process.*, 89:1195–1204, Jun. 2009.
- [16] A. Carini and S. Malatini. "Optimal variable step-size NLMS algorithms with auxiliary noise power scheduling for feedforward active noise control". *IEEE Trans. Audio, Speech, Language Process.*, 16:1383–1395, Nov. 2008.
- [17] A. Benallal, and A. Benkrid. "A simplified FTF-type algorithm for adaptive filtering". *Signal Process.*, 87(5):904–917, May 2007.
- [18] J. Cioffi, and T. Kailath. "Fast, recursive-least-squares transversal filters for adaptive filtering". *IEEE Trans. Acoust. Speech Signal Process.*, 32(2):304–337, Apr. 1984.
- [19] M. Belanger. *Adaptive Digital Filters and Signal Analysis*. Marcel Dekker, New York, 1987.
- [20] S. Binde. "A numerically stable fast transversal filter with leakage correction". *IEEE Signal Process. Lett.*, 2(6):114–116, Jun. 1995.
- [21] S. Liu, Y. Ma, and Y. Huang. "Sea clutter cancellation for passive radar sensor exploiting multi-channel adaptive filters". *IEEE Sensors J.*, 19(3):982–995, Feb. 2019.



Muhammad Saeed Aslam is pursuing PhD in Electrical Engineering from The University of Adelaide. He received the Master degree in control systems engineering from the Pakistan Institute of Engineering and Applied Sciences (PIEAS), Islamabad, Pakistan, in 2009 and the Bachelor degree in Electrical engineering from the University of Engineering and Technology (UET), Lahore, Pakistan, in 2007. His research interests include digital signal processing, filter design theory, adaptive algorithms, system identification, and active noise control.



Peng Shi (M-95/SM-98/F-15) received the PhD degree in Electrical Engineering from the University of Newcastle, Australia in 1994. He was awarded the Doctor of Science degree from the University of Glamorgan, Wales in 2006; and the Doctor of Engineering degree from the University of Adelaide, Australia in 2015. He is now a professor at the University of Adelaide. His research interests include system and control theory, autonomous and robotic systems, and cyber-physical systems. He has served on the editorial board of a number of journals, including *Automatica*; *IEEE Transactions on Automatic Control*; *Cybernetics*; *Fuzzy Systems*; *Circuits and Systems*. He is a Member-at-Large of Board of Governors, IEEE SMC Society, and an IEEE SMC Society Distinguished Lecturer. He is a Fellow of the Institute of Electrical and Electronic Engineers, Institution of Engineering and Technology; and the Institute of Engineers, Australia.



Cheng-Chew Lim received the B.Sc. degree (Hons.) in electronic and electrical engineering and Ph.D. degree in electronic and electrical engineering from Loughborough University, Leicestershire, U.K. He is currently a Professor with the University of Adelaide, Adelaide, SA, Australia. His research interests include control and systems theory, autonomous systems, machine learning, and optimization techniques and applications. Dr Lim serves as an Associate Editor for the *IEEE Transactions on Systems, Man, and Cybernetics: Systems* and an Editorial Board

Member for the *Journal of Industrial and Management Optimization*, and has served as a Guest Editor for a number of journals, including *Discrete and Continuous Dynamical System-Series B*.

Chapter 4

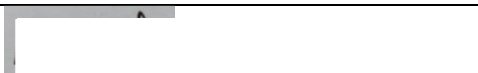
Robust Active Noise Control Design by Optimal Weighted Least Squares Approach

AN optimal weighting factor based least squares algorithm is derived for noise controllers in active noise control systems with a bounded narrowband disturbance. The proposed method updates the weighting factor in relation to the new information in the current data to improve the convergence speed and steady state error. The weighting factor is also used to vary the frequency of the feed-forward and feedback filter updates. Detailed analysis is provided for stability and robustness of the proposed method.

Statement of Authorship

Title of Paper	Robust Active Noise Control Design by Optimal Weighted Least Squares Approach
Publication Status	Submitted for Publication
Publication Details	Muhammad Saeed Aslam, Peng Shi, Cheng-Chew Lim (2019). Robust Active Noise Control Design by Optimal Weighted Least Squares Approach, <i>IEEE Transactions on Circuits and Systems I: Regular Papers</i> , 66(10), pp. 3955–3967.


Principal Author


Name of Principal Author (Candidate)	Muhammad Saeed Aslam		
Contribution to the Paper	Designed the core idea and performed analysis on the concept, interpreted data, wrote manuscript and acted as corresponding author		
Overall percentage (%)	80%		
Certification:	This paper reports on original research I conducted during the period of my Higher Degree by Research candidature and is not subject to any obligations or contractual agreements with a third party that would constrain its inclusion in this thesis. I am the primary author of this paper.		
Signature		Date	8/11/2020

Co-Author Contributions

By signing the Statement of Authorship, each author certifies that:

- the candidate's stated contribution to the publication is accurate (as detailed above);
- permission is granted for the candidate to include the publication in the thesis; and
- the sum of all co-author contributions is equal to 100% less the candidate's stated contribution.

Name of Co-Author	Peng Shi		
Contribution to the Paper	Supervised development of work, helped in refining core concept and manuscript evaluation.		
Signature		Date	8 Nov 2020

Name of Co-Author	Cheng-Chew Lim		
Contribution to the Paper	Supervised development of work, helped in data interpretation and manuscript evaluation.		
Signature		Date	8/11/2020

Please cut and paste additional co-author panels here as required.

Robust Active Noise Control Design by Optimal Weighted Least Squares Approach

Muhammad Saeed Aslam¹, Peng Shi², *Fellow, IEEE*, and Cheng-Chew Lim³, *Senior Member, IEEE*

Abstract—An optimal strategy is derived for robust performance of feedforward and feedback noise controllers in active noise control systems with a bounded narrowband disturbance. The designed recursive algorithm updates the weighting factor to make sure that controller updates are performed when the current measurement data contain new information to improve the estimation quality. This significantly reduces the computational complexity by allowing fewer updates in the steady state and persistent updates otherwise. The presented algorithm can guarantee non-increasing and positive-definite covariance matrices for feedforward and feedback filters, and this results in a bounded and non-increasing estimation error. Moreover, the proposed algorithm achieves fast convergence with improved performance in steady-state noise reduction. In simulations, the comparison of the proposed method with the established methods under benchmark conditions demonstrates the improvement in the overall performance.

Index Terms—Robust active noise control, selective filtering, weighted least squares algorithm, hybrid control.

I. INTRODUCTION

ACTIVE noise control (ANC) is a popular technique for attenuating low frequency noises by using a controlled secondary source that generates a similar amplitude cancelling noise with opposite phase [1]. Last decade has seen the commercialization of numerous products using ANC, such as headphones, mobile phones and automobiles. In addition, ANC has been used in diverse applications ranging from aircraft cabin noise, air conditioning ducts, incubators to magnetic resonance imaging scanner [2]. Prominent control strategies used for triggering the secondary source are feedforward control [2]–[6] and feedback control [5], [7]–[10]. A single channel feedforward ANC system uses an error microphone and a reference microphone. The error microphone detects the residual error which is also used to oversee the performance of ANC system. The reference microphone detects the primary noise that needs to be cancelled. The feedback control strategy requires only an error microphone to cancel the predictable

Manuscript received December 14, 2018; revised March 10, 2019 and April 1, 2019; accepted April 1, 2019. Date of publication April 24, 2019; date of current version September 27, 2019. This paper was recommended by Associate Editor G. Jovanovic Dolecek. (*Corresponding author: Muhammad Saeed Aslam.*)

The authors are with the School of Electrical and Electronic Engineering, The University of Adelaide, Adelaide, SA 5005, Australia (e-mail: muhammad.aslam@adelaide.edu.au; peng.shi@adelaide.edu.au; cheng.lim@adelaide.edu.au).

Color versions of one or more of the figures in this article are available online at <http://ieeexplore.ieee.org>.

Digital Object Identifier 10.1109/TCSI.2019.2910290

1549-8328 © 2019 IEEE. Personal use is permitted, but republication/redistribution requires IEEE permission. See http://www.ieee.org/publications_standards/publications/rights/index.html for more information.

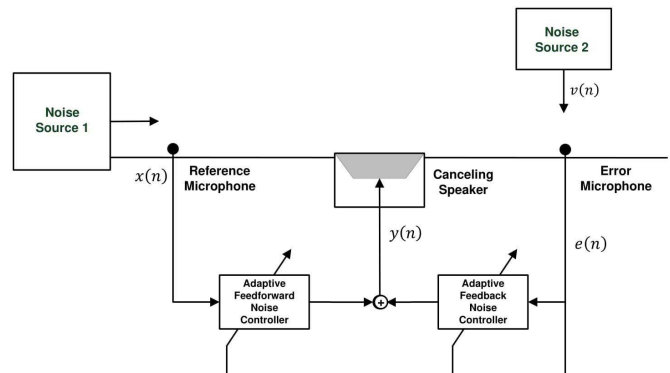


Fig. 1. Block diagram of a hybrid ANC system.

noise components in the primary noise [5]. The use of both strategies is dependent on the application circumstances. Feedforward control is commonly implemented when available reference noise is independent, and correlated with the primary noise. Feedback control is used when sensing or internal generation of completely coherent reference signal is not possible which include spatially incoherent turbulence noise, multi-source noise, noise from multiple propagation paths and induced resonance [5].

In practice, situations arise where disturbances are detected at error microphone that are uncorrelated with the reference signal. These disturbances can result from different reasons like noise generated by other automobiles in electronic muffler case or a neighboring machinery in an industrial application [5], [8]. In such cases, a combination of feedforward and feedback schemes is used. This control structure is referred as hybrid ANC system in which the cancelling signal is calculated based on the outputs of both the reference microphone and the error microphone as shown in Fig. 1. The primary noise correlated with the reference signal is attenuated by the feedforward controller, and the feedback controller removes the narrowband components of primary noise that are not detected by the reference microphone. Besides, the periodic components are most intense in many ANC applications, and the feedback controller enforces the reduction of spectral peaks in the primary noise, which eases the operation of feedforward controller.

Numerous methods exist in the literature addressing the disturbances at the error microphone. An algorithm comprising of two notch filters is presented in [11] to reduce the uncorrelated narrowband disturbance for single-frequency narrowband

ANC systems. To address the multi-frequency narrowband ANC systems, the use of a high-order adaptive filter is proposed in [12]. This method improves the convergence of the feedforward filter without mitigating the disturbance detected by the error microphone. In [13], a feedback controller scheme is included in the system of [12] to mitigate the narrowband disturbance. This method uses an additional filter, apart from feedforward and feedback noise controllers, to obtain the appropriate error signals for each noise controller. In contrast, conventional hybrid ANC systems [14] uses the same error signal for adapting both feedforward and feedback controllers. The presence of both feedforward and feedback controllers makes the design of ANC system more flexible, and often improves the system performance even when there is an uncorrelated narrowband disturbance detected by the error microphone. A variable step size scheme was proposed in [10] for a conventional hybrid system to improve the convergence characteristics. In conventional hybrid systems, feedforward and feedback systems are coupled which means that simultaneous optimization of both filters is required for stable system design, and this issue is resolved in [9] by modifying the error signal used for feedforward controller, and the reference signal for feedback controller. In [8], the decoupling technique of [9] is modified for the hybrid structure of [13], and a variable step size scheme is developed for the additional filter to enhance the convergence speed.

All the techniques mentioned above use the filtered-x least mean square (FxLMS) adaptive algorithm [14] for updating the noise filters. This variant of LMS algorithm is usually preferred due to its attractive features like computational simplicity, unbiased convergence and robustness [14]–[18]. However, eigen-spread of the input signal can critically alter the convergence properties of the LMS algorithm [18], [19]. Apart from [10], all the algorithms compromise the system flexibility by using fixed step sizes for noise control filters. A suitable solution is to use the least squares (LS) algorithm that has convergence speed and steady-state error significantly better than the LMS algorithm [2], [5]. These algorithms require relatively large number of computations for improved performance. Recently, LMS-Newton algorithm is proposed in [2] for feedforward control filter. The computational complexity is reduced by use of selective updating.

The motivation for developing the proposed algorithm is to achieve the advantages of LMS and LS algorithms without inheriting the negative aspects. More specifically, the desirable features of LMS algorithm include ease of implementation and small computations, while LS algorithm converges at a relatively fast rate. LMS algorithm convergence speed is relatively slower than LS algorithm and depends on the eigen-spread of the input signal. LS algorithm requires relatively high computations than LMS algorithm. The proposed algorithm design focuses on achieving fast convergence independent of input signal characteristics with relatively reduced computations. These characteristics can be achieved by using optimal weighting factor. As a small valued forgetting factor results in fast convergence but large steady state mis-adjustment. Similarly, a large forgetting factor slows down the convergence speed to reduce the steady state mis-adjustment. The motivation for

the proposed algorithm is to derive a variable factor that has a small value during transition phase for fast convergence, and a large value in the steady state to achieve small steady state error. The derivation of the proposed variable factor makes use of new information in the data. Therefore, reliable decision regarding filter updates can be made to reduce the overall computations with fast convergence and low steady state error.

The distinct features of the proposed algorithm are as follows

- 1) The derived algorithm has an optimal adaptive strategy which updates the weighting factor to achieve fast convergence in the transition phase and small steady state error. In conventional LS approaches, the filter updates are performed with a fixed parameter. The performance of LMS algorithms is compromised by the characteristics of the input signal [2].
- 2) The designed algorithm presents an optimal scheme to make decision on the filter updates. The decision is calculated on the basis of sufficient new information in the current observed data to improve the controller performance. A significant reduction in computations is achieved by avoiding controller updates which do not contribute to system performance. In conventional approaches, the filter updates are performed on each iteration irrespective of improvement achieved in the outcome.
- 3) The proposed weighting factor is simple to compute, and is also used to decide on filter update.
- 4) The presented algorithm can guarantee positive definite covariance matrices which results in a bounded and non-increasing error in filter estimates which strengthens the reliability of the system.
- 5) The filter estimates obtained by the proposed algorithm are shown to converge to a region containing the actual filter. Moreover, upper bound for filter estimation error is derived for detailed convergence analysis.

The organization of this paper is as follows: In Section II, ANC system model is described. Filtered-x optimally weighted recursive least squares (FxOWRLS) algorithm and its convergence properties are derived in Section III for feedforward control filter. FxOWRLS algorithm for feedback control filter is provided in Section IV. The computational requirements are discussed in Section V. Analysis of the computer simulations is given in Section VI with concluding remarks in Section VII.

II. ANC SYSTEM MODEL

The block diagram of the proposed methodology is given in Fig. 2. The objective of the ANC system is to attenuate residual error, $e(n)$, using the feedforward noise control filter $W_f(z)$ and feedback noise control filter $W_b(z)$ (where n is for iteration, and z is for z -transform). Outputs of both $W_f(z)$ and $W_b(z)$ are used to generate the control signal $y(n)$. The reference signal for $W_f(z)$ is $x_f(n)$ which is detected by the reference microphone, while estimated signal $x_b(n)$ is the reference signal for $W_b(z)$. The control signal, $y(n)$, is obtained by summing the control signals, $y_1(n)$ and $y_2(n)$,

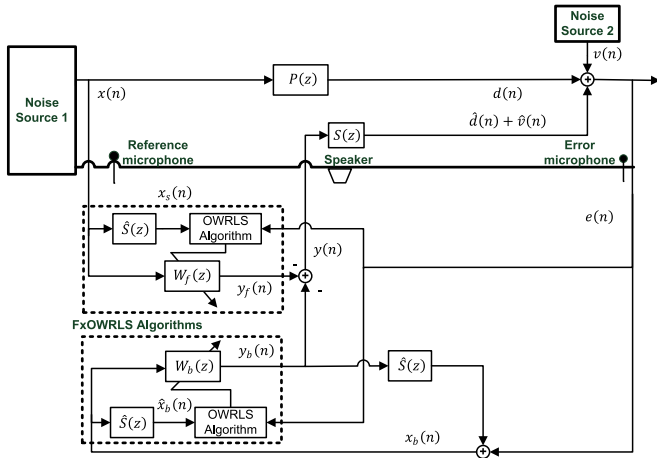


Fig. 2. Block diagram of the proposed method.

from $W_f(z)$ and $W_b(z)$, respectively

$$\begin{aligned} y(n) &= y_1(n) + y_2(n) \\ &= \mathbf{w}_f^T(n) \mathbf{x}_f(n) + \mathbf{w}_b^T(n) \mathbf{x}_b(n), \end{aligned} \quad (1)$$

where $\mathbf{w}_f(n)$ and $\mathbf{w}_b(n)$ are the coefficient vectors of $W_f(z)$ and $W_b(z)$, respectively, with

$$\mathbf{w}_f(n) = [w_{f,1}(n), w_{f,2}(n), \dots, w_{f,L_f}(n)]^T, \quad (2)$$

$$\mathbf{w}_b(n) = [w_{b,1}(n), w_{b,2}(n), \dots, w_{b,L_b}(n)]^T. \quad (3)$$

The lengths of $\mathbf{w}_f(n)$ and $\mathbf{w}_b(n)$ are L_f and L_b , respectively. Signal vectors $\mathbf{x}_f(n)$ and $\mathbf{x}_b(n)$ constitute the recent samples of $x(n)$ and $x_b(n)$, respectively

$$\mathbf{x}_f(n) = [x(n), x(n-1), \dots, x(n-(L_f-1))]^T, \quad (4)$$

$$\mathbf{x}_b(n) = [x_b(n), x_b(n-1), \dots, x_b(n-(L_b-1))]^T. \quad (5)$$

and $x_b(n)$ is the reference signal for $W_b(z)$

$$x_b(n) = e(n) + \hat{s}(n) * y_2(n), \quad (6)$$

where $*$ denotes the linear convolution and $\hat{s}(n)$ is the impulse response of estimated secondary path $\hat{S}(z)$. Signal, $e(n)$, is detected by an error microphone

$$\begin{aligned} e(n) &= d(n) + v(n) - (\hat{d}(n) + \hat{v}(n)) \\ &= p(n) * x(n) + v(n) - s(n) * y(n), \end{aligned} \quad (7)$$

where $p(n)$ is the impulse response of primary path $P(z)$, and $s(n)$ is the impulse response of secondary path $S(z)$. The uncorrelated disturbance, $v(n)$, in (7) is the noise component detected by the error microphone that is uncorrelated with $x(n)$, and $\hat{d}(n) + \hat{v}(n)$ is the noise cancelling signal. Filtered forms of reference signals, $\hat{x}_f(n)$ and $\hat{x}_b(n)$, are used to update the coefficients of $W_f(z)$ and $W_b(z)$, respectively. The filtered-x weighted recursive least squares (FxWRLS) algorithm [20] for $W_f(z)$ can be given as

$$\mathbf{w}_f(n) = \mathbf{w}_f(n-1) + \lambda_f P_f^{-1}(n) \hat{\mathbf{x}}_s(n) e(n),$$

where λ_f is the weighting factor and

$$\begin{aligned} P_f(n) &= P_f(n-1) + \lambda_f \hat{\mathbf{x}}_s(n) \hat{\mathbf{x}}_s^T(n), \\ \hat{\mathbf{x}}_s(n) &= [\hat{x}_s(n), \hat{x}_s(n-1), \dots, \hat{x}_s(n-(L_f-1))]^T, \\ \hat{x}_s(n) &= \hat{s}(n) * x(n). \end{aligned} \quad (8)$$

Using the matrix inversion lemma [18] and (8), $P_f^{-1}(n)$ can be written as

$$\begin{aligned} P_f^{-1}(n) &= P_f^{-1}(n-1) - \frac{\lambda_f P_f^{-1}(n-1) \hat{\mathbf{x}}_s(n) \hat{\mathbf{x}}_s^T(n) P_f^{-1}(n-1)}{1 + \lambda_f G_f(n)}, \\ G_f(n) &= \hat{\mathbf{x}}_s^T(n) P_f^{-1}(n-1) \hat{\mathbf{x}}_s(n). \end{aligned}$$

The FxWRLS algorithm for $W_b(z)$ with weighting factor, λ_b , can be given as

$$\begin{aligned} \mathbf{w}_b(n) &= \mathbf{w}_b(n-1) + \lambda_b P_b^{-1}(n) \hat{\mathbf{x}}_b(n) e(n), \\ P_b(n) &= P_b(n-1) + \lambda_b \hat{\mathbf{x}}_b(n) \hat{\mathbf{x}}_b^T(n), \\ P_b^{-1}(n) &= P_b^{-1}(n-1) - \frac{\lambda_b P_b^{-1}(n-1) \hat{\mathbf{x}}_b(n) \hat{\mathbf{x}}_b^T(n) P_b^{-1}(n-1)}{1 + \lambda_b G_b(n)}, \\ G_b(n) &= \hat{\mathbf{x}}_b^T(n) P_b^{-1}(n-1) \hat{\mathbf{x}}_b(n), \\ \hat{\mathbf{x}}_b(n) &= [\hat{x}_b(n), \hat{x}_b(n-1), \dots, \hat{x}_b(n-(L_b-1))]^T, \\ \hat{x}_b(n) &= \hat{s}(n) * x_b(n). \end{aligned}$$

For the conventional hybrid ANC system, the optimal filters are: $W_b(z) = -1/S(z)$ and $W_f(z) = -P(z)/[S(z)(1 + S(z)W_b(z))]$ [9]. Thus, filters $W_b(z)$ and $W_f(z)$ are coupled, and the phase difference between $S(z)/[1 + S(z)W_b(z)]$ and $S(z)$ may become greater than $\pi/2$ radians to cause the divergence of $W_f(z)$ [5], [8], [9]. This issue is resolved in the proposed algorithm. From Fig. 2, z -transform of the residual error signal can be expressed as

$$\begin{aligned} E(z) &= D(z) - \hat{D}(z) + V(z) \\ &= P(z)X(z) - S(z)Y(z) + V(z). \end{aligned} \quad (9)$$

Expression (1) becomes

$$Y(z) = W_f(z)X(z) + W_b(z)X_b(z). \quad (10)$$

Expression (6) can be written as

$$X_b(z) = \frac{E(z)}{1 + \hat{S}(z)W_b(z)}. \quad (11)$$

Substitute (10) and (11) in (9) and simplify the resulting expression

$$E(z) = \frac{1 + \hat{S}(z)W_b(z)}{1 + [\hat{S}(z) - S(z)]W_b(z)} [P(z)X(z) + V(z) + S(z)Y(z)]. \quad (12)$$

In this paper, the design of adaptive algorithms for noise control filters, $W_f(z)$ and $W_b(z)$, is addressed. Therefore, it is assumed that exact estimate of secondary path has been obtained, i.e., $\hat{S}(z) = S(z)$. Details on secondary path estimation can be found in [3], [4], [21]–[24]. If $\hat{S}(z) = S(z)$, expression (12) becomes

$$\begin{aligned} E(z) &= [1 + S(z)W_b(z)]V(z) \\ &\quad + [1 + S(z)W_b(z)][P(z) + S(z)W_f(z)]X(z). \end{aligned} \quad (13)$$

The first term in (13) is responsible for cancelling disturbance $v(n)$ and results in optimal $W_b(z)$ to be

$$W_b(z) = -\frac{1}{S(z)}. \quad (14)$$

The second term in (13) is responsible for the cancellation of $d(n)$, and optimal $W_f(z)$ is

$$W_f(z) = -\frac{P(z)}{S(z)}. \quad (15)$$

From (14) and (15), it is clear that the feedforward and feedback filters in the proposed method are decoupled, and can be updated independently. It can be observed from the second term in (13) that $W_f(z)$ and $W_b(z)$ are cascaded. The term $[1 + S(z)W_b(z)][P(z) + S(z)W_f(z)]$ is a product of both control structures. Filter $W_f(z)$ approximates (15) to achieve a negligible $[P(z) + S(z)W_f(z)]$, and $W_b(z)$ approximates (14) to mitigate the term $[1 + S(z)W_b(z)]$. Therefore, both filters are able to attenuate the noise independently.

III. FILTERED-X OPTIMALLY WEIGHTED RECURSIVE LEAST SQUARES ALGORITHM FOR $W_f(z)$

In practical parameter estimation schemes, the observation data is corrupted by noise. Normally, the noise is modeled as a stochastic process described by mean, covariance and noise autocorrelation model. The stochastic approach has two limitations. First, it is difficult to give an accurate statistical features to model the noise if it is not random. Second, the samples of the observation data, in most circumstances, are insufficient to determine the statistics [25]. An appropriate assumption is to consider the noise to be unknown but bounded. This situation arises frequently in control and signal processing. In speech processing systems, a similar bound is obeyed by disturbances in speech-band signals [20], [26]. In this section, FxOWRLS algorithm for feedforward noise control filter $W_f(z)$ is derived. The problem of interest for $W_f(z)$ is to cancel $d(n)$ in (7) and it can be written as [5]

$$\begin{aligned} e(n) &= p(n) * x(n) - s(n) * y(n) + v(n) \\ &= d(n) - s(n) * [\mathbf{w}_f^T(n)\mathbf{x}_f(n) + \mathbf{w}_b^T(n)\mathbf{x}_b(n)] + v(n) \\ &\approx d(n) - \mathbf{w}_f^T(n)\mathbf{x}_s(n) + v_f(n) \\ &= d_f(n) - \mathbf{w}_f^T(n)\mathbf{x}_s(n), \end{aligned} \quad (16)$$

where $v_f(n)$ acts as disturbance for $W_f(z)$ and

$$\begin{aligned} \mathbf{x}_s(n) &= [x_s(n), x_s(n-1), \dots, x_s(n-(L_f-1))]^T, \\ x_s(n) &= s(n) * x(n). \end{aligned}$$

Feedforward subsystem controlled by $W_f(z)$ can be given by

$$\begin{aligned} d_f(n) &= d(n) + v_f(n) \\ &= \mathbf{w}_f^T(n)\mathbf{x}_s(n) + v_f(n), \end{aligned} \quad (17)$$

where $d(n)$ is written in terms of the desired filter coefficients. Assume that $v_f(n)$ is bounded in magnitude for each n

$$v_f^2(n) \leq \gamma_f^2. \quad (18)$$

and γ_f is a known bound. Let $S_f(n)$ be a subset of \mathbb{R}^{L_f} defined by

$$S_f(n) = \{\mathbf{w}_f : (d_f(n) - \mathbf{w}_f^T \mathbf{x}_s(n))^2 \leq \gamma_f^2, \mathbf{w}_f \in \mathbb{R}^{L_f}\}.$$

The subset $S_f(n)$ is a convex polytope from a geometrical perspective [20]. Thus, a convex polytope in parameter space can be obtained from recent observation data, (17) and (18). Each $S_f(n)$ can be regarded as a degenerate ellipsoid in \mathbb{R}^{L_f} [20], [26]. Thus, the set of \mathbf{w}_f after n measurements is uniform with the measured data and the system. The set can be given by

$$\Theta_f(n) = \bigcap_{i=1}^n S_f(i).$$

Modeled controller, \mathbf{w}_f , must be contained by this intersection and any bounding ellipsoids. The recursive algorithm begins with adequately large ellipsoid that has all possible values of \mathbf{w}_f . After acquiring $(e(1), x(1))$, it identifies an ellipsoid, $E_f(1)$ bounding the intersection of $S_f(1)$ and initial ellipsoid. Similarly, a sequence of bounding ellipsoids, $E_f(n)$ can be obtained. The center of $E_f(n)$ defines the estimate for \mathbf{w}_f at iteration n . Assume that the actual coefficient vector \mathbf{w}_f^* lies within ellipsoid $E_f(n-1)$ at instant $(n-1)$ which is given by

$$\begin{aligned} E_f(n-1) &= \{\mathbf{w}_f : (\mathbf{w}_f - \mathbf{w}_f(n-1))^T P_f(n-1) \\ &\quad \times (\mathbf{w}_f - \mathbf{w}_f(n-1)) \leq \sigma_f^2(n-1)\}, \end{aligned}$$

where $P_f(n-1)$ is a $L_f \times L_f$ positive definite symmetric matrix and $\sigma_f(n-1)$ is a scalar. The estimate of the desired controller coefficients at instant $(n-1)$, $\mathbf{w}_f(n-1)$, is also the center of the ellipsoid $E_f(n-1)$. Now, the set of \mathbf{w}_f which is consistent with $S_f(n)$, $E_f(n-1)$, and the system is $S_f(n) \cap E_f(n-1)$. Generally, $S_f(n) \cap E_f(n-1)$ is not a regular convex set. Therefore, it is desired to obtain an ellipsoid $E_f(n)$ with $E_f(n) \supset (E_f(n-1) \cup S_f(n))$. Consequently, an ellipsoid bounding $S_f(n) \cup E_f(n-1)$ can be defined as

$$\begin{aligned} &(\mathbf{w}_f - \mathbf{w}_f(n-1))^T P_f(n-1) (\mathbf{w}_f - \mathbf{w}_f(n-1)) \\ &+ \lambda_f(n) (d_f(n) - \mathbf{w}_f^T \mathbf{x}_s(n))^2 \leq \sigma_f^2(n-1) + \lambda_f(n) \gamma_f^2, \end{aligned} \quad (19)$$

where variable weighting factor $\lambda_f(n) \geq 0$.

Theorem 1 The ellipsoid defined in (19) along with (16) and the following equalities

$$\mathbf{w}_f(n) = \mathbf{w}_f(n-1) + \lambda_f(n) P_f^{-1}(n) \mathbf{x}_s(n) e(n), \quad (20)$$

$$P_f(n) = P_f(n-1) + \lambda_f(n) \mathbf{x}_s(n) \mathbf{x}_s^T(n), \quad (21)$$

$$\mathbf{x}_s(n) = [x_s(n), x_s(n-1), \dots, x_s(n-(L_f-1))]^T, \quad (22)$$

$$x_s(n) = s(n) * x(n), \quad (23)$$

$$P_f^{-1}(n) = P_f^{-1}(n-1) \left(1 - \frac{\lambda_f(n) \mathbf{x}_s(n) \mathbf{x}_s^T(n) P_f^{-1}(n-1)}{1 + \lambda_f(n) G_f(n)} \right), \quad (24)$$

$$G_f(n) = \mathbf{x}_s^T(n) P_f^{-1}(n-1) \mathbf{x}_s(n), \quad (25)$$

$$\sigma_f^2(n) = \sigma_f^2(n-1) + \lambda_f(n) \gamma_f^2 - \frac{\lambda_f(n) e^2(n)}{1 + \lambda_f(n) G_f(n)}, \quad (26)$$

is analogous to the ellipsoid

$$E_f(n) = \{\mathbf{w}_f : (\mathbf{w}_f - \mathbf{w}_f(n))^T P_f(n)(\mathbf{w}_f - \mathbf{w}_f(n)) \leq \sigma_f^2(n), \quad (27)$$

where $P_f(n)$ is a $L_f \times L_f$ positive definite symmetric matrix, $\lambda_f(n)$, $\sigma_f(n)$, $\sigma_f(n-1)$, γ_f , $e(n)$ and $x(n)$ are scalars, and $\mathbf{w}_f(n)$, $\mathbf{w}_f(n-1)$ and $\mathbf{x}_s(n)$ are L_f dimensional vectors.

Proof: Expand the left hand side of (19) and substitute $P_f(n-1)$ from (21)

$$\begin{aligned} & \mathbf{w}_f^T P_f(n) \mathbf{w}_f - 2\mathbf{w}_f^T P_f(n-1) \mathbf{w}_f(n-1) + \lambda_f(n) d_f^2(n) \\ & + \mathbf{w}_f^T(n-1) P_f(n-1) \mathbf{w}_f(n-1) - 2\lambda_f(n) d_f(n) \mathbf{w}_f^T(n) \mathbf{x}_s(n) \\ & \leq \sigma_f^2(n-1) + \lambda_f(n) \gamma_f^2. \end{aligned} \quad (28)$$

The first term in $\mathbf{w}_f^T P_f(n) \mathbf{w}_f$ can be written as

$$\begin{aligned} \mathbf{w}_f^T P_f(n) \mathbf{w}_f &= (\mathbf{w}_f - \mathbf{w}_f(n))^T P_f(n)(\mathbf{w}_f - \mathbf{w}_f(n)) \\ & + 2\mathbf{w}_f^T P_f(n) \mathbf{w}_f(n) - \mathbf{w}_f^T(n) P_f(n) \mathbf{w}_f(n). \end{aligned} \quad (29)$$

Substitute (29) into (28) and simplify the resulting expression

$$\begin{aligned} & (\mathbf{w}_f - \mathbf{w}_f(n))^T P_f(n)(\mathbf{w}_f - \mathbf{w}_f(n)) - \mathbf{w}_f^T(n) P_f(n) \mathbf{w}_f(n) \\ & + \mathbf{w}_f^T(n-1) P_f(n-1) \mathbf{w}_f(n-1) + \lambda_f(n) d_f^2(n) \leq \sigma_f^2(n-1) \\ & + \lambda_f(n) \gamma_f^2. \end{aligned} \quad (30)$$

Substitute (24) into (20) and simplify the resulting expression

$$\mathbf{w}_f(n) = \mathbf{w}_f(n-1) + \frac{\lambda_f(n) P_f^{-1}(n-1) \mathbf{x}_s(n) e(n)}{1 + \lambda_f(n) G_f(n)}. \quad (31)$$

Multiply both sides of (24) with $P_f(n-1) \mathbf{w}_f(n-1) + \lambda_f(n) \mathbf{x}_s(n) d_f(n)$ results in

$$\begin{aligned} & P_f^{-1}(n) [P_f(n-1) \mathbf{w}_f(n-1) + \lambda_f(n) \mathbf{x}_s(n) d_f(n)] \\ & = \mathbf{w}_f(n-1) + \frac{\lambda_f(n) P_f^{-1}(n-1) \mathbf{x}_s(n) e(n)}{1 + \lambda_f(n) G_f(n)}, \end{aligned} \quad (32)$$

Compare (31) and (32) to obtain

$$\mathbf{w}_f(n) = P_f^{-1}(n) [P_f(n-1) \mathbf{w}_f(n-1) + \lambda_f(n) \mathbf{x}_s(n) d_f(n)]. \quad (33)$$

From (33), obtain the expression for $\mathbf{w}_f^T(n-1) P_f(n-1) \mathbf{w}_f(n-1)$ by using (20)

$$\begin{aligned} & \mathbf{w}_f^T(n-1) P_f(n-1) \mathbf{w}_f(n-1) = \mathbf{w}_f^T(n) P_f(n) \mathbf{w}_f(n) \\ & - \lambda_f(n) \mathbf{w}_f^T(n) \mathbf{x}_s(n) e(n) - \lambda_f(n) \mathbf{w}_f^T(n-1) \mathbf{x}_s(n) d_f(n), \end{aligned} \quad (34)$$

Substitute (34) into (30) to obtain

$$\begin{aligned} & (\mathbf{w}_f - \mathbf{w}_f(n))^T P_f(n)(\mathbf{w}_f - \mathbf{w}_f(n)) + \lambda_f(n) d_f^2(n) \\ & - \lambda_f(n) \mathbf{w}_f^T(n) \mathbf{x}_s(n) e(n) - \lambda_f(n) \mathbf{w}_f^T(n-1) \mathbf{x}_s(n) d_f(n) \\ & \leq \sigma_f^2(n-1) + \lambda_f(n) \gamma_f^2. \end{aligned}$$

Using (31)

$$\begin{aligned} & (\mathbf{w}_f - \mathbf{w}_f(n))^T P_f(n)(\mathbf{w}_f - \mathbf{w}_f(n)) \leq \sigma_f^2(n-1) + \lambda_f(n) \gamma_f^2 \\ & - \frac{\lambda_f(n) e^2(n)}{1 + \lambda_f(n) G_f(n)}, \end{aligned}$$

which is equivalent to (27) with the definition of $\sigma_f^2(n)$ in (26). \square

A. Optimum Value for $\lambda_f(n)$

It is established in Theorem 1 that (27), with the equalities provided in (20)-(26), is a bounding ellipsoid. An optimal bounding ellipsoid corresponds to a minimum $\sigma_f^2(n)$ in (26), since $\sigma_f^2(n)$ stands for the bound on the filter estimation error. From analytical perspective, a natural bound on a Lyapunov function (see Theorem 2) is also $\sigma_f^2(n)$. Thus, minimization of $\sigma_f^2(n)$ with respect to $\lambda_f(n)$ can improve the convergence with a computationally simple evaluation criterion.

It is clear from (26), $\sigma_f^2(n) = \sigma_f^2(n-1)$ for $\lambda_f(n) = 0$. This means $\sigma_f^2(n) \leq \sigma_f^2(n-1)$ for the optimum value of $\lambda_f(n)$. Thus if

$$\frac{d\sigma_f^2(n)}{d\lambda_f(n)} \geq 0, \quad \text{for } \lambda_f(n) \geq 0,$$

then the new data does not have information to improve $\sigma_f^2(n)$, and filter update is not required. Hence zero is the optimum value for $\lambda_f(n)$. From (26)

$$\frac{d\sigma_f^2(n)}{d\lambda_f(n)} = \gamma_f^2 - \frac{e^2(n)}{(1 + \lambda_f(n) G_f(n))^2},$$

and

$$\frac{d^2\sigma_f^2(n)}{d\lambda_f^2(n)} = \frac{2e^2(n) G_f(n)}{(1 + \lambda_f(n) G_f(n))^3}.$$

If $e^2(n) G_f(n) \neq 0$, the positive definiteness of $P_f^{-1}(n)$ implies that $d^2\sigma_f^2(n)/d\lambda_f^2(n)$ has the same sign as $(1 + \lambda_f(n) G_f(n))$. Therefore, $d^2\sigma_f^2(n)/d\lambda_f^2(n) \geq 0$ and $\sigma_f^2(n)$ is minimized for positive $\lambda_f(n)$. Set $d\sigma_f^2(n)/d\lambda_f(n) = 0$ and write the expression in terms of $\lambda_f(n)$

$$\lambda_f(n) = \frac{|e(n)| - \gamma_f}{\gamma_f G_f(n)}, \quad \text{if } |e(n)| > \gamma_f \quad (35)$$

where the positive value of $\lambda_f(n)$ is guaranteed by the if-check. Similarly, $\lambda_f(n) = 0$ for $|e(n)| < \gamma_f$. FxOWRLS algorithm for $W_f(z)$ can be implemented by (20) to (26) with optimal weighting factor $\lambda_f(n)$ provided in (35).

B. Convergence Analysis

The convergence properties of the proposed algorithm are established in this section. The filter estimate obtained by the proposed algorithm is shown to converge to a region containing the actual filter. The derived method can guarantee positive definite covariance matrix which results in a bounded and non-increasing error in filter estimate. Finally, upper bound for error in filter estimate is derived. These properties strengthen the reliability of the system.

Theorem 2: Suppose $\mathbf{w}_f^* \in E_f(0)$, then $\mathbf{w}_f^* \in E_f(n)$ for all n .

Proof: Consider using the Lyapunov function

$$V_f(n) = \Delta \mathbf{w}_f^T(n) P_f(n) \Delta \mathbf{w}_f(n) \quad (36)$$

where $\Delta \mathbf{w}_f(n) = \mathbf{w}_f^* - \mathbf{w}_f(n)$. Using (16), (17), (20) and (21), expression (36) can be written as

$$V_f(n) = V_f(n-1) + \lambda_f(n)v_f^2(n) - \lambda_f(n)e^2(n)[1 - \lambda_f(n)\mathbf{x}_s^T(n)P_f^{-1}(n)\mathbf{x}_s(n)]. \quad (37)$$

From (24), $\mathbf{x}_s^T(n)P_f^{-1}(n)\mathbf{x}_s(n)$ can be given by

$$\mathbf{x}_s^T(n)P_f^{-1}(n)\mathbf{x}_s(n) = \frac{G_f(n)}{1 + \lambda_f(n)G_f(n)}. \quad (38)$$

Substitute (38) in (37) and simplify the resulting expression

$$V_f(n) = V_f(n-1) + \lambda_f(n)\left[v_f^2(n) - \frac{e^2(n)}{1 + \lambda_f(n)G_f(n)}\right] \leq V_f(n-1) + \lambda_f(n)\left[\gamma_f^2 - \frac{e^2(n)}{1 + \lambda_f(n)G_f(n)}\right], \quad (39)$$

Using (26)

$$V_f(n) - \sigma_f^2(n) \leq V_f(n-1) - \sigma_f^2(n-1).$$

Note that

$$V_f(n-1) \leq \sigma_f^2(n-1) \text{ if and only if } \mathbf{w}_f^* \in E_f(n-1)$$

which implies

$$V_f(n) \leq \sigma_f^2(n) \text{ implies } \mathbf{w}_f^* \in E_f(n).$$

This completes the proof of Theorem 2. \square

Remark 1: The proposed method is established on $\mathbf{w}_f^* \in E_f(0)$ and the filter estimates obtained by the proposed algorithm converge to a region containing the actual filter.

Theorem 3: For any bounded filtered- x vector sequence $\mathbf{x}_s(n)$, the proposed algorithm exhibits the following properties

- 1) $\|\Delta \mathbf{w}_f(n)\|$ is bounded and non-increasing
- 2) $\lim_{n \rightarrow \infty} \|\Delta \mathbf{w}_f(n) - \Delta \mathbf{w}_f(n-1)\|^2 = 0$
- 3) $e^2(n)$ is bounded
- 4) $\lim_{n \rightarrow \infty} \lambda_f(n) = 0$

Proof: Each of the aforementioned properties are proven in sequence.

(1): Define

$$f(\lambda_f(n)) = \lambda_f(n)\left[\gamma_f^2 - \frac{e^2(n)}{1 + \lambda_f(n)G_f(n)}\right]. \quad (40)$$

Then (39) can be written as

$$V_f(n) \leq V_f(n-1) + f(\lambda_f(n)). \quad (41)$$

Term $f(\lambda_f(n)) \leq 0$ for

$$\lambda_f(n) \in [0, \frac{1}{\gamma_f^2 G_f(n)}(e^2(n) - \gamma_f^2)].$$

This means that

$$V_f(n) \leq V_f(n-1),$$

or

$$\Delta \mathbf{w}_f^T(n)P_f(n)\Delta \mathbf{w}_f(n) \leq \Delta \mathbf{w}_f^T(n-1)P_f(n-1)\Delta \mathbf{w}_f(n-1).$$

From (21), we have

$$P_f(n) \geq P_f(n-1),$$

which means

$$\|\Delta \mathbf{w}_f(n)\|^2 \leq \|\Delta \mathbf{w}_f(n-1)\|^2. \quad (42)$$

Thus, $\|\Delta \mathbf{w}_f(n)\|$ is bounded and non-increasing. This is the most desirable property for selective updating of adaptive filters [18].

(2): From (41)

$$V_f(n) \leq V_f(0) + \sum_{i=1}^n f(\lambda_f(i)) \leq V_f(0).$$

This implies bounded and non-increasing property of $V_f(n)$. Therefore, $\lim_{n \rightarrow \infty} V_f(n)$ exists. Thus

$$-\sum_{i=1}^{\infty} f(\lambda_f(i)) \leq \infty \text{ and } \lim_{n \rightarrow \infty} f(\lambda_f(n)) = 0. \quad (43)$$

Using $\lambda_f(n)$ from (35), expression (24) becomes

$$P_f^{-1}(n) = P_f^{-1}(n-1) - \frac{P_f^{-1}(n-1)\mathbf{x}_s(n)\mathbf{x}_s^T(n)P_f^{-1}(n-1)}{G_f(n)}\left(1 - \frac{\gamma_f}{|e(n)|}\right), \quad (44)$$

for $\gamma_f < |e(n)|$, and otherwise $P_f^{-1}(n) = P_f^{-1}(n-1)$. Similarly, by using (35) and (44), expression (20) can be written as

$$\mathbf{w}_f(n) = \mathbf{w}_f(n-1) + \frac{P_f^{-1}(n-1)\mathbf{x}_s(n)}{|e(n)|G_f(n)}(|e(n)| - \gamma_f)e(n), \quad (45)$$

for $|e(n)| > \gamma_f$. Therefore, $\|\Delta \mathbf{w}_f(n) - \Delta \mathbf{w}_f(n-1)\|^2$ can be obtained from (45)

$$\begin{aligned} \|\Delta \mathbf{w}_f(n) - \Delta \mathbf{w}_f(n-1)\|^2 &\leq \frac{\mathbf{x}_s^T(n)K_f^2(n-1)\mathbf{x}_s(n)(|e(n)| - \gamma_f)^2}{G_f^2(n)} \\ &\leq \frac{\lambda_{\max}(P_f^{-1}(n-1))}{G_f(n)}(|e(n)| - \gamma_f)^2 \\ &\leq \frac{\lambda_{\max}(P_f^{-1}(0))}{G_f(n)}(|e(n)| - \gamma_f)^2, \end{aligned} \quad (46)$$

where $K_f(n-1) = P_f^{-1}(n-1)$. Writing (46) in terms of $\lambda_f(n)$ gives

$$\|\Delta \mathbf{w}_f(n) - \Delta \mathbf{w}_f(n-1)\|^2 \leq \lambda_{\max}(P_f^{-1}(0))\lambda_f(n) \times (|e(n)| - \gamma_f)\gamma_f. \quad (47)$$

In the derivation of (35), it was mentioned that filter update is not performed when $\gamma_f^2 \geq e^2(n)$ and this means $\|\Delta \mathbf{w}_f(n) - \Delta \mathbf{w}_f(n-1)\|^2 = 0$. Otherwise (35) is used to obtain optimal $\lambda_f(n)$. Using (35), expression (40) can be written as

$$f(\lambda_f(n)) = \lambda_f(n)(\gamma_f - |e(n)|)\gamma_f, \quad (48)$$

and (47) becomes

$$\|\Delta \mathbf{w}_f(n) - \Delta \mathbf{w}_f(n-1)\|^2 \leq -\lambda_{\max}(P(0))f(\lambda_f(n)),$$

TABLE I

COMPUTATIONAL REQUIREMENTS FOR VARIOUS HYBRID ANC SYSTEMS

	Additions	Multiplications
Hybrid [14]	$2L_f + 2L_b + 3L_s - 3$	$2L_f + 2L_b + 3L_s + 2$
Akhtar's method [13]	$2L_f + 2L_b + 2L_h + 3L_s - 3$	$2L_f + 2L_b + 2L_h + 3L_s + 3$
Laleh's method [10]	$2L_f + 2L_b + 3L_s + 7$	$2L_f + 2L_b + 3L_s + 18$
Wu's method [9]	$2L_f + 2L_b + 3L_s - 3$	$2L_f + 2L_b + 3L_s + 2$
Trideba's method [8]	$2L_f + 2L_b + 3L_h + 3L_s - 2$	$2L_f + 2L_b + 3L_h + 3L_s + 11$
Proposed method maximum ^a	$L_f^2 + L_b^2 + 3(L_f + L_b + L_s) - 1$	$L_f^2 + L_b^2 + 5(L_f + L_b) + 3L_s + 3$
Proposed method minimum ^b	$L_f + L_b + 3L_s - 1$	$L_f + L_b + 3L_s + 1$

^a maximum: Both $\mathbf{w}_f(n)$ and $\mathbf{w}_b(n)$ are updated.

^b minimum: Without controller update.

and

$$\lim_{n \rightarrow \infty} \|\Delta \mathbf{w}_f(n) - \Delta \mathbf{w}_f(n-1)\|^2 = 0.$$

This proves (2).

(3): From (16) and (17), we get

$$e(n) = \mathbf{x}_s^T(n) \Delta \mathbf{w}_f(n-1) + v_f(n), \quad (49)$$

and

$$|e(n)| \leq \|\mathbf{x}_s(n)\| \|\Delta \mathbf{w}_f(n-1)\| + |v_f(n)|. \quad (50)$$

 From (18) and (42), $|v_f(n)| \leq \gamma_f$ and $\|\Delta \mathbf{w}_f(n-1)\|^2 \leq \|\Delta \mathbf{w}_f(0)\|^2$. Filtered-x reference vector $\mathbf{x}_s(n)$ is also bounded. It follows from (50) that $e^2(n)$ is bounded.

 (4): From (43) and (48), it can be seen that $\lim_{n \rightarrow \infty} \lambda_f(n) = 0$. \square

Remark 2: It should be noted that the proposed method can guarantee positive definite covariance matrix and results in a bounded and non-increasing error in filter estimate. The reliability of the system strengthens as $e^2(n)$ remains bounded. The small value of $\lambda_f(n)$ with large iteration shows that the system has reached the steady state and updating the noise control filter will not improve the system performance. Therefore, computations can be avoided without compromising the system performance.

A condition of persistent excitation is imposed to establish the result on the convergent region. The filtered-x reference vector $\{\mathbf{x}_s^T(n)\}$ is said to be persistently exciting, if there exist positive constants a_1 and a_2 for some constant integer M and all k such that [20]

$$0 < a_1 \mathbf{I} \leq \sum_{j=k}^{k+M} \mathbf{x}_s(j) \mathbf{x}_s^T(j) \leq a_2 \mathbf{I} < \infty. \quad (51)$$

Theorem 4: If the filtered-x reference vector $\{\mathbf{x}_s^T(n)\}$ is persistently exciting, then the noise filter estimate given by the proposed algorithm converges to a region as specified below

$$\lim_{n \rightarrow \infty} \|\Delta \mathbf{w}_f(n)\|^2 \leq \frac{4M\gamma_f^2}{a_1}.$$

TABLE II

COMPUTATIONAL REQUIREMENTS FOR VARIOUS FEEDFORWARD ANC SYSTEMS

	Additions	Multiplications
Shakeel's method [23]	$4L_f + 2L_s - 1$	$4L_f + 2L_s + 5$
Lopes's method [24]	$4L_f + 2L_s - 1$	$4L_f + 2L_s + 5$
Saeed's method [3]	$2L_f + L_s - 2$	$2L_f + L_s + 1$
Saeed's method [2]		
$\mathbf{w}_f(n)$ is updated	$L_f^2 + 3L_f + L_s + 1$	$L_f^2 + 5L_f + L_s + 3$
No filter update	$L_f + L_s + 1$	$L_f + L_s + 3$
Proposed method*		
$\mathbf{w}_f(n)$ is updated	$L_f^2 + 3L_f + L_s - 1$	$L_f^2 + 5L_f + L_s + 1$
No filter update	$L_f + L_s - 1$	$L_f + L_s$

* Feedforward noise control filter only.

TABLE III

NORMALIZED MEMORY REQUIREMENTS FOR VARIOUS ANC SYSTEMS

	Number of variables to be stored
Shakeel's method [23]	$3L_f + 2L_s + 9$
Lopes's method [24]	$3L_f + 2L_s + 10$
Saeed's method [3]	$3L_f + 2L_s + 4$
Hybrid [14]	$3L_f + 3L_b + 4L_s + 7$
Akhtar's method [13]	$3L_f + 3L_b + 2L_h + 4L_s + 11$
Laleh's method [10]	$3L_f + 3L_b + 4L_s + 13$
Wu's method [9]	$3L_f + 3L_b + 4L_s + 7$
Trideba's method [8]	$3L_f + 3L_b + 2L_h + 4L_s + 17$
Saeed's method [2]	$L_f^2 + 3L_f + 2L_s + 7$
Proposed method ($W_f(z)$ only)	$L_f^2 + 3L_f + 2L_s + 9$
Proposed method	$L_f^2 + L_b^2 + 3L_f + 3L_b + 4L_s + 11$

TABLE IV

PARAMETER VALUES USED IN THE SIMULATIONS

	Parameters
Shakeel's method [23]	$\mu_1 = 3 \times 10^{-1}, \mu_2 = 8 \times 10^{-2}, \lambda = 0.99, \alpha = 0.997, \gamma_{max} = 0.9, \gamma_{min} = 0.3$
Lopes's method [24]	$\mu = 0.5, \mu_s = 0.5, \lambda = 0.9, k_r = 0.1, \beta = 40, A = 2$
Saeed's method [3]	$\mu_w = 1 \times 10^{-4}, \lambda = 0.99$
Hybrid [14]	$\mu_{wf} = 1 \times 10^{-5}, \mu_{wb} = 1 \times 10^{-6}$
Akhtar's method [13]	$\mu_{wf} = 1 \times 10^{-5}, \mu_{wb} = 5 \times 10^{-6}, \mu_{wh} = 1 \times 10^{-3}$
Laleh's method [10]	$\lambda = 0.99, Constant_{wf} = 16, Constant_{wb} = 16$
Wu's method [9]	$\mu_{wf} = 1 \times 10^{-5}, \mu_{wb} = 1 \times 10^{-6}$
Trideba's method [8]	$\mu_{wf} = 1 \times 10^{-5}, \mu_{wb} = 5 \times 10^{-6}, \mu_{wh} = 1 \times 10^{-3}$
Saeed's method [2]	$\alpha = 0.99, \beta_w = 1.5$
Proposed method	$\lambda = 0.99, \gamma_f = \gamma_b = 0.05$

Proof: Define

$$\dot{e}(n) = \mathbf{x}_s^T(n) \Delta \mathbf{w}_f(n) + v_f(n).$$

Using (45) and (49)

$$\dot{e}(n) = \frac{e(n)}{1 + \lambda_f(n) G_f(n)}.$$

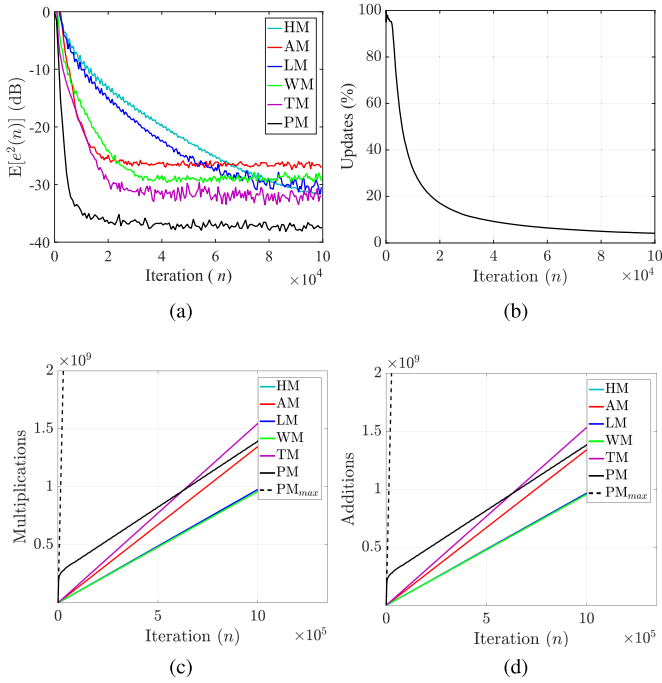


Fig. 3. Performance comparison for Case 1. (a) The mean-squared error. (b) Update percentage. (c) Total multiplications. (d) Total additions.

Thus $|\dot{e}(n)| \leq |e(n)|$ and

$$\begin{aligned} |\mathbf{x}_s^T(n) \Delta \mathbf{w}_f(n)| &\leq |\mathbf{x}_s^T(n) \Delta \mathbf{w}_f(n-1)| \\ &\leq |\mathbf{x}_s^T(n) \Delta \mathbf{w}_f(n-1) + v_f(n)| + |v_f(n)| \\ &\leq |e(n)| + \gamma_f. \end{aligned}$$

From the fact that

$$\lim_{n \rightarrow \infty} \lambda_f(n) = \lim_{n \rightarrow \infty} \frac{1}{\gamma_f G_f(n)} [|e(n)| - \gamma_f] = 0$$

we have

$$\limsup_{n \rightarrow \infty} |e(n)| \leq \gamma_f,$$

and

$$\begin{aligned} \limsup_{n \rightarrow \infty} (\mathbf{x}_s^T(n) \Delta \mathbf{w}_f(n))^2 &\leq \limsup_{n \rightarrow \infty} (|e(n)| + \gamma_f)^2 \\ &\leq 4\gamma_f^2. \end{aligned}$$

That is

$$\limsup_{n \rightarrow \infty} \sum_{i=n}^{n+M} \Delta \mathbf{w}_f^T(i) \mathbf{x}_s(i) \mathbf{x}_s^T(i) \Delta \mathbf{w}_f(i) \leq 4M\gamma_f^2.$$

Using Schwartz's inequality [26], we get

$$\limsup_{n \rightarrow \infty} \Delta \mathbf{w}_f^T(n) \left(\sum_{i=n}^{n+M} \mathbf{x}_s(i) \mathbf{x}_s^T(i) \right) \Delta \mathbf{w}_f(n) \leq 4M\gamma_f^2.$$

From (51), we obtain

$$\begin{aligned} a_1 \lim_{n \rightarrow \infty} \|\Delta \mathbf{w}_f(n)\|^2 &\leq \lim_{n \rightarrow \infty} \Delta \mathbf{w}_f^T(n) \\ &\quad \times \left(\sum_{i=n}^{n+M} \mathbf{x}_s(i) \mathbf{x}_s^T(i) \right) \Delta \mathbf{w}_f(n) \\ &\leq 4M\gamma_f^2. \end{aligned}$$

This completes the proof and gives a bound for error in filter estimates in terms of persistent excitation condition (51) and disturbance bound $\gamma_f(n)$. \square

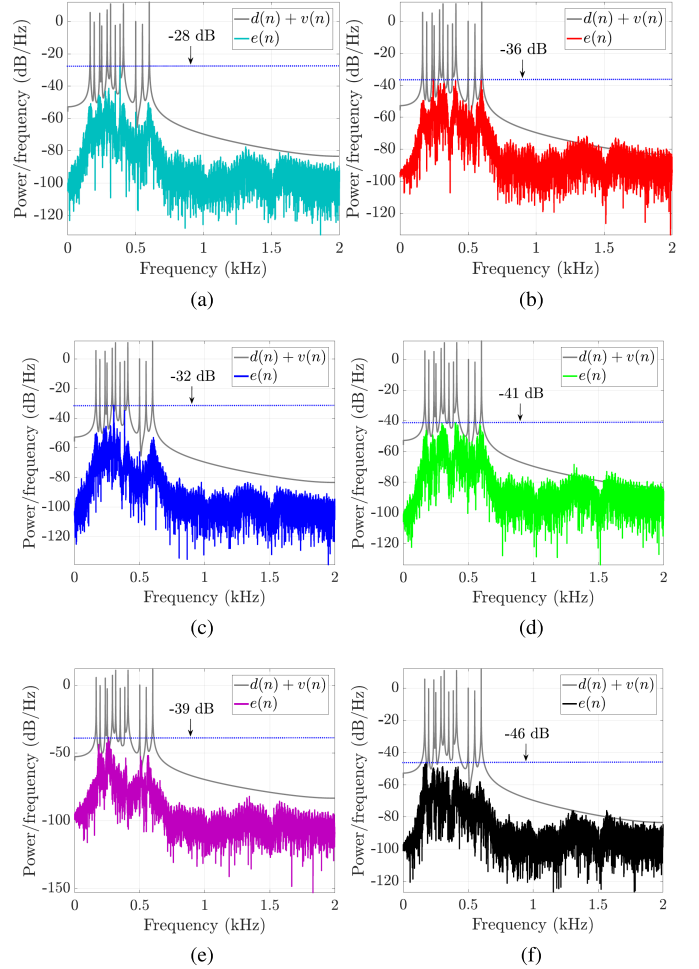


Fig. 4. Power spectra comparison for Case 1. (a) HM. (b) AM. (c) LM. (d) WM. (e) TM. (f) PM.

Remark 3: For a controllable and observable system, persistent excitation can be guaranteed by $\{\mathbf{x}_s(n)\}$ if the frequency of the input signal $x(n)$ is sufficiently rich, and either $x(n)$ and noise are uncorrelated or excitation level of $x(n)$ is enough to outdo the effect of the noise signal [20], [26].

IV. FILTERED-X OPTIMALLY WEIGHTED RECURSIVE LEAST SQUARES ALGORITHM FOR $W_b(z)$

Following the procedure for $W_f(z)$, FxOWRLS algorithm for $W_b(z)$ can be written as

$$\mathbf{w}_b(n) = \mathbf{w}_b(n-1) + \lambda_b P_b^{-1}(n) \mathbf{x}_b(n) e(n), \quad (52)$$

$$P_b(n) = P_b(n-1) + \lambda_b(n) \mathbf{x}_b(n) \mathbf{x}_b^T(n), \quad (53)$$

$$P_b^{-1}(n) = P_b^{-1}(n-1) \left(1 - \frac{\lambda_b(n) \mathbf{x}_b(n) \mathbf{x}_b^T(n) P_b^{-1}(n-1)}{1 + \lambda_b(n) G_b(n)} \right), \quad (54)$$

$$G_b(n) = \mathbf{x}_b^T(n) P_b^{-1}(n-1) \mathbf{x}_b(n), \quad (55)$$

$$\mathbf{x}_b(n) = [x_b(n), x_b(n-1), \dots, x_b(n-(L_b-1))]^T, \quad (56)$$

$$x_b(n) = s(n) * x_b(n), \quad (57)$$

$$\lambda_b(n) = \frac{|e(n)| - \gamma_b}{\gamma_b G_b(n)}, \quad \text{if } |e(n)| > \gamma_b. \quad (58)$$

where γ_b is a scalar bound for disturbance to $W_b(z)$.

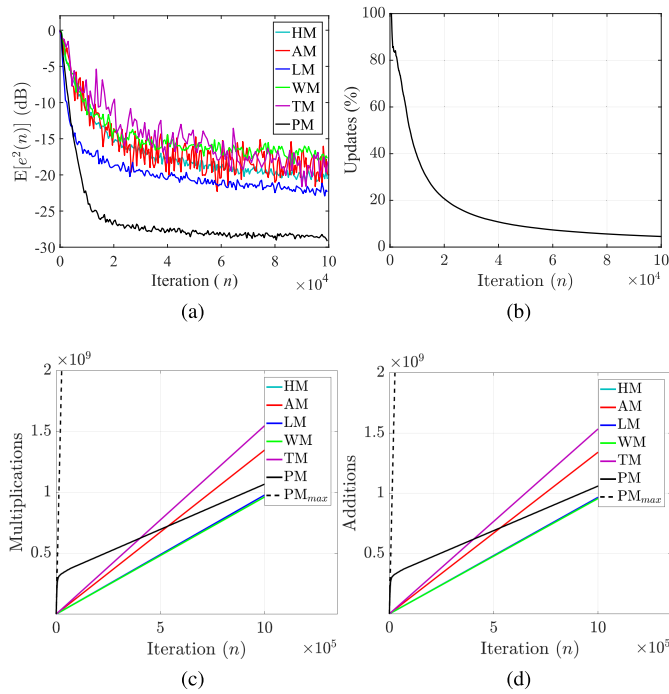


Fig. 5. Performance comparison for Case 2. (a) The mean-squared error. (b) Update percentage. (c) Total multiplications. (d) Total additions.

V. COMPUTATIONAL COMPLEXITY

This section presents the computational complexity of various methods discussed in this paper using standard figure of merit which is the number of multiplications and additions per iteration as given in Table I [2], [3], [18], [23]. Computational complexity could be a secondary issue with the evolution of economical and powerful signal processing hardware, but reduced computational demand is a preferred feature for processors running multiple applications such as mobile phones and noise cancelling headphones. Moreover, reduced operations can contribute to lowering power consumption for long battery life. Algorithms in [8]–[10], [13], [14] use LMS variants with low computational needs. In the proposed algorithm, expressions (24) and (54) require high computations. Computations of the FxOWRLS algorithms for $W_f(z)$ and $W_b(z)$ are calculated by implementation scheme of [27]. In Table I, there are two possible entries for the proposed algorithm at each iteration. In the maximum entry, both $W_f(z)$ and $W_b(z)$ are updated and the operations for the proposed method are large in comparison with the previous methods. In the minimum entry, no filter update is performed and the proposed method requires less computations than previous methods. Computational complexity of the proposed method with only feedforward filter and the previously established feedforward ANC systems [2], [3], [23], [24] is presented in Table II. At start-up and during perturbations, computations for the proposed method switch to maximum entry while minimum entry is valid in the steady state. The decision to switch between maximum and minimum entry is based on expressions (35) and (58). Apart from the operations required per iteration, memory usage is a reasonable measure taking into account the adaptive algorithms discussed in this paper.

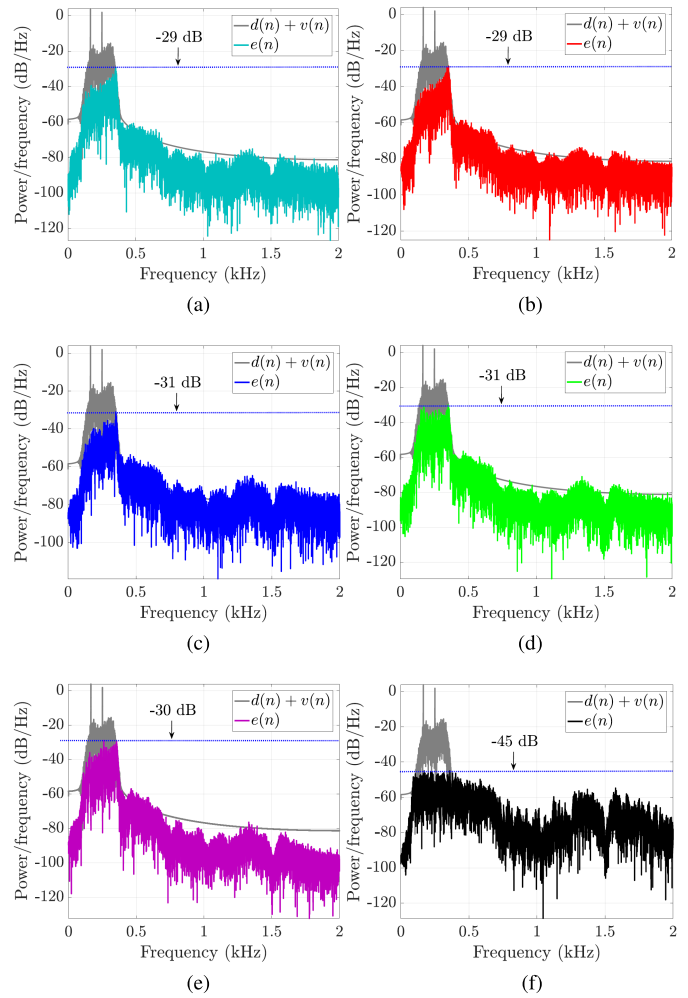


Fig. 6. Power spectra comparison for Case 2. (a) HM. (b) AM. (c) LM. (d) WM. (e) TM. (f) PM.

In terms of normalized memory requirements, the number of variables to be stored at each iteration are listed in Table III. The term normalized refers to number of variables used as unit of memory instead of bytes. Method in [2] and the proposed method require more variables due to the LS method than the methods reported in [3], [8]–[10], [13], [14], [23], [24]. The high memory requirement is the cost for improving the convergence and steady state performance. The memory requirements are fixed throughout the operation while multiplications and additions performed at each iteration may be different. Therefore, only multiplications and additions are considered in Section VI.

VI. CASE STUDIES

The performance of the proposed algorithm, under standard disturbance conditions, is compared with Hybrid (HM) [14], Akhtar (AM) [13], Laleh (LM) [10], Wu (WM) [9] and Trideba (TM) [8] in terms of mean-squared error, convergence speed, computational complexity and number of tunable parameters. Simulations are performed using parameter values listed in Table IV and sampling frequency is 4 kHz. Benchmark acoustic paths are taken from [5]. Coefficient vectors of

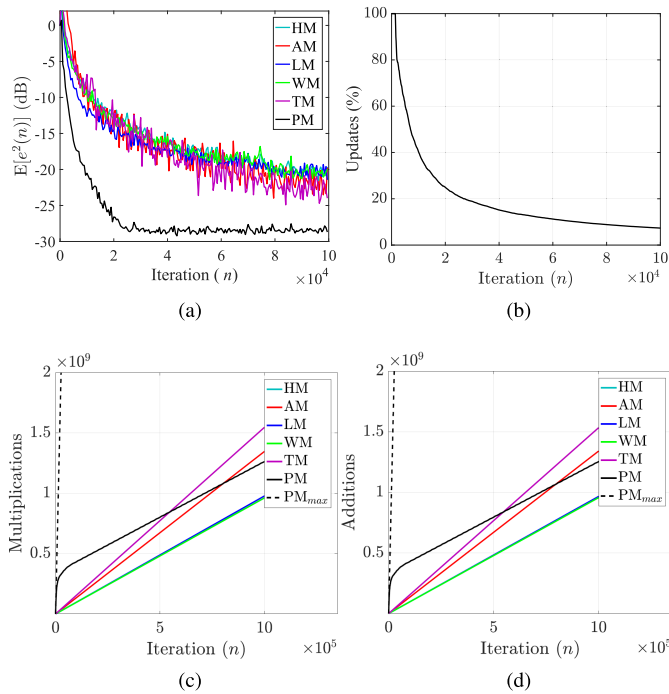


Fig. 7. Performance comparison for Case 3. (a) The mean-squared error. (b) Update percentage. (c) Total multiplications. (d) Total additions.

length 256, 64, 192 and 192 are taken for $P(z)$, $S(z)$, $W_f(z)$ and $W_b(z)$, respectively. The cases presented for demonstrating the improved performance are general and adopted from the relevant literature [2], [3], [8]–[10]. Moreover, simulation results are obtained by averaging over 20 independent runs.

A. Case 1

The reference signal used in this case is a multi-tonal signal consisting of frequencies 165, 235, 290, 315, 410 and 600 Hz, and the disturbance signal is a multi-tonal signal consisting of frequencies 195, 250, 350, 385, 500 and 550 Hz [8], [13]. The variances of both $x(n)$ and $v(n)$ are adjusted to 1.0. Reference signal is mixed with Gaussian noise to achieve a SNR of 30 dB. The proposed method converges in 8000 iterations to a mean-squared error of -37 dB as shown in Fig. 3(a). The convergence rate is more than twice than existing results in literature, and the steady state error is improved by 6 dB. The optimal weighting factor plays a big role to improve the convergence rate and steady state error. The variable weighting factor has helped in reducing the frequency of the filter updates by 90% as can be seen from the plot of the percentage updates in Fig. 3(b). The reduction in updates is translated into a considerable reduction in computations as can be seen in Fig. 3(c) and (d), where PM_{max} is used for computations if updates are performed at each iteration. Power spectra in Fig. 4 compares the steady state performance in frequency to highlight the contribution of the proposed method.

B. Case 2

For this case, a broadband reference signal is formed by filtering a zero mean unit variance Gaussian noise through

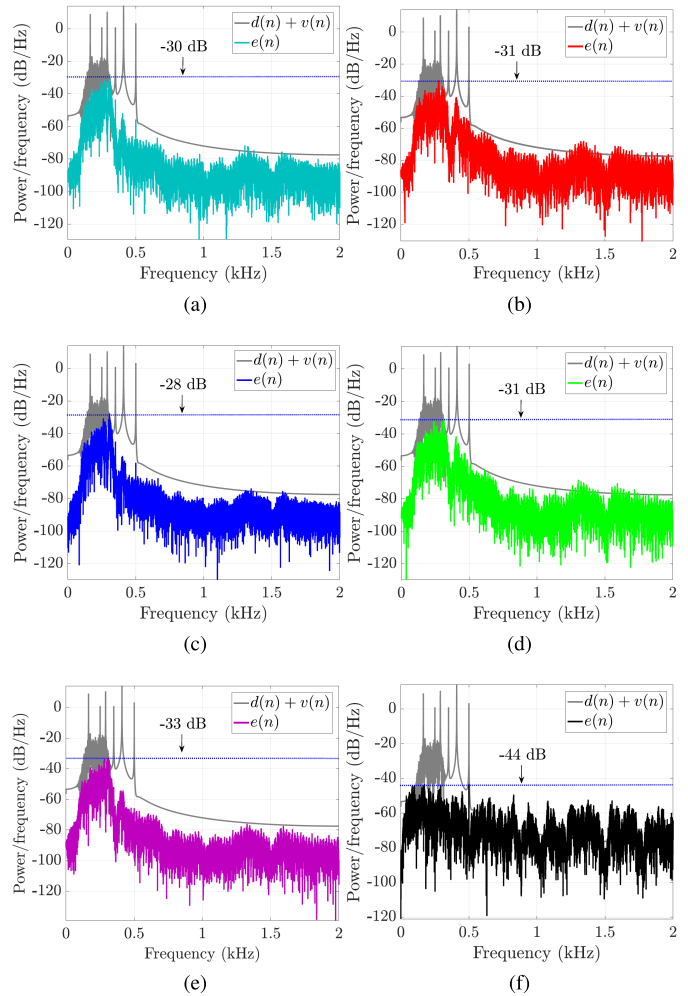


Fig. 8. Power spectra comparison for Case 3. (a) HM. (b) AM. (c) LM. (d) WM. (e) TM. (f) PM.

a bandpass filter with passband 100–350 Hz, and a Gaussian noise is added to attain the SNR of 30 dB. Broadband noise occurs in ducts [5]. The disturbance signal is a unit variance multi-tonal signal consisting of frequencies 165 and 250 Hz [8], [13]. Results for various performance measures are given in Fig. 5. The presented method converges in 10000 iterations to a mean-squared error of -28.5 dB, which is a reduction of at least 6.5 dB over the previous residual noise levels as shown in Fig. 5(a). The noteworthy improvement in convergence speed not only highlights the superior performance of the proposed algorithm but helps to reduce the computational requirements as fewer updates are required in the steady state (see Fig. 5(b), (c) and (d)). The noise reduction performance of various methods can be observed from the power spectra provided in Fig. 6.

C. Case 3

This case investigates the reference signal comprising of multi-tonal and broadband signals. The multi-tonal part is a unit variance signal consisting of tones with frequencies: 165, 290 and 410 Hz. The broadband part is obtained by

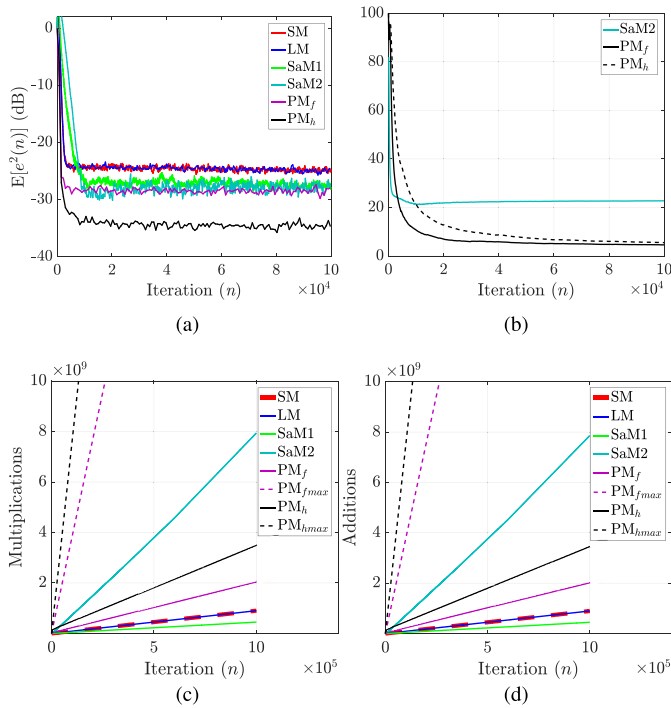


Fig. 9. Performance comparison for Case 4. (a) The mean-squared error. (b) Update percentage. (c) Total multiplications. (d) Total additions.

filtering a zero mean unit variance Gaussian noise through a 100-300 Hz bandpass filter. SNR of 30 dB is achieved by adding reference signal with Gaussian noise. The disturbance signal is a unit variance multi-tonal signal consisting of frequencies 250, 350 and 500 Hz [8], [13]. The designed weighting factor exhibits improved performance by superior convergence rate and reduced steady state mean-squared error (see Fig. 7(a)). Iterations required for convergence are reduced by half compared to existing results in literature. In steady state, the noise reduction performance is improved by at least 6 dB with comparable computational requirements as can be seen in Fig. 7. The corresponding power spectra in the steady state is presented in Fig. 8 to highlight the improved performance achieved by the proposed method.

D. Case 4

In this case, the proposed algorithm investigates the feedforward ANC systems: Shakeel (SM) [23], Lopes (LM) [24], Saeed (SaM1) [3] and Saeed's method (SaM2) [2]. Therefore, the disturbance is not considered in this case. The reference signal is the same multi-tonal signal as used in case 1. The proposed algorithm with only feedforward noise controller is labeled as PM_f , and with hybrid configuration is referred as PM_h . The methods, SM and LM, improve the convergence speed with slightly high residual noise, while SaM1 and SaM2 reduce the steady state residual noise by taking relatively more iterations (see Fig. 9(a)). Simulation results show that both, PM_f and PM_h , exhibit noteworthy improvement in the convergence speed. PM_f converges to the same steady state $E[e^2(n)]$ as SaM2 with superior

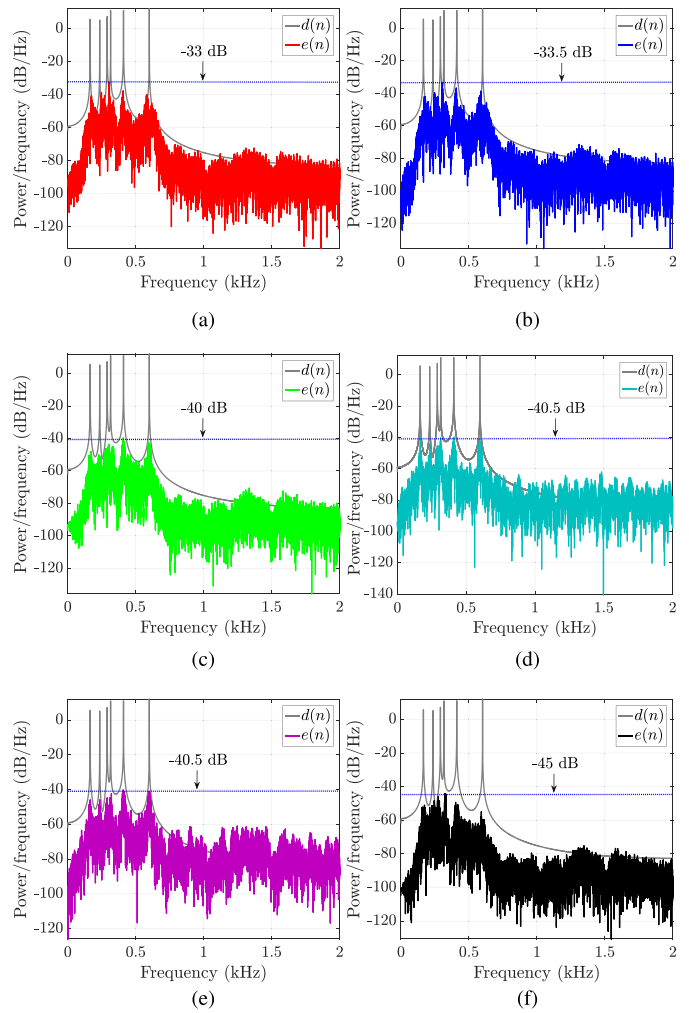


Fig. 10. Power spectra comparison for Case 4. (a) SM. (b) LM. (c) SaM1. (d) SaM2. (e) PM_f . (f) PM_h .

convergence rate as shown in Fig. 9(a). PM_h improves the convergence speed with at least 5 dB improvement in the noise reduction (see Fig. 9(a)). The proposed method, PM_h , achieves significant improvement in all performance aspects. The rate of filter updates decreases with iterations, but still the computational complexity of PM_f and PM_h is lower than the method reported in [2] and slightly higher than the previous methods [3], [23], [24] as shown in Fig. 9, where PM_{fmax} and PM_{hmax} represent the computations if updates are performed on every iteration for PM_f and PM_h . Power spectra in the steady state are shown in Fig. 10 and the proposed method demonstrates significant enhancement.

VII. CONCLUSIONS

This paper derives filtered-x optimal weighting recursive least squares algorithms for feedforward and feedback noise control filters in hybrid ANC systems with bounded narrowband disturbances. The proposed algorithms use optimal weighting factors that are adjusted at each iteration on the basis of new information in the recent observation data. These weight factors are also used to decide on effective

filter updates. Therefore, reducing computational complexity in the long term operation of the ANC system by avoiding the filter updates that do not improve the system performance. In the presence of bounded narrowband disturbance, cessation of filter updates is ensured once the absolute residual error becomes less than the disturbance bound. For the proposed algorithm, the filter estimation error is bounded and non-increasing which reinforces the reliability of the filter estimates. The filter estimates of the proposed algorithm are shown to converge to a region containing the actual filter along with derivation of upper bound on filter estimation error. The presented algorithm for feedforward and feedback noise control filters provide fast convergence, reduced computations and improved steady state performance independent of input signal eigen-spread which slows down the LMS algorithms. In comparison with the previous methods, the proposed design reduces the mean-squared error by at least 6 dB for broadband, multi-tonal and their mixture reference noises in the presence of multi-tonal disturbance noise. Future work includes detailed analysis on application of the proposed algorithm for multi-channel systems and exploring new controller design techniques [28].

REFERENCES

- [1] P. Lueg, "Process of silencing sound oscillations," U.S. Patent 2043416 A, Jun. 9, 1936.
- [2] M. S. Aslam, P. Shi, and C.-C. Lim, "Variable threshold-based selective updating algorithms in feed-forward active noise control systems," *IEEE Trans. Circuits Syst. I, Reg. Papers*, vol. 66, no. 2, pp. 782–795, Feb. 2019.
- [3] M. S. Aslam, "Maximum likelihood least squares identification method for active noise control systems with autoregressive moving average noise," *Automatica*, vol. 69, pp. 1–11, Jul. 2016.
- [4] M. S. Aslam and M. A. Z. Raja, "A new adaptive strategy to improve online secondary path modeling in active noise control systems using fractional signal processing approach," *Signal Process.*, vol. 107, pp. 433–443, Feb. 2015.
- [5] S. M. Kuo and D. R. Morgan, *Active Noise Control Systems—Algorithms DSP Implementations*. Hoboken, NJ, USA: Wiley, 1996.
- [6] M. A. Z. Raja, M. S. Aslam, N. I. Chaudhary, and W. U. Khan, "Bio-inspired heuristics hybrid with interior-point method for active noise control systems without identification of secondary path," *Frontiers Inf. Technol. Electron. Eng.*, vol. 19, no. 2, pp. 246–259, Feb. 2018.
- [7] A. Yanou, "Reduction of noise in on-demand type feedback control systems," *Int. J. Innov. Comput. Inf. Control*, vol. 14, no. 3, pp. 1123–1131, 2018.
- [8] T. Padhi, M. Chandra, A. Kar, and M. N. S. Swamy, "Design and analysis of an improved hybrid active noise control system," *Appl. Acoust.*, vol. 127, pp. 260–269, Dec. 2017.
- [9] L. Wu, X. Qiu, I. S. Burnett, and Y. Guo, "Decoupling feedforward and feedback structures in hybrid active noise control systems for uncorrelated narrowband disturbances," *J. Sound Vib.*, vol. 350, pp. 1–10, Aug. 2015.
- [10] L. Mokhtarpour and H. Hassanpour, "A self-tuning hybrid active noise control system," *J. Franklin Inst.*, vol. 349, no. 5, pp. 1904–1914, 2012.
- [11] S. M. Kuo and M. Ji, "Passband disturbance reduction in periodic active noise control systems," *IEEE Trans. Speech Audio Process.*, vol. 4, no. 2, pp. 96–103, Mar. 1996.
- [12] X. Sun and S. M. Kuo, "Active narrowband noise control systems using cascading adaptive filters," *IEEE Trans. Audio, Speech, Language Process.*, vol. 15, no. 2, pp. 586–592, Feb. 2007.
- [13] M. T. Akhtar and W. Mitsuhashi, "Improving performance of hybrid active noise control systems for uncorrelated narrowband disturbances," *IEEE Trans. Audio, Speech, Language Process.*, vol. 19, no. 7, pp. 2058–2066, Sep. 2011.
- [14] S. M. Kuo and D. Vijayan, "A secondary path modeling technique for active noise control systems," *IEEE Trans. Speech Audio Process.*, vol. 5, no. 4, pp. 374–377, Jul. 1997.
- [15] L. J. Eriksson and M. C. Allie, "Use of random noise for on-line transducer modeling in an adaptive active attenuation system," *J. Acoust. Soc. Amer.*, vol. 85, no. 2, pp. 797–802, 1989.
- [16] M. Zhang, H. Lan, and W. Ser, "Cross-updated active noise control system with online secondary path modeling," *IEEE Trans. Speech Audio Process.*, vol. 9, no. 5, pp. 598–602, Jul. 2001.
- [17] M. Zhang, H. Lan, and W. Ser, "A robust online secondary path modeling method with auxiliary noise power scheduling strategy and norm constraint manipulation," *IEEE Trans. Speech Audio Process.*, vol. 11, no. 1, pp. 45–53, Jan. 2003.
- [18] P. S. R. Diniz, *Adaptive Filtering Algorithms and Practical Implementation*. New York, NY, USA: Springer, 2008.
- [19] G.-O. Glentis, K. Berberidis, and S. Theodoridis, "Efficient least squares adaptive algorithms for FIR transversal filtering," *IEEE Signal Process. Mag.*, vol. 16, no. 4, pp. 13–41, Jul. 1999.
- [20] S. Dasgupta and Y.-F. Huang, "Asymptotically convergent modified recursive least-squares with data-dependent updating and forgetting factor for systems with bounded noise," *IEEE Trans. Inf. Theory*, vol. 33, no. 3, pp. 383–392, May 1987.
- [21] A. Carini and S. Malatini, "Optimal variable step-size NLMS algorithms with auxiliary noise power scheduling for feedforward active noise control," *IEEE Trans. Audio, Speech, Language Process.*, vol. 16, no. 8, pp. 1383–1395, Nov. 2008.
- [22] P. Davari and H. Hassanpour, "Designing a new robust on-line secondary path modeling technique for feedforward active noise control systems," *Signal Process.*, vol. 89, pp. 1195–1204, Jun. 2009.
- [23] S. Ahmed, M. T. Akhtar, and X. Zhang, "Robust auxiliary-noise-power scheduling in active noise control systems with online secondary path modeling," *IEEE/ACM Trans. Audio, Speech, Language Process.*, vol. 21, no. 4, pp. 749–761, Apr. 2013.
- [24] P. A. C. Lopes and J. A. B. Gerald, "Auxiliary noise power scheduling algorithm for active noise control with online secondary path modeling and sudden changes," *IEEE Signal Process. Lett.*, vol. 22, no. 10, pp. 1590–1594, Oct. 2015.
- [25] G. Belforte, B. Bona, and V. Cerone, "Parameter estimation algorithms for a set-membership description of uncertainty," *Automatica*, vol. 26, no. 5, pp. 887–898, 1990.
- [26] G. Tan, C. Wen, and Y. C. Soh, "Identification for systems with bounded noise," *IEEE Trans. Autom. Control*, vol. 42, no. 7, pp. 996–1001, Jul. 1997.
- [27] A. H. Sayed, *Adapt Filters*. Hoboken, NJ, USA: Wiley, 2008.
- [28] K. Sun, S. Mou, J. Qiu, T. Wang, and H. Gao, "Adaptive fuzzy control for non-triangular structural stochastic switched nonlinear systems with full state constraints," *IEEE Trans. Fuzzy Syst.*, to be published. doi: 10.1109/TFUZZ.2018.2883374.



Muhammad Saeed Aslam received the bachelor's degree in electrical engineering from the University of Engineering and Technology (UET), Lahore, Pakistan, in 2007, and the master's degree in control systems engineering from the Pakistan Institute of Engineering and Applied Sciences (PIEAS), Islamabad, Pakistan, in 2009. He is currently pursuing the Ph.D. degree in electrical engineering with The University of Adelaide. His research interests include digital signal processing, filter design theory, adaptive algorithms, system identification, and active noise control.



Peng Shi (M'95–SM'98–F'15) received the Ph.D. degree in electrical engineering from The University of Newcastle, Australia, in 1994, the Ph.D. degree in mathematics from the University of South Australia in 1998, the D.Sc. degree from the University of Glamorgan, U.K., in 2006, and the D.Eng. degree from The University of Adelaide, Australia, in 2015.

He is currently a Professor with The University of Adelaide. His research interests include system and control theory, intelligent systems, and operational research.

Dr. Shi is a Member-at-Large of the Board of Governors of the IEEE SMC Society and an IEEE Distinguished Lecturer. He is a fellow of the Institution of Engineering and Technology and the Institute of Engineers, Australia. He received the Andrew Sage Best Transactions Paper Award from the IEEE SMC Society in 2016. He has served on the editorial board of a number of journals in the fields of automation, fuzzy systems, cybernetics, signal processing, and information sciences.



Cheng-Chew Lim received the B.Sc. degree (Hons.) in electronic and electrical engineering and the Ph.D. degree in electronic and electrical engineering from Loughborough University, Leicestershire, U.K. He is currently a Professor with The University of Adelaide, Adelaide, SA, Australia. His research interests include control and systems' theory, autonomous systems, machine learning, and optimization techniques and applications. He has served as a Guest Editor for a number of journals, including *Discrete and Continuous Dynamical System-Series B*.

He serves as an Associate Editor for the IEEE TRANSACTIONS ON SYSTEMS, MAN, AND CYBERNETICS: SYSTEMS and an Editorial Board Member of the *Journal of Industrial and Management Optimization*.

Chapter 5

Self-adapting variable step size strategies for active noise control systems with acoustic feedback

S_{ELF-ADAPTING} variable step size based normalized least mean square algorithms are derived and analyzed for the active noise control systems with acoustic feedback path. The proposed variable step size is designed for rapid convergence and low mis-adjustment. Moreover, auxiliary noise power is varied in relation with status of the predictor filter to introduce auxiliary noise at startup or in case of perturbation only. A low auxiliary noise gain in the steady state improves noise reduction. Feedback compensation and predictor filters are not updated in the steady state to reduce computations.

Statement of Authorship

Title of Paper	Self-Adapting Variable Step Size Strategies for Active Noise Control Systems with Acoustic Feedback
Publication Status	Published
Publication Details	Muhammad Saeed Aslam, Peng Shi, Cheng-Chew Lim (2020). Self-Adapting Variable Step Size Strategies for Active Noise Control Systems with Acoustic Feedback, <i>Automatica</i> , https://doi.org/10.1016/j.automatica.2020.109354 .

Principal Author

Name of Principal Author (Candidate)	Muhammad Saeed Aslam		
Contribution to the Paper	Designed the core idea and performed analysis on the concept, interpreted data, wrote manuscript and acted as corresponding author		
Overall percentage (%)	80%		
Certification:	This paper reports on original research I conducted during the period of my Higher Degree by Research candidature and is not subject to any obligations or contractual agreements with a third party that would constrain its inclusion in this thesis. I am the primary author of this paper.		
Signature	<input type="text"/>	Date	8/11/2020

Co-Author Contributions

By signing the Statement of Authorship, each author certifies that:

- the candidate's stated contribution to the publication is accurate (as detailed above);
- permission is granted for the candidate to include the publication in the thesis; and
- the sum of all co-author contributions is equal to 100% less the candidate's stated contribution.

Name of Co-Author	Peng Shi		
Contribution to the Paper	Supervised development of work, helped in refining core concept and manuscript evaluation.		
Signature	<	Date	8 Nov 2020

Name of Co-Author	Cheng-Chew Lim		
Contribution to the Paper	Supervised development of work, helped in data interpretation and manuscript evaluation.		
Signature	<input type="text"/>	Date	8/11/2020

Please cut and paste additional co-author panels here as required.



Contents lists available at ScienceDirect

Automatica

journal homepage: www.elsevier.com/locate/automatica

Brief paper

Self-adapting variable step size strategies for active noise control systems with acoustic feedback[☆]

Muhammad Saeed Aslam^{*}, Peng Shi, Cheng-Chew Lim

School of Electrical and Electronic Engineering, The University of Adelaide, SA, 5005, Australia

ARTICLE INFO

Article history:

Received 25 February 2019

Received in revised form 21 June 2020

Accepted 26 September 2020

Available online xxxxx

Keywords:

Parameter estimation

FxLMS

Online feedback path estimation

Self-adapting variable step size

Active noise control

ABSTRACT

Self-adapting variable step size (SAVSS) normalized least mean square (NLMS) algorithms are derived and analysed for the active noise control systems with acoustic feedback path. The objective of the proposed SAVSS scheme is to resolve the conflicting requirements of rapid convergence and low misadjustment. A tuningless power scheduling scheme is proposed that varies the gain according to the output of the predictor filter, and switches to a low gain on the basis of a minimum criteria. In the steady state, a low gain auxiliary noise significantly improves noise reduction performance, and the update of the feedback compensation filter and predictor filter is discontinued to reduce computations. Simulations are performed with narrowband noises to validate the improved performance of the proposed method in comparison with established state-of-the-art methods.

© 2020 Published by Elsevier Ltd.

1. Introduction

Active noise control (ANC) is a technique preferred for attenuating the low frequency noises by generating a cancelling noise with the identical amplitude and opposite phase by using the controlled secondary sources (Lueg, 1936). Generally, reference microphones are used to obtain reference of primary noises to adapt noise control filters. The outputs of noise control filters trigger the speakers to cancel the primary noise at the error microphones. Sometimes, acoustics from speakers reflect back to the reference microphones and destabilize the system. Consider the basic configuration of ANC system with acoustic feedback in Fig. 1 to familiarize with the common structure and building blocks. Microphones are used for detecting the residual signal $e(n)$ and the reference signal $x(n)$ where n is the time variable. Primary noise, $d(n)$, results from $x(n)$ passing through primary path $P(z)$. Cancelling noise, $\hat{d}(n)$, is formed by $x(n)$ passing through adaptive noise controller $W(z)$ and secondary path $S(z)$. Filtered-x least mean square (FxLMS) algorithm is used to update $W(z)$ due to its computational simplicity, unbiased convergence and robustness (Aslam, 2016; Aslam & Raja, 2015; Aslam, Shi, & Lim, 2019). When reflections of the output from speaker travel back towards the reference microphone through feedback path $F(z)$,

the feedback signal $x_f(n)$ also becomes available at the reference microphone. The signal $x_f(n)$ forms a closed loop which causes instability if left unattended. Therefore, compensation of $F(z)$ via estimated feedback path $\hat{F}(z)$ is a necessity. Overall, obtaining $\hat{S}(z)$ and $\hat{F}(z)$ is critical for the stable system operation. The estimation of $\hat{F}(z)$ is the issue addressed in this paper in detail. Therefore, it is assumed that an exact $\hat{S}(z)$ is already available i.e., $\hat{S}(z) = S(z)$. See Ahmed and Akhtar (2017), Kuo and Morgan (1996), Liao and Lin (2007) and Zhang, Lan, and Ser (2001, 2003) for more details on estimating $\hat{S}(z)$.

Time varying $\hat{F}(z)$ is estimated online by inducing an auxiliary noise signal at the output of $W(z)$ (Ahmed & Akhtar, 2017; Ahmed, Akhtar, & Zhang, 2013, 2015; Akhtar & Mitsuhashi, 2011; Kuo, 2002; Kuo & Luan, 1994). In Kuo (2002), fixed gain auxiliary noise and fixed step size parameters are used for $\hat{F}(z)$ and $W(z)$. Bounded step size parameter for $\hat{F}(z)$ increases from small to large value in Akhtar and Mitsuhashi (2011) to improve the convergence speed. In Ahmed and Akhtar (2017) and Ahmed et al. (2013, 2015), gain scheduling is designed for auxiliary noise in relation with estimation accuracy. The method in Ahmed et al. (2013) uses fixed step sizes for adaptive filters, therefore a variable step size scheme is introduced for the single channel ANC systems in Ahmed et al. (2015) which is extended to the multi-channel systems in Ahmed and Akhtar (2017). Similar to Akhtar and Mitsuhashi (2011), the step size strategy of Ahmed and Akhtar (2017) and Ahmed et al. (2015) also increases from a small value at the start up to a large value in the steady state, which may lead to a large steady state error. The power variation schemes of Ahmed and Akhtar (2017) and Ahmed et al. (2013, 2015) have a noteworthy contribution in the residual error from

[☆] The material in this paper was not presented at any conference. This paper was recommended for publication in revised form by Associate Editor Alessandro Chiuso under the direction of Editor Torsten Söderström.

^{*} Corresponding author.

E-mail addresses: muhammad.aslam@adelaide.edu.au (M.S. Aslam), peng.shi@adelaide.edu.au (P. Shi), cheng.lim@adelaide.edu.au (C.-C. Lim).

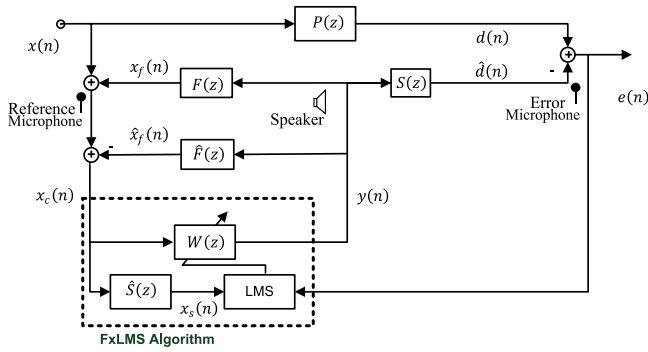


Fig. 1. Feed-forward ANC system with acoustic feedback.

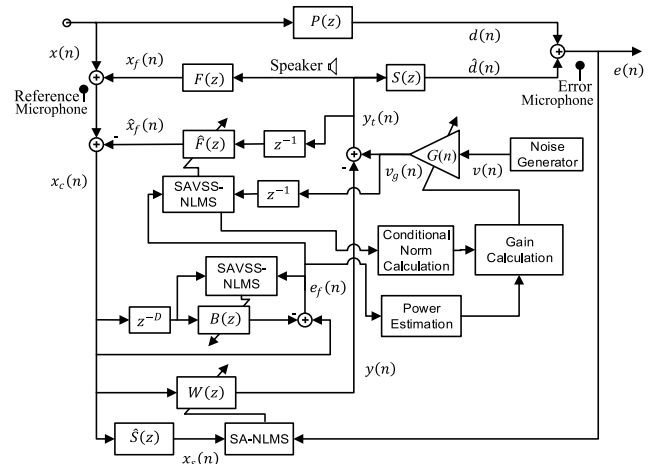


Fig. 2. Block diagram of the proposed ANC system.

the auxiliary noise in the steady state, which is a disturbance for the $W(z)$. In Ahmed and Akhtar (2017), an increasing step size is used only for $\hat{F}(z)$, and variable auxiliary noise gain is significant in the steady state which degrades the system performance. The proposed step size for $\hat{F}(z)$ and $W(z)$ varies appropriately to deliver fast performance and low steady state error. Also, proposed auxiliary noise gain is negligible in the steady state to improve noise reduction. Filter updates are also stopped in the steady state to reduce computations.

The distinct contributions made in this paper are

(1) A self-adapting variable step size based normalized least mean square (SAVSS-NLMS) algorithm is derived for $\hat{F}(z)$.

- Unlike the previous methods (Ahmed & Akhtar, 2017; Ahmed et al., 2013, 2015; Akhtar & Mitsuhashi, 2011; Kuo, 2002; Kuo & Luan, 1994), the proposed step size parameter is time varying and self-adapts by using the statistical information to maintain stability and make system robust to perturbations in acoustic paths.
- The proposed step size varies appropriately to deliver fast convergence along with small steady state error.
- Unlike the previous works (Ahmed & Akhtar, 2017; Ahmed et al., 2013, 2015; Akhtar & Mitsuhashi, 2011; Kuo, 2002; Kuo & Luan, 1994), the proposed method reduces computational complexity by stopping the updates of $\hat{F}(z)$ and $B(z)$ along with their associated step sizes after system convergence.
- Superior convergence speed of the presented method requires significant auxiliary noise for relatively reduced iterations.

(2) A scheme is formulated for the gain variation of auxiliary noise according to the accuracy of $\hat{F}(z)$.

- In the presented approach, the gain of the auxiliary noise is significant in learning phase and becomes negligible in the steady state. Thus, the approach results in improved noise reduction.
- Continuous auxiliary noise injection in Ahmed and Akhtar (2017), Ahmed et al. (2013, 2015), Akhtar and Mitsuhashi (2011), Kuo (2002) and Kuo and Luan (1994) slows down the convergence of $W(z)$. In the proposed method, a negligible auxiliary noise in the steady state results in an accurate reference signal for improved $W(z)$ performance.
- It helps the system in maintaining stability when perturbations exit in acoustic paths.

(3) A novel SAVSS based filtered-x normalized least mean square (SAVSS-FxNLMS) algorithm is derived for $W(z)$. The

step size parameter adapts by using the statistical information to achieve the fast convergence and improved noise reduction properties. The proposed scheme is robust to the perturbations in acoustic paths and offers reduced computational requirements in long term operation in comparison with (Ahmed & Akhtar, 2017; Ahmed et al., 2013, 2015; Akhtar & Mitsuhashi, 2011; Kuo, 2002; Kuo & Luan, 1994).

The organization of upcoming sections is as follows: Section 2 describes the system model for the proposed ANC structure. The SAVSS-NLMS algorithm is derived for the online identification and compensation of $F(z)$ in Section 3. The derivation of SAVSS-NLMS algorithm for $\hat{F}(z)$ is presented in Section 3.1 along with the analysis and the practical considerations. The SAVSS-NLMS algorithm is presented for prediction filter in Section 3.2. A strategy for variable power auxiliary signal is provided in Section 4. Section 5 derives a SAVSS-FxNLMS algorithm for $W(z)$. Section 6 presents the computational requirements. Computer simulations are discussed in Section 7 while concluding remarks are given in Section 8.

2. Single channel ANC system model

The schematic of the proposed methodology for single channel ANC system is given in Fig. 2. The impulse response vectors for the primary path $P(z)$, the secondary path $S(z)$ and the feedback path $F(z)$ are

$$\mathbf{p}(n) = [p(n), p(n-1), \dots, p(n-L_p+1)]^T, \in \mathbb{R}^{L_p} \quad 72$$

$$\mathbf{s}(n) = [s(n), s(n-1), \dots, s(n-L_s+1)]^T, \in \mathbb{R}^{L_s} \quad 73$$

$$\mathbf{f}(n) = [f(n), f(n-1), \dots, f(n-L_f+1)]^T, \in \mathbb{R}^{L_f} \quad 74$$

The primary signal, $d(n)$, is

$$d(n) = \mathbf{p}^T(n)\mathbf{x}_p(n), \quad (1) \quad 76$$

where $\mathbf{x}_p(n) = [x(n), x(n-1), \dots, x(n-L_p+1)]^T$ and $x(n)$ is the primary noise. The reference signal, $x_r(n)$, is

$$x_r(n) = x(n) + x_f(n), \quad (2) \quad 79$$

where $x_f(n)$, the acoustic feedback signal, is given as

$$x_f(n) = \mathbf{f}^T(n)\mathbf{y}_f(n), \quad (3) \quad 77$$

$$\mathbf{y}_f(n) = [y_t(n), y_t(n-1), \dots, y_t(n-L_f+1)]^T, \quad (4) \quad 78$$

$$y_t(n) = y(n) + v_g(n), \quad (5) \quad 79$$

1 and $y(n)$ is the output of the noise control filter $W(z)$ and the
2 modified gain auxiliary signal, $v_g(n)$, is

$$3 \quad v_g(n) = G(n)v(n), \quad (6)$$

4 where $G(n)$ is a variable gain function ($G(n)$ is discussed in Sec-
5 tion 4) and $v(n)$ is a white noise sequence that has zero mean with
6 unit variance. It is assumed that $x(n)$ and $v(n)$ are uncorrelated.
7 The residual error signal, $e(n)$, is

$$8 \quad e(n) = d(n) - \hat{d}(n), \quad (7)$$

9 where $\hat{d}(n) = \mathbf{s}^T(n)\mathbf{y}_s(n)$, $\mathbf{y}_s(n) = [y_t(n), y_t(n-1), \dots, y_t(n-
10 L_s+1)]^T$, and $y_t(n)$ is provided in (5). Control signal, $y(n)$, can
11 be computed as

$$12 \quad y(n) = \mathbf{w}^T(n)\mathbf{x}_w(n), \quad (8)$$

13 where $\mathbf{w}(n) = [w_0(n), w_1(n), \dots, w_{(L_w-1)}(n)]^T$, $\mathbf{x}_w(n) = [x_c(n),
14 x_c(n-1), \dots, x_c(n-(L_w-1))]^T$, and feedback compensated signal
15 $x_c(n)$ is

$$16 \quad x_c(n) = x_r(n) - \hat{x}_f(n). \quad (9)$$

17 Reference signal $x_r(n)$ is provided in (2) and $\hat{x}_f(n)$ is the output of
18 $\hat{F}(z)$

$$19 \quad \hat{x}_f(n) = \hat{\mathbf{f}}^T(n)\mathbf{y}_d(n), \quad (10)$$

20 where $\hat{\mathbf{f}}(n) = [\hat{f}_0(n), \hat{f}_1(n), \dots, \hat{f}_{(L_f-1)}(n)]^T$ and

$$21 \quad \mathbf{y}_d(n) = \mathbf{y}_f(n-1) \quad (11)
= [y_t(n-1), y_t(n-2), \dots, y_t(n-L_f)]^T.$$

22 In the next section, SAVSS-NLMS algorithms are derived for $\hat{F}(z)$
23 and $B(z)$.

24 3. Feedback path compensation

25 The functionality of feedback compensation is to remove the
26 effects of $F(z)$ from $x_r(n)$ i.e., $x_c(n) \approx x(n)$. For this purpose, two
27 filters are used. Filter $\hat{F}(z)$ is used to neutralize the contribution
28 of $F(z)$, while filter $B(z)$ is employed to provide a suitable error
29 signal for adapting $\hat{F}(z)$. Signal $v_g(n)$ is introduced for estimating
30 $\hat{F}(z)$. The error signal for the adaptive algorithm is the signal
31 obtained after filtering $x_c(n)$, which has $v_g(n)$ along with $x(n)$ and
32 filtered $x(n)$. Using (2), (3), (10) and (11), Eq. (9) can be written
33 as

$$34 \quad x_c(n) = x_r(n) - \hat{f}(n) * y_t(n-1) \quad (12)
= x(n) + \delta f(n) * [w(n) * x_c(n-1) + v_g(n-1)],$$

35 where $*$ denotes linear convolution and $\delta f(n)$ stands for the
36 feedback path estimation error. The inherent delay for feedback
37 is also incorporated in this expression. Terms like $\delta f(n) * v_g(n)$
38 carry the desired error signal for $\hat{F}(z)$ and this is addressed by
39 a predictor filter $B(z)$. This filter has $x_c(n)$ as input, and its error
40 signal is

$$41 \quad e_f(n) = x_c(n) - \mathbf{b}^T(n)\mathbf{x}_b(n), \quad (13)$$

42 where $\mathbf{b}(n) = [b_0(n), b_1(n), \dots, b_{(L_b-1)}(n)]^T$ and

$$43 \quad \mathbf{x}_b(n) = [x_c(n-D), x_c(n-D-1), \dots, x_c(n-D-L_b+1)]^T. \quad (14)$$

44 Delay D ensures that $v_g(n)$ components required for $\hat{F}(z)$ are
45 decorrelated while the narrowband components remain corre-
46 lated in $x_c(n)$, and D can be selected from the correlation between
47 $x_c(n)$ and $x_c(n-D)$

$$48 \quad E[x_c(n)x_c(n-D)] = E[(x(n) + \delta f(n) * y(n-1) +
= \delta f(n) * v_g(n-1))(x(n-D) + \delta f(n) * y(n-D-1) +
+ \delta f(n) * v_g(n-D-1))]. \quad (15)$$

where $E[\cdot]$ denotes mathematical expectation and it is assumed
that the change in $\delta f(n)$ is negligible in the interval D . From (8)
and (9)

$$y(n-1) = w(n) * (x(n-1) + C_{fw}(n)) * \quad (16)
(y(n-2) + v_g(n-2)),$$

where $C_{fw}(n) = \delta f(n) * w(n)$. It is clear from (16) that $x_c(n)$ will
become unbounded if $F(z)$ is not neutralized. With improvement
in estimation accuracy, $\delta f(n)$ will approach a null response and
terms like $\delta f(n) * y(n-1)$ and $\delta f(n) * y(n-D-1)$ in (15) become
negligible. As $v_g(n)$ is uncorrelated with $x(n)$, (15) becomes (Kuo
& Vijayan, 1997)

$$E[x_c(n)x_c(n-D)] = E[x(n)x(n-D)] + \quad (17)
= \sum_{i=0}^{L_f-1} \delta f_i(n) \sum_{j=0}^{L_f-1} \delta f_j(n) E[v_g(n-i-1)v_g(n-j-D-1)].$$

Since $v(n)$ is a zero mean white noise, the last term in (17) for
 $D \geq L_f$ becomes (Kuo & Vijayan, 1997)

$$E[v_g(n-i-1)v_g(n-j-D-1)] = 0. \text{ for } i < L_f, 0 \leq j \quad (18)$$

Therefore, the auxiliary signal components in $x_c(n)$ and $x_c(n-
D)$ are uncorrelated for $D \geq L_f$. Consequently, $B(z)$ is able to
predict $x(n)$ component that remains correlated in $x_c(n)$ for $D \geq
L_f$. The correlated component will be absent in $e_f(n)$ after the
convergence of $B(z)$, and (13) becomes $e_f(n) \approx \delta f(n) * v_g(n-
1)$ which is equivalent to a modelling error without $x(n)$, thus
preventing $\hat{F}(z)$ from being interfered by the narrowband signal.
Therefore, $\hat{F}(z)$ can model $F(z)$ correctly. However, if delay $D <
L_f$, then the second term in (17) will not be zero, resulting in
cancelling the auxiliary signal components by $B(z)$ and degrading
the convergence of $\hat{F}(z)$. In the next subsection, derivation of the
proposed variable step size strategy is presented.

3.1. Self-adapting variable step size strategy for $\hat{F}(z)$

This section derives SAVSS-NLMS algorithm for $\hat{F}(z)$. From (2)
and (3)

$$x_r(n) = \mathbf{f}^T(n)\mathbf{v}_g(n) + v_{xx}(n), \quad (19)$$

$$\mathbf{v}_g(n) = [v_g(n), v_g(n-1), \dots, v_g(n-L_f+1)]^T, \quad (20)$$

$$v_{xx}(n) = \mathbf{f}^T(n)\mathbf{y}(n) + x(n), \quad (21)$$

and $v_{xx}(n)$ is disturbance for $\hat{F}(z)$.

3.1.1. Derivation of the algorithm

The *a priori* error signal from (13) is

$$e_f(n) = \mathbf{v}_g^T(n)[\mathbf{f}(n) - \hat{\mathbf{f}}(n)] + v_x(n), \quad (22)$$

$$v_x(n) = v_{xx} - \mathbf{b}^T(n)\mathbf{x}_b(n), \quad (23)$$

where $v_{xx}(n)$ is given in (20) and $\mathbf{x}_b(n)$ is defined in (14). The term
 $\mathbf{b}^T(n)\mathbf{x}_b(n)$ gives predictable part of $x_c(n)$. After the convergence of
 $B(z)$, $x(n)$ terms become insignificant in $v_x(n)$, and $e_f(n)$ becomes
representative of the feedback path modelling error. Similarly, the
a posteriori error signal can be given as

$$e_f(n) = \mathbf{v}_g^T(n)[\mathbf{f}(n) - \hat{\mathbf{f}}(n+1)] + v_x(n), \quad (24)$$

where $\hat{\mathbf{f}}(n+1)$ can be written as

$$\hat{\mathbf{f}}(n+1) = \hat{\mathbf{f}}(n) + \mu_f(n)\mathbf{v}_g(n)e_f(n), \quad (25)$$

where $\mu_f(n)$ is the step size parameter. For NLMS algorithm,
replace (24) in (23) and substitute $v_x(n) = 0$ with the requirement
 $e_f(n) = 0$. Assume $e_f(n) \neq 0$, for all n , then $\mu_{NLMS}(n) =
[\mathbf{v}_g^T(n)\mathbf{v}_g(n)]^{-1}$ and is suitable for noiseless case. In the presence

of $v_x(n)$, finding $\mu_f(n)$ that cancels (23) introduces disturbance in $\hat{\mathbf{f}}(n+1)$ since $\mathbf{v}_g^T(n)[\mathbf{f}(n) - \hat{\mathbf{f}}(n+1)] = -v_x(n) \neq 0$, for all n . It is appropriate to have $\mathbf{v}_g^T(n)[\mathbf{f}(n) - \hat{\mathbf{f}}(n+1)] = 0$, for all n . This means $\varepsilon_f(n) = v_x(n)$. For the proposed $\mu_f(n)$, consider

$$E[\varepsilon_f^2(n)] = \sigma_{v_x}^2, \text{ for all } n \quad (25)$$

where $\sigma_{v_x}^2 = E[v_x^2(n)]$. Use (21), (23) and (24) to obtain

$$\varepsilon_f(n) = [1 - \mu_f(n)\mathbf{v}_g^T(n)\mathbf{v}_g(n)]e_f(n). \quad (26)$$

From (26), $E[\varepsilon_f^2(n)]$ can be written as (Benesty, Rey, Vega, & Tressens, 2006)

$$E\{\varepsilon_f^2(n)\} = [1 - \mu_f(n)L_f\sigma_{v_g}^2]^2\sigma_{e_f}^2(n), \quad (27)$$

where $\sigma_{v_g}^2 = E[v_g^2(n)]$ and $\sigma_{e_f}^2(n) = E[e_f^2(n)]$. Equating (27) with (25) results in

$$\sigma_{v_x}^2 = [1 - \mu_f(n)L_f\sigma_{v_g}^2]^2\sigma_{e_f}^2(n). \quad (28)$$

Solve (28) for $\mu_f(n)$

$$\mu_f(n) = \frac{\alpha_f(n)}{L_f\sigma_{v_g}^2}, \quad (29)$$

$$\alpha_f(n) = \left[1 - \frac{\sigma_{v_x}}{\sigma_{e_f}(n)}\right], \quad (30)$$

where $0 \leq \alpha_f(n) \leq 1$. During the transition phase, $\sigma_{e_f}(n) \gg \sigma_{v_x}$, which is appropriate for fast convergence. While, $\sigma_{e_f}(n) \approx \sigma_{v_x}$ and $\mu_f \approx 0$ in the steady state to result in a low misadjustment.

3.1.2. Convergence of the misalignment

The analysis in this section is based on the independence assumptions as the resulting predictions for LMS algorithm match for the simulations and practical performance (Farhang-Boroujeny, 1999).

Independence Assumption

- (1) The auxiliary data vectors $\mathbf{v}_g(1), \mathbf{v}_g(2), \dots, \mathbf{v}_g(n)$ are statistically independent.
- (2) At time k , desired output of $F(z)$ is dependent on $\mathbf{v}_g(k)$. The current desired output of $F(z)$ and $\mathbf{v}_g(k)$ are statistically independent of all past outputs of $F(z)$, $\mathbf{f}^T(i)\mathbf{v}_g(i)$ for $i = 1, 2, \dots, k-1$.

Let the misalignment vector be $\mathbf{m}_f(n) = \mathbf{f}(n) - \hat{\mathbf{f}}(n)$. Subtract $\mathbf{f}(n)$ from both sides of (24)

$$\mathbf{m}_f(n+1) = \mathbf{m}_f(n) - \frac{\alpha_f(n)}{L_f\sigma_{v_g}^2}\mathbf{v}_g(n)e_f(n), \quad (31)$$

Take l_2 norm and mathematical expectation

$$E[\|\mathbf{m}_f(n+1)\|_2^2] = E[\|\mathbf{m}_f(n)\|_2^2] - 2\frac{\alpha_f(n)}{L_f\sigma_{v_g}^2}E[\mathbf{v}_g^T(n)\mathbf{m}_f(n)e_f(n)] + \frac{\alpha_f^2(n)}{L_f^2\sigma_{v_g}^4}E[e_f^2(n)\mathbf{x}_g^T(n)\mathbf{v}_g(n)]. \quad (32)$$

Using $\mathbf{m}_f(n)$ definition, (21) becomes

$$e_f(n) = \mathbf{v}_g^T(n)\mathbf{m}_f(n) + v_x(n). \quad (33)$$

Substitute (33) into (32) and remove uncorrelated terms

$$E[\mathbf{v}_g^T(n)\mathbf{m}_f(n)e_f(n)] = E[\mathbf{v}_g^T(n)\mathbf{m}_f(n)\mathbf{v}_g^T(n)\mathbf{m}_f(n)] = E[(\mathbf{v}_g^T(n)\mathbf{m}_f(n))^2]. \quad (34)$$

Using the independence assumption to evaluate (34), then $(\mathbf{v}_g(n), x_r(n))$ are independent of $\{(\mathbf{v}_g(n-1), x_r(n-1)), (\mathbf{v}_g(n-2), x_r(n-2)), \dots\}$ (Ardekani & Abdulla, 2013; Farhang-Boroujeny, 1999). Similarly, $\mathbf{m}_f(n+1)$ is independent of $\mathbf{v}_g(n)$ and depends only on

$\{(\mathbf{v}_g(n-1), x_r(n-1)), (\mathbf{v}_g(n-2), x_r(n-2)), \dots\}$. Vectors $\mathbf{v}_g(n)$ and $\mathbf{v}_g(n-1)$ have (L_f-1) common terms. Nevertheless, anticipations by the independence assumption match the actual performance and the simulations of the LMS algorithm (Farhang-Boroujeny, 1999). Explanation by weakly-dependence assumption states that affect on $\mathbf{f}(n)$ by $\{(\mathbf{v}_g(n-1), x_r(n-1)), (\mathbf{v}_g(n-2), x_r(n-2)), \dots\}$ becomes negligible for small $\mu_f(n)$. Thus, $\hat{\mathbf{f}}(n)$ and $\mathbf{m}_f(n)$ are independent of $\mathbf{f}^T(k)\mathbf{v}_g(k)$ and $\mathbf{v}_g(k)$. Therefore, (34) becomes

$$E[(\mathbf{v}_g^T(n)\mathbf{m}_f(n))^2] = E[\text{tr}[\mathbf{m}_f^T(n)\mathbf{R}_{v_g v_g}\mathbf{m}_f(n)]] = \text{tr}[E[\mathbf{m}_f(n)\mathbf{m}_f^T(n)]\mathbf{R}_{v_g v_g}], \quad (35)$$

where $\mathbf{R}_{v_g v_g} = E[\mathbf{v}_g(n)\mathbf{v}_g^T(n)]$ and $\text{tr}[\cdot]$ denotes the trace of a matrix. In the steady state, $[\mathbf{m}_f(n)\mathbf{m}_f^T(n)]$ is close to a diagonal matrix, since errors of the individual coefficients become uncorrelated. Therefore, (35) becomes

$$E[\mathbf{v}_g^T(n)\mathbf{m}_f(n)e_f(n)] = \sigma_{v_g}^2 E[\|\mathbf{m}_f(n)\|_2^2]. \quad (36)$$

The last expectation term from (32) can be expressed as

$$E[e_f^2(n)\mathbf{v}_g^T(n)\mathbf{v}_g(n)] = \text{tr}[E[e_f^2(n)\mathbf{v}_g(n)\mathbf{v}_g^T(n)]]. \quad (37)$$

Substitute (33) and remove uncorrelated terms

$$E[e_f^2(n)\mathbf{v}_g^T(n)\mathbf{v}_g(n)] = \text{tr}[E[v_x^2(n)\mathbf{v}_g^T(n)\mathbf{v}_g(n)] + E[\mathbf{v}_g(n)\mathbf{v}_g^T(n)\mathbf{m}_f(n)\mathbf{m}_f^T(n)\mathbf{v}_g(n)\mathbf{v}_g^T(n)]]. \quad (37)$$

Using independence assumption, the last expectation term on the right hand side of (37) can be written as

$$E[\mathbf{v}_g(n)\mathbf{v}_g^T(n)\mathbf{m}_f(n)\mathbf{m}_f^T(n)\mathbf{v}_g(n)\mathbf{v}_g^T(n)] = E[\mathbf{v}_g(n)\mathbf{v}_g^T(n)\mathbf{K}(n)\mathbf{v}_g(n)\mathbf{v}_g^T(n)], \quad (38)$$

where $\mathbf{K}(n) = E[\mathbf{m}_f(n)\mathbf{m}_f^T(n)]$. Using the procedure proposed in Farhang-Boroujeny (1999), (38) can be written as

$$E[\mathbf{v}_g(n)\mathbf{v}_g^T(n)\mathbf{K}(n)\mathbf{v}_g(n)\mathbf{v}_g^T(n)] = \sigma_{v_g}^4 E[\|\mathbf{m}_f(n)\|_2^2]\mathbf{I}_{L_f} + 2\sigma_{v_g}^4 E[\mathbf{m}_f(n)\mathbf{m}_f^T(n)], \quad (39)$$

where \mathbf{I}_{L_f} is an identity matrix of order L_f . Substitute (39) in (37) results in

$$E[e_f^2(n)\mathbf{v}_g^T(n)\mathbf{v}_g(n)] = \text{tr}[\sigma_{v_g}^4 E[\|\mathbf{m}_f(n)\|_2^2]\mathbf{I}_{L_f} + 2\sigma_{v_g}^4 E[\mathbf{m}_f(n)\mathbf{m}_f^T(n)] + L_f\sigma_{v_g}^2\sigma_{v_x}^2] = (L_f+2)\sigma_{v_g}^4 E[\|\mathbf{m}_f(n)\|_2^2] + L_f\sigma_{v_g}^2\sigma_{v_x}^2. \quad (40)$$

Substituting (36) and (40) in (32) results in

$$E[\|\mathbf{m}_f(n+1)\|_2^2] = g(\alpha_f(n), L_f)E[\|\mathbf{m}_f(n)\|_2^2] + h(\alpha_f(n), L_f, \sigma_{v_g}^2, \sigma_{v_x}^2), \quad (41)$$

where

$$g(\alpha_f(n), L_f) = 1 - 2\frac{\alpha_f(n)}{L_f} + \frac{(L_f+2)\alpha_f^2(n)}{L_f^2}, \quad (42)$$

$$h(\alpha_f(n), L_f, \sigma_{v_g}^2, \sigma_{v_x}^2) = \frac{\alpha_f^2(n)}{L_f\sigma_{v_g}^2}\sigma_{v_x}^2. \quad (43)$$

Expression (41) relates misalignment with convergence rate and misadjustment. The term $g(\alpha_f(n), L_f)$ influences the convergence rate of the algorithm, and its minimum value results in fastest convergence with $\alpha_f(n)$ as the reference parameter

$$\alpha_f(n) |_{\text{FC}} = \frac{L_f}{L_f+2}, \quad (44)$$

where subscript FC denotes fast convergence. For long filters $L_f \gg 2$, the fastest convergence is possible for $\alpha_f(n) \approx 1$, which is an established result (Haykin & Widrow, 2003; Sulyman & Zerguine, 2003). For the proposed $\alpha_f(n)$ in (30), (21) shows that $e_f(n) > v_x(n)$ for large estimation errors, $\mathbf{f}(n) - \hat{\mathbf{f}}(n)$. This happens at the system startup or in case of perturbation in $\mathbf{f}(n)$. If $e_f(n) \gg v_x(n)$,

then $\sigma_{e_f}(n)$ is also greater than σ_{v_x} and $\alpha_f(n) \approx 1$ from (30) which ensures fast convergence.

The stability condition is expressed by the non-increasing $E[\|\mathbf{m}_f(n+1)\|_2^2]$ in (41). The decreasing trend in (41) can be obtained by $g(\alpha_f(n), L_f) < 1$. From (42), we get

$$g(\alpha_f(n), L_f) |_{\text{stable}} = \frac{2L_f}{L_f+2}, \quad (44)$$

where subscript 'stable' denotes stability condition. For $L_f \gg 2$, (44) reduces to $\alpha_f(n) |_{\text{stable}} < 2$ and using (30)

$$\left[1 - \frac{\sigma_{v_x}}{\sigma_{e_f}(n)} \right] < 2.$$

This condition is always true since $\sigma_{e_f}(n) > \sigma_{v_x}$. The minimum value of $\sigma_{e_f}(n)$ occurs at $\mathbf{f}(n) \approx \hat{\mathbf{f}}(n)$, which means $\sigma_{e_f}(n) \approx \sigma_{v_x}$ and $\alpha_f(n) \approx 0$. When $e_f(n) \gg v_x(n)$, then $\alpha_f(n) \approx 1$. Thus, $\alpha_f(n)$ is always within the stability limit.

The term $h(\alpha_f(n), L_f, \sigma_{v_g}^2, \sigma_{v_x}^2)$ in (41) influences the misadjustment which increases with increase in $\sigma_{v_x}^2$ and decreases with increase in $\sigma_{v_g}^2$. The misadjustment is minimum when (43) reaches its minimum for $\alpha_f(n) \approx 0$ (Haykin & Widrow, 2003). Desired minimum misadjustment occurs when $\sigma_{e_f}^2 \approx \sigma_{v_x}^2$ in the steady state and $\alpha_f(n) \approx 0$ from (30).

3.1.3. Practical considerations

The first consideration is to avoid the divisions by small numbers by adding a positive constant ϵ_f to the denominator in (29). Normally, $\sigma_{e_f}(n) \geq \sigma_{v_x}$ and $\alpha_f(n) \geq 0$. For implementation, $\sigma_{e_f}^2(n)$ is

$$\sigma_{e_f}^2(n) = \beta \sigma_{e_f}^2(n-1) + (1-\beta)e_f^2(n), \quad (45)$$

where β is a forgetting factor. Also, (45) may give $\sigma_{e_f}(n) < \sigma_{v_x}$ and $\alpha_f(n) < 0$. The safety check is to set $\mu_f(n) = 0$ for $\alpha_f(n) < 0$. Moreover, (30) is not implementable due to unavailable term σ_{v_x} . Therefore, we derive the disturbance signal energy estimate, $\hat{\sigma}_{v_x}^2(n)$, to implement (30). The cross-correlation between $\mathbf{v}_g(n)$ and $e_f(n)$ is $\mathbf{r}_f(n) = E[\mathbf{v}_g(n)e_f(n)]$. Use (33) and remove uncorrelated terms to get

$$\mathbf{r}_f(n) = \mathbf{R}_{v_g v_g} \mathbf{m}_f(n), \quad (46)$$

where $\mathbf{R}_{v_g v_g} = E[\mathbf{v}_g(n)\mathbf{v}_g^T(n)]$ and $\mathbf{m}_f(n) = \mathbf{f}(n) - \hat{\mathbf{f}}(n)$. The variance of $e_f(n)$ is

$$\begin{aligned} \sigma_{e_f}^2(n) &= E[e_f^2(n)] \\ &= \mathbf{m}_f^T(n) \mathbf{R}_{v_g v_g} \mathbf{m}_f(n) + \sigma_{v_x}^2(n), \end{aligned} \quad (47)$$

where $\sigma_{v_x}^2(n)$ is the power of the part of $e_f(n)$ that is contributed by $x(n)$. From (46) and (47), the term $\sigma_{v_x}^2(n)$ can be written as (Iqbal & Grant, 2008)

$$\sigma_{v_x}^2(n) = \sigma_{e_f}^2(n) - \frac{\mathbf{r}_f^T(n)\mathbf{r}_f(n)}{\sigma_{v_g}^2(n)}, \quad (48)$$

where $\sigma_{v_g}^2(n)$ is the variance of the auxiliary noise. Estimated values of $\sigma_{e_f}^2(n)$, $\mathbf{r}_f(n)$ and $\sigma_{v_g}^2(n)$ are used in (48) to evaluate $\hat{\sigma}_{v_x}^2(n)$ by using the exponential recursive weighting algorithm

$$\hat{\sigma}_{v_x}^2(n) = \beta \hat{\sigma}_{v_x}^2(n-1) + (1-\beta) \left(\hat{\sigma}_{e_f}^2(n) - \frac{\hat{\mathbf{r}}_f^T(n)\hat{\mathbf{r}}_f(n)}{\hat{\sigma}_{v_g}^2(n)} \right), \quad (49)$$

$$\hat{\sigma}_{e_f}^2(n) = \beta \hat{\sigma}_{e_f}^2(n-1) + (1-\beta)e_f^2(n), \quad (50)$$

$$\hat{\sigma}_{v_g}^2(n) = \beta \hat{\sigma}_{v_g}^2(n-1) + (1-\beta)v_g^2(n), \quad (51)$$

$$\hat{\mathbf{r}}_f(n) = \beta \hat{\mathbf{r}}_f(n-1) + (1-\beta)\mathbf{v}_g(n)e_f(n). \quad (52)$$

Expressions (24), (29), (30) and (49) to (52) can be used to implement the SAVSS-NLMS algorithm for $\hat{F}(z)$.

3.2. Self-adapting VSS-NLMS algorithm for $B(z)$

The SAVSS-NLMS algorithm for $B(z)$ is obtained by following the procedure given in Section 3.1. Corresponding analysis is also valid. Filter $B(z)$ predicts the contribution of $x(n)$ in $x_c(n)$. The update expression for $B(z)$ is

$$\mathbf{b}(n+1) = \mathbf{b}(n) + \mu_b(n)\mathbf{x}_b(n)e_f(n), \quad (53)$$

where $e_f(n)$ and $\mathbf{x}_b(n)$ are defined in (13) and (14) respectively. From (21) and (22)

$$e_f(n) = v_{gb} + v_x(n), \quad (54)$$

where $v_{gb} = \mathbf{v}_g^T(n)[\mathbf{f}(n) - \hat{\mathbf{f}}(n)]$ is the disturbance term and $v_x(n)$ is the error signal for $B(z)$. After the convergence of $F(z)$, v_{gb} becomes very small and $e_f(n)$ becomes the prediction error. This means $F(z)$ and $B(z)$ reduce disturbance for each other. Parameter $\mu_b(n)$ in (54) is

$$\mu_b(n) = \left[1 - \frac{\hat{\sigma}_{v_{gb}}}{\hat{\sigma}_{e_f}(n)} \right] \frac{1}{L_b \sigma_{x_b}^2}. \quad (55)$$

Similar to (49)–(52), $\hat{\sigma}_{v_{gb}}^2(n)$ can be written as

$$\hat{\sigma}_{v_{gb}}^2(n) = \beta \hat{\sigma}_{v_{gb}}^2(n-1) + (1-\beta) \left(\hat{\sigma}_{e_b}^2(n) - \frac{\hat{\mathbf{r}}_b^T(n)\hat{\mathbf{r}}_b(n)}{\hat{\sigma}_{x_b}^2(n)} \right), \quad (56)$$

$$\hat{\sigma}_{e_b}^2(n) = \beta \hat{\sigma}_{e_b}^2(n-1) + (1-\beta)e_b^2(n), \quad (57)$$

$$\hat{\sigma}_{x_b}^2(n) = \beta \hat{\sigma}_{x_b}^2(n-1) + (1-\beta)x_c^2(n-D), \quad (58)$$

$$\hat{\mathbf{r}}_b(n) = \beta \hat{\mathbf{r}}_b(n-1) + (1-\beta)\mathbf{x}_b(n)e_f(n). \quad (59)$$

Expressions (53)–(59) are implementable for $B(z)$, and a scheme for $G(n)$ is designed in the next section.

4. Design of auxiliary noise gain $G(n)$

A suitable $G(n)$ should have a large value when $\hat{F}(z)$ estimation is poor, and be negligible in the steady state. The error signal for the effective performance of $\hat{F}(z)$ is $e_f(n)$ as it has information for estimating $\hat{F}(z)$ as well as $x(n)$. In Ahmed and Akhtar (2017), $G(n)$ is obtained by

$$G(n) = \sqrt{\frac{\hat{\sigma}_{e_f}^2(n-1)}{\hat{\mathbf{f}}^T(n)\hat{\mathbf{f}}(n)}}, \quad (60)$$

where $\hat{\sigma}_{e_f}^2(n)$ is provided in (50). Expression (60) makes the power of $\mathbf{v}_g^T(n)\hat{\mathbf{f}}(n)$ equal to $\hat{\sigma}_{e_f}^2(n-1)$, and maintains significant auxiliary noise in $e(n)$ in the steady state. In order to reduce $G(n)$ in the steady state,

$$f_{e_f,k}(n) = \beta f_{e_f,k}(n-1) + (1-\beta) |e_f(n)|^k, \quad \text{for } k = 2, 5. \quad (61)$$

where $|\cdot|$ denotes the absolute value. It is clear from (61) that $f_{e_f,5}(n) < f_{e_f,2}(n)$ for $|e_f(n)| < 1$. Hence, $f_{e_f,5}(n)$ is preferred for small $e_f(n)$ in the steady state. Therefore, we propose

$$G(n) = \sqrt{\frac{f_{e_f,5}(n)}{\hat{\mathbf{f}}^T(n)\hat{\mathbf{f}}(n)}}, \quad \text{if } \min(f_{e_f,2}(n), f_{e_f,5}(n)) = f_{e_f,5}(n) \quad (62)$$

where $\min(\cdot)$ selects the minimum of the available values. By using (62), $G(n)$ becomes negligible by switching to $f_{e_f,5}(n)$ in the steady state. Values $k > 5$ are equally valid for (61) and (62) in the steady state. Therefore, $k = 5$ is used. For $|e_f(n)| > 1$, $f_{e_f,5}(n) > f_{e_f,2}(n)$. Therefore, $f_{e_f,2}(n)$ may be selected for $|e_f(n)| > 1$ as is used in Ahmed and Akhtar (2017). However, this selection does not ensure the improvement in $\hat{F}(z)$ without considering the

power of $x(n)$ in $x_c(n)$. Therefore, the proposed $G(n)$ at the system initialization or in case of perturbation is

$$G(n) = \sqrt{\frac{\hat{\sigma}_{y_b}^2(n)}{\hat{\mathbf{f}}^T(n)\hat{\mathbf{f}}(n)}}, \quad (63)$$

$$\hat{\sigma}_{y_b}^2(n) = \beta\hat{\sigma}_{y_b}^2(n-1) + (1-\beta)(\mathbf{b}^T(n)\mathbf{x}_b(n)), \quad (64)$$

where $\hat{\sigma}_{y_b}^2(n)$ is the power of the output of $B(z)$. Use of (63) during the large error times is advantageous as this signal only contains the predictable part of $x_c(n)$ and it cannot inflate with increase in the accuracy of $\hat{F}(z)$. The proposed method introduces a bounded gain during poor estimation stage and negligible auxiliary noise in the steady state. When $G(n)$ is small for $\min(f_{ef,2}(n), f_{ef,5}(n)) = f_{ef,5}(n)$, it is reasonable to stop updating $\hat{F}(z)$ and $B(z)$. The validity of convergence analysis for proposed $G(n)$ in Section 3.1.2 can be established intuitively for the maximum value of $G(n)$ as is demonstrated in Ahmed and Akhtar (2017) with the same maximum value. The convergence analysis in Section 3.1.2 is valid for variable gain. However, detailed convergence analysis with explicit $G(n)$ term is complex and will be addressed in a future work.

5. Self-adapting FxNLMS algorithm for $W(z)$

The SAVSS-FxNLMS algorithm for $W(z)$ is obtained by following the procedure used for $\hat{F}(z)$ and $B(z)$. Therefore, only implementable expressions are presented. The expression for updating the coefficient vector is

$$\mathbf{w}(n+1) = \mathbf{w}(n) + \mu_w(n)\mathbf{x}_s(n)e(n), \quad (65)$$

$$\mathbf{x}_s(n) = [x_s(n), x_s(n-1), \dots, x_s(n-L_w+1)]^T,$$

$$x_s(n) = s(n) * x_c(n), \quad (66)$$

where $\mu_w(n)$ is step size, and $e(n)$ from (7) becomes

$$e(n) = d(n) - s(n) * y(n) + v_{gw}(n), \quad (67)$$

where $v_{gw}(n) = s(n) * v_g(n)$ is the disturbance for $W(z)$, $d(n) - s(n) * y(n)$ is the desired error signal for $W(z)$, and $\mu_w(n)$ in (65) is

$$\mu_w(n) = \left[1 - \frac{\hat{\sigma}_{v_{gw}}}{\hat{\sigma}_e(n)}\right] \frac{1}{L_w\sigma_{x_s}^2}. \quad (68)$$

Similar to (49)–(52), $\hat{\sigma}_{v_{gw}}^2(n)$ can be written as

$$\hat{\sigma}_{v_{gw}}^2(n) = \beta\hat{\sigma}_{v_{gw}}^2(n-1) + (1-\beta)\left(\hat{\sigma}_e^2(n) - \frac{\hat{\mathbf{r}}_w^T(n)\hat{\mathbf{r}}_w(n)}{\hat{\sigma}_{x_s}^2(n)}\right), \quad (69)$$

$$\hat{\sigma}_e^2(n) = \beta\hat{\sigma}_e^2(n-1) + (1-\beta)e^2(n), \quad (70)$$

$$\hat{\sigma}_{x_s}^2(n) = \beta\hat{\sigma}_{x_s}^2(n-1) + (1-\beta)x_s^2(n), \quad (71)$$

$$\hat{\mathbf{r}}_w(n) = \beta\hat{\mathbf{r}}_w(n-1) + (1-\beta)\mathbf{x}_s(n)e(n). \quad (72)$$

6. Computational complexity

The computational complexity of the proposed and the established methods is compared in terms of the number of multiplications and additions, which is standard in relevant literature and established research work (Ahmed & Akhtar, 2017; Ahmed et al., 2015; Diniz, 2008; Kuo & Morgan, 1996). Reduction in computational complexity is preferred for processors running multiple applications and to reduce power consumption for long battery life. Table 1 lists the computational complexity for the algorithms, where there are two entries for the proposed method since it stops updating $\hat{F}(z)$ and $B(z)$ when $G(n)$ is negligible. The algorithm in Akhtar and Mitsuhashi (2011) is simple and computationally least expensive of the previous methods. In Ahmed

Table 1
Computational requirements for various ANC systems.

Method	Additions	Multiplications
Kuo (2002)	$3L_f + 2L_w + L_s + 2L_b$	$3L_f + 2L_w + L_s + 2L_b + 3$
Akhtar and Mitsuhashi (2011)	$2L_f + 2L_w + L_s + 2L_b + 6$	$2L_f + 2L_w + L_s + 2L_b + 11$
Ahmed et al. (2013)	$3L_f + 2L_w + L_s + 2L_b$	$3L_f + 2L_w + L_s + 2L_b + 9$
Ahmed and Akhtar (2017)	$3L_f + 2L_w + L_s + 2L_b - 1$	$3L_f + 2L_w + L_s + 2L_b + 7$
Proposed Maximum ^a	$5L_f + 4L_w + L_s + 4L_b + 11$	$5L_f + 4L_w + L_s + 4L_b + 22$
Proposed Minimum ^b	$L_f + 2L_w + L_s + L_b$	$L_f + 2L_w + L_s + L_b + 5$

^aFilters $\hat{\mathbf{f}}(n)$, $\mathbf{b}(n)$ and $\mathbf{w}(n)$ are updated.

^bOnly $\mathbf{w}(n)$ is updated.

Table 2
Normalized memory requirements for various ANC systems.

Method	Number of variables to be stored
Kuo (2002)	$3L_f + 2L_w + L_s + 2L_b + L_D + 7^a$
Akhtar and Mitsuhashi (2011)	$2L_f + 2L_w + L_s + 2L_b + 16$
Ahmed et al. (2013)	$2L_f + 2L_w + L_s + 2L_b + 15$
Ahmed and Akhtar (2017)	$4L_f + 2L_w + L_s + 2L_b + 14$
Proposed	$4L_f + 3L_w + L_s + 3L_b + 27$

^a L_D is length of decorrelation delay.

and Akhtar (2017), Ahmed et al. (2013), $G(n)$ calculation increases computations compared with Akhtar and Mitsuhashi (2011). For the proposed method

- SAVSS-NLMS algorithms are used for $\hat{F}(z)$, $B(z)$ and $W(z)$, which increases the computational cost compared with the fixed step size. 38
- $L_f\sigma_{v_g}^2$ or $\mathbf{v}_g^T(n)\mathbf{v}_g(n)$ can be used to normalize in (29). Evaluating $L_f\sigma_{v_g}^2$ using (51) requires 4 multiplications and 1 addition. For $\mathbf{v}_g^T(n)\mathbf{v}_g(n)$ 39
- $\mathbf{v}_g^T(n+1)\mathbf{v}_g(n+1) = \mathbf{v}_g^T(n)\mathbf{v}_g(n) + v_g^2(n+1) - v_g^2(n-L_f+1)$, which requires only 1 multiplication and 2 additions. Similar implementation can be used for (55) and (68). 40
- At the system start up or in case of perturbation, $\hat{F}(z)$ update and $G(n)$ calculation is required. This stage requires maximum computations as labelled in Table 1. However, minimum computations are required during the steady state. This also saves L_f multiplications and $L_f - 1$ additions for the calculation of $G(n)$. 41

Memory usage is also taken into account by the number of variables stored at each iteration as listed in Table 2. The proposed method and Ahmed and Akhtar (2017) require slightly more variables. It is difficult to intuitively decide on methods from Tables 1 and 2. Therefore, computations are plotted against time using Table 1 in the next section. 42

7. Case studies

Simulation studies are conducted for the proposed algorithm (PM), Kuo (KM) (Kuo, 2002), Akhtar (AM) (Akhtar & Mitsuhashi, 2011), Shakeel (SM1) (Ahmed et al., 2013) and Shakeel (SM2) (Ahmed & Akhtar, 2017) under standard conditions to compare the performance in terms of the mean squared-error $E[e^2(n)]$, the relative $F(z)$ identification error 43

$$\Delta F(n) = 10\log_{10} \left(\frac{\|\mathbf{f}(n) - \hat{\mathbf{f}}(n)\|^2}{\|\mathbf{f}(n)\|^2} \right), \quad (73) \quad 44$$

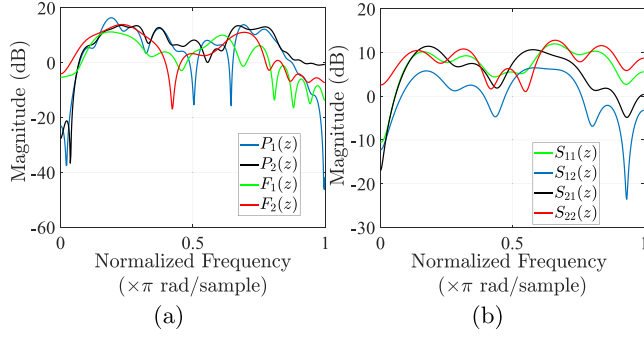


Fig. 3. Amplitude response for acoustic paths.

Table 3
Parameter values used in simulations.

Method	Case 1	Case 2
Kuo (2002)	$\beta = 0.99, \mu_w = 3e^{-5}, \mu_h = 5e^{-4}, \mu_f = 5e^{-3}$	$\beta = 0.99, \mu_w = 1e^{-5}, \mu_h = 2e^{-4}, \mu_f = 3e^{-3}$
Akhtar and Mitsuhashi (2011)	$\beta = 0.99, \mu_w = 3e^{-5}, \mu_h = 5e^{-4}, \mu_{f_{\min}} = 3e^{-4}, \mu_{f_{\max}} = 5e^{-3}$	$\beta = 0.99, \mu_w = 1e^{-5}, \mu_h = 2e^{-4}, \mu_{f_{\min}} = 5e^{-4}, \mu_{f_{\max}} = 3e^{-3}$
Ahmed et al. (2013)	$\mu_h = 5e^{-4}, \mu_f = 1e^{-3}, \beta = 0.99, \mu_w = 3e^{-5}$	$\mu_h = 2e^{-4}, \mu_f = 8e^{-4}, \beta = 0.99, \mu_w = 1e^{-5}$
Ahmed and Akhtar (2017)	$\beta = 0.99, \mu_w = 3e^{-5}, \mu_h = 5e^{-4}, \mu_f = 1e^{-3}$	$\beta = 0.99, \mu_w = 1e^{-5}, \mu_h = 2e^{-4}, \mu_f = 8e^{-4}$
Proposed	$\beta = 0.99, D = L_f$	$\beta = 0.99, D = L_f$

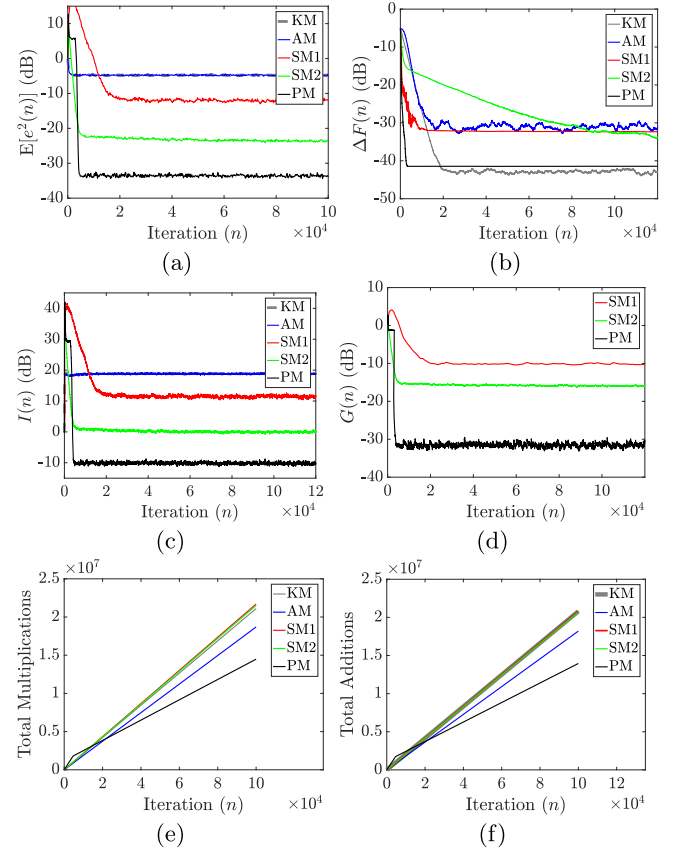


Fig. 4. Performance results for Case 1.

1 convergence speed, number of tunable parameters, computa-
2 tional complexity, $G(n)$ and interference in the gradient for
3 $W(z)$

$$4 \quad I(n) = \beta I(n-1) + (1-\beta) \|\mathbf{x}_{s,a}(n)e(n) - \mathbf{x}_{s,a}(n)e_a(n)\|, \quad (74)$$

5 where $\mathbf{x}_{s,a}(n)e_a(n)$ is the gradient in the absence of $F(z)$. The
6 sampling frequency is 2 kHz and $v(n)$ is a zero mean white
7 noise of unit variance. Primary $\{P_1(z), P_2(z)\}$ paths, secondary
8 $\{S_{11}(z), S_{12}(z), S_{21}(z), S_{22}(z)\}$ paths, feedback $\{F_1(z), F_2(z)\}$
9 paths, and $W(z)$ are considered as FIR filters of order 48, 16, 32
10 and 32 respectively. Like Ahmed and Akhtar (2017) and Akhtar
11 and Mitsuhashi (2011), acoustic paths are the experimental data
12 provided in Kuo and Morgan (1996) (see Fig. 3). Similar to
13 Ahmed and Akhtar (2017), $\hat{F}(z)$ is initialized with a $\Delta F(n)$ of
14 -5 dB. The values for various parameters are provided in Table 3
15 and results are obtained by averaging over 20 runs.

16 7.1. Case 1

17 In this case, $x(n)$ is a tone of 500 Hz with variance of 2.0.
18 Such noise is produced by machines like fans, generators and
19 compressors (Aslam, 2016). Gaussian noise is mixed to have SNR
20 $= 30$ dB. The acoustic paths used are $P(z) = P_1(z), S(z) =$
21 $S_{11}(z), F(z) = F_1(z)$. In Fig. 4, the proposed method reduces
22 $E[e^2(n)]$ to a steady state value of -35 dB in 4600 iterations,
23 which is an improvement of at least 11 dB. Accurate $\Delta F(n)$
24 with considerably reduced computations can be seen in Fig. 4(b),
25 (e) and (f). The improvement in $E[e^2(n)]$ is imminent from Fig. 4(c)
26 and (d). Term $I(n)$ is reduced by at least 10 dB, and $G(n)$ is
27 reduced by at least 15 dB in the steady state. KM and AM have a
28 fixed $G(n)$ of 0.05. The proposed method requires at least 24%
29 less computations after 100,000 iterations (see Fig. 4(e) and (f)).
30 The proposed ANC system reduces $e(n)$ in minimum iterations and

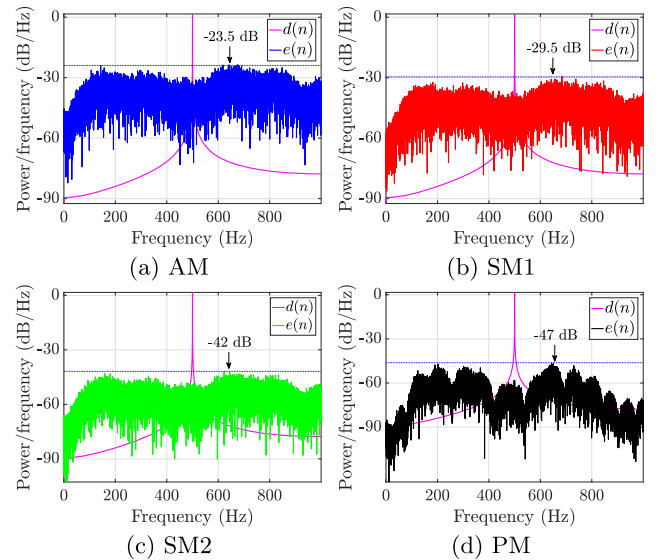


Fig. 5. Power spectra of $d(n)$ and $e(n)$ in Case 1.

31 computations. Power spectra for various methods are shown in
32 Fig. 5.

33 7.2. Case 2

34 In this case, $x(n)$ is a multi-tonal signal of frequencies: 100,
35 150, 300, 400 and 450 Hz, with variance of 2.0. Gaussian noise
36 is mixed for SNR $= 30$ dB. The acoustic paths at startup are

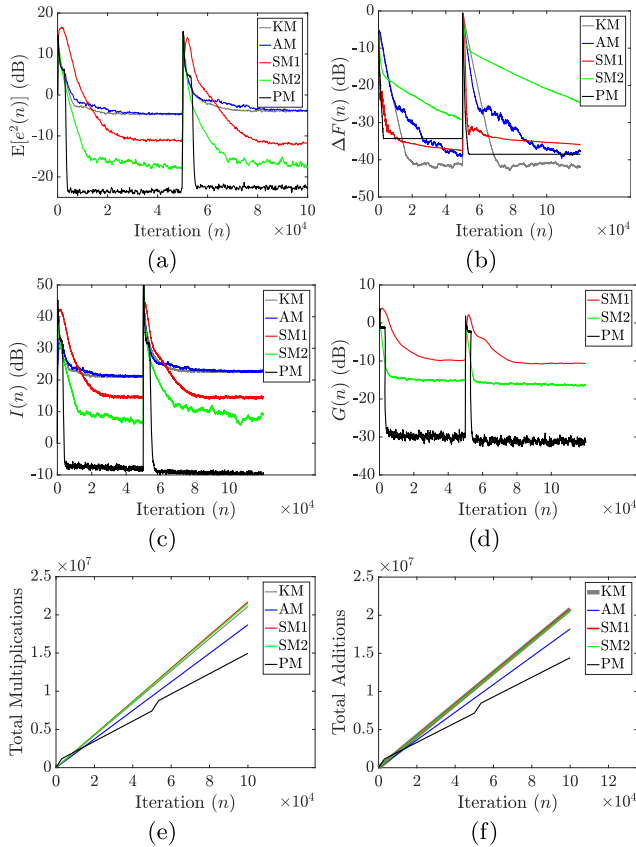


Fig. 6. Performance results for Case 2.

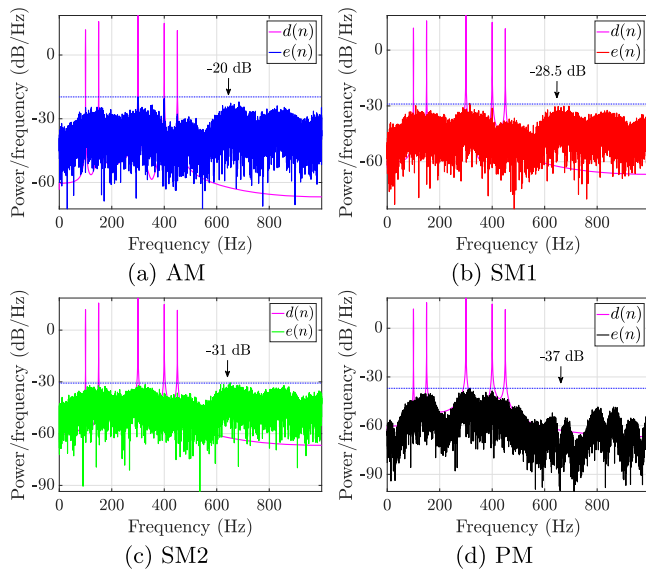


Fig. 7. Power spectra of $d(n)$ and $e(n)$ in Case 2.

steady state. KM and AM have $G(n) = 0.05$. The computations for PM in Fig. 6(e) and (f) are at least 17% less after 100,000 iterations with acoustic perturbation. The robustness of PM is validated by a similar performance before and after the perturbation in the acoustic paths. The proposed method has shown improvement in all desirable areas. Moreover, the power spectra shown in Fig. 7 validate the improved performance of PM.

8. Conclusions

This paper introduces SAVSS-NLMS adaptive algorithms used for $\hat{F}(z)$, $B(z)$ and $W(z)$. In the proposed schemes, the step size varies according to the system requirement unlike the previous methods which use either fixed or an increase only type step sizes. A novel and simple $G(n)$ is presented that responds effectively to the acoustic changes with negligible steady state power. Filter updates for $\hat{F}(z)$ and $B(z)$ and their corresponding step sizes are discontinued when $G(n)$ is negligible to significantly reduce the operational needs of the proposed algorithm. Also, small $G(n)$ reduces interference at the input and output of $W(z)$ and improves the noise reduction. The proposed method provides unprecedented balance between fast convergence and reduced computations while providing significantly improved steady state performance and robustness to acoustic path perturbation.

References

- Ahmed, S., & Akhtar, M. T. (2017). Gain scheduling of auxiliary noise and variable step-size for online acoustic feedback cancellation in narrow-band active noise control systems. *IEEE/ACM Transactions on Audio, Speech, and Language Processing*, 25(2), 333–343.
- Ahmed, S., Akhtar, M. T., & Zhang, X. (2013). Online acoustic feedback mitigation with improved noise-reduction performance in active noise control systems. *IET Signal Processing*, 7(6), 505–514.
- Ahmed, S., Akhtar, M. T., & Zhang, X. (2015). Variable step-size based-adaptive algorithm for acoustic feedback cancellation during online operation of ANC systems. In *IEEE China summit and international conference on signal and information processing* (pp. 74–78).
- Akhtar, M. T., & Mitsuhashi, W. (2011). Variable step-size based method for acoustic feedback modeling and neutralization in active noise control systems. *Applied Acoustics*, 72(5), 297–304.
- Ardekani, I. T., & Abdulla, W. H. (2013). Stochastic modelling and analysis of filtered-x least-mean-square adaptation algorithm. *IET Signal Processing*, 7(6), 486–496.
- Aslam, M. S. (2016). Maximum likelihood least squares identification method for active noise control systems with autoregressive moving average noise. *Automatica*, 69, 1–11.
- Aslam, M. S., & Raja, M. A. Z. (2015). A new adaptive strategy to improve online secondary path modeling in active noise control systems using fractional signal processing approach. *Signal Processing*, 107, 433–443.
- Aslam, M. S., Shi, P., & Lim, C. C. (2019). Variable threshold-based selective updating algorithms in feed-forward active noise control systems. *IEEE Transactions on Circuits and Systems. I. Regular Papers*, 66(2), 782–795.
- Benesty, J., Rey, H., Vega, L. R., & Tressens, S. (2006). A nonparametric VSS NLMS algorithm. *IEEE Signal Processing Letters*, 13(10), 581–584.
- Diniz, P. S. R. (2008). *Adaptive filtering: Algorithms and practical implementation*. New York, NY, USA: Springer.
- Farhang-Boroujeny, B. (1999). *Adaptive filters: Theory and applications*. John Wiley and Sons Ltd.
- Haykin, S., & Widrow, B. (2003). *Least-mean-square adaptive filters*. Hoboken, NJ: Wiley.
- Iqbal, M. A., & Grant, S. L. (2008). Novel variable step size NLMS algorithms for echo cancellation. In *IEEE International conference on acoustics, speech and signal processing* (pp. 241–244).
- Kuo, S. M. (2002). Active noise control system and method for on-line feedback path modeling. Patent US6418227.
- Kuo, S. M., & Luan, J. (1994). On-line modeling and feedback compensation for multiple-channel active noise control systems. *Applied Signal Processing*, 1(2), 64–75.
- Kuo, S. M., & Morgan, D. R. (1996). *Active noise control systems—Algorithms and DSP implementations*. New York: Wiley.

1 $P(z) = P_1(z), S(z) = S_{11}(z), F(z) = F_1(z)$ which change to
 2 $P(z) = P_2(z), S(z) = S_{22}(z), F(z) = F_2(z)$ at $n = 50,000$.
 3 In Fig. 6, the proposed algorithm converges in 3000 iterations
 4 at start up with an improvement of at least 5.5 dB in $E[e^2(n)]$
 5 and $\Delta F(n) = -34$ dB. The convergence speed is significantly
 6 improved by using PM as shown in Fig. 6(a). In Fig. 6(c) and (d),
 7 PM reduces $I(n)$ by at least 10 dB and $G(n)$ by at least 15 dB in the

- 1 Kuo, S. M., & Vijayan, D. (1997). A secondary path modeling technique for active
2 noise control systems. *IEEE Transactions on Speech and Audio Processing*, 5,
3 374–377.
- 4 Liao, C.-W., & Lin, J.-Y. (2007). New FIR filter-based adaptive algorithms incorpo-
5 rating with commutation error to improve active noise control performance.
6 *Automatica*, 43(2), 325–331.
- 7 Lueg, P. (1936). Process of silencing sound oscillations. Patent US2043416 A.
- 8 Sulyman, A. I., & Zerguine, A. (2003). Convergence and steady-state analysis of
9 a variable step-size NLMS algorithm. *Signal Processing*, 83(6), 1255–1273.
- 10 Zhang, M., Lan, H., & Ser, W. (2001). Cross-updated active noise control system
11 with online secondary path modeling. *IEEE Transactions on Speech and Audio*
12 *Processing*, 9, 598–602.
- 13 Zhang, M., Lan, H., & Ser, W. (2003). A robust online secondary path modeling
14 method with auxiliary noise power scheduling strategy and norm constraint
15 manipulation. *IEEE Transactions on Speech and Audio Processing*, 11, 45–53.



16 **Muhammad Saeed Aslam** is pursuing Ph.D. in Elec-
17 trical Engineering from The University of Adelaide.
18 He received the Master degree in control systems
19 engineering from the Pakistan Institute of Engineering
20 and Applied Sciences (PIEAS), Islamabad, Pakistan, in
21 2009 and the Bachelor degree in Electrical engineering
22 from the University of Engineering and Technology
23 (UET), Lahore, Pakistan, in 2007. His research interests
24 include digital signal processing, filter design theory,
25 adaptive algorithms, system identification, and active
26 noise control.
27



28 **Peng Shi** received the Ph.D. degree in Electrical Engi-
29 neering from the University of Newcastle, Australia in
30 1994. He was awarded the Doctor of Science degree
31 from the University of Glamorgan, Wales in 2006; and
32 the Doctor of Engineering degree from the University
33 of Adelaide, Australia in 2015. He is now a professor
34 at the University of Adelaide. His research interests
35 include system and control theory, autonomous and
36 robotic systems, and cyber-physical systems. He has
37 served on the editorial board of a number of journals,
38 including *Automatica*; *IEEE Transactions on (Automatic*
39 *Control*; *Cybernetics*; *Fuzzy Systems*; *Circuits and Systems*). He is a Member-
40 at-Large of Board of Governors, IEEE SMC Society, and an IEEE SMC Society
41 Distinguished Lecturer. He is a Fellow of the Institute of Electrical and Electronic
42 Engineers, Institution of Engineering and Technology; and the Institute of
43 Engineers, Australia.
44



45 **Cheng-Chew Lim** received the B.Sc. degree (Hons.) in
46 electronic and electrical engineering and Ph.D. degree
47 in electronic and electrical engineering from Lough-
48 borough University, Leicestershire, U.K. He is currently
49 a Professor with the University of Adelaide, Adelaide,
50 SA, Australia. His research interests include control and
51 systems theory, autonomous systems, machine learn-
52 ing, and optimization techniques and applications. Dr.
53 Lim serves as an Associate Editor for the *IEEE Trans-*
54 *actions of Systems, Man, and Cybernetics: Systems* and
55 an Editorial Board Member for the *Journal of Industrial*
56 *and Management Optimization*, and has served as a Guest Editor for a number
57 of journals, including *Discrete and Continuous Dynamical System-Series B*.
58

Chapter 6

New control structure for estimation-less acoustic feedback neutralization in active noise control systems

A new control structure is designed to cancel out narrowband noises in active noise control systems with acoustic feedback. Unlike the conventional approach which involves the estimation of feedback path, the proposed method involves frequency estimation algorithm to generate the reference signal internally. A two-tap noise controller is used for each tone. Performance analysis is provide to demonstrate the undiased frequency estimate, error in time varying frequency estimation and noise reduction performance.

Statement of Authorship

Title of Paper	New Control Structure for Estimation-less Acoustic Feedback Neutralization in Active Noise Control Systems
Publication Status	Submitted for Publication
Publication Details	Muhammad Saeed Aslam, Peng Shi, Cheng-Chew Lim (2020). New Control Structure for Estimation-less Acoustic Feedback Neutralization in Active Noise Control Systems, <i>Automatica</i> , under review.

Principal Author

Name of Principal Author (Candidate)	Muhammad Saeed Aslam		
Contribution to the Paper	Designed the core idea and performed analysis on the concept, interpreted data, wrote manuscript and acted as corresponding author		
Overall percentage (%)	80%		
Certification:	This paper reports on original research I conducted during the period of my Higher Degree by Research candidature and is not subject to any obligations or contractual agreements with a third party that would constrain its inclusion in this thesis. I am the primary author of this paper.		
Signature		Date	8/11/2020

Co-Author Contributions

By signing the Statement of Authorship, each author certifies that:

- i. the candidate's stated contribution to the publication is accurate (as detailed above);
- ii. permission is granted for the candidate to include the publication in the thesis; and
- iii. the sum of all co-author contributions is equal to 100% less the candidate's stated contribution.

Name of Co-Author	Peng Shi		
Contribution to the Paper	Supervised development of work, helped in refining core concept and manuscript evaluation.		
Signature		Date	8 Nov 2020

Name of Co-Author	Cheng-Chew Lim		
Contribution to the Paper	Supervised development of work, helped in data interpretation and manuscript evaluation.		
Signature		Date	8/11/2020

Please cut and paste additional co-author panels here as required.

New control structure for estimation-less acoustic feedback neutralization in active noise control systems[★]

Muhammad Saeed Aslam^a, Peng Shi^a, Cheng-Chew Lim^a

^a*School of Electrical and Electronic Engineering, The University of Adelaide, SA, 5005, Australia*

Abstract

A new control structure is proposed to cancel out narrowband noises for ANC systems with acoustic feedback. The proposed control structure does not require estimate of feedback path to neutralize it. Instead, a frequency estimation algorithm is designed to estimate the frequencies of tones in the reference signal. Using each frequency estimate, reference signals are internally generated for a two-tap noise controller. Performance analysis is provided for proposed frequency estimation algorithm to establish unbiased estimates and good tracking ability. Finally, simulations are performed for benchmark conditions to demonstrate the contribution of the proposed control structure.

Key words: Parameter estimation, notch filter, feedback path neutralization, active noise control.

1 Introduction

Active noise control (ANC) systems are popular choice for reducing the low frequency noises in numerous daily use applications including headphones, mobile phones, incubators and automobiles[1–3]. In a conventional ANC system, reference and error microphones are used to obtain reference and error signals respectively. Adaptive algorithm uses the reference and error signals to update the noise control filter coefficients. Noise control filter derives the speaker to

★

Email addresses: muhammad.aslam@adelaide.edu.au (Muhammad Saeed Aslam), peng.shi@adelaide.edu.au (Peng Shi), cheng.lim@adelaide.edu.au (Cheng-Chew Lim).

produce the cancelling acoustics at the error microphone. In certain scenarios, reflections of acoustics from speaker reach the reference microphones and this phenomenon is referred as acoustic feedback. Acoustic feedback forms a de-stabilizing closed loop of reference signal.

The de-stabilizing acoustic feedback is neutralized by using specialized equipment (directional reference microphone and speaker) or electronically by estimating the acoustic feedback path [1,4]. Electronic acoustic feedback neutralization is a challenging task and numerous methods have been developed in the recent past [1,5–10]. The general structure for an ANC system with acoustic feedback is given in Fig. 1 where n is the time, $x(n)$ is the reference signal, $x_f(n)$ is the acoustic feedback signal, $\hat{x}_f(n)$ is the acoustic feedback neutralization signal, $x_c(n)$ is the input signal for noise controller, $d(n)$ is the primary noise, $e(n)$ is the residual error signal, $y(n)$ is the controller output signal, and $\hat{d}(n)$ is the cancelling signal. $P(z)$ represents the primary acoustic path, $S(z)$ represents the secondary path, $F(z)$ represents the feedback path, $\hat{F}(z)$ represents the estimated feedback path, and $W(z)$ represents the noise control filter. Signal $x(n)$ passes through $P(z)$ to form $d(n)$ and $\hat{d}(n)$ results from $y(n)$ passing through $S(z)$. Acoustic reflections of $y(n)$ corrupt $x(n)$ in the form of $x_f(n)$. In order to obtain $x(n)$, $\hat{x}_f(n)$ is obtained by passing $y(n)$ through $\hat{F}(z)$. Signal $\hat{x}_f(n)$ neutralizes $x_f(n)$ to provide a genuine $x(n)$ for $W(z)$. Therefore, accuracy of $\hat{F}(z)$ is critical for the performance of $W(z)$.

Apart from the dependence on the accuracy of $\hat{F}(z)$, there are some critical aspects of the use of FIR noise control filter to bear in mind. When the reference signal has a large number of frequencies or the frequencies are closely spaced, the filter length needs to be large to provide good filtering ($L_w \gg 2M$ where L_w is the length of noise control filter and M is the number of sinusoids). However, a high-order filter normally suffers from large excess mean square error, slow convergence and high numerical error [4]. In the authors' view, all the previous methods [1,5–8,11] obtain $\hat{F}(z)$ to neutralize the acoustic feedback. In this paper, a new control structure is proposed to cancel narrowband noises in ANC systems with acoustic feedback that does not require the estimation of $\hat{F}(z)$. A frequency estimation algorithm is proposed to estimate the frequencies of narrowband noises in the reference signal. Then, sinusoids corresponding to estimated frequencies are generated internally. These reference signals are used to derive the noise controllers for each tone. The distinct features presented in this paper in comparison with the previous established methods are as follows

- (1) A new robust control structure is proposed to cancel narrowband noises without acoustic feedback path estimation.
- (2) Since $\hat{F}(z)$ is not obtained for the proposed method, auxiliary noise is not introduced at any time. This reduces the noise level by significant margin.

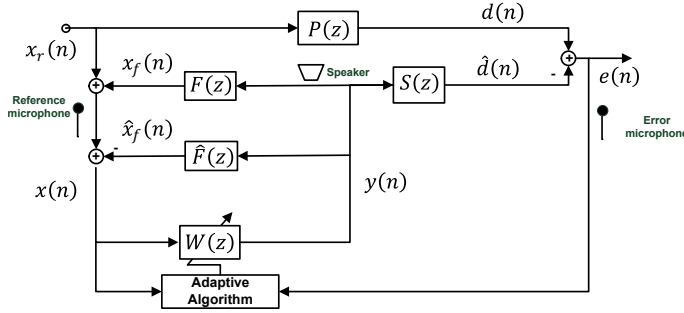


Fig. 1. ANC system with acoustic feedback.

- (3) Simple two-tap controllers are used to cancel each tone. Therefore, any number of tones can be handled without suffering poor convergence or numerical error.
- (4) The proposed frequency estimation algorithm can estimate and track closely spaced frequencies as well.

The organization of the paper is as follows: Section 2 presents the proposed ANC structure with frequency estimation algorithm presented in Section 3. Performance analysis of the proposed frequency estimation algorithm is presented in Section 4. Computations required for the proposed control structure are given in Section 5. Simulation results and discussions are given in Section 6 with conclusions provided in Section 7.

2 Proposed ANC Structure

The structure of the proposed method is provided in Fig. 2, where $p(n)$, $f(n)$ and $s(n)$ represent the impulse responses for the primary path $P(z)$, the feedback path $F(z)$ and the secondary path $S(z)$ respectively. At the reference microphone, the corrupted reference signal $x(n)$ is detected

$$x(n) = x_r(n) + x_f(n), \quad (1)$$

where $x(n)$ is the genuine reference signal in the absence of $F(z)$ and $x_f(n)$ is the signal contributed by $F(z)$ at the reference microphone. Since narrowband noises are considered in this paper, $x(n)$ can be written as

$$x(n) = \sum_{i=1}^M C_i [e^{j(\omega_i n + \phi_{xi})} + e^{-j(\omega_i n + \phi_{xi})}] + v(n), \quad (2)$$

where C_i , ϕ_{xi} and ω_i represent the amplitude, phase and angular frequency, respectively. Measurement noise, $v(n)$, is considered as zero mean Gaussian noise. ω_i can be written as

$$\omega_i = 2\pi \frac{f_i}{f_s}, \quad (3)$$

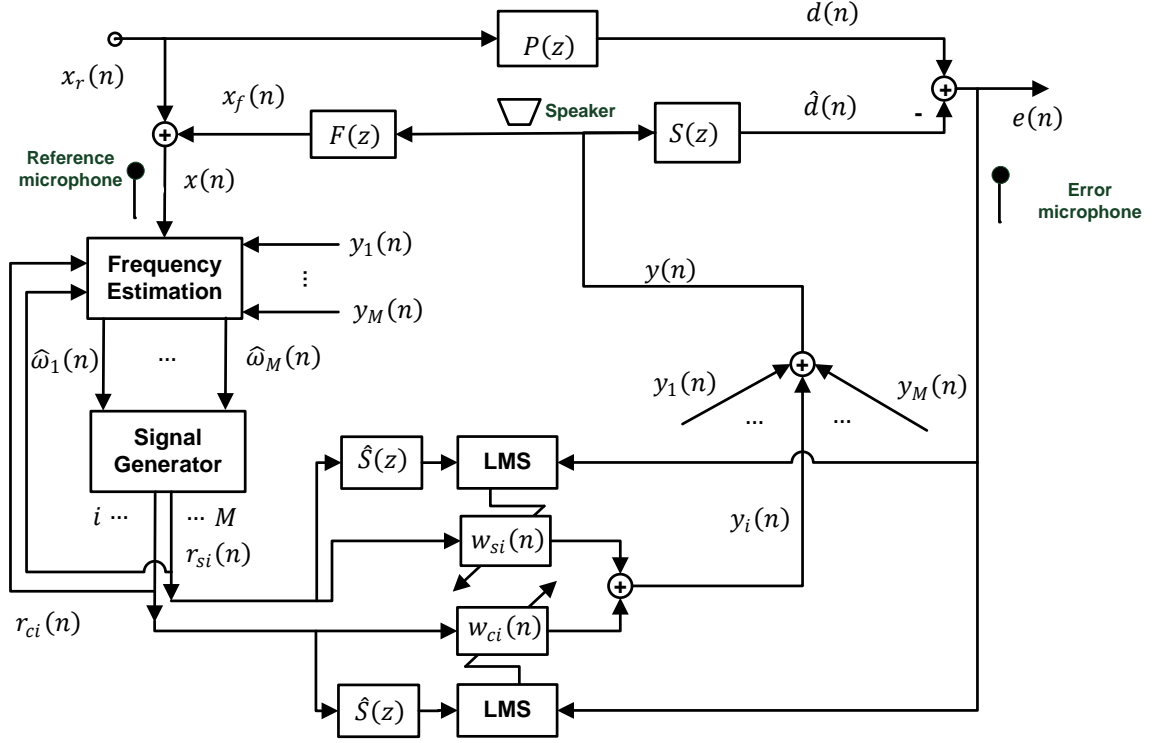


Fig. 2. Proposed control structure for ANC system with acoustic feedback.

where f_i denotes the i th frequency and f_s presents the sampling frequency. Signal $x(n)$ is used as an input to the frequency estimation algorithm. Let $\hat{\omega}_1, \hat{\omega}_2, \dots, \hat{\omega}_M$ be the estimated frequencies obtained from the estimation algorithm (where $\hat{\omega}_i = 2\pi \hat{f}_i / f_s$). A signal generator is used to obtain two periodic signals corresponding to each $\hat{\omega}_i$

$$r_{ci}(n) = \cos(\hat{\omega}_i n), \quad (4)$$

$$r_{si}(n) = \sin(\hat{\omega}_i n). \quad (5)$$

For each ω_i , noise control signal is obtained by

$$y_i(n) = w_{ci}(n)r_{ci}(n) + w_{si}(n)r_{si}(n), \quad (6)$$

where $w_{ci}(n)$ and $w_{si}(n)$ are the noise control weights. The net control signal for all frequencies $\hat{\omega}_1, \hat{\omega}_2, \dots, \hat{\omega}_M$ is

$$y(n) = \sum_{i=1}^M y_i(n). \quad (7)$$

The cancelling signal $\hat{d}(n)$ is obtained by

$$\hat{d}(n) = s(n) * y(n), \quad (8)$$

where $*$ denotes linear convolution. Signal $\hat{d}(n)$ is used to cancel out the primary noise $d(n)$ at the error microphone

$$d(n) = p(n) * x_r(n). \quad (9)$$

The error signal $e(n)$ received at the error microphone is

$$e(n) = d(n) - \hat{d}(n), \quad (10)$$

Expressions (4), (5) and (8) are used to update the noise control weights in (6)

$$w_{ci}(n+1) = w_{ci}(n) + \mu \hat{r}_{ci}(n) e(n), \quad (11)$$

$$w_{si}(n+1) = w_{si}(n) + \mu \hat{r}_{si}(n) e(n), \quad (12)$$

where

$$\hat{r}_{ci}(n) = \hat{s}(n) * r_{ci}(n), \quad (13)$$

$$\hat{r}_{si}(n) = \hat{s}(n) * r_{si}(n), \quad (14)$$

and μ is the step size parameter and $\hat{s}(n)$ is the estimated secondary path impulse response. Since acoustic feedback neutralization is the area of focus in this paper, it is assumed that accurate $\hat{s}(n)$ has already been obtained. In the next section, estimation of $\hat{\omega}_1, \hat{\omega}_2, \dots, \hat{\omega}_M$ is addressed in detail.

3 Frequency Estimation

The block diagram for frequency estimation process is given in Fig. 3. For each $\hat{\omega}_i$ for $i = 1, 2, \dots, M-1$, the following steps are conducted

- (1) Let $u_i(n)$ be the input signal, then enhance $u_i(n)$ by passing through an all-pole enhancing filter to produce $\hat{u}_i(n)$.
- (2) Recursively calculate frequency $\hat{\omega}_i$ from $\hat{u}_i(n)$.
- (3) Remove $\hat{\omega}_i$ from $u_i(n)$ using notch filter centered at $\hat{\omega}_i$ and use the resulting signal as input for estimating frequency $\hat{\omega}_{i+1}$.

The first step enhances the target frequency $\hat{\omega}_i$ by using[12]

$$E_i(q^{-1}) = \frac{1}{1+2\alpha k_i q^{-1} + \alpha^2 q^{-2}}, \quad (15)$$

where q^{-1} represents unit time delay, $0 < \alpha < 1$ and k_i is defined as

$$k_i = -\cos(\hat{\omega}_i), \quad (16)$$

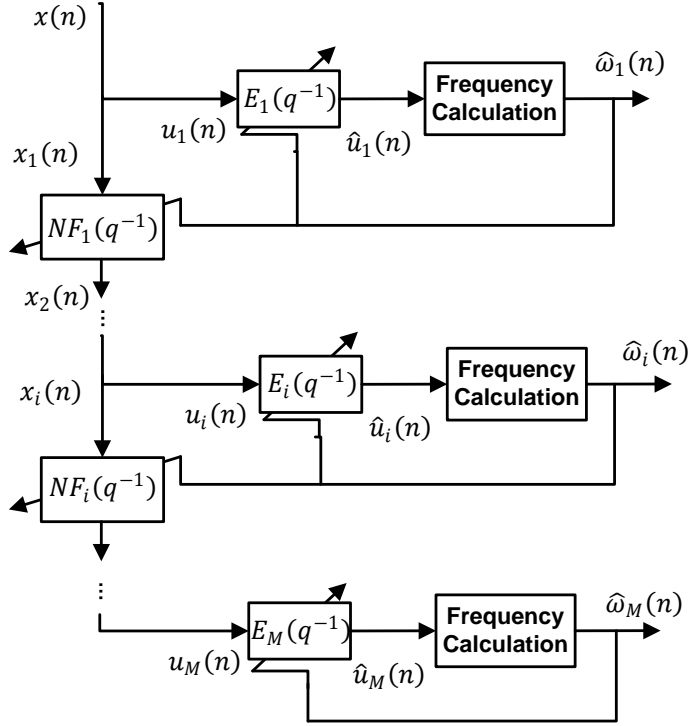


Fig. 3. Frequency estimation algorithm.

In the second step, the Burg algorithm [13] is used to recursively estimate the $\hat{\omega}_i$ from $\hat{u}_i(n)$ (output of $E_i(q^{-1})$). Define the intermediate variables

$$B_i(n) = \lambda B_i(n-1) + 2(1-\lambda)\hat{u}_i^2(n-1), \quad (17)$$

$$A_i(n) = \lambda A_i(n-1) + (1-\lambda)\hat{u}_i(n-1)[\hat{u}_i(n) + \hat{u}_i(n-2)], \quad (18)$$

where $0.9 < \lambda < 1$ is the forgetting factor. The angular frequency estimation is as follows

$$\hat{k}_i(n) = -\frac{A_i(n)}{B_i(n)+\eta}, \quad (19)$$

where η is a small number added in the denominator to avoid division by zero. Estimation from (19) is smoothen out by

$$k_i(n) = \gamma k_i(n-1) + (1-\gamma)\hat{k}_i(n), \quad (20)$$

where $0.9 < \gamma < 1$. Finally, $\hat{\omega}_i$ can be written as

$$\hat{\omega}_i = \cos^{-1}(k_i(n)). \quad (21)$$

The last step prepares the input signal for next frequency estimation. Therefore, it is not required for $i = M$. The input signal for $\hat{\omega}_{i+1}$ estimation is obtained by removing the $\hat{\omega}_i$ frequency component using the notch filter centered at $\hat{\omega}_i$

$$NF_i(q^{-1}) = \frac{1+2k_i q^{-1}+q^{-2}}{1+2\alpha k_i q^{-1}+\alpha^2 q^{-2}}. \quad (22)$$

For M frequencies, there will be M enhancing filters given in (15) and $M - 1$ notch filters given in (22). Notch filters are connected series to make the output of i th notch filter to be the input of $(i + 1)$ th notch filter. In this way multiple stages cannot converge to same frequency. As the frequencies are estimated, the corresponding tones are eliminated. The already estimated frequencies are not available to the next stage and this reduces the interference in the frequency estimates as explained in Section 4.1.

4 Performance analysis

Performance of the frequency estimation algorithm is analysis in terms of offset, frequency deviation and noise reduction. The off-set, ζ , represents the bias in frequency estimation resulting from interfering frequencies or low signal-to-noise (SNR) ratio. Frequency deviation, ψ , results from the time-varying frequencies.

4.1 Offset

Offset can be defined as the difference between $-\cos(\omega_i)$ and $-\cos(\hat{\omega}_i)$ for ω_i in the steady state

$$\zeta_i = -\cos(\omega_i) - \hat{k}_m. \quad (23)$$

The offset can result from the interference from other tones in $u_i(n)$ and the measurement noise. From [14], (17)-(19) can be written as

$$B_i(n) = \lambda B_i(n-1) + 2(1-\lambda)u_i^2(n-1), \quad (24)$$

$$y_u(n) = u_i(n) + 2\hat{k}_i(n-1)u_i(n-1) + u_i(n-1), \quad (25)$$

$$\hat{k}_i(n) = \hat{k}_i(n-1) - \frac{1-\lambda}{B_i(n)}u_i(n-1)y_u(n), \quad (26)$$

where $y_u(n)$ is obtained from the numerator in (22)

$$y_u(n) = (1 + 2k_iq^{-1} + q^{-2})u_i(n), \quad (27)$$

For a slowly varying frequency, the convergence of $\hat{k}_i(n)$ is conditioned by

$$E[u_i(n-1)y_u(n)] = 0, \quad (28)$$

In a steady state, let $k_i(\infty) = \hat{k}_i(\infty) \rightarrow k_i$ and substitute (22) and (27) into (28)

$$E\{u_i(n-1)[u_i(n) + 2k_iu_i(n-1) + u_i(n-2)]\} = 0, \quad (29)$$

Also, (29) can also be expressed as

$$R_u(0)\hat{k}_i + R_u(1) = 0, \quad (30)$$

where $R_u(l) = E[u_i(n)u_i(n-l)]$. From [15], $R_u(0)$, $R_u(1)$ can be derived as

$$R_u(0) = \frac{D_m^2 |E(e^{j\omega_m})|^2}{2} + \frac{(1+\alpha^2)\sigma^2}{(1-\alpha^2)[(1+\alpha^2)^2 - 4\alpha^2\hat{k}_i^2]}, \quad (31)$$

$$R_x(1) = \frac{D_m^2 \cos(\omega_m) |E(e^{j\omega_m})|^2}{2} + \frac{(2\alpha\sigma^2\hat{k}_i)}{(1-\alpha^2)[(1+\alpha^2)^2 - 4\alpha^2\hat{k}_i^2]}, \quad (32)$$

where σ^2 represents the variance of measurement noise and D_m^2 is the variance of tone with angular frequency ω_m . Substitute (15), (31) and (32) into (30)

$$\frac{D_m^2 [\hat{k}_i + \cos(\omega_m)]}{2|1 + 2\hat{k}_i\alpha e^{-j\omega_m} + \alpha^2 e^{-2j\omega_m}|^2} + \frac{\hat{k}_i(1-\alpha)\sigma^2}{(1+\alpha)[(1-\alpha^2)^2 + 4\alpha^2(1-\hat{k}_i^2)]} = 0. \quad (33)$$

Extending (33) to include impact of multiple tones with ω_m where $m = 1, 2, \dots, M$)

$$\sum_{m=1}^M \frac{D_m^2 [\hat{k}_i + \cos(\omega_m)]}{2|1 + 2\hat{k}_i\alpha e^{-j\omega_m} + \alpha^2 e^{-2j\omega_m}|^2} + \frac{\hat{k}_i(1-\alpha)\sigma^2}{(1+\alpha)[(1-\alpha^2)^2 + 4\alpha^2(1-\hat{k}_i^2)]} = 0, \quad (34)$$

For cases with high SNR, the second term in (34) becomes negligible

$$\sum_{m=1}^M \frac{D_m^2 [\hat{k}_i + \cos(\omega_m)]}{|1 + 2\hat{k}_i\alpha e^{-j\omega_m} + \alpha^2 e^{-2j\omega_m}|^2} = 0, \quad (35)$$

It is clear from (35) that estimate \hat{k}_i is at a bias to one of $\cos(\omega_m)$. In order to move forward with high order (35) for the explicit expression of bias, let \hat{k}_i be close to $-\cos(\omega_i)$

$$\hat{k}_i = -\cos(\omega_i) + \Delta k_i, \quad (36)$$

where Δk_i is much smaller than unity. Substitute (36) in (35)

$$\sum_{m=1}^M \frac{D_m^2 [-\cos(\omega_i) + \Delta k_i + \cos(\omega_m)]}{|1 + 2\hat{k}_i\alpha e^{-j\omega_m} + \alpha^2 e^{-2j\omega_m}|^2} = 0, \quad (37)$$

The denominator in (35) for each m can be written as

$$\begin{aligned} |J(e^{j\omega_m})|^2 &= |1 + 2\hat{k}_i\alpha e^{-j\omega_m} + \alpha^2 e^{-2j\omega_m}|^2 \\ &= |F_m + 2\alpha e^{-2j\omega_m} \Delta_m|^2 \end{aligned} \quad (38)$$

where

$$F_m = 1 - 2\cos(\omega_m)\alpha e^{-j\omega_m} + \alpha^2 e^{-2j\omega_m}, \quad (39)$$

$$\Delta_m = \cos(\omega_m) - \cos(\omega_i) + \Delta k_i, \quad (40)$$

Expanding (38)

$$|J(e^{j\omega_m})|^2 = |F_m|^2 + 4\alpha^2\Delta_m^2 + 4\alpha(1-\alpha)^2\cos(\omega_m)\Delta_m. \quad (41)$$

For $m = i$, (40) becomes

$$|J(e^{j\omega_i})|^2 = |F_i|^2 + 4\alpha^2\Delta k_i^2 + 4\alpha(1-\alpha)^2\cos(\omega_i)\Delta k_i. \quad (42)$$

where $|F_i|^2 = (1-\alpha)^2[(1+\alpha)^2 - 4\alpha\cos^2(\omega_i)]$ and

$$|D(e^{j\omega_m})|^2 = (1-\alpha)^2[(1+\alpha)^2 - 4\alpha\cos^2(\omega_m)] + 4\alpha^2\Delta_m^2 + 4\alpha(1-\alpha)^2\cos(\omega_m)\Delta_m, \quad (43)$$

for $m \neq i$. For $(1-\alpha) \ll 1$ and $\Delta k_i \ll 1$, we assume

$$\begin{aligned} (1-\alpha)^2 &\ll 1 \\ \Delta k_i^2 &\ll \Delta k_i \\ \Delta k_i(1-\alpha)^2 &\ll \Delta k_i \\ \Delta k_i(1-\alpha)^2 &\ll (1-\alpha)^2 \end{aligned} \quad (44)$$

Substitute (42) and (43) into (35) and use (44) to ignore the higher-order terms of Δk_i and $(1-\alpha)$

$$\begin{aligned} (1-\alpha)^2[(1+\alpha)^2 - 4\alpha\cos^2(\omega_m)] \sum_{m=1, m \neq i}^M \{D_m^2[\cos(\omega_m) - \cos(\omega_i)] \\ \prod_{l \neq m, l > i}^M 4\alpha^2[\cos(\omega_l) - \cos(\omega_i)]^2\} + \\ D_i^2 \Delta k_i \prod_{y=1, y \neq i}^M 4\alpha^2[\cos(\omega_y) - \cos(\omega_i)]^2 = 0, \end{aligned} \quad (45)$$

Rearranging (45) to obtain

$$\begin{aligned} \Delta k_i = & -[(1+\alpha)^2 4\alpha\cos^2(\omega_i)](1-\alpha)^2 \\ & \frac{\sum_{m=1, m \neq i}^M \{D_m^2[\cos(\omega_i) - \cos(\omega_1)] \prod_{l \neq m, l > i}^M 4\alpha^2[\cos(\omega_l) - \cos(\omega_1)]^2\}}{D_i^2 \Delta k_i \prod_{y=1, y \neq i}^M 4\alpha^2[\cos(\omega_l) - \cos(\omega_i)]^2} \\ & - \frac{[(1+\alpha)^2 4\alpha\cos^2(\omega_i)](1-\alpha)^2}{4\alpha^2} \sum_{m=1, m \neq i}^M \frac{D_m^2}{D_i^2[\cos(\omega_m) - \cos(\omega_i)]}, \end{aligned} \quad (46)$$

For small $(1-\alpha)$, expression for offset ζ_i in ω_i can be obtained from (46)

$$\begin{aligned} \zeta_i = & -\Delta k_i \\ & \approx (1-\alpha)^2 \sin^2(\omega_i) \sum_{m=1, m \neq i}^M \frac{D_m^2}{D_i^2[\cos(\omega_m) - \cos(\omega_i)]}, \end{aligned} \quad (47)$$

where D_m^2 represents the variance of tones with ω_m for $m = 1, 2, \dots, M$ in signal $u_i(n)$ used for estimation of ω_i . The proposed algorithm estimates the

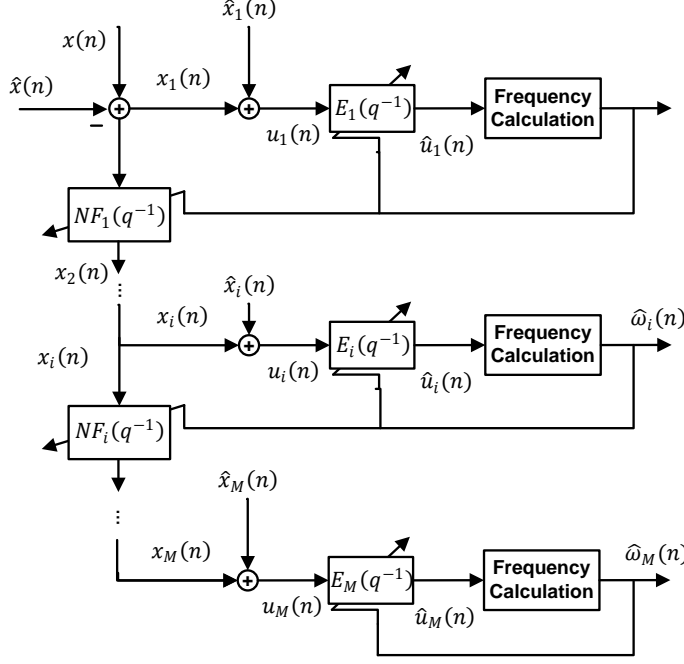


Fig. 4. Frequency estimation with compensation of interfering tones.

frequencies from ω_1 to ω_M in an orderly manner. Sinusoids with frequencies ω_i for $i = 1, 2, \dots, l-1$ are removed from signal $u_l(n)$ used for detection of ω_l while $M-l$ interfering frequencies are still present. Therefore, $D_m^2 = 0, m < i$ and bias ζ_i in (47) becomes

$$\zeta_i = (1 - \alpha)^2 \sin^2(\omega_i) \sum_{m=i+1}^M \frac{D_m^2}{D_i^2 [\cos(\omega_m) - \cos(\omega_i)]}, \quad (48)$$

where $i = 1, 2, \dots, M-1$. For $i = M$, sinusoids with frequencies ω_i for $i = 1, 2, \dots, M-1$ are removed and estimation is unbiased for ω_M . It is clear from (48) that offset ζ_i can be reduced by choosing $(1 - \alpha)$ to a small value. However, the convergence speed can deteriorate for α close to 1. For (i)th stage of frequency estimation, the frequencies $\hat{\omega}_{i+1}, \hat{\omega}_{i+2}, \dots, \hat{\omega}_M$ are disturbance frequencies which can lead to biased results and deteriorate performance of the ANC system. To remove the interfering frequencies for any ω_i , adaptive filters are introduced as shown in Figs. 4 and 5. Similar to (11) and (12), these adaptive filters are updated by

$$z_{1i}(n+1) = z_{1i}(n) + \mu_z r_{ci}(n)(x(n) - \hat{x}(n)), \quad (49)$$

$$z_{2i}(n+1) = z_{2i}(n) + \mu_z r_{si}(n)(x(n) - \hat{x}(n)), \quad (50)$$

where μ_z is the step size and signals $\{r_{ci}(n), r_{si}(n)\}$ are given in (4) and (5), respectively. The term for $\hat{x}(n)$ is the sum of outputs from $\{z_{1i}(n+1), z_{2i}(n+1)\}$ for $i = 1, 2, \dots, M$

$$\hat{x}(n) = \sum_{i=1}^M \hat{x}_i(n) = \sum_{i=1}^M z_{1i}(n)r_{ci}(n) + z_{2i}(n)r_{si}(n). \quad (51)$$

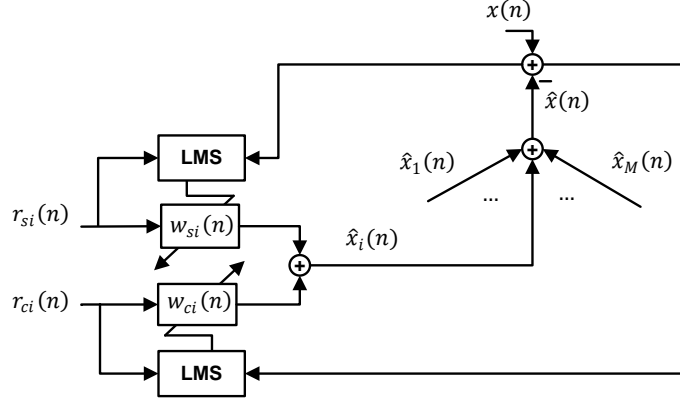


Fig. 5. Adaptive filters for removing interfering tones.

Signal $\hat{x}(n)$ is removed from $x(n)$ before the use of any $NF_i(q^{-1})$ and the input signal for $E_i(q^{-1})$ are modified as (see Fig. 4)

$$u_i(n) = x_i(n) + \hat{x}_i(n). \quad (52)$$

By introducing these changes, interfering frequencies for each ω_i are eliminated before frequency calculation. Therefore, $D_m^2 \rightarrow 0, m \neq i$ in (48) and estimates for ω_i are unbiased for $i = 1, 2, \dots, M$ in the steady state.

4.2 Frequency Estimation Error

For constant frequency, \hat{k}_i has the following form

$$\hat{k}_i = -\cos(\hat{\omega}_i), \quad (53)$$

However, it is important to consider the time-delay for time-varying frequency

$$\hat{k}_i = -\cos(\omega_i - \Delta\omega_i), \quad (54)$$

where ω_i is the target angular frequency and time-delay angular frequency $\Delta\omega_i$ results from varying frequency. From (17) and (18), (54) can be written as [16]

$$\cos(\omega_i - \Delta\omega_i) \approx \frac{\sum_{j=1}^{\text{inf}} \lambda^j \cos(\omega - jv_{\omega_i})}{\sum_{j=1}^{\text{inf}} \lambda^j}, \quad (55)$$

where v_{ω_i} denotes a constant rate of change in ω_i . Sampling frequency can be set to make v_{ω_i} small. Then, a Taylor series approximation of (55) can be expressed as

$$\begin{aligned} \cos(\omega_i - \Delta\omega_i) &\approx \frac{\sum_{j=1}^{\text{inf}} \lambda^j \cos(\omega_i)}{\sum_{j=1}^{\text{inf}} \lambda^j} + \frac{\sum_{j=1}^{\text{inf}} \lambda^j j v_{\omega_i} \sin(\omega_i)}{\sum_{j=1}^{\text{inf}} \lambda^j} \\ &= \cos(\omega_i) + \frac{\lambda v_{\omega_i} \sin(\omega_i)}{1-\lambda}, \end{aligned} \quad (56)$$

From (56), the time-delay deviation becomes

$$\begin{aligned} k_i - \hat{k}_i &= -\cos(\omega_i) + \cos(\omega_i - \Delta\omega_i) \\ &= \frac{\lambda v \omega_i \sin(\omega_i)}{1-\lambda}. \end{aligned} \quad (57)$$

Using (48) and (57), the error in estimation of frequency f_i can be written as

$$\Delta f_i = \frac{f_s}{2\pi} \cos^{-1}[\cos(\omega_i) + (\zeta_i + \frac{\lambda v \omega_i \sin(\omega_i)}{1-\lambda})] - f_i, \quad (58)$$

where f_s denotes the sampling frequency. Frequency estimation is dependent on $k_i - \hat{k}_i$ and can be reduced by setting a high sampling frequency.

4.3 Analysis of noise reduction

From [17], noise reduction for difference $\Delta\omega_i = 2\pi\Delta f_i/f_s = \omega_i - \hat{\omega}_i$ can be written as

$$NR_i = \frac{\hat{D}_s^2 D_s^2}{2-2\cos(\Delta\omega_i)} [\mu - \frac{\cos(\Delta\phi_s) - \cos(\Delta\omega_i - \Delta\phi_s)}{\hat{D}_s D_s}]^2 + \cos^2(\frac{2\Delta\phi_s - \Delta\omega_i}{2}), \quad (59)$$

where NR_i represents the mean square noise reduction for $\Delta\omega_i$, $\Delta\phi_s$ is the estimated secondary path phase error, D_s^2 is the secondary path gain at ω_i , and \hat{D}_s^2 is the estimated secondary path gain at $\hat{\omega}_i$. For large μ and small $\Delta\omega_i$ with accurate secondary path estimate available, it can be shown for (58) that [17]

$$|\frac{\cos(\Delta\phi_s) - \cos(\Delta\omega_i - \Delta\phi_s)}{\hat{D}_s D_s}| \approx |\frac{\Delta\omega_i \sin(\Delta\phi_s)}{\hat{D}_s D_s}| \ll \mu \quad (60)$$

and

$$\cos^2(\frac{2\Delta\phi_s - \Delta\omega_i}{2}) \leq 1 \ll \frac{\hat{D}_s^2 D_s^2 \mu^2}{2-2\cos(\Delta\omega_i)}. \quad (61)$$

Therefore, (59) becomes

$$NR_i \approx \frac{\rho_f}{1-\cos(\Delta\omega_i)}, \quad (62)$$

where ρ_f represents a constant for f_i . Substitute (58) into (62)

$$NR_i = \frac{\rho_f}{1-\cos\{\cos^{-1}[\cos(\omega_i) + (\zeta_i + \frac{\lambda v \omega_i \sin(\omega_i)}{1-\lambda})] - \omega_i\}}, \quad (63)$$

Therefore, noise reduction performance is related to the offset ζ_i and $k_i - \hat{k}_i$. The term ζ_i has been reduced in the proposed method while $k_i - \hat{k}_i$ can be reduced by setting sampling frequency as high as possible.

Table 1

Computational requirements for ANC systems discussed in this paper.

	Additions	Multiplications
Kuo's method [7]	$3L_f + 2L_w + L_s + 2L_b$	$3L_f + 2L_w + L_s + 2L_b + 3$
Akhtar's method [11]	$2L_f + 2L_w + L_s + 2L_b + 6$	$2L_f + 2L_w + L_s + 2L_b + 11$
Shakeel's method [8]	$3L_f + 2L_w + L_s + 2L_b$	$3L_f + 2L_w + L_s + 2L_b + 9$
Shakeel's method [5]	$3L_f + 2L_w + L_s + 2L_b - 1$	$3L_f + 2L_w + L_s + 2L_b + 7$
Saeed's method maximum ¹	$5L_f + 4L_w + L_s + 4L_b + 11$	$5L_f + 4L_w + L_s + 4L_b + 22$
minimum ²	$L_f + 2L_w + L_s + L_b$	$L_f + 2L_w + L_s + L_b + 5$
Proposed method	$(2L_s + 22)M$	$(2L_s + 28)M$

¹ Filters $\hat{\mathbf{f}}(n)$, $\mathbf{b}(n)$ and $\mathbf{w}(n)$ are updated.² Only $\mathbf{w}(n)$ is updated.

Table 2

Memory requirements for various ANC systems.

	Number of variables
Kuo's Method [7]	$3L_f + 2L_w + L_s + 2L_b + L_D + 7^*$
Akhtar's Method [11]	$2L_f + 2L_w + L_s + 2L_b + 16$
Shakeel's Method [8]	$2L_f + 2L_w + L_s + 2L_b + 15$
Shakeel's Method [5]	$4L_f + 2L_w + L_s + 2L_b + 14$
Saeed's Method	$4L_f + 3L_w + L_s + 3L_b + 27$
Proposed Method	$4L_f + 3L_w + L_s + 3L_b + 27$

* L_D is length of decorrelation delay.

5 Computational Complexity

The computational complexity of the proposed method is provided in Table 1 for comparison where L_s , L_w , L_f and L_b represent the length of secondary path estimation filter, noise control filter, feedback path neutralization filter and predictor filter respectively. The proposed control structure requires less computations compared to the previous methods which makes it suitable for implementation with high sampling frequency. Setting high sampling frequency can help reduce the time-delay in frequency estimation as derived in subsection 4.2. Moreover, reducing computations translates well into power usage and processing resources required. The number of variables to be stored in memory at each iteration is given in Table 2. For small number of tones,

Table 3

Parameter values used in the simulations.

	Case 1	Case 2
Kuo's Method [7]	$\beta = 0.99, \mu_w = 3e^{-5}, \mu_h = 5e^{-4}, \mu_f = 5e^{-3}$	$\beta = 0.99, \mu_w = 1e^{-5}, \mu_h = 2e^{-4}, \mu_f = 3e^{-3}$
Akhtar's Method [11]	$\beta = 0.99, \mu_w = 3e^{-5}, \mu_h = 5e^{-4}, \mu_{f_{\min}} = 3e^{-4}, \mu_{f_{\max}} = 5e^{-3}$	$\beta = 0.99, \mu_w = 1e^{-5}, \mu_h = 2e^{-4}, \mu_{f_{\min}} = 5e^{-4}, \mu_{f_{\max}} = 3e^{-3}$
Shakeel's Method [8]	$\mu_h = 5e^{-4}, \mu_f = 1e^{-3}, \beta = 0.99, \mu_w = 3e^{-5}$	$\mu_h = 2e^{-4}, \mu_f = 8e^{-4}, \beta = 0.99, \mu_w = 1e^{-5}$
Shakeel's Method [5]	$\beta = 0.99, \mu_w = 3e^{-5}, \mu_h = 5e^{-4}, \mu_f = 1e^{-3}$	$\beta = 0.99, \mu_w = 1e^{-5}, \mu_h = 2e^{-4}, \mu_f = 8e^{-4}$
Saeed's Method	$\beta = 0.99, D = L_f$	$\beta = 0.99, D = L_f$
Proposed Method	$\alpha = 0.995, \lambda = 0.99, \gamma = 0.99, \eta = 1e^{-6}, \mu = 1e^{-2}, \mu_z = 1e^{-4}$	$\alpha = 0.995, \lambda = 0.99, \gamma = 0.99, \eta = 1e^{-6}, \mu = 1e^{-2}, \mu_z = 1e^{-4}$

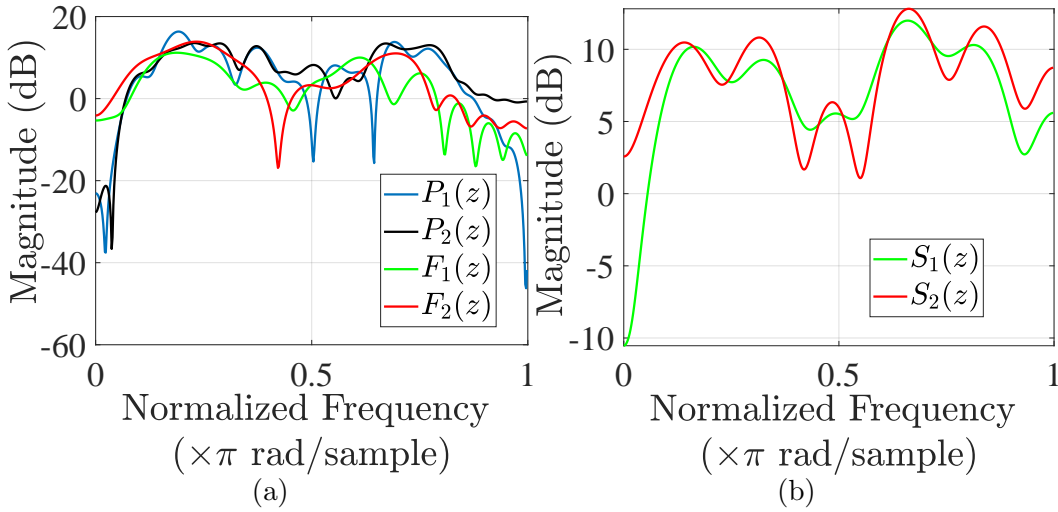


Fig. 6. Amplitude responses for primary, secondary and acoustic feedback paths.

the proposed method requires less computations and memory for implementation. However, all the previous methods make use of FIR filters for secondary path estimation filter, noise control filter, feedback path neutralization filter and prediction filter. This means that these methods can only handle a small number of well spaced frequencies [4]. The proposed method can handle large number of frequencies and even if they are a few hertz apart.

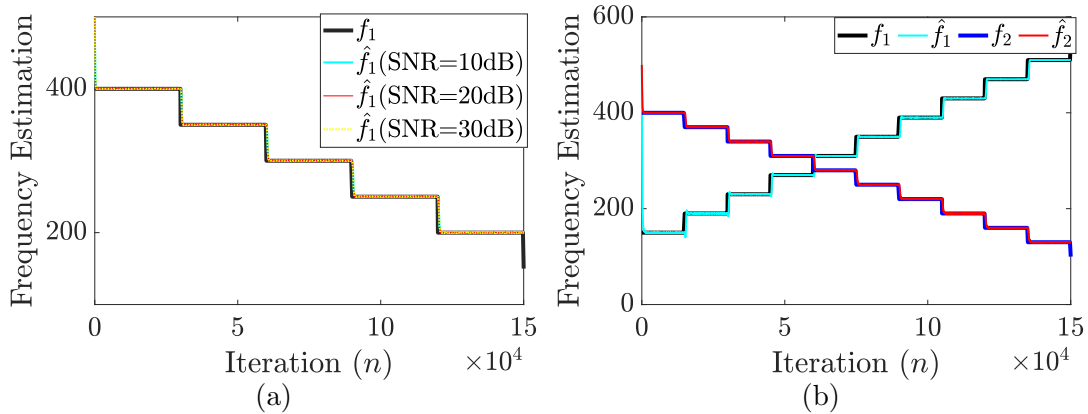


Fig. 7. Case 1 plots for frequency estimation (a) SNR (b) Time-varying frequency.

6 Case Studies

The proposed method is simulated under standard conditions to demonstrate its performance in comparison with Kuo (KM) [7], Akhtar (AM) [11], Shakeel (SM1) [8], Shakeel (SM2) [5] and Saeed (SaM) [1]. The proposed method does not involve acoustic feedback path estimation and auxiliary noise injection, hence all the methods are compared in terms of mean squared-error $E[e^2(n)]$ only. Impulse responses for primary paths, secondary paths, feedback paths and $W(z)$ are taken as FIR filters of length 48, 16, 32 and 32 respectively. Similar to [1,5,11], acoustic paths are obtained from [4] with amplitude responses provided in Fig. 6. Parameter settings are listed in Table 3 with $f_s = 2\text{KHz}$ and ensemble average is obtained over 20 independent runs.

6.1 Case 1

In this case, the proposed frequency estimation algorithm is analyzed under different conditions. In Fig. 7 (a), the proposed algorithm is tested for frequency estimation under different SNR conditions and a single time-varying frequency. Frequency estimation does not deteriorate with change in SNR which validates the robust behavior. In Fig. 7 (b), there are two time-varying tones that start from a different frequency but with time the frequencies get close to each other and settle to well apart frequency values. The algorithm demonstrates stable behavior and tracks both the tones with excellent precision.

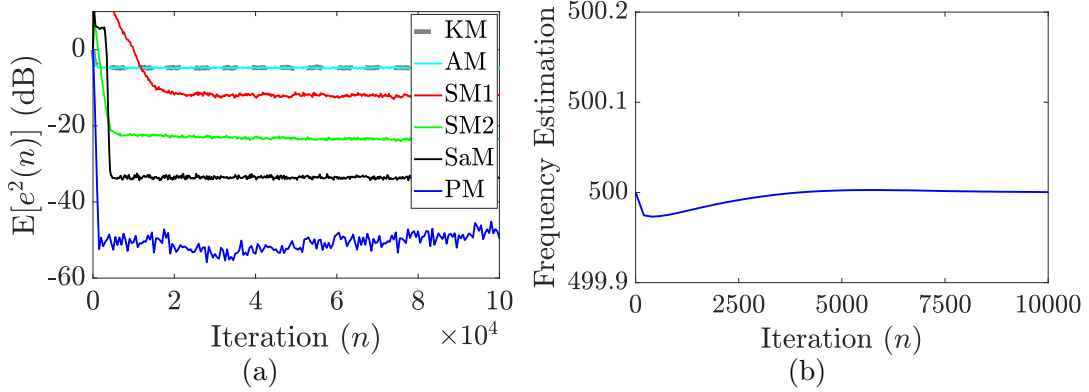


Fig. 8. Case 2 plots for: (a) The mean-squared error $E[e^2(n)]$ (dB). (b) Frequency estimation.

6.2 Case 2

In this case, $x_r(n)$ is a sinusoid with frequency 500 Hz and variance 2.0. Tonal noise is typical of machines like fans, generators and compressors [1,18]. SNR is adjusted to 30 dB and $\{P_1(z), S_1(z), F_1(z)\}$ are used as the acoustic paths. Simulation results are provided in Fig. 8. The proposed method improves the noise reduction performance by 15dB by reducing $E[e^2(n)]$ to 50dB in steady state at a significantly improved convergence rate. Power spectra for various methods are shown in Fig. 9 to highlight the contribution of the proposed method. Unlike, the proposed method does not require the estimate of $F(z)$ or injection of auxiliary noise.

6.3 Case 3

In this case, $x_r(n)$ comprises of sinusoids with frequencies: 100, 150, 300, 400 and 450 Hz, and variance 2.0. SNR is set to 30 dB and perturbation is introduced by changing acoustic paths from $\{P_1(z), S_1(z), F_1(z)\}$ to $\{P_2(z), S_2(z), F(z) = F_2(z)\}$ at $n = 50000$. Simulation results are provided in Fig. 10. The proposed algorithm improves the $E[e^2(n)]$ by more than 15dB in the steady state with noticeably improved convergence speed. At the time of perturbation, the noise levels stay much lower than the previous methods and convergence speed is superior after the perturbation in acoustic paths. There is no significant impact on the frequency estimates by the perturbations. Moreover, the power spectra of the primary noise, $d(n)$, and the residual noise, $e(n)$, are shown in Fig. 11 to validate the improved performance of the proposed method with the established methods.

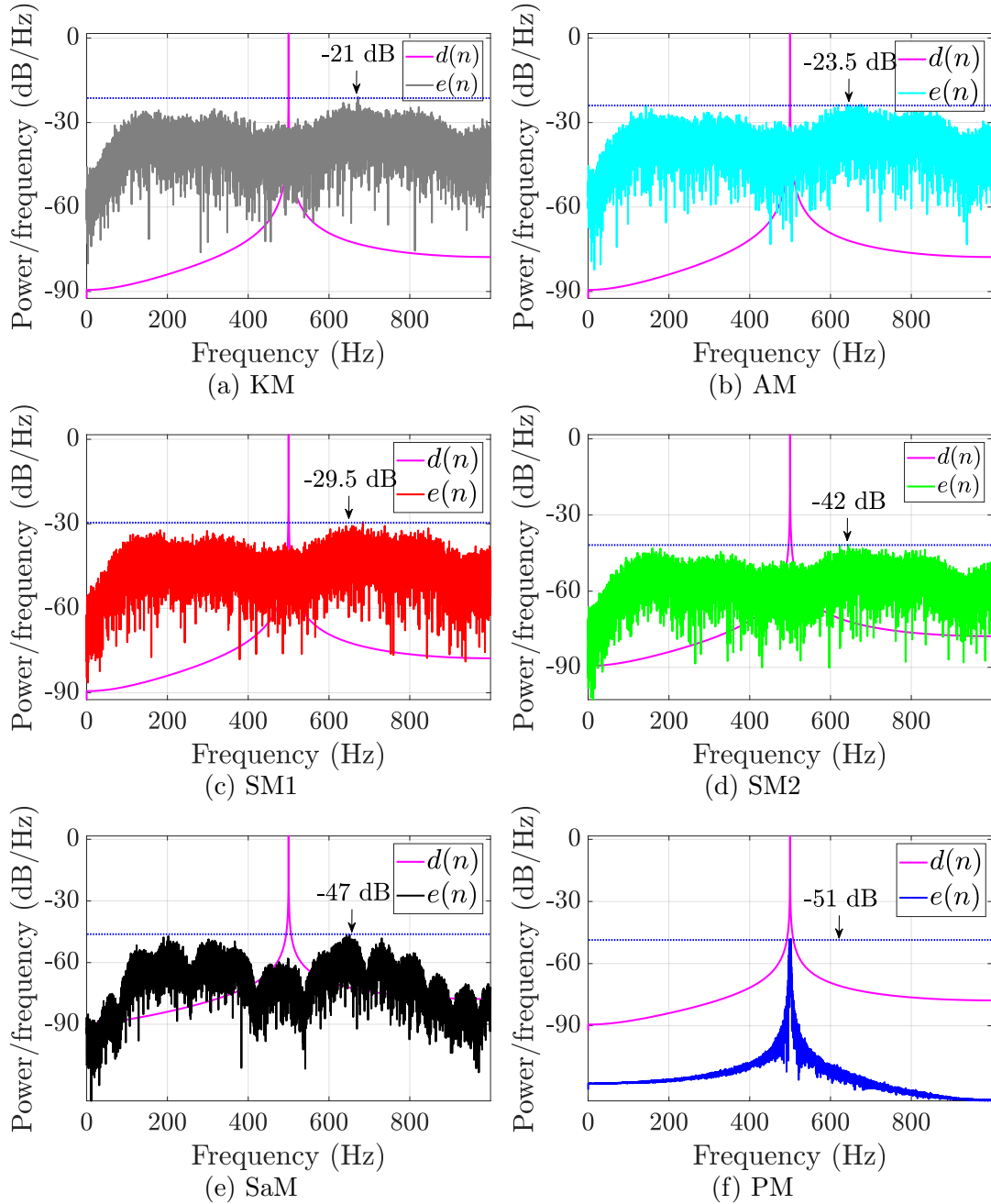


Fig. 9. Power spectra of $d(n)$ and $e(n)$ for various methods in Case 2.

7 Conclusions

This paper introduces a novel control structure to counter the narrowband noises in ANC systems with acoustic feedback. The proposed control structure uses a frequency estimation algorithm to generate reference signals internally. There are two-tap noise control filter for each tonal frequency. Performance analysis shows that proposed frequency estimation algorithm can produce unbiased estimates with adequate tracking capability. The proposed

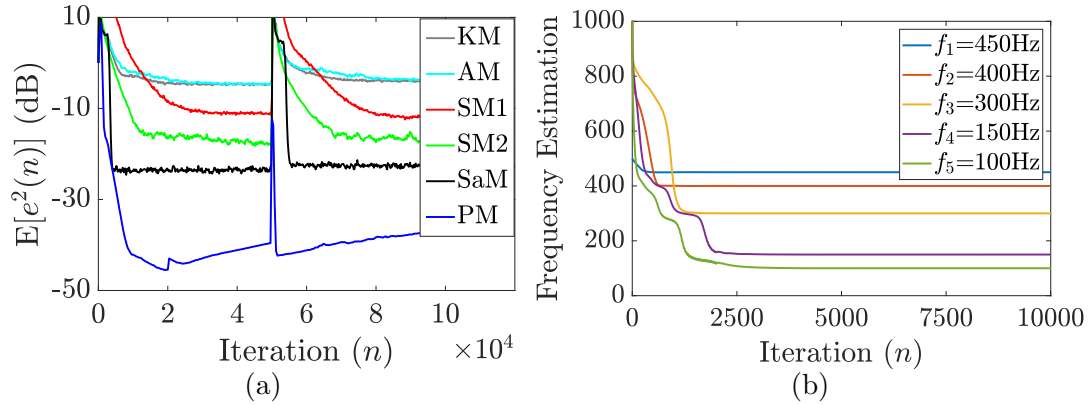


Fig. 10. Case 3 plots for: (a) The mean-squared error $E[e^2(n)]$ (dB). (b) Frequency estimation.

method does not require estimate of acoustic feedback path or introduction of auxiliary noise. This contributes significantly in keeping the noise levels low. The proposed control structure improves the noise reduction levels by more than 15dB for single tone and multi-tonal noises. The robust performance under perturbation, appreciable frequency tracking, improved convergence speed and significantly reduced residual noise are prominent contributions of the proposed control structure.

References

- [1] M. S. Aslam, P. Shi, and C. C. Lim. Self-adapting variable step size strategies for active noise control systems with acoustic feedback. *Automatica*, 123:109354, 2021.
- [2] M. S. Aslam, P. Shi, and C. C. Lim. Robust active noise control design by optimal weighted least squares approach. *IEEE Transactions on Circuits and Systems I: Regular Papers*, 66(10):3955–3967, 2019.
- [3] M. S. Aslam, P. Shi, and C. C. Lim. Variable threshold-based selective updating algorithms in feed-forward active noise control systems. *IEEE Transactions on Circuits and Systems I: Regular Papers*, 66(2):782–795, 2019.
- [4] S. M. Kuo and D. R. Morgan. *Active noise control systems—algorithms and DSP implementations*. Wiley, New York, 1996.
- [5] S. Ahmed and M. T. Akhtar. Gain scheduling of auxiliary noise and variable step-size for online acoustic feedback cancellation in narrow-band active noise control systems. *IEEE/ACM Transactions on Audio, Speech, and Language Processing*, 25(2):333–343, 2017.
- [6] S. Ahmed, M. T. Akhtar, and X. Zhang. Variable step-size based-adaptive algorithm for acoustic feedback cancellation during online operation of ANC

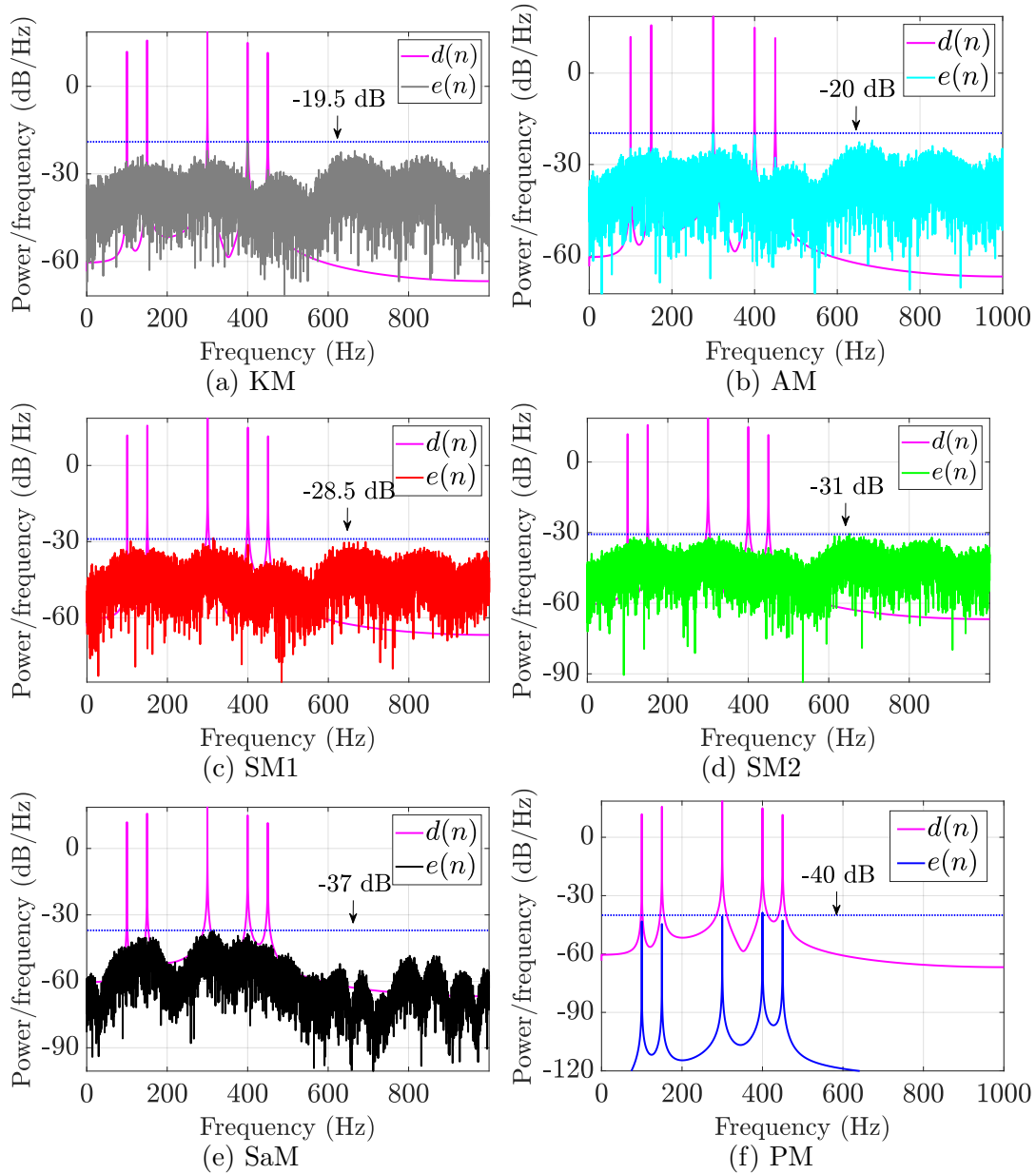


Fig. 11. Power spectra of $d(n)$ and $e(n)$ for various methods in Case 3.

systems. *IEEE China Summit and International Conference on Signal and Information Processing*, pages 74–78, 2015.

- [7] S. M. Kuo. Active noise control system and method for on-line feedback path modeling, 2002. Patent US6418227.
- [8] S. Ahmed, M. T. Akhtar, and X. Zhang. Online acoustic feedback mitigation with improved noise-reduction performance in active noise control systems. *IET Signal Processing*, 7(6):505–514, 2013.
- [9] S. M. Kuo and J. Luan. On-line modeling and feedback compensation for multiple-channel active noise control systems. *Applied Signal Processing*, 1(2):64–75, 1994.

- [10] L. J. Eriksson. Active sound attenuation system with on-line feedback path cancellation, 1987. Patent US4677677.
- [11] M. T. Akhtar and W. Mitsuhashi. Variable step-size based method for acoustic feedback modeling and neutralization in active noise control systems. *Applied Acoustics*, 72(5):297–304, 2011.
- [12] N. I. Cho and S. U. Lee. On the adaptive lattice notch filter for the detection of sinusoids. *IEEE Transactions on Circuits and Systems II: Analog and Digital Signal Processing*, 40(7):405–416, 1993.
- [13] J. Makhoul and L. Cosell. Adaptive lattice analysis of speech. *IEEE Transactions on Acoustics, Speech, and Signal Processing*, 29(3):654–659, 1981.
- [14] T. Söderström and L. Ljung. *Theory and Practice of Recursive Identification*. MIT, Cambridge, MA, 1983.
- [15] S. Haykin. *Adaptive filter theory*. Prentice Hall, Upper Saddle River, NJ, fourth edition, 2002.
- [16] H. Jeon, T. Chang, S. Yu, and S. M. Kuo. A narrowband active noise control system with frequency corrector. *IEEE Transactions on Audio, Speech, and Language Processing*, 19(4):990–1002, 2011.
- [17] H. Jeon, T. Chang, and S. M. Kuo. Analysis of frequency mismatch in narrowband active noise control. *IEEE Transactions on Audio, Speech, and Language Processing*, 18(6):1632–1642, 2010.
- [18] M. S. Aslam. Maximum likelihood least squares identification method for active noise control systems with autoregressive moving average noise. *Automatica*, 69:1–11, 2016.

Chapter 7

Thesis Conclusion

DESIGN of efficient control methods for various configurations of ANC systems are the prime focus of this thesis. Efficiency of the presented designs has been measured in terms of noise reduction, convergence rate, robustness, memory usage and computational cost. Noise reduction, robustness and convergence rate are directly related to the performance of the ANC systems, while computational requirements and memory usage are related to implementation domain. Low memory and computational requirements make the algorithm implementable in devices running multiple applications and use less power for extended battery life. Summary of this thesis is provided in this chapter along with directions for future research work.

7.1 Summary

In Chapter 2 computationally efficient self updating adaptive algorithms are derived for noise control and secondary path estimation filters. The proposed variable threshold based filtered-x self updating LMS-Newton algorithm provides fast convergence and improved noise reduction while requiring reduced computations for noise control filter. The proposed method performance is independent of the properties of input signal, which sometimes degrade the performance of least mean squares algorithm. For secondary path estimation, a simple auxiliary noise gain variation method is proposed that injects noise only at the startup or for perturbations. During steady state, auxiliary noise is negligible. Variable threshold effectively reduces the computations without deteriorating the performance of the ANC system.

Development of new recursive least squares algorithm is further explored in Chapter 3. The derived fast recursive least squares algorithm uses only forward prediction to obtain the adaptation gain. Using only forward prediction, eliminates the instability arising from the backward prediction in the conventional fast recursive least squares algorithm. Detailed convergence analysis establishes the stable behavior along with fast convergence speed and tracking capability. Rigorous simulations are performed to demonstrate the improved performance with low computations and numerical stability under quantization errors.

Chapter 4 addresses the ANC systems with narrowband disturbances at the error microphone. For feedforward and feedback noise control filters, filtered-x optimal weighting recursive least squares algorithm is derived. Optimal weighting factors are updated recursively in relation with new information in the current measurements. Decision on filter updates is also based on these weight factors to reduce the computational complexity. The proposed method produces reliable estimates as estimation error is bounded and nonincreasing as shown by detailed stability analysis. The presented algorithm delivers improved performance by combining the advantages of least mean squares and least squares algorithm.

In Chapter 5 acoustic feedback at the reference microphone is addressed. For feedback path neutralization filter, predictor filter and noise control filter, self adapting variable step sizes are derived to achieve robust performance and fast convergence. Auxiliary noise gain scheduling for feedback path estimation is designed to introduce minimum noise in the steady state. This reduces the interference to the noise control filter and

helps improve the noise reduction performance. Feedback path neutralization filter, predictor filter and their corresponding step size updates are discontinued for negligible auxiliary noise gain to reduce the computations.

In Chapter 6, a new control structure is designed to address narrowband noises in ANC systems with acoustic feedback. The proposed structure does not require the feedback path estimation. A frequency estimation algorithm is developed to internally generate the reference signals for noise controllers. There is a two tap noise controller for each frequency which works much better, in terms of convergence and steady state error, than the standard FIR noise controllers implemented in the relevant literature.

The research work presented in this thesis is focused on developing algorithms that require minimum computations possible for superior noise reduction. Thus, making them suitable for implementation with high sampling frequency to achieve fast convergence and improved tracking capability.

7.2 Future work

The directions for future work are

- Designing the control structure that does not require estimation of secondary path for the feed-forward controller and/or the acoustic feedback path estimation.
- Developing control structure for disturbances at the error microphone that can handle any number of tones. As normal FIR filter can handle small number of tonal noises with well spaced frequencies.
- Scaling up the control structure presented in Chapter 6 to multi-channel systems.
- Developing mixed control structures to handle most kind of practical noises to improve the robustness and noise reduction performance.

References

- AHMED-S., AKHTAR-M. T., AND ZHANG-X. (2013a). Online acoustic feedback mitigation with improved noise-reduction performance in active noise control systems, *IET Signal Processing*, **7(6)**, pp. 505–514.
- AHMED-S., AKHTAR-M. T., AND ZHANG-X. (2013b). Robust auxiliary-noise-power scheduling in active noise control systems with online secondary path modeling, *IEEE Transactions on Audio, Speech and Language Processing*, **21**, pp. 749–761.
- AHMED-S., AKHTAR-M. T., AND ZHANG-X. (2015). Variable step-size based-adaptive algorithm for acoustic feedback cancellation during online operation of ANC systems, *IEEE China Summit and International Conference on Signal and Information Processing*, pp. 74–78.
- AHMED-S., AND AKHTAR-M. T. (2017). Gain scheduling of auxiliary noise and variable step-size for online acoustic feedback cancellation in narrow-band active noise control systems, *IEEE/ACM Transactions on Audio, Speech, and Language Processing*, **25(2)**, pp. 333–343.
- AKHTAR-M. T., ABE-M., AND KAWAMATA-M. (2006). A new variable step size LMS algorithm-based method for improved online secondary path modeling in active noise control systems, *IEEE Transactions on Audio, Speech and Language Processing*, **12**, pp. 720–726.
- AKHTAR-M. T., ABE-M., AND KAWAMATA-M. (2007). Noise power scheduling in active noise control systems with online secondary path modeling, *IEICE Electronics Express*, **4**, pp. 66–71.
- AKHTAR-M. T., AND MITSUHASHI-W. (2011a). Improving performance of hybrid active noise control systems for uncorrelated narrowband disturbances, *IEEE Transactions on Audio, Speech, and Language Processing*, **19(7)**, pp. 2058–2066.
- AKHTAR-M. T., AND MITSUHASHI-W. (2011b). Variable step-size based method for acoustic feedback modeling and neutralization in active noise control systems, *Applied Acoustics*, **72(5)**, pp. 297–304.
- ARDEKANI-I. T., AND ABDULLA-W. H. (2012). Effects of imperfect secondary path modeling on adaptive active noise control systems, *IEEE Transactions on Signal Processing*, **20**, pp. 1252–1262.
- ASLAM-M. S. (2016). Maximum likelihood least squares identification method for active noise control systems with autoregressive moving average noise, *Automatica*, **69**, pp. 1–11.
- ASLAM-M. S., AND RAJA-M. A. Z. (2015). A new adaptive strategy to improve online secondary path modeling in active noise control systems using fractional signal processing approach, *Signal Processing*, **107**, pp. 433–443.
- ASLAM-M. S., SHI-P., AND LIM-C. (2019a). Robust active noise control design by optimal weighted least squares approach, *IEEE Transactions on Circuits and Systems I: Regular Papers*, **66(10)**, pp. 3955–3967.

References

- ASLAM-M. S., SHI-P., AND LIM-C. (2019b). Variable threshold-based selective updating algorithms in feed-forward active noise control systems, *IEEE Transactions on Circuits and Systems I: Regular Papers*, **66**(2), pp. 782–795.
- ASLAM-M. S., SHI-P., AND LIM-C. (2021). Self-adapting variable step size strategies for active noise control systems with acoustic feedback, *Automatica*, **123**, p. 109354.
- BASIN-M., SHI-P., AND CALDERON-ALVAREZ-D. (2011). Joint state filtering and parameter estimation for linear time-delay systems, *Signal Processing*, **91**(4), pp. 782–792.
- BOUCHARD-M. (2002). Numerically stable fast convergence least-squares algorithms for multichannel active sound cancellation systems and sound deconvolution systems, *Signal Processing*, **82**(5), pp. 721–736.
- BOUCHARD-M., AND QUEDNAU-S. (2000). Multichannel recursive-least-square algorithms and fast-transversal-filter algorithms for active noise control and sound reproduction systems, *IEEE Transactions on Speech and Audio Processing*, **8**(5), pp. 606–618.
- CARINI-A., AND MALATINI-S. (2008). Optimal variable step-size NLMS algorithms with auxiliary noise power scheduling for feedforward active noise control, *IEEE Transactions on Audio, Speech and Language Processing*, **16**, pp. 1383–1395.
- CHANG-C. Y., AND CHEN-D. R. (2010). Active noise cancellation without secondary path identification by using an adaptive genetic algorithm, *IEEE Transactions on Instrumentation and Measurement*, **59**, pp. 2315–2327.
- DAVARI-P., AND HASSANPOUR-H. (2009). Designing a new robust online secondary path modeling technique for feedforward active noise control systems, *Signal Processing*, **89**, pp. 1195–1204.
- DINIZ-P. S. R. (2008). *Adaptive filtering: algorithms and practical implementation*, Springer, New York, NY, USA.
- EGHTESADI-K., AND LEVENTHALL-H. G. (1981). Active attenuation of noise: The Chelsea dipole, *Journal of Sound and Vibration*, **75**(1), pp. 127–134.
- ERIKSSON-L. J. (1987). Active sound attenuation system with on-line feedback path cancellation. Patent US4677677.
- ERIKSSON-L. J., AND ALLIE-M. C. (1989). Use of random noise for on-line transducer modeling in an adaptive active attenuation system, *Journal of the Acoustical Society of America*, **85**, pp. 797–802.
- GAIOTTO-S. (2013). A tuning-less approach in secondary path modeling in active noise control systems, *IEEE Transactions on Audio, Speech and Language Processing*, **21**, pp. 444–448.
- GEORGE-N. V., AND PANDA-G. (2012). A particle-swarm-optimization-based decentralized nonlinear active noise control system, *IEEE Transactions on Instrumentation and Measurement*, **61**, pp. 3378–3386.
- GLENTIS-G. O., BERBERIDIS-K., AND THEODORIDIS-S. (1999). Efficient least squares adaptive algorithms for FIR transversal filtering, *IEEE Signal Processing Magazine*, **16**(4), pp. 13–41.

- HONG-M., AND SÖDERSTRÖM-T. (2009). Relations between bias-eliminating least squares, the frisch scheme and extended compensated least squares methods for identifying errors-in-variables systems, *Automatica*, **45(1)**, pp. 277–282.
- HONG-M., SÖDERSTRÖM-T., AND ZHENG-W. (2007). Accuracy analysis of bias-eliminating least squares estimates for errors-in-variables systems, *Automatica*, **43(9)**, pp. 1590–1596.
- HUFFEL-S. V., MARKOVSKY-I., R. J. VACCARO-R., AND SÖDERSTRÖM-T. (2007). Total least squares and errors-in-variables modeling, *Automatica*, **87(10)**, pp. 2281–2282.
- KAJIKAWA-Y., GAN-W. S., AND KUO-S. M. (2012). Recent advances on active noise control : open issues and innovative applications, *APSIPA Transactions on Signal and Information Processing*, **1**, pp. 1–21.
- KUO-S. M. (2002). Active noise control system and method for on-line feedback path modeling. Patent US6418227.
- KUO-S. M., AND LUAN-J. (1994). On-line modeling and feedback compensation for multiple-channel active noise control systems, *Applied Signal Processing*, **1(2)**, pp. 64–75.
- KUO-S. M., AND MORGAN-D. R. (1996). *Active noise control systems—algorithms and DSP implementations*, Wiley, New York.
- KUO-S. M., AND VIJAYAN-D. (1997). A secondary path modeling technique for active noise control systems, *IEEE Transactions on Speech and Audio Processing*, **5**, pp. 374–377.
- LEE-H. M., HUA-Y., WANG-Z., LIM-K. M., AND LEE-H. P. (2021). A review of the application of active noise control technologies on windows: Challenges and limitations, *Applied Acoustics*, **174**, p. 107753.
- LIAO-C.-W., AND LIN-J.-Y. (2007). New FIR filter-based adaptive algorithms incorporating with commutation error to improve active noise control performance, *Automatica*, **43(2)**, pp. 325–331.
- LIN-J.-Y., AND LIAO-C.-W. (2008). New IIR filter-based adaptive algorithm in active noise control applications: Commutation error-introduced LMS algorithm and associated convergence assessment by a deterministic approach, *Automatica*, **44(11)**, pp. 2916–2922.
- LOPES-P. A. C., AND GERALD-J. A. B. (2015). Auxiliary noise power scheduling algorithm for active noise control with online secondary path modeling and sudden changes, *IEEE Signal Processing Letters*, **22**, pp. 1590–1594.
- LOPES-P. A. C., GERALD-J. A. B., AND PIEDADE-M. S. (2017). The MMF \times LMS algorithm for active noise control with on-line secondary path modelling, *Digital Signal Processing*, **60**, pp. 75–80.
- LUEG-P. (1936). Process of silencing sound oscillations. Patent US2043416 A.
- MOKHTARPOUR-L., AND HASSANPOUR-H. (2012). A self-tuning hybrid active noise control system, *Journal of the Franklin Institute*, **349(5)**, pp. 1904 – 1914.
- MONTAZERI-A., AND POSHTAN-J. (2011). A new adaptive recursive RLS-based fast-array IIR filter for active noise and vibration control systems, *Signal Processing*, **91(1)**, pp. 98–113.

References

- PADHI-T., CHANDRA-M., KAR-A., AND SWAMY-M. (2017). Design and analysis of an improved hybrid active noise control system, *Applied Acoustics*, **127**, pp. 260 – 269.
- REDDY-M. R., PANAH-I. M., AND BRIGGS-R. (2011). Hybrid FxRLS-FxNLMS adaptive algorithm for active noise control in fMRI application, *IEEE Transactions on Control Systems Technology*, **19**(2), pp. 474–480.
- ROUT-N. K., DAS-D. P., AND PANDA-G. (2012). Particle swarm optimization based active noise control algorithm without secondary path identification, *IEEE Transactions on Instrumentation and Measurement*, **61**, pp. 554–563.
- SATO-N., AND SONE-T. (1996). Influence of modeling error on noise reduction performance of active noise control systems using filtered-x LMS algorithm, *Journal of the Acoustical Society of Japan (E)*, **17**, pp. 195–202.
- SHI-P., LUAN-X., AND LIU-F. (2012). H_∞ filtering for discrete-time systems with stochastic incomplete measurement and mixed delays, *IEEE Transactions on Industrial Electronics*, **59**(6), pp. 2732–2739.
- SHI-P., SU-X., AND LI-F. (2016). Dissipativity-based filtering for fuzzy switched systems with stochastic perturbation, *IEEE Transactions on Automatic Control*, **61**(6), pp. 1694–1699.
- SHI-P., YIN-Y., AND LIU-F. (2013). Gain-scheduled worst case control on nonlinear stochastic systems subject to actuator saturation and unknown information, *Journal of Optimization Theory and Applications*, **156**(3), pp. 844–858.
- SNYDER-S. D., AND HANSEN-C. H. (1994). The effect of transfer function estimation errors on the filtered-x LMS algorithms, *IEEE Transactions on Signal Processing*, **42**, pp. 950–953.
- SÖDERSTRÖM-T. (2007). Errors-in-variables methods in system identification, *Automatica*, **43**(6), pp. 939–958.
- SÖDERSTRÖM-T. (2013). Comparing some classes of bias-compensating least squares methods, *Automatica*, **49**(3), pp. 840–845.
- SUN-X., AND KUO-S. M. (2007). Active narrowband noise control systems using cascading adaptive filters, *IEEE Transactions on Audio, Speech, and Language Processing*, **15**(2), pp. 586–592.
- SWINBANKS-M. A. (1973). The active control of sound propagation in long ducts, *Journal of Sound and Vibration*, **27**(3), pp. 411–436.
- TOBIAS-O. J., BERMUDEZ-J. C. M., AND BERSHAD-N. J. (2000). Mean weight behavior of the filtered-x LMS algorithm, *IEEE Transactions on Signal Processing*, **48**, pp. 1061–1075.
- WARNAKA-G. E., POOLE-L. A., AND TICHY-J. (1984). Active acoustic attenuators. Patent US4473906.
- WU-B., AND BODSON-M. (2004). Multi-channel active noise control for periodic sources—indirect approach, *Automatica*, **40**(2), pp. 203–212.
- WU-L., QIU-X., BURNETT-I. S., AND GUO-Y. (2015). Decoupling feedforward and feedback structures in hybrid active noise control systems for uncorrelated narrowband disturbances, *Journal of Sound and Vibration*, **350**, pp. 1 – 10.

- ZHANG-M., LAN-H., AND SER-W. (2001). Cross-updated active noise control system with online secondary path modeling, *IEEE Transactions on Speech and Audio Processing*, **9**, pp. 598–602.
- ZHANG-M., LAN-H., AND SER-W. (2003). A robust online secondary path modeling method with auxiliary noise power scheduling strategy and norm constraint manipulation, *IEEE Transactions on Speech and Audio Processing*, **11**, pp. 45–53.